Investigating stress responses in models of Amyotrophic Lateral Sclerosis

---

Benjamin Clarke

Institute of Neurology

Academic Supervisors:

Prof. Linda Greensmith and Dr. Bernadett Kalmar

A Thesis submitted for the degree of

Doctor of Philosophy

University College London

2019

Declaration

I, Benjamin Clarke, confirm that the work presented in this Thesis is my own. Where information has been derived from other sources, I confirm that this has been indicated in the Thesis.

Abstract

The ability of motor neurons and surrounding glia to respond to stressful conditions is crucial for their survival in injury or disease states. Amyotrophic lateral sclerosis (ALS) is a fatal neurodegenerative disease defined by the loss of both upper and lower motor neurons resulting in muscle paralysis. Several pathomechanisms in both motor neurons and glial cells contribute to motor neuron death in ALS. Among these, dysfunction in stress responsive pathways involved in inflammation, proteostasis and mitochondrial function are known to be important.

Since ALS is defined by loss of motor neurons in specific anatomical areas, with spinal motor neurons most affected, regional differences in glial stress responses may contribute towards this specific pattern of damage. In this Thesis, a regional difference in the NO-iNOS-NF-κB inflammatory pathway was observed, with spinal cord glia displaying a stronger response than cortical glia. While this regional difference was observed, no clear differences were found in the inflammatory responses of glia from mutant SOD1 (mSOD1) models of ALS. However, mSOD1 glia were unable to activate the heat shock response (HSR), a cytoprotective response involving the upregulation of heat shock proteins (Hsps), as effectively as wildtype glia. Reduced activation of the HSR increased the inflammatory responses of mSOD1 glia. Therefore, dysregulation of the HSR may further exacerbate an inherent ability of spinal cord glia to promote inflammatory damage in ALS.

Mitochondrial dysfunction is also an important pathomechanism in ALS. Several Hsps are specifically localised to mitochondria. mSOD1 spinal cord motor neurons expressed lower levels mitochondrial Hsps TRAP1 and Hsp60. In a cellular ALS model of oxidative stress, overexpression of these proteins was protective to mitochondrial functions in motor neurons, while knockdown was detrimental.

Together, these data suggest that manipulating stress responses of motor neurons and glia may be a viable therapeutic target for ALS.

Acknowledgements

I would first like to thank Linda Greensmith for giving me the opportunity to undertake this PhD and for her supervision and advice over the last 4 years. I would also like to thank Bernadett Kalmar for her advice and support both in and out of the lab, and for enduring my many, many questions. I must also thank Rickie Patani for allowing me to work in his lab during the final months of my PhD and for all of his advice and supervision.

When I started this PhD, I don't think that I fully comprehended the level of mental resilience needed to deal with the regular frustration and failure that a PhD naturally entails. Thankfully, I have been lucky enough to have the support of many fellow students and post-docs, without whom I would not be writing this Thesis. I would therefore like to thank all the members of the Greensmith, Schiavo, Fratta and Patani labs for being there for me, whether it be in the lab, over a pint at the Perserverance or the Queen's Larder, at a "fancy" Friday lunch or on the football pitch on a Monday evening.

Finally, I would like to thank my family and friends for their help and support. Particularly to Olivia, who even though for most of this PhD was on the other side of the Atlantic, was still able to keep me sane.

"You can't always get what you want

But if you try sometimes you might find

You get what you need"

Impact statement

In neurodegenerative conditions or following injury, the ability of neurons and glia to respond to stressful conditions is vitally important for their continued function and survival. In chronic neurodegenerative diseases such as Amyotrophic lateral sclerosis (ALS), the loss of stress responsive mechanisms may contribute towards the specific loss of upper and lower motor neurons from the brain and spinal cord. Therefore, unravelling the molecular mechanisms that underlie the stress responses of motor neurons and glia that become dysfunctional in ALS may provide a therapeutic target for future treatments.

Motor neurons and surrounding glia that provide neuronal support are known to be molecularly and functionally diverse in different areas of the brain and spinal cord. Data presented in this Thesis shows that glia from the spinal cord are more readily activated by induction of inflammatory stress than glia from the cortex. While there were no clear differences found in induced pro-inflammatory signalling in glia from a mutant SOD1 mouse model of ALS compared to controls, this regional difference may have important implications for injury and disease where activation of inflammatory pathways occur. For example, in mutant SOD1 mice, motor neuron degeneration is known to occur primarily in the spinal cord compared with the brain. It is possible that the relative greater reactivity of spinal cord glia may play a role in this regional difference in motor neuron vulnerability to death.

The heat shock response is a pro-survival mechanism involving the upregulation of heat shock proteins, a family of protein chaperones that maintain protein homeostasis and inhibit apoptosis. Results presented in this Thesis suggests that the heat shock response is dysfunctional in glia from mutant SOD1 mice. Loss of this important cytoprotective mechanism in glia may exacerbate damaging inflammatory signalling, as well as contributing to loss of protein homeostasis in motor neurons. It is likely that both of these mechanisms contribute towards motor neuron death induced by dysfunctional glial cells in ALS.

Mitochondrial dysfunction is also thought to play an important role in motor neuron death in ALS. The data in this Thesis shows that the expression of mitochondrial heat shock proteins are reduced in motor neurons of mutant SOD1 mice. Manipulation of the levels of these proteins demonstrates that these

proteins are protective to motor neurons under conditions of oxidative stress, which is known to occur in ALS. Thus, mitochondrial heat shock proteins may be an attractive therapeutic target for ALS.

Taken together, the results presented in this Thesis show that differences in stress responsive pathways may contribute to motor neuron death in ALS, and suggest that manipulation of these mechanisms may be beneficial in treating the disease.

Table of contents

List of figures

List of diagrams

List of tables

Abbreviations

6-OHDA	Oxidopamine
ALS	Amyotrophic lateral sclerosis
ANG	Angiogenin
ANXA11	Annexin A11
BMP4	Bone morphogenetic protein 4
BSA	Bovine serum albumin
C1q	Complement component 1q
C9orf72	Chromosome 9 open reading frame 72
CHCHD10	Coiled-coil-helix-coiled-helix-coiled Domain containing 10
CHMP2B	Charged Multivesicular Body Protein 2B
CHOP	C/EBP homologous protein
CNS	Central nervous system
CSF	Cerebrospinal fluid
DAO	D-amino acid oxidase
DCTN1	Dynactin subunit 1
DHE	Dihydroethidium
DIV	Days *In Vitro*
DNase	Deoxyribonuclease
EAAT2	Excitatory amino acid transporter 2
EDTA	Ethylenediaminetetraacetic acid
EGTA	Egtazic acid
eNOS	Endothelial nitric oxide synthase
ENU	N-ethyl-N-nitrosourea
EWSR1	EWS RNA-binding protein 1
FACS	Fluorescence activated cell sorting
fALS	Familial amyotrophic lateral sclerosis
FBS	Foetal bovine serum
FGF2	Fibroblast growth factor 2
FIG4	FIG4 Phosphoinositide 5-Phosphatase
FOXG1	Forkhead box protein G1
FTD	Frontotemporal dementia
FUS	Fused in sarcoma
GDNF	Glial cell derived neurotrophic factor

GPC	Glial precursor cell
GTPP	Gamitrinib-triphenylphosphonium
H_2O_2	Hydrogen peroxide
HBSS	Hanks balanced salt solution
HNRNPA1/2	Heterogeneous nuclear ribonucleoprotein A1/2
HOXA4	Homeobox A4
HSF-1	Heat shock factor 1
Hsps	Heat shock proteins
HSR	Heat shock response
IBMPFD	Inclusion Body Myopathy with early-onset Paget disease and frontotemporal dementia
IKK	IκB kinase
IL-1α	Interleukin 1 alpha
IL-2	Interleukin 2
iNOS	Inducible nitric oxide synthase
iPSC	Induced pluripotent stem cell
KIF5A	Kinesin family member 5A
LCD	Low complexity domain
LIF	Leukocyte inhibitory factor
LPS	Lipopolysaccharide
MATR3	Matrin 3
MND	Motor neuron disease
MSP	Multisystem proteinopathy
mtDNA	Mitochondrial DNA
mtHsp	Mitochondrial heat shock protein
mtUPR	Mitochondrial unfolded protein response
NEK1	NimA-related protein kinase 1
NF-κB	Nuclear factor κ-light-chain-enhancer of activated B cells
NKX6.1	NK6 homeobox 1
NMJ	Neuromuscular junction
NO	Nitric oxide
nNOS	Neuronal nitric oxide synthase
NPC	Neural precursor cell
OPTN	Optineurin
ΔOTC	Mutant ornithine transcarbamylase

OTX2	Orthodenticle homeobox 2
PBS	Phosphate buffered saline
PD	Parkinson’s disease
PCR	Polymerase chain reaction
PFN1	Profilin 1
qPCR	Quantitative polymerase chain reaction
RAN	Repeat-associated non-ATG
RIPA	Radioimmunoprecipitation buffer
RNA	Ribonucleic acid
ROCK	Rho-associated protein kinase
ROS	Reactive oxide species
sALS	Sporadic amyotrophic lateral sclerosis
SETX	Senataxin
SIGMAR1	Sigma Non-Opioid Intracellular Receptor 1
SOD1	Superoxide dismutase 1
mSOD1	Mutant superoxide dismutase 1
SQSTM1	Sequestosome 1
STAT-1α	Signal transducer and activator of transcription 1 alpha
TAF15	TATA-Box Binding Protein Associated Factor 15
TARDBP	TAR DNA-binding protein 43
TBK1	TANK binding kinase 1
TBS	Tris buffered saline
TBST	Tris buffered saline 0.1% Tween 20
TIA1	TIA1 Cytotoxic Granule Associated RNA-Binding Protein
TMRM	Tetramethylrhodamine
TNF-α	Tumour necrosis factor alpha
TRAP1	TNF-α receptor associated protein 1
TUBA4A	Tubulin Alpha 4a
UBQLN2	Ubiquilin 2
UPS	Ubiquitin-proteasome system
VAPB	VAMP Associated Protein B and C
VCP	Valosin containing protein

Chapter 1: General Introduction

1.1 Aetiology and clinical symptoms of ALS

Motor neuron diseases are a group of neurological disorders characterised by the degeneration and death of motor neurons. Amyotrophic lateral sclerosis (ALS), also known as Lou Gehrig's disease in the USA and often referred to as Motor Neurone Disease (MND) in the UK, is the most common adult onset MND, characterised by the death of both upper and lower motor neurons in the motor cortex, brainstem and spinal cord (Al-Chalabi et al., 2017). Motor neurons are responsible for the transmission of commands from the brain to skeletal muscles in order to elicit movement. Loss of motor neurons from the brain and spinal cord results in extensive paralysis, with patients usually succumbing to the disease within 2-5 years of diagnosis. Typically, cause of death is respiratory failure due to the denervation of the respiratory muscles (Niedermeyer et al., 2019).

The phenotype of ALS is heterogeneous with respect to the age, site of onset, rate of progression and the predominance of upper or lower motor neuron death (Brown and Al-Chalabi, 2017). The onset of disease usually starts with a focal weakness presenting asymmetrically in the limbs. However, a third of cases begin with bulbar symptoms such as difficulty with speech or swallowing and ~5% of patients first present with respiratory issues (Kiernan et al., 2011). Upper motor neuron loss results in symptoms of spasticity and hyperreflexia while lower motor neuron loss causes fasciculations and muscle wasting (Statland et al., 2015). Sensory and autonomic nervous systems are not affected in the vast majority of ALS cases. Although the disease is primarily associated with motor symptoms, up to 50% of patients experience some form of behavioural impairment or cognitive decline, ~15% of which are consistent with a diagnosis of frontotemporal dementia (FTD) (Phukan et al., 2012; Bang et al., 2015).

There is evidence of selective vulnerability of motor neuron subtypes in ALS. Fast firing motor neurons that innervate fast twitch voluntary skeletal muscles are the most vulnerable in ALS, with slower firing motor neurons that innervate slow twitch postural muscles showing more resistance to disease (Dengler et al., 1990; Kanning et al., 2010). Furthermore, motor neurons in the oculomotor nucleus that innervate the muscles controlling the eyes and those in Onuf's nucleus that

innervate the pelvic floor muscles are most resistant to degeneration, usually remaining functional until death (Nijssen et al., 2017).

The incidence of ALS is 2.6 per 100,000 of the population, with a lifetime risk of 1:400 for those of European ancestry (Alonso et al., 2009). Incidence of the disease is more common in men than in women at a ratio of 1.3:1 (McCombe and Henderson, 2010). The onset of symptoms is typically between 55-75 years old, however, around 5% of cases present with an onset of younger than 30 years old. Importantly, there are currently no effective disease-modifying treatments available to treat ALS. Riluzole and Edavarone are the only FDA-approved treatments, modestly increasing lifespan by only a few months (Kiernan et al., 2011; Abe et al., 2017).

1.2 Genetic causes and pathological features of ALS

In the last 10 years, the number of genes found to cause ALS has increased dramatically, with more than 20 genes now identified (Taylor et al., 2016). These genes were first found in hereditary cases of ALS, also known as familial ALS (fALS), which account for ~5-10% of patients (Renton et al., 2014). Although they only represent a minority of overall ALS cases, fALS patients are mostly clinically indistinguishable to those with sporadic ALS (sALS) and share many neuropathological features. fALS cases can be inherited in an autosomal dominant or recessive pattern of inheritance, with varying levels of penetrance (Turner et al., 2017). A genetic basis for disease is not restricted to fALS, as mutations in genes found in fALS cases have been identified in up to 25% of apparently sALS cases (Cady et al., 2015).

Around half of cases of fALS are caused by mutations in either chromosome 9 open reading frame 72 (*C9orf72*) or Cu/Zn-superoxide dismutase 1 (*SOD1*) (Taylor et al., 2016), encoding two multifunctional proteins whose roles are discussed below. Many other rarer ALS-causing genes and risk factors have been identified. Interestingly, many of these genes can be grouped according to their functions, suggesting that common pathomechanisms exist in ALS. These include genes encoding proteins involved in: i) protein homeostasis: optineurin (*OPTN*), TANK-binding kinase 1 (*TBK1*), valosin-containing protein (*VCP*), vesicle-associated membrane protein-associated protein B (*VAPB*), ubiquilin 2 (*UBQLN2*), sequestosome 1 (*SQSTM1*), annexin A11 (*ANXA11*); ii) RNA

metabolism: TAR DNA-binding protein (*TARDBP*), fused in sarcoma (*FUS*), heterogeneous nuclear ribonucleoprotein A1 (*HNRNPA1*), matrin 3 (*MATR3*), TATA-box binding protein-associated factor 15 (*TAF15*), ewing sarcoma breakpoint region 1 (*EWSR1*), senataxin *(SETX)*; iii) axonal transport: dynactin subunit 1 (*DCTN1*) and kinesin family member 5A (*KIF5A*); iv) cytoskeletal maintenance: profilin 1 (*PFN1*) and tubulin beta-4A (*TUBA4A*); and v) mitochondrial function: *VAPB, TBK1,* coiled-coil-helix-coiled-coil-helix domain-containing 10 (*CHCHD10*) and sigma non-opioid intracellular receptor 1 (*SIGMAR1*) (Cook and Petrucelli, 2019) (Table 1.1).

Many ALS patients have mutations in more than one of these genes, suggesting that in some cases ALS may be an oligogenic disease (van Blitterswijk et al., 2012; Nguyen et al., 2018). Despite these recent advances in identifying ALS-associated mutations, the majority of cases have no known cause. It is thought that environmental factors also play a role in ALS, but these have been difficult to identify and prove in epidemiological studies (Hardiman et al., 2017). Others have proposed that like cancer, ALS may be a complex disease that involves several “steps”, with mathematical and statistical modelling suggesting that this may involve up to six steps to result in an ALS pathology (AI-Chalabi et al., 2014). Below the most common genes known to be causative for ALS are summarised in order of frequency among fALS cases, as well as some rarer genetic causes that display the diverse cellular roles of these genes in ALS pathomechanisms.

1.2.1 *C9orf72*

A hexanucleotide repeat expansion in the first intron of *C9orf72* is the most common known cause of fALS. The normal functions of C9orf72 are still not fully understood, however, it is clear that it is involved in autophagy (Farg et al., 2014) and has a role in inflammatory processes (O'Rourke et al., 2016). Hexanucleotide expansions of GGGGCC repeats in intronic domains of C9orf72 numbering in the hundreds or thousands are found in ALS patients, whereas healthy individuals typically have no more than 11 repeats. The mechanism of C9orf72 toxicity is not well understood but may be due to either a toxic gain-of-function by accumulation of RNA-binding proteins, or the production of toxic dipeptide repeat proteins by non-canonical repeat-associated non-ATG (RAN) translation (Mizielinska et al., 2014; Kumar et al., 2017; Balendra and Isaacs, 2018), although a loss-of-function mechanism has not yet been excluded (Webster et al., 2016).

Gene	fALS cases (%)	Main role	Mutations	References
C9orf72	25	Guanine nuclear exchange factor	Intronic GGGGCC repeat	(DeJesus-Hernandez et al., 2011; Renton et al., 2011)
SOD1	20	Superoxide dismutase	>150	(Rosen, 1993)
TARDBP	5	RNA metabolism	>40	(Sreedharan et al., 2008)
FUS	4	RNA metabolism	>40	(Kwiatkowski et al., 2009; Vance et al., 2009)
OPTN	4	Autophagy	>10	(Maruyama et al., 2010)
TBK1	1-3	Autophagy, immunity, mitochondrial quality control	>10	(Cirulli et al., 2015; Freischmidt et al., 2015)
VCP	1-2	Autophagy	>5	(Johnson et al., 2010)
SQSTM1	<1	Autophagy	>10	(Fecto et al., 2011)
VAPB	<1	Autophagy, mitochondrial maintenance	<5	(Nishimura et al., 2004)
CHMP2B	<1	Autophagy	<10	(Parkinson et al., 2006)
UBQLN2	<1	Proteasome	>10	(Deng et al., 2011)
HNRNPA1/HNRNPB1	<1	RNA metabolism, nucleocytoplasmic transport	<5	(Kim et al., 2013)
MATR3	<1	RNA metabolism, nucleocytoplasmic transport	<5	(Johnson et al., 2014)

TAF15	<1	RNA metabolism, nucleocytoplasmic transport	<10	(Couthouis et al., 2011; Ticozzi et al., 2011)
EWSR1	<1	RNA metabolism, nucleocytoplasmic transport	<10	(Couthouis et al., 2012)
DCTN1	<1	Axonal transport	>10	(Puls et al., 2003)
KIF5A	<1	Axonal transport	<10	(Brenner et al., 2018; Nicolas et al., 2018)
PFN1	<1	Cytoskeleton	<10	(Wu et al., 2012)
TUBA4A	<1	Cytoskeleton	>5	(Smith et al., 2014)
CHCHD10	<1	Mitochondrial maintenance	<5	(Bannwarth et al., 2014)
SIGMAR1	<1	Mitochondrial maintenance	<5	(Luty et al., 2010)
DAO	<1	D-serine metabolism	<5	(Mitchell et al., 2010)
NEK1	<1	DNA repair	<10	(Brenner et al., 2016)
ANG	<1	Angiogenesis	>10	(Greenway et al., 2006)
ANXA11	<1	Vesicle trafficking	<10	(Smith et al., 2017a)
TIA1	<1	Stress granule formation	<10	(Mackenzie et al., 2017)
SETX	<1	DNA/RNA helicase	<10	(Chen et al., 2004)
FIG4	<1	Lipid phosphatase	<10	(Chow et al., 2009)

Table 1.1. ALS-associated genes. Over 20 genes have been linked with ALS, encoding proteins with diverse cellular functions. Several ALS genes share common cellular functions, suggesting that common pathomechanisms exist across different ALS-causing mutations.

1.2.2 *SOD1*

Mutations in *SOD1* were the first to be identified as causative for ALS and account for ~20% of fALS cases and ~2% of sALS cases (Rosen, 1993). Currently, over 150 mutations in *SOD1* have been linked to ALS, most of which are missense mutations that follow an autosomal dominant pattern of inheritance. ALS-causing mutations in *SOD1* occur throughout the five exons of the gene. Some of these mutations display considerable phenotypic heterogeneity. For example, the A4V mutation, the most common in the North American population, is associated with a rapidly progressive form of ALS with an average survival of one year post-diagnosis (Juneja et al., 1997). In contrast, the D90A mutation is associated with a milder disease course, with patients surviving for over 10 years after diagnosis (Giannini et al., 2010).

SOD1 is a ubiquitously expressed protein that has several known functions, most notably as an antioxidant enzyme removing damaging superoxide molecules by conversion to hydrogen peroxide (H_2O_2) and water. SOD1 has additional roles as a transcription factor activated in response to oxidative stress and in stabilising mRNAs and regulating energy metabolism (Tsang et al., 2014; Bunton-Stasyshyn et al., 2015). It has been proposed that due to the relative abundance of the protein in cells SOD1 is likely to have additional unknown functions (Beckman et al., 1993; Wei et al., 2001; Reddi and Culotta, 2013). While SOD1 is predominantly a cytosolic protein, small but significant amounts have been found in the nucleus and mitochondria (Crapo et al., 1992; Sturtz et al., 2001).

ALS-causing mutations in *SOD1* can affect both the active site and stability of the protein. However, there is little correlation between the loss of enzymatic activity and disease severity in mice harbouring different SOD1 mutations, suggesting that loss of SOD1 enzymatic function is not a primary mechanism of disease (Ratovitski et al., 1999). Several studies have suggested that instead a toxic gain-of-function drives mutant SOD1 (mSOD1) pathology, likely through an increased propensity of mSOD1 to misfold and form aggregates (Shinder et al., 2001; Stathopulos et al., 2003; Hough et al., 2004; Rakhit et al., 2004). It has been proposed that aggregates of SOD1 may spread to nearby cells through a prion-like mechanism where wildtype proteins are sequestered, seeding further misfolding and aggregation (Munch et al., 2011). Indeed, mSOD1 is more likely to form fibrils than wildtype SOD1 and spinal cord homogenates from mSOD1

mice promote fibrillogenic seeding of wildtype SOD1 *in vitro* (Chia et al., 2010). This prion-like mechanism of SOD1 toxicity may explain the spread of clinical symptoms from a focal site of muscle weakness seen in ALS patients.

Accumulation of cytoplasmic SOD1 aggregates is observed in SOD1 fALS cases as well as mSOD1 overexpressing mouse models (Rakhit et al., 2007; Kerman et al., 2010; Da Cruz et al., 2017). However, there is some controversy over the presence of misfolded SOD1 in sALS cases. Several studies have reported that misfolded SOD1 is present in the spinal cords of sALS patients using conformation-sensitive antibodies (Bosco et al., 2010; Forsberg et al., 2010). Other groups have suggested that even though there are no SOD1 mutations present in these patients, oxidation or demetallation of wildtype SOD1 results in misfolding (Estevez et al., 1998; Ezzi et al., 2007), which in turn may contribute to motor neuron death in sALS cases (Bosco et al., 2010). However, other groups have found no evidence of misfolded SOD1 in sALS cases using the same techniques. A recent comprehensive study using several commercially available antibodies recognising misfolded SOD1 found no evidence of misfolded SOD1 in over 50 sALS cases (Da Cruz et al., 2017). This study suggests that evidence of misfolded SOD1 in sALS cases may be false positives as glycoproteinacous inclusions found in elderly tissue can be mistaken for positive signals. Thus, misfolded aggregates of SOD1 are unlikely to be present in sALS.

Loss-of-function mechanisms are not thought to play a major role in mSOD1 mediated toxicity as $SOD1^{-/-}$ mice do not display an overt ALS phenotype (Reaume et al., 1996). Furthermore, elevating levels of wildtype SOD1 has no effect on disease course in SOD1 mutant overexpressing mice (Bruijn et al., 1998), suggesting that loss of SOD1 function is not responsible for disease. However, loss of SOD1 may still play a modulatory role in motor neuron death as $SOD1^{-/-}$ mice display a mild, late-onset motor neuropathy and $SOD1^{-/-}$ motor neurons are more vulnerable to axotomy than wildtype mice (Reaume et al., 1996; Fischer et al., 2012; Saccon et al., 2013). In addition, the $SOD1^{D83G}$ N-ethyl-N-nitrosourea (ENU) induced mouse model of ALS shows a loss-of-function peripheral neuropathy phenotype due to loss of SOD1 dismutase activity, prior to a toxic gain-of-function in the Central Nervous System (CNS) that causes motor neuron death, suggesting a possible role for loss-of-function of SOD1 in ALS (Joyce et al., 2015).

1.2.2.1 Mutant SOD1 mouse models of ALS

The majority of studies investigating pathological mechanisms involved in ALS have used mSOD1 overexpressing transgenic mice. This is not only because mutations in *SOD1* were the first to be associated with ALS, but also because the mSOD1 mouse model remains the best available model to recapitulate the motor neuron death and muscle paralysis phenotypes of the disease. The first and most commonly used mSOD1 mouse harbours the glycine to alanine at position 93 (G93A) mutation (Gurney et al., 1994) (Diagram 1.1). In these mSOD1 overexpressing models, disease progression is correlated with the copy number of the mutant transgene and depends on mouse gender and genetic background (Heiman-Patterson et al., 2005; Nardo et al., 2016).

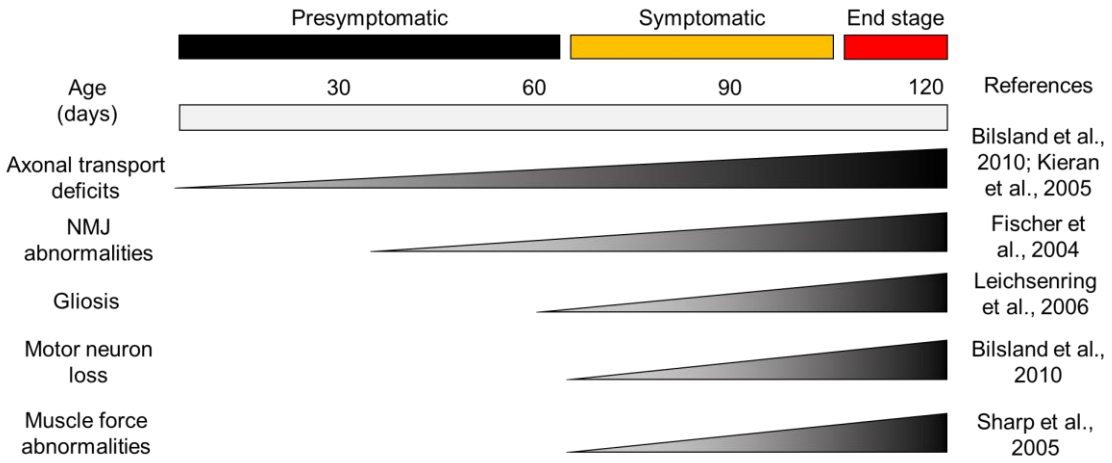

Diagram 1.1. Pathology of the SOD1^{G93A} mouse model of ALS. Mice overexpressing SOD1^{G93A} undergo an adult-onset loss of motor neurons, leading to muscle paralysis and premature death. NMJ: neuromuscular junction.

Mice overexpressing mSOD1 model several aspects of ALS pathology including muscle denervation, motor neuron loss and muscle wasting (Gurney et al., 1994; Fischer et al., 2004). Examination of motor neurons and glia of these mice reveals the accumulation of cytoplasmic aggregates of SOD1 at symptomatic ages (Bruijn et al., 1997; Johnston et al., 2000). Fast firing motor neurons are predominantly affected, while slower firing, fatigue-resistant motor neurons are less vulnerable (Frey et al., 2000). By late stage of disease, over 50% of motor neurons are lost (Sharp et al., 2005; Bilsland et al., 2010). An obvious caveat of these models is that artificial overexpression of the mutant protein does not occur

in ALS. In addition, mitochondria in mSOD1 overexpressing mice undergo vacuolisation, which is not seen in ALS patient motor neurons. $SOD1^{WT}$ overexpressor mice also exhibit mitochondrial vacuolisation and a phenotype of a late onset motor neuropathy (Jaarsma et al., 2000). Thus, the overexpression of SOD1 may account for at least part of the pathology observed in these mice.

1.2.3 *TARDBP* and *FUS*

TARDBP and *FUS* encode RNA-binding proteins involved in several aspects of RNA metabolism including transcription, alternative splicing, transport and local translation. Although mutations in TDP-43 account for only around 5% of fALS and 1% of sALS cases, TDP-43 mislocalises from the nucleus to the cytoplasm in the vast majority (95%) of ALS cases (Neumann et al., 2006; Mackenzie et al., 2007). TDP-43 can be found in cytoplasmic aggregates of misfolded proteins, however, some motor neurons that have a loss of TDP-43 from the nucleus do not contain aggregates, suggesting that TDP-43 nuclear depletion does not inevitably result in cytoplasmic aggregation (Braak et al., 2017). Moreover, TDP-43 mislocalisation is not essential for an ALS phenotype, as TDP-43 pathology is absent in patients with SOD1 or FUS mutations (Saberi et al., 2015). Some aggregates observed in ALS patients with TDP-43 mislocalisation are TDP-43 negative (Al-Sarraj et al., 2011). TDP-43 pathology is present not only in ALS, but is also seen in cases of FTD, indicating that ALS-FTD is a disease spectrum of disorders that shares TDP-43 pathology (Neumann et al., 2006).

The majority of ALS mutations in TDP-43 occur in the low complexity domain (LCD) of the protein, located towards the C terminus of the protein (Buratti, 2015). An ENU induced mutation in the TDP-43 C terminal domain has been found to result in a late onset motor neuropathy phenotype in mice (Fratta et al., 2018). Mechanisms of TDP-43 pathology include the loss of its nuclear functions or a gain-of-toxic function in the cytoplasm. However, the study of TDP-43 has been challenging, as TDP-43 is auto-regulated and overexpression of wildtype TDP-43 is toxic to neurons, while knockout of *TARDBP* in mice is embryonically lethal. Mouse models expressing heterozygous mutations in TDP-43, Cre inducible TDP-43 knockout mice and mice expressing mutant TDP-43 under neuronal specific promoters have all failed to recapitulate the phenotype of ALS as effectively as mSOD1 overexpressing models (Philips and Rothstein, 2015).

Mutations in *FUS* account for around 5% of fALS cases, including rare juvenile forms of the disease (Conte et al., 2012). FUS shares many commonalities with TDP-43 as it is also an RNA-binding protein that mislocalises from the nucleus to the cytoplasm in ALS. Recently, FUS mislocalisation but not aggregation has been found to occur in motor neurons of sALS cases (Tyzack et al., 2019). Most ALS-causing mutations in *FUS* are found in either the LCD or C terminal region, which contains the nuclear localisation signal of the protein (Deng et al., 2014). However, no TDP-43 pathology is observed in FUS mutant models and patients, suggesting that distinct pathological pathways occur in FUS-ALS. FUS and TDP-43 regulate the metabolism of different RNAs under physiological conditions, but loss of these proteins results in the downregulation of a number of common RNAs, suggesting that common loss-of-function mechanisms may occur in ALS (Lagier-Tourenne et al., 2012). Overexpression of FUS is toxic and knockout mice die before birth, however, mice heterozygous for a knockin FUS truncation mutation develop late onset motor neuron death (Devoy et al., 2017), but as with models of TDP-43-ALS, do not fully recapitulate the phenotype of ALS as effectively as mSOD1 models.

1.2.4 *TBK1, OPTN* and *VCP*

Rare ALS-causing mutations (between 1-3% of fALS cases) occur in either *TBK1*, *OPTN* or *VCP* genes, encoding proteins that are all involved in autophagy, a mechanism where cells degrade or recycle dysfunctional cellular components.

TBK1 is a member of the IκB kinase (IKK) family of proteins and plays important roles in both autophagy and inflammation. Most of the first ALS-causing mutations in TBK1 were found to cause a premature truncation of the protein and therefore TBK1 mutants were thought to act primarily through a loss-of-function mechanism (Freischmidt et al., 2015; Oakes et al., 2017). More recent studies have discovered that missense mutations in TBK1 are more common, although many have not been validated for their pathogenicity (Oakes et al., 2017). TBK1 knockout mice die of liver dysfunction before adulthood, however, $TBK1^{+/-}$ mice are viable. These heterozygous mice do not develop any motor symptoms but when crossed with mSOD1 overexpressing mice reduce inflammation and exacerbate dysfunction of autophagy pathways (Brenner et al., 2019). It is likely that both of these processes are important in the development of disease,

however, the relative contributions of each of these TBK1-mediated processes to ALS remains unclear.

OPTN is an autophagy adaptor protein that plays a major role in the polyubiquitination of proteins, marking them for degradation (Markovinovic et al., 2017). Interestingly, OPTN has been shown to mediate autophagy under the control of TBK1, providing a link between these two ALS related proteins (Richter et al., 2016). As with *TBK1* mutations, ALS-causing mutations in *OPTN* are thought to occur predominantly through a loss-of-function mechanism. $OPTN^{-/-}$ mice do not exhibit motor neuron death but do undergo axonal degeneration and denervation (Ito et al., 2016).

VCP is a multifunctional type II AAA-ATPase with diverse roles including cell cycle control, DNA repair, autophagy and proteostasis. Importantly, VCP binds ubiquitinated proteins to direct them towards autophagic degradation pathways (Meyer and Weihl, 2014). Mutations in *VCP* not only cause ALS but can also result in a multisystem disease known as multisystem proteinopathy (MSP), previously referred to as inclusion body myopathy with early-onset Paget disease and frontotemporal dementia (IBMPFD), a disease of neurons, bone and muscle (Al-Tahan et al., 2018). *VCP* mutations may cause abnormal ATPase activity or altered binding of VCP to co-factors. Interestingly, mutations in *VCP* result in TDP-43 pathology in the brain and muscle of mouse models and iPSC-derived motor neurons (Custer et al., 2010; Hall et al., 2017).

1.2.5 *DCTN1* and *KIF5A*

Rare mutations (<1% of fALS cases) in genes that are involved in axonal transport can also cause ALS. Axonal transport is the process by which cargoes move from the soma to the axon terminal (anterograde) or from the axon terminal back to the soma (retrograde). Mutations in *DCTN1*, which is involved in retrograde axonal transport, are causative for ALS (Puls et al., 2003). Dynactin acts as a link between cargoes and dynein, the motor protein that moves cargoes in a retrograde direction along microtubules. Moreover, mutations in *KIF5A*, encoding a protein that belongs to the kinesin family of proteins involved in anterograde axonal transport also cause ALS (Brenner et al., 2018; Nicolas et al., 2018).

1.2.6 *CHCHD10*

Rare mutations (<1% of fALS cases) in *CHCHD10* have been implicated as causative in ALS, as well as other Parkinson-like disorders and myopathies (Burstein et al., 2018). CHCHD10 is a mitochondrial protein that is located in the intermembrane space. The function of CHCHD10 is not well understood however it is thought to play a role in cristae maintenance and iron homeostasis (Genin et al., 2016; Burstein et al., 2018). CHCHD10 knockout mice are viable with no overt phenotype, however, *CHCHD10* knockin mutant mice display mitochondrial pathology and motor neuron loss (Genin et al., 2019). Although only a very small number of reported mutations in *CHCHD10* give rise to a pure ALS phenotype, it is important to consider that dysfunction in this mitochondrial protein is sufficient to cause an ALS phenotype.

1.3 ALS pathomechanisms

As previously discussed, studies of the genetic basis of ALS have shown that many ALS-causing genes are involved in common cellular processes including protein homeostasis, RNA metabolism, axonal transport and mitochondrial function (Hardiman et al., 2017). Dysfunction in each of these cellular functions can result in oxidative stress and excitotoxicity, ultimately leading to motor neuron death. Importantly, ALS pathomechanisms are not mutually exclusive, with dysfunction in one process leading to global cellular dysfunction that culminates in motor neuron death. The intrinsic properties of motor neurons as post-mitotic, highly metabolically active cells with long axons that require effective protein homeostasis and transport is likely to make these cells more susceptible to damage and dysfunction (Vandoorne et al., 2018).

It is important to consider that ALS-causing genes are not solely expressed in motor neurons, with many highly expressed in other cell types. It is now clear that cells that interact with motor neurons, including oligodendrocytes, astrocytes and microglia, can contribute to motor neuron death through non-cell autonomous mechanisms (Philips and Rothstein, 2014). Since mutations in *SOD1* were the first discovered to cause ALS and SOD1 mouse models remain the best at recapitulating the ALS phenotype, most of our understanding of the pathomechanisms of ALS have been performed in models of SOD1-ALS. Some

of the key pathomechanisms that have been proposed to play a role in ALS are discussed below (Diagram 1.2).

1.3.1 Protein dyshomeostasis

The presence of misfolded proteins in motor neurons and surrounding glial cells is universal in ALS, suggesting that there is a common dysfunction of proteostatic cellular mechanisms in all ALS cases (Neumann et al., 2006; Shaw et al., 2008; Kalmar and Greensmith, 2017). The accumulation of aggregates of misfolded proteins may not be the main toxic driving force but rather a maladaptive consequence of an inability to maintain protein homeostasis (Kalmar et al., 2014). Maintenance of protein homeostasis is a fundamental requirement for effective cellular function. Cells are equipped with many levels of quality control systems to properly maintain proteins or recycle and degrade misfolded proteins that have become misfolded (Webster et al., 2017). These include protein chaperones, the

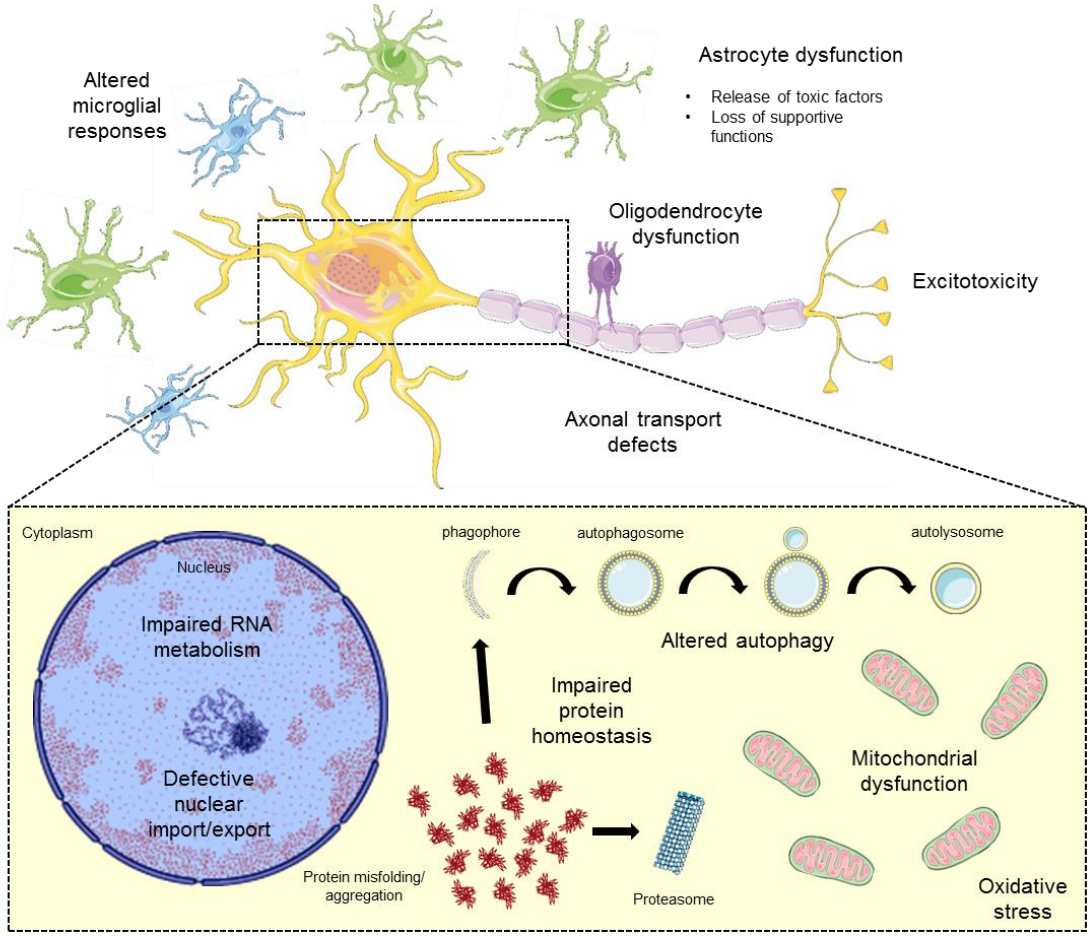

Diagram 1.2. Summary of pathomechanisms in ALS. Several mechanisms, both autonomous and non-cell autonomous, have been implicated in motor neuron death in ALS.

ubiquitin-proteasome system (UPS) and autophagy. Each of these aspects of protein homeostasis have been shown to be dysfunctional in models of ALS.

1.3.1.1 Protein chaperones and the heat shock response

Protein chaperones are proteins that preferentially bind to hydrophobic residues of nascent or misfolded proteins in order to refold them back to their functional conformation. Protein chaperones are not only able to prevent the aggregation of misfolded proteins through this action but can also function in disassembling protein aggregates (Yerbury et al., 2013).

The human chaperone network consists of over 300 genes, several of which are specialised for individual cellular compartments such as the endoplasmic reticulum or mitochondria (Brehme et al., 2014). The majority of protein chaperones consist of a superfamily of proteins known as heat shock proteins (Hsps). Hsps are categorised according to their molecular weight: Hsp90, Hsp70, Hsp60, Hsp40 and small Hsps. Together, protein chaperones make up around 10% of all of the total protein in the cytosol, half of which consist of Hsp70 and Hsp90 isoforms (Finka and Goloubinoff, 2013). Binding of Hsps to client proteins is typically ATP-dependent, with the exception of Hsp40 co-chaperones and small Hsps that do not act as “foldases” but instead act as “holdases”, inhibiting aggregation and facilitating other chaperones. In addition to their roles as protein chaperones, many Hsps also have additional functions including roles in maintaining the cytoskeleton, autophagy, apoptotic signalling and regulating inflammation (Liao et al., 1995; Yenari et al., 2005; Dokladny et al., 2013; Kennedy et al., 2014). The subcellular location of different Hsps, their relative expression in different tissues and their responses to different stressors varies greatly, suggesting that there are fine-tuned cell-type and stress-specific responses to stressful conditions (Sala et al., 2017; San Gil et al., 2017).

In addition to pathways that maintain protein homeostasis under normal cellular conditions, cells have evolved pathways to respond to stressful conditions that induce protein misfolding. Among these pathways is the heat shock response (HSR), a highly conserved ubiquitous pro-survival pathway activated in response to stressful conditions. After exposure to stressful conditions, the transcription factor heat shock factor 1 (HSF-1) trimerises and translocates to the nucleus

where it binds to short DNA sequences called heat shock elements, resulting in the upregulation of several Hsps that function to prevent protein aggregation (Morimoto et al., 1996; Brown, 2007).

The HSR was originally named due to the increase in expression of proteins following exposure to heat stress (Ritossa, 1962). However, the name HSR is a slight misnomer as the HSR has been reported to be activated after exposure to a wide variety of other stressors. These include artificial stressors such as acidic conditions (Mosser et al., 1990) and UV radiation (Trautinger et al., 1996) but also endogenous stressors such as oxidative stress (Welch et al., 1991), ischaemia (Zhang et al., 2008) and neurodegenerative conditions (Leak, 2014). Furthermore, several Hsps are not upregulated in response to any stressful conditions and instead are constitutively expressed.

Dysfunctional protein homeostasis is a characteristic hallmark of several neurodegenerative diseases, including Alzheimer's disease, Parkinson's disease, Huntington's disease and ALS. It has been suggested that ageing may be a primary factor in the failure of protein homeostasis that contributes to the development of these late onset neurodegenerative conditions (Boisvert et al., 2018). It has also been proposed that ageing may lead to loss of epigenetic control of HSF-1 through reduction in the expression of the deacetylase sirtuin-1, which regulates the ability of HSF-1 to bind to DNA (Westerheide et al., 2009). Since age is a major risk factor for most neurodegenerative diseases, protein dyshomeostasis may play a fundamental role in the pathogenesis of these diseases (Boisvert et al., 2018). The HSR is therefore an attractive therapeutic target to improve protein homeostasis, with potential benefits for many neurodegenerative diseases (Brehme et al., 2014; Calderwood and Murshid, 2017; Kalmar and Greensmith, 2017).

1.3.1.2 Heat shock proteins in ALS

Several studies have demonstrated that protein homeostasis is disrupted in ALS. Aggregates of misfolded proteins are present in spinal cord motor neurons and glia of ALS models and patients (Garofalo et al., 1991; Kato et al., 1997; Watanabe et al., 2001). Several Hsps have been found in these aggregates including Hsp70 and Hsp27 (Shinder et al., 2001; Okado-Matsumoto and Fridovich, 2002; Matsumoto et al., 2005), suggesting that cytosolic Hsps are

caught up in these aggregates, possibly rendering cells defenceless to any further proteotoxic stress. For example, Hsps may become trapped in aggregates because mSOD1 has a higher binding affinity to Hsp70 than wildtype SOD1, increasing the probability of Hsp70 sequestering in aggregates (Matsumoto et al., 2005). In addition, chaperoning activity is reduced in the spinal cord of $SOD1^{G93A}$ mice (Bruening et al., 1999; Tummala et al., 2005). Furthermore, levels of Hsp70 have been reported to become decreased at symptomatic ages of $SOD1^{G93A}$ mice (Liu et al., 2005). Therefore, increasing levels of Hsps may be a beneficial therapeutic strategy in ALS.

Aberrant expression of Hsps has been observed more recently in other models of ALS. For example, models of mutant TDP-43 show deficits in Hsp expression. The constitutive Hsc-70 has been shown to be reduced in mouse primary motor neurons transfected with mutant TDP-43 constructs (Coyne et al., 2017) and Hsps are downregulated in spinal cord lysates of mutant TDP-43 mice and sporadic ALS patients (Chen et al., 2016). Other recent studies have found that ALS-causing mutations can in fact induce the HSR. Two studies have found that in models of mutant C9orf72 or FUS, there is an increase in the expression of Hsp mRNAs as well as transcripts of HSF-1, although these studies did not investigate Hsp protein levels (Lopez-Erauskin et al., 2018; Mordes et al., 2018). Overall, in most models of ALS it seems that there is a loss of Hsp function at the level of protein expression due to either a reduced expression of Hsps or the sequestering of Hsps into aggregates, which is likely to contribute to a loss of proteostasis and eventual death.

The conflicting results regarding Hsp expression in different ALS models might not be a result of differential HSRs in various models but may rather represent different stages of the disease, with the initial phases characterised by a transient increase in Hsp expression, followed by a depletion of these proteins as the disease progresses. Alternatively, it is also possible that the disease condition has varying effects in different cell types and the compound effect measured might give different outcomes in each model, depending on the involvement of glial, interneuron and motor neuron stress responses.

Increasing the levels of Hsps may be an attractive therapeutic strategy to boost the proteostatic capacity of motor neurons in ALS. Attempts to increase the levels of Hsps have had varying levels of success. Overexpression of Hsp70 in primary

motor neurons has been shown to reduce the number of SOD1 aggregates and improve cell viability (Bruening et al., 1999). However, overexpression of Hsp70 *in vivo* has only elicited modest benefits in ALS models. Crossing mSOD1 expressing mice with mice overexpressing a Hsp70 transgene which increases the levels of Hsp70 by more than 10 times the normal level has no affect on disease progression (Liu et al., 2005). Furthermore, increasing levels of individual Hsps such as injection of recombinant Hsp70 (Gifondorwa et al., 2007) or overexpression of Hsp27 (Sharp et al., 2008) has only elicited modest benefits in mSOD1 mice. This indicates that purely targeting a single member of the Hsp superfamily might be insufficient to achieve a therapeutic benefit in conditions of protein misfolding and concerted induction of Hsp70 with its interacting co-chaperone partners or other Hsps may be required to combat protein dyshomeostasis more effectively (Kalmar et al., 2014).

Pharmacological approaches to increase Hsps have been more successful in mSOD1 models of ALS. Arimoclomol, a hydroxylamine derivative, has been shown to rescue motor neuron death, improve muscle function and increase the lifespan of mSOD1 mice (Kieran et al., 2004; Kalmar et al., 2008). Furthermore, arimoclomol has shown some promise in a recent phase II trial for ALS patients harbouring mSOD1 mutations (Benatar et al., 2018) and a phase III clinical trial is underway to establish clinical efficacy of this drug candidate for treatment of ALS (https://clinicaltrials.gov/ct2/show/NCT03836716). The mechanism of action of arimoclomol and other hydroxylamine derivatives is thought to be due to enhanced binding of HSF-1 to DNA, increasing the production of Hsps under stressful conditions (Hargitai et al., 2003). Arimoclomol has also been shown to be neuroprotective in a nerve injury model of motor neuron degeneration (Kalmar et al., 2002). In this study, neuroprotection correlated with an increase in Hsp70 not in motor neurons but instead in surrounding glial cells. Therefore, arimoclomol's protective effects may at least partly be due to its actions in glial cells. Another inducer of the HSR, the Hsp90 inhibitor 17-AAG, has also been shown to have beneficial effects in a TDP-43 model of ALS, in preventing ROS-induced aggregation of TDP-43, providing evidence that upregulation of the HSR may have potential therapeutic benefits in non-SOD1-ALS (Chang et al., 2013).

1.3.1.3 Ubiquitin-proteasome system dysfunction

The UPS is a proteolysis mechanism that removes misfolded proteins by enzymatically tagging them with polyubiquitin chains, resulting in their transport to the proteasome where they are degraded (Shahheydari et al., 2017). The presence of ubiquitinated aggregates in ALS spinal cords implicates dysfunction of the UPS in ALS pathomechanisms (Basso et al., 2006; Neumann et al., 2006). Motor neuron specific inhibition of the proteasome using conditional knockout of proteasomal subunit *Rpt3* results in protein aggregation, spinal motor neuron loss and locomotor dysfunction, showing that proteasomal inhibition can partially recapitulate an ALS phenotype (Tashiro et al., 2012).

Direct evidence for UPS dysfunction in ALS comes from the discovery of mutations in UPS-associated genes *VCP, UBQLN2* and *VAPB* in ALS patients. Reduced proteasomal activity has also been found in ALS models and patient tissue. Spinal cord lysates from presymptomatic $SOD1^{G93A}$ and post-mortem sALS cases have reduced proteasomal activity, with reduced expression of subunits involved in catalytic activity (Kabashi et al., 2004; Kabashi et al., 2008; Kabashi et al., 2012).

1.3.1.4 Autophagy dysfunction

Autophagy is the process by which proteins and organelles are directed to lysosomes for degradation via the formation of membranous structures called autophagosomes. Evidence for both impairment and maladaptive overactivation of autophagy has been reported in ALS models (Nguyen et al., 2019). The first evidence of autophagy playing a role in ALS came from the finding that impairment of autophagy via silencing of the essential autophagy gene, *atg7*, increases SOD1 accumulation (Kabuta et al., 2006). Creation of a motor neuron specific conditional *atg7* knockout mouse was found to extend lifespan but hastened the onset of disease when crossed with $SOD1^{G93A}$ mice, suggesting that autophagy is beneficial early on in the disease but plays a detrimental role at later stages (Rudnick et al., 2017).

Direct evidence for autophagy dysfunction in ALS comes from studies showing that aggregates found in motor neurons from post-mortem ALS cases or presymptomatic $SOD1^{G93A}$ mice are positive for the autophagy related proteins p62 and LC3-II (Sasaki, 2011; Xie et al., 2015). Furthermore, several autophagy

related genes have been found to cause ALS including *OPTN*, *TBK1*, *VCP*, *SQSTM1*, *VAPB* and *CHMP2B*. There is also evidence for C9orf72 playing a role in autophagy as depletion of C9orf72 results in p62 accumulation and iNeurons transdifferentiated from C9orf72-ALS patient fibroblasts exhibit reduced C9orf72 levels and impaired autophagy (Webster et al., 2016).

1.3.2 RNA metabolism defects

Deficits in RNA metabolism have become an intense area of ALS research since the discovery of ALS-causing mutations in genes encoding the RNA-binding proteins TDP-43 and FUS and the observation of nuclear RNA foci in C9orf72-ALS patients (Neumann et al., 2006; DeJesus-Hernandez et al., 2011). Furthermore, rarer mutations in genes encoding RNA-binding proteins *HNRNPA1/HNRNPB1*, *MATR3*, *TAF15* and *EWSR1* have also been associated with ALS (Couthouis et al., 2011; Couthouis et al., 2012; Kim et al., 2013; Johnson et al., 2014).

Mislocalisation of RNA-binding proteins is seen in the vast majority of ALS cases (Mackenzie et al., 2007; Deng et al., 2010; Luisier et al., 2018). Redistribution of RNA-binding proteins from the nucleus to the cytoplasm results in a loss of normal alternative splicing in the nucleus causing the abnormal retention of cryptic splice sites or the skipping of usually conserved exons (Polymenidou et al., 2011; Fratta et al., 2018). Mislocalisation may also result in aberrant cytoplasmic functions of RNA-binding proteins. RNA-binding proteins are also found in aggregates of misfolded protein in ALS models and patient tissue (Neumann et al., 2006). Although TDP-43 mislocalisation is not found in SOD1-ALS cases, a recent study has shown that another RNA-binding protein SFPQ is mislocalised in the $SOD1^{G93A}$ mouse, suggesting that deficits in RNA-binding proteins may be common to all forms of ALS (Luisier et al., 2018).

1.3.2.1 Nucleocytoplasmic shuttling dysfunction

Mislocalisation of RNA-binding proteins from the nucleus to the cytoplasm may be due to deficits in transport across the nuclear pore. Proteins involved in nuclear pore transport are mislocalised in spinal motor neurons of symptomatic $SOD1^{G93A}$ mice (Zhang et al., 2006). Furthermore, there is also evidence of nucleocytoplasmic transport deficits in C9orf72-ALS (Freibaum et al., 2015; Xiao et al., 2015; Zhang et al., 2015). Deficits in nucleocytoplasmic transport may be

a consequence of aggregation of toxic proteins in the cytoplasm inhibiting mRNA export (Woerner et al., 2016). Interestingly, a recent study has shown that proteins involved in nuclear import may act as protein chaperones and disaggregases, preventing mislocalised RNA-binding proteins from accumulation (Guo et al., 2018). In this study, binding of these nuclear import proteins to mutant ALS proteins was reduced compared to wildtype proteins, possibly limiting the ability of nuclear import proteins to relocalise RNA-binding proteins to the nucleus.

1.3.2.2 Stress granules in ALS

Stress granules are dynamic structures consisting of RNA and proteins that regulate mRNA translation by transiently sequestering mRNAs under conditions of cellular stress. The formation of stress granules is dependent on the ability of proteins to undergo liquid-liquid phase separation, which is dictated by the presence of LCDs present in RNA-binding proteins such as TDP-43 and FUS (Molliex et al., 2015). ALS-causing mutations in these RNA-binding proteins are more common in their LCDs, altering their ability to undergo phase separation (Murakami et al., 2015). Expression of either mutant C9orf72, SOD1, TDP-43 or FUS all results in altered dynamics of stress granules (Baron et al., 2013; Boeynaems et al., 2017; Gopal et al., 2017; Mateju et al., 2017). It has been hypothesised that stress granules may be the seed for aggregates of misfolded proteins in ALS. However, recent evidence suggests that aggregation of TDP-43 and stress granule formation occur independently of one another (Gasset-Rosa et al., 2019). Nevertheless, dysfunctional stress granule dynamics may still adversely affect many other cellular processes by abnormally sequestering RNAs and proteins, contributing to motor neuron death in ALS.

1.3.3 Oxidative stress

Oxidative stress is a term used to describe the process whereby accumulation of reactive oxide species (ROS) leads to cellular damage and cell death. ROS are products of partial oxidation of O_2 that form unstable and reactive intermediates.

The production of ROS such as $O_2^{\cdot -}$ and H_2O_2 is a normal physiological process that occurs during oxidative phosphorylation within mitochondria, during fatty acid beta oxidation in peroxisomes and in metabolic processes catalysed by cytochrome P450 enzymes in cell membranes or the endoplasmic reticulum.

These oxidative processes involve electron transfer between molecules. Some escaping electrons can react with either $O_{2\cdot}$ to form $O_{2\cdot^-}$ or H_2O_2 or form hydroxyl radicals. Alone these products are not particularly damaging, however, when combined with other species such as nitric oxide (NO) or superoxide more damaging species such as peroxynitrite are formed. The presence of high levels of ROS causes damage to several different parts of the cell including oxidation of proteins or DNA and the peroxidation of lipids.

Oxidative stress is thought to increase with age, a major risk factor in many neurodegenerative diseases, including ALS, due to excessive production of ROS (Barber and Shaw, 2010). Increased oxidative stress has been reported in both fALS and sALS patient spinal cords, as well as mSOD1 overexpressing models. ROS have been implicated in causing increases in the nitrosylation of proteins (Abe et al., 1995; Beal et al., 1997), lipid peroxidation (Shibata et al., 2001) and DNA damage (Ferrante et al., 1997). Levels of the ROS-producing enzyme NADPH oxidase are increased in symptomatic mSOD1 mice (Wu et al., 2006) and knockout of this enzyme rescues motor neuron death and extends survival (Marden et al., 2007). Oxidative stress may also play a role in sALS as ROS can cause oxidation of $SOD1^{WT}$ (Ezzi et al., 2007) and modify TDP-43 to cause aggregation (Cohen et al., 2015). Furthermore, increasing levels of anti-oxidant proteins has been shown to reduce mislocalisation of TDP-43 (Finelli et al., 2015). ROS production also reduces the levels of Hsps Hsp70 and Hsp27, which may contribute to the aggregation of TDP-43 (Chang et al., 2013).

1.3.4 Mitochondrial dysfunction

Mitochondria are dynamic, double-membrane bound organelles that have a number of vitally important cellular functions including ATP production, calcium buffering and apoptotic signalling (Moehle et al., 2019). The intrinsic properties of motor neurons make them more susceptible to mitochondrial dysfunction than other cell types. Motor neurons are especially dependent on energy production from mitochondria as high amounts of ATP are required for axonal transport over long distances (Vandoorne et al., 2018). Furthermore, mitochondria are one of the main sites of ROS production. ROS damage mitochondria by nitrating proteins, altering membrane permeability, causing mtDNA mutations and dysfunction of the respiratory chain through the disruption of Fe-S clusters. Mitochondrial dysfunction has been heavily implicated in the pathology of ALS,

as either a primary cause of pathology or as a secondary event occurring downstream of other factors (Smith et al., 2017b).

Mitochondria have been found to be morphologically abnormal in post-mortem spinal cords of sALS patients (Sasaki and Iwata, 2007). In this study, electron microscopy revealed several different abnormalities including filamentous structures inside the inner compartment of mitochondria, with some patients exhibiting swollen mitochondria with stubby protrusions on the outer membrane. Mitochondria also degenerate in the spinal cord of $SOD1^{G93A}$ mice (Wong et al., 1995), however unlike sporadic ALS patients, $SOD1^{G93A}$ mice present with vacuolisations as the predominant mitochondrial abnormality (Kong and Xu, 1998). In addition, mitochondria appear fragmented and rounder in $SOD1^{G93A}$ rat E15 spinal motor neurons (Song et al., 2013) and presymptomatic $SOD1^{G37R}$ mouse motor neurons (Vande Velde et al., 2011).

mSOD1 is known to localise to mitochondria and cause damage. mSOD1 protein has been found to accumulate at mitochondria on the outer membrane, but can also be found in the intermembrane space and the matrix (Jaarsma et al., 2001; Liu et al., 2004; Vijayvergiya et al., 2005). It is not fully understood how mSOD1 causes damage to mitochondria, although mSOD1 is known to interact with and inhibit VDAC1 at the outer mitochondrial membrane to influence calcium signalling (Israelson et al., 2010). mSOD1 is also implicated in causing a toxic conformational change in the apoptosis-related protein, Bcl-2 (Pedrini et al., 2010). Furthermore, transgenic mice with mSOD1 targeted to the intermembrane space of mitochondria develop motor neuron loss, muscle atrophy and have to be euthanised at one year of age, suggesting that specific mutant SOD1 expression to mitochondria is sufficient to cause a MND-like pathology (Igoudjil et al., 2011). Conversely, targeting wildtype SOD1 to mitochondria in SOD1 knockout mice rescues motor neuron denervation (Fischer et al., 2011).

Several other ALS-associated mutant proteins are known to localise to mitochondria and cause damage. Mutant TDP-43 has been shown to localise to mitochondria and inhibit the formation of complex I (Wang et al., 2016) while mitochondrial respiratory chain genes are downregulated in the spinal cord of a mutant FUS knockin mouse (Devoy et al., 2017). Furthermore, dipeptide repeats produced in C9orf72-ALS bind preferentially to mitochondrial ribosomal proteins and cause mitochondrial dysfunction (Lopez-Gonzalez et al., 2016; Choi et al.,

2019). Other genes known to cause ALS also encode proteins that localise to mitochondria (*CHCHD10*, *VAPB* and *OPTN*).

There is extensive evidence for mitochondrial dysfunction in ALS models. Mitochondrial dysfunction can be causative of many ALS pathomechanisms including calcium dyshomeostasis, oxidative stress and axonal transport deficits. Several studies have reported mitochondrial respiratory chain defects in the $SOD1^{G93A}$ mouse, although there are contradictory accounts over exactly which respiratory chain subunits are affected (Jung et al., 2002; Mattiazzi et al., 2002; Kirkinezos et al., 2005). In addition, a decrease in mitochondrial membrane potential is observed in embryonic motor neurons when co-cultured with $SOD1^{G93A}$ expressing astrocytes from post-natal day 0-3 mice, implicating mitochondrial dysfunction as an early pathological event in ALS (Bilsland et al., 2008). Abnormal calcium handling is also found in $SOD1^{G93A}$ motor neurons (Damiano et al., 2006; Lautenschlager et al., 2013). Increasing calcium buffering capacity reduced mSOD1 inclusions but did not affect survival of mSOD1 mice, suggesting that ameliorating deficits in calcium buffering is insufficient to affect disease progression in mSOD1 mice (Parone et al., 2013).

There is also evidence for dysfunction in the transport of mitochondria in ALS models. Mitochondrial transport speed is slower in both the anterograde and retrograde directions in both primary motor neurons cultures and in sciatic nerves of presymptomatic $SOD1^{G93A}$ mice compared to wildtype mice (Bilsland et al., 2010; Song et al., 2013). Specifically targeting mSOD1 to the intermembrane space of mitochondria was sufficient to induce deficits in mitochondrial transport, suggesting that deficits in mitochondrial transport are caused by the direct interaction between mutant proteins and not secondary to other mSOD1 pathomechanisms (Magrane et al., 2009).

1.3.5 Axonal transport and cytoskeletal dysfunction

Axonal transport is the process by which neurons move cargoes containing organelles or proteins along microtubules in an anterograde or retrograde direction. Motor neurons have unusually long axons that reach distant skeletal muscle targets up to a metre away from their cell body and are therefore uniquely reliant on axonal transport for their maintenance. Mutations in genes associated with axonal transport have been identified in rare cases of fALS including *DCTN1*,

KIF5A, *PFN1* and *TUBA4A* (Puls et al., 2003; Wu et al., 2012; Smith et al., 2014; Nicolas et al., 2018). Reduction in the speed of axonal transport has been reported in mSOD1 overexpressing models (Kieran et al., 2005; Bilsland et al., 2010; Gibbs et al., 2018) and mutant TDP43 models of ALS, but not in mutant FUS mice (Sleigh, bioRxiv 2018) suggesting that axonal transport deficits may not be universal in ALS cases.

Deficits in the cytoskeleton may also contribute to the death of motor neurons in ALS. Stathmin-2 has been reported to be involved in axonal maintenance and regeneration (Shin et al., 2014). Stathmin-2 is highly downregulated in TDP-43 mutant cells and motor neurons from sporadic and C9orf72-ALS patients due to loss of TDP-43 function (Melamed et al., 2019). Therefore, ALS mutant proteins can cause axonal transport and cytoskeletal deficits.

1.3.6 Excitotoxicity

Excitotoxicity is the pathological process in which neurons are overstimulated by glutamate, the major excitatory neurotransmitter in the CNS. At the synapse, glutamate is released from the presynaptic terminal and binds to ionotropic (NMDA, AMPA and kainate) and metabotropic (mGlu) post-synaptic receptors in order to cause depolarisation and the subsequent transmission of action potentials. This process involves the influx of calcium into the post-synaptic neuron. While calcium is required for normal function, high levels of calcium are detrimental to the neuron through the pathological activation of enzymes that damage the cell membrane, DNA and cytoskeleton (van Damme et al., 2005b).

Several studies have suggested that excitotoxicity plays a role in ALS. The only licensed treatment in the UK for ALS is Riluzole, which is thought to act by reducing excitotoxicity (Doble, 1996; Mohammadi et al., 2001; Albo et al., 2004). It has been suggested that motor neurons are more vulnerable to excitotoxic damage than other cell types as they express more AMPA receptors that lack the GluA2 subunit, which is responsible for the calcium impermeability of these channels (Van Damme et al., 2002). Furthermore, reduced expression of the calcium binding proteins calbindin and parvalbumin are not present in motor neurons, increasing their susceptibility to excitotoxic damage (Alexianu et al., 1994).

There is also some evidence of an increased release of glutamate from presynaptic terminals in ALS. An increased glutamate concentration has been found in the cerebrospinal fluid (CSF) of ALS patients (Rothstein et al., 1990). Furthermore, synaptosomes from spinal cords of $SOD1^{G93A}$ mice contain higher levels of glutamate both under basal conditions and in response to stimulation from presymptomatic ages (Milanese et al., 2011).

Changes in the composition of post-synaptic receptors could also contribute to excitotoxicity in ALS. Loss of the calcium impermeable GluA2 subunit of AMPA receptors exacerbates disease progression and motor neuron death in the $SOD1^{G93A}$ mouse (Van Damme et al., 2005a). Post transcriptional editing of the GluA2 subunit of AMPA receptors is also reduced in sALS spinal cord, suggesting that dysfunction of this process contributes to excitotoxicity in ALS (Kawahara et al., 2004).

Loss of glutamate uptake mechanisms may also contribute to excitotoxicity in ALS. Reduction in the expression of excitatory amino acid transporter 2 (EAAT2), a transporter expressed by astrocytes that removes glutamate from the synapse, is observed in ALS post-mortem motor cortex and spinal cord (Rothstein et al., 1995b). Furthermore, primary astrocyte cultures from $SOD1^{G93A}$ mice fail to uptake glutamate as efficiently as wildtype cultures (Benkler et al., 2013) and pharmacological blockade of glutamate uptake results in motor neuron death in $SOD1^{G93A}$ rat organotypic slice cultures (Yin and Weiss, 2012). Together, these studies show that loss of glutamate uptake may play an important role in the death of motor neurons in ALS.

1.3.7 Glial non-cell autonomous mechanisms of motor neuron death

Although much of the focus of ALS research has been into autonomous mechanisms of motor neuron death, cell types other than motor neurons are now known to contribute towards motor neuron death in ALS. Glial cells including oligodendrocytes, astrocytes and microglia are supportive cells that under normal conditions maintain motor neuron function and survival. However, it is now clear that glial cells undergo dysfunction in ALS, contributing to motor neuron death.

Most work on the individual contributions of different glial cells to motor neuron death has been performed in mSOD1 models. Restricting expression of $SOD1^{G93A}$ to neurons results in an incomplete recapitulation of disease in mice,

highlighting the requirement of non-neuronal cells for pathology (Pramatarova et al., 2001; Jaarsma et al., 2008). More direct evidence for the contribution of non-neuronal cells to motor neuron death in ALS has been demonstrated in chimeric mice expressing different levels of mSOD1 in different cell populations (Clement et al., 2003). Chimeras with a higher proportion of non-neuronal cells expressing mSOD1 have been shown to undergo more extensive motor neuron death and exhibit a shorter lifespan. Therefore, it is clear that non-neuronal cells are important in motor neuron death in ALS.

Under conditions of stress, astrocytes and microglia adopt a “reactive” phenotype, undergoing extensive changes in gene expression, resulting in altered cellular functions (Wilhelmsson et al., 2006; Sofroniew, 2009; Liddelow and Barres, 2017). Glial reactivity is not a binary response, instead glia respond in a graded and context-dependent way to different stressors (Burda and Sofroniew, 2017). Stress responses of glia can be pro- or anti-inflammatory, with subsequent beneficial or detrimental effects on the survival of motor neurons (Anderson et al., 2016; Liddelow et al., 2017). Different stimuli can induce different patterns of reactivity in glia and therefore a distinct reactive signature is likely to occur in ALS, albeit perhaps with common biochemical pathways (Zamanian et al., 2012; Chiu et al., 2013; Phatnani et al., 2013).

1.3.7.1 Astrocytes

Astrocytes perform numerous functions to support neurons in the CNS including regulating synaptic transmission, recycling neurotransmitters, providing metabolic support, regulating blood flow and protecting neurons from injury or infection by becoming reactive (Sofroniew and Vinters, 2010). However, it is now clear that astrocytes become detrimental to motor neuron survival in ALS (Serio and Patani, 2018). Populations of reactive astrocytes become hypertrophic in ALS tissue and models (Bruijn et al., 1997; Hall et al., 1998; Levine et al., 1999; Haidet-Phillips et al., 2011).

While astrocyte-restricted expression of mSOD1 is not sufficient to cause motor neuron death in wildtype mice (Gong et al., 2000), several studies have shown that astrocytes play an important modulatory role in mSOD1 models. Deletion of the mSOD1 gene specifically in astrocytes results in delayed death of mSOD1 mice (Yamanaka et al., 2008). While it is clear from this study that astrocytes are

involved in the later stages of disease, contradictory results have been found regarding whether or not this affects the onset of disease in these mice (Wang et al., 2011).

Several studies have suggested that astrocytes also play a role during the early stages of disease. RNA-Seq of different cell types throughout the lifespan of mSOD1 mice revealed that many genes are dysregulated at disease onset in astrocytes (Sun et al., 2015). Furthermore, astrocytes from neonatal SOD1 mice are toxic to motor neurons in co-culture (Nagai et al., 2007; Bilsland et al., 2008), and transplantation of mSOD1 astrocyte precursors into the spinal cords of wildtype rats has been shown to be toxic to motor neurons (Papadeas et al., 2011). Therefore, astrocytes appear to be damaging to motor neurons at an early disease phase, as well as later stages of disease in mSOD1 mice.

Co-culture paradigms have also been employed to demonstrate toxicity of astrocytes from sALS post-mortem tissue to motor neurons (Haidet-Phillips et al., 2011; Re et al., 2014), suggesting that astrocyte involvement in ALS is not restricted to SOD1-ALS cases. It has also been shown that both C9orf72 and FUS mutant astrocytes induce non-cell autonomous motor neuron death in co-culture (Meyer et al., 2014; Kia et al., 2018; Varcianna et al., 2019). However, TDP-43 mutant astrocytes are not toxic to motor neurons in co-culture but instead undergo cell death themselves (Serio et al., 2013). Thus, different ALS-causing mutations may confer damage to motor neurons through different mechanisms.

Non-cell autonomous motor neuron death mediated by astrocytes may be due to a release of toxic factors, dysfunction of metabolic support of motor neurons or the failure to induce adaptive mechanisms that provide protection to motor neurons. Since it has also been shown that there is a loss of astrocytes themselves in mutant TDP-43 and SOD1 models, the absence of astrocytes or the replacement of protective astrocytes with functionally aberrant astrocytes may also lead to motor neuron death (Rossi et al., 2008; Serio et al., 2013; Sloan and Barres, 2013).

Much research into the mechanisms of astrocyte-mediated motor neuron death has focused on the release of toxic factors. Several toxic factors have been implicated in astrocyte-mediated motor neuron death including TNF- α (Hensley et al., 2003), NO (Lee et al., 2009), NGF (Ferraiuolo et al., 2011), IL-1β (Meissner

et al., 2010), TGF-β (Endo et al., 2015), prostaglandins (de Boer et al., 2014), lipocalin 2 (Bi et al., 2013) and even mutant SOD1 itself (Urushitani et al., 2006). Motor neuron death induced by mutant astrocyte conditioned media has been shown to be rescued by antioxidants or sodium channel blockers, implicating mitochondrial dysfunction, oxidative stress and hyperexcitability as mechanisms of non-cell autonomous motor neuron death (Cassina et al., 2008; Fritz et al., 2013; Rojas et al., 2014).

The loss of the regular functions of astrocytes has also been implicated in contributing to motor neuron death in ALS. Reduction of the glutamate transporter EAAT2 has been observed in symptomatic mSOD1 mice and post-mortem ALS spinal cords (Rothstein et al., 1995a; Bruijn et al., 1997). Astrocytes are responsible for up to 90% of glutamate recycling and therefore loss of this receptor is likely to contribute towards glutamate-induced excitotoxicity (Kim et al., 2011). Furthermore, loss of the glia-specific potassium channel Kir4.1 is known to lead to neuronal hyperexcitability (Nwaobi et al., 2016). Both $SOD1^{G93A}$ spinal cords (Kaiser et al., 2006) and $SOD1^{D90A}$ expressing iPSC-derived astrocytes display a reduced expression of this channel (Kelley et al., 2018). Dysfunction of astrocytes has also been shown to result in a loss of the major histocompatibility complex I in $SOD1^{G93A}$ motor neurons and post-mortem ALS tissue, contributing to disease progression in $SOD1^{G93A}$ mice (Song et al., 2016).

Dysfunctional metabolic support from astrocytes to motor neurons has also been linked to motor neuron death in ALS. A recent study found that the levels of many metabolites of cultured astrocytes from neonatal $SOD1^{G93A}$ mice were dysregulated compared to wildtype cultures (Madji Hounoum et al., 2017). Lactate was found to be one of the most highly downregulated metabolites in $SOD1^{G93A}$ astrocytes. Decreased lactate has been found in the spinal cords of presymptomatic $SOD1^{G93A}$ mice and supplementing wildtype motor neurons co-cultured with $SOD1^{G93A}$ astrocytes with lactate improves motor neuron viability (Ferraiuolo et al., 2011). Dysfunctional metabolic support has also been observed in mutant C9orf72 astrocytes where reduction in the enzyme adenosine deaminase results in toxicity due to overproduction of adenosine and the loss of the supportive substrate inosine (Allen et al., 2019).

Finally, the loss of astrocytic neuroprotective pathways activated in response to stress may occur in ALS. In response to nerve ligation, a model of neuronal

damage, mSOD1 astrocytes are unable to effectively activate a neuroprotective STAT3-dependent mechanism (Tyzack et al., 2017). In this study, mass spectroscopy of iPSC-derived $SOD1^{D90A}$ astrocytes revealed that several STAT3 regulators were downregulated. Therefore, astrocytes can confer toxicity to motor neurons through both gain-of-toxic function and loss-of-function mechanisms.

1.3.7.2 Microglia

Microglia are the innate immune cells of the CNS, constantly surveying their local environment and responding to injury or infection. Unlike astrocytes that form from neural precursors, microglia are derived from the mesoderm and migrate into the CNS during embryonic development (Alliot et al., 1999). Proliferation of microglia is observed in tissue from post-mortem ALS spinal cords as well as in mSOD1 mouse spinal cords (Hall et al., 1998; Alexianu et al., 2001; Henkel et al., 2004; Nikodemova et al., 2014). Deleting mSOD1 specifically from microglia in mSOD1 overexpressing mice, or transplanting wildtype microglia into mSOD1 mice, has been shown to result in increased survival but has little effect on the onset of disease, suggesting that microglia play a role in the late disease phase (Beers et al., 2006; Boillee et al., 2006).

In co-culture, microglia from symptomatic mSOD1 mice are neurotoxic to motor neurons (Frakes et al., 2014). However, contradictory evidence has been given regarding the neurotoxic potential of microglia from presymptomatic mSOD1 mice. While an earlier study found that microglia from neonatal mice kill motor neurons in co-culture (Xiao et al., 2007), subsequent studies have failed to see an effect (Liao et al., 2012; Frakes et al., 2014). Microglia from neonatal mSOD1 mice were more toxic than wildtype mice to motor neurons in co-culture following stimulation with lipopolysaccharide (LPS), suggesting that mSOD1 expression exacerbates pro-inflammatory signalling even at presymptomatic ages (Xiao et al., 2007). Furthermore, incubation of wildtype microglia from neonatal mice with recombinant mSOD1 protein, but not $SOD1^{WT}$, caused a pro-inflammatory response that was toxic to motor neurons (Zhao et al., 2010).

Microglia are also reported to be dysfunctional in non-mSOD1 models. Microglia from C9orf72 knockout mice display abnormal endosomal trafficking leading to a pro-inflammatory state, albeit without resulting neurodegeneration (O'Rourke et al., 2016). Overexpression of TDP-43 also results in an exacerbated pro-

inflammatory response in microglia treated with LPS, leading to neuronal toxicity (Swarup et al., 2011). Furthermore, expression of mutant TDP-43 has been shown to activate pro-inflammatory microglial responses more strongly than wildtype TDP-43 (Zhao et al., 2015). Therefore, microglial dysfunction may be common to different genetic causes of ALS.

Like astrocytes, it is thought that microglia release factors that contribute to motor neuron death in ALS. These factors include nitric oxide (Frakes et al., 2014), pro-inflammatory cytokines such as TNF-α and IL-1α (Chiu et al., 2013) and ROS (Marden et al., 2007; Harraz et al., 2008). Release of factors from microglia can direct astrocytic pro-inflammatory responses, which can have subsequent detrimental effects on motor neurons. A combination of TNF-α, IL-1α and C1q released from microglia is able to cause a switch in astrocytes towards a neurotoxic phenotype (Liddelow et al., 2017). Conversely, astrocytes are able to influence microglial inflammatory responses. For example, TGF-β released from astrocytes reduces microglial inflammatory responses (Endo et al., 2015). Therefore, microglial-astroglial crosstalk may be important in non-cell autonomous mechanisms of motor neuron death in ALS.

1.3.7.3 Oligodendrocytes

Oligodendrocytes provide support to neurons by ensheathing axons with myelin, aiding the transmission of action potentials. Oligodendrocytes are lost in mSOD1 models and in ALS post-mortem tissue, and progenitor cells that attempt to replace these cells are unable to sufficiently mature and remyelinate neurons (Kang et al., 2013; Philips et al., 2013). Furthermore, removal of mSOD1 from oligodendrocytes results in delayed disease onset and extended survival in $SOD1^{G37R}$ mice, suggesting that oligodendrocytes are important in the pathogenesis of mSOD1 disease (Kang et al., 2013). Oligodendrocytes also function to provide motor neurons with metabolic support. Lactate transporter MCT1, which is enriched in oligodendrocytes, is downregulated in mSOD1 models and in the motor cortex of ALS patients (Lee et al., 2012). Decreased lactate production has been observed in mSOD1 oligodendrocytes and motor neuron death induced by oligodendrocyte conditioned media is rescued by the addition of lactate (Ferraiuolo et al., 2016). Therefore, altered metabolic support of oligodendrocytes contributes towards motor neuron death in ALS.

1.4 Aims

It is clear that several pathological processes contribute towards the death of motor neurons in ALS. Among these, the ability of motor neurons and glia to activate stress responsive pathways may become dysfunctional in ALS, contributing to motor neuron death. The aim of this Thesis is to explore the roles of different stress responses in models of ALS.

The specific aims of this Thesis are to:

1) Determine whether there are any differences in the inflammatory responses or the HSR in glia from different regions of the CNS.
2) Assess the inflammatory responses and the HSR in glia from mSOD1 models of ALS.
3) Investigate whether mitochondrial heat shock proteins are protective in models of ALS.

Chapter 2: General methods

Reagents were purchased from Sigma-Aldrich or Thermo Fisher Scientific unless otherwise stated.

2.1 Breeding and maintenance of SOD1^{G93A} and wildtype mice

All experiments were performed in accordance with the Animals (Scientific Procedures) Act 1986 following approval from the Institute of Neurology Ethical Review Committee. Mice were housed in individually ventilated cages on a 12 hour light/dark cycle with food and water made available ad libitum.

Transgenic SOD1^{G93A} (B6SJL-Tg(SOD1*G93A) 1Gur/J) mice, overexpressing human mutant SOD1^{G93A} (glycine to alanine substitution at position 93) protein. This mouse line, which has a high copy number (25 times) of the transgene in addition to endogenous mouse SOD1, was originally obtained from Jackson Laboratories (USA) along with wildtype (WT) littermates. Mice were repeatedly backcrossed and then maintained by breeding heterozygous male carriers with female (C57BL/6×SJL) F1 hybrids. Experiments performed by Jing Yip, a previous PhD student in the Greensmith lab, also utilised SOD1^{WT} (TgN(SOD1)2Gur) mice, overexpressing human wildtype SOD1 mice at similar levels to SOD1^{G93A} mice.

2.2 PCR genotyping

Tail biopsies from SOD1^{G93A} mice and WT littermates were genotyped for expression of the human SOD1^{G93A} by PCR amplification of genomic DNA extracted from either ear or tail biopsies. Biopsies were digested in rapid digestion buffer (10 mM Tris-HCl pH 8.3, 50 mM KCl, 0.1 mg/ml gelatin, 0.45% NP40, 0.45% Tween 20) containing 20 mg/ml proteinase K first at 55°C for 15 minutes and then 95°C for 10 minutes to stop the reaction.

DNA was then amplified using primer pairs for interleukin 2 (IL-2): forward (CTA GGC CAC AGA ATT GAA AGA TCT), reverse (GTA GGT GGA AAT TCT AGC ATC ATC) and SOD1: forward (CAT CAG CCC TAA TCC ATC TGA) and reverse (CGC GAC TAA CAA TCA AAG TGA). 0.25 µl of each primer were added to a reaction mix containing 2 µl DNA, 15 µl Megamix Blue (Taq polymerase in a reaction buffer (2.75 mM MgCl2, 220 µM dNTPs, blue agarose loading dye and stabilizer, Microzone Ltd)) and 9 µl H_2O. PCR cycling conditions were as follows:

95 °C for 30 seconds, 60 °C for 30 seconds, 72 °C for 45 seconds repeated 35 times and finally 72 °C for 2 minutes. PCR products were analysed by electrophoresis (100 V for 30 minutes) in Tris/Borate/ethylenediaminetetraacetic acid (EDTA) buffer (90 mM Tris-HCl, 90 mM boric acid, 2 mM EDTA, pH 8.0) using a 2% agarose gel stained with GelRed and visualised using a ChemiDoc imager (Biorad). Presence of a lower band at 236bp was indicative of $SOD1^{G93A}$ expression.

2.3 Primary mixed cortical and spinal cord derived glial cultures

Primary mixed glial cultures were obtained from $SOD1^{G93A}$ and WT littermate mice at postnatal day 2-3 based on a previously described protocol (McCarthy and de Vellis, 1980). Mice were humanely killed by decapitation and spinal cords and cortices were dissected and meninges removed. Tissue was dissociated in 0.025% trypsin, 0.017% (w/v) DNase I, 0.3% (w/v) bovine serum albumin (BSA), 1% penicillin/streptomycin in Hanks balanced salt solution (HBSS) for 10 minutes at 37°C. Foetal bovine serum (FBS) was used to inhibit the proteolytic reaction. Tissue was triturated 10-15 times and then filtered through a 100 µm nylon strainer before being centrifuged at 1000 *g* for 5 minutes. The resulting cell pellet was resuspended in feeding media containing 15% FBS, 1% penicillin/streptomycin in Dulbecco's Modified Eagle Medium (DMEM)+Glutamax and plated on 10 µg/ml poly-D-lysine coated 12 well plates or glass coverslips in 24 well plates in feeding media. Tissue was plated at a ratio of 1 cortex in 18 wells of a 24 well plate or 1 spinal cord in 10 wells of a 24 well plate. Cells were maintained under standard culture conditions (37°C and 5% CO_2) and media was replenished every 3 days.

2.3.1 Treatment of primary mixed glial cultures

After being maintained for 12 days *in vitro* (DIV 12), primary cortical and spinal cord mixed glial cultures from WT and $SOD1^{G93A}$ mice were treated with different concentrations of the inflammatory inducers dissolved in phosphate buffered saline (PBS; Oxiod): 10-200 ng/ml tumour necrosis factor alpha (TNF-α) (Cell Signaling), 100 ng/ml interleukin 1 alpha (IL-1α), 1000 ng/ml Complement component 1q (C1q) or 2-100 µg/ml LPS (all Sigma-Aldrich) or exposed to heat stress at 42°C for 30 minutes. In instances where cultures were treated with both LPS and heat shocked, cultures were heat shocked at 42°C for 30 minutes,

immediately treated with LPS and then incubated at 37°C for 24 hours. Cells were subsequently processed for immunoblotting, immunostaining, qPCR or fluorescence-activated cell sorting (FACS) analysis 24 hours later.

2.4 Induced pluripotent stem cell (iPSC) culture

Human induced pluripotent stem cells (iPSCs) consisted of 4 control lines including an isogenic control ($SOD1^{D90D}$) line and 2 ALS mutant $SOD1^{D90A}$ lines. iPSCs were differentiated into astrocytes patterned to the ventral spinal cord based on (Hall et al., 2017) or the cortex, adapting a protocol to obtain cortical neurons from iPSCs (Shi et al., 2012).

2.4.1 Differentiation of human iPSCs to astrocytes

iPSCs were maintained on Geltrex coated 6-well plates in Essential 8 media (Gibco) containing Essential 8 substrate. iPSCs were thawed with media containing 10 µM rho-associated protein kinase (ROCK) inhibitor Y-2763 (StemCell Technologies) to improve cell survival. iPSCs were split using 0.5 mM EDTA at least twice to recover from freezing before inductions were started.

Once iPSCs had reached 100% confluency cells were changed into N2B27 media (1x N2 supplement, 1x B-27 supplement, 1x glutamax, 0.5% Penicillin-Streptomycin, 0.5% non-essential amino acids, 5 µg/ml insulin, 100 µM β-mercaptoethanol in DMEM:F12 and neurobasal media 1:1). To direct iPSCs to a cortical fate patterning media was supplemented with 1µM Dorsamorphin and 10µM SB431542 (both StemCell Technologies) for 10 days followed by 8 days in N2B27. To direct iPSCs to a ventral spinal cord fate patterning media was supplemented with 1µM Dorsamorphin, 2µM SB431542 and 3µM CHIR9902 for 8 days, followed by 0.5µM retinoic acid and 1µM Purmorphamine (both StemCell Technologies) for 6 days and then 0.1µM Purmorphamine for 4 days. iPSCs were split using 10 mg/ml dispase and replated in media containing 10 µM Y-2763. Dispase splits were performed at days 10 and 16 for cortical patterned cells and days 5 and 10 for spinal patterned cells. Cells were fed with fresh media every day.

18 days after the start of iPSC inductions, both cortical and spinal cord patterned neural precursor cells (NPCs) were cycled in N2B27 media containing 10 ng/ml fibroblast growth factor 2 (FGF2) for 60 days. Cells were split at least once a

week and maintained at less than 90% confluency. Cells were then terminally differentiated into astrocytes using N2B27 media supplemented with 10 ng/ml bone morphogenetic protein 4 (BMP4) and 20 ng/ml leukemia inhibitory factor (LIF) for 3 weeks.

2.4.2 Treatment of iPSC-derived astrocytes

iPSC-derived astrocytes were treated with inflammatory inducers: 80 µg/ml LPS, a combination of 100 ng/ml TNF-α, 100 ng/ml IL-1α and 1 µg/ml C1q or exposed to heat stress of 42-43°C for 30 minutes to 2 hours and then incubated at 37°C for 4-120 hours.

2.5 qPCR measurements

Glial cultures or iPSC-derived NPCs or astrocytes were lysed in 1 ml Trizol. 0.2 ml of chloroform was added and lysates were centrifuged at 12,000 *g* for 15 minutes. Supernatant was extracted and 500 µl isopropanol and 2 µl pellet paint were added to precipitate RNA. Samples were centrifuged again and the pellet resuspended in 1 ml 70% ethanol. Samples were then centrifuged at 7500 *g* for 5 minutes. Pellets were resuspended in 15 µl of RNAse free water and RNA content was measured using a Nanodrop. RNA was stored at -80 °C.

750 ng of RNA was made up to 10 µl and added to 1 µl of hexamers, 1 µl 10 mM dNTPs and 1 µl 50 µM olig dTs and incubated at 65°C for 5 minutes. Then this mix was added to 4 µl RT buffer, 1 µl 0.1 M DTT, 1 µl RnaseOut RNAse inhibitor and 1 µl SuperScript IV. Reverse transcription to obtain cDNA was performed by heating the samples to 37°C for 10 minutes, 50°C for 80 minutes and then 72°C for 15 minutes. cDNA was stored at -80°C until needed.

qPCR was performed using 1 µl cDNA diluted 1:10, 0.3 µM primers (Table. 2.1), 4 µl distilled water and 10 µl Sybergreen reaction mix using the Applied Biosystems 7500 Real-Time PCR System (Thermo Fisher Scientific). cT values were taken and normalised to a GAPDH loading control using the comparative threshold cycle (ddCt) method.

Gene	Species	Forward	Reverse
otx2	Mouse	GAGAGCGGAACCTTCCTCAG	AGCTATCAAAGTAGAGGTGGCG
nkx6.1	Mouse	GACAGCAAATCTTCGCCCTG	ACCAGACCTTGACCTGACTC
gapdh	Mouse	GGAGAGTGTTTCCTCGTCCC	ATGAAGGGGTCGTTGATGGC
hspa1a	Mouse	GCGAGGCTGACAAGAAGAAG	GGCCTCTAATCCACCTCCTC
OTX2	Human	TAAAAATTGCTAGAGCAGCC	CATGGGAGGTTAGAAAAAGTC
NKX6.1	Human	GTTTGGCCTATTCGTTGGGGA	GTGCTTCTTCCTCCACTTGGT
HOXA4	Human	ACGCTCTGTTTGTCTGAGCGCC	AGAGGCCGAGGCCGAATTGGA
FOXG1	Human	AGGAGGGCGAGAAGAAGAAC	TCACGAAGCACTTGTTGAGG
GAPDH	Human	ATGACATCAAGAAGGTGGTG	CATACCAGGAAATGAGCTTG

Table 2.1. Primers used for qPCR.

2.6 Immunofluorescence

For immunofluorescence, cells were fixed in 4% paraformaldehyde (PFA) in PBS for 10 minutes and then washed with PBS. Brains and spinal cords of 90 day old adult female WT and $SOD1^{G93A}$ mice were fixed in 4% PFA for 1 hour at room temperature and then added to a 30% sucrose solution in PBS overnight at 4°C. Tissue was then mounted and 20 µm sections were cut using a cryostat and stored at -20°C. Antigen retrieval was performed on sections when required using 10 mM sodium citrate buffer heated to 95°C and added to the slides for 20 minutes. For immunofluorescence staining with the ALDH1L1 antibody, cells were first immersed in ice-cold methanol for 10 minutes.

Sections or cells were then blocked for 1 hour at room temperature in blocking solution consisting of 5% normal donkey or goat serum (Vector Laboratories) and 0.1% Triton X-100 in PBS. Primary antibodies (Table. 2.2) were then added in blocking solution overnight at 4°C or for 1 hour at room temperature. The following day, sections or cells were washed thrice with PBS and then incubated with HRP-conjugated secondary antibodies (Table. 2.2) in blocking solution for 1 hour at room temperature. After another set of three PBS washes, a 1 mg/ml DAPI stain was applied in PBS (1:2000) to label nuclei and then sections or cells were mounted with Mowiol mounting media and stored at 4°C.

2.6.1 Image analysis

Imaging was performed using the 40x or 63x objectives of confocal microscopes (Zeiss LSM 710 or Zeiss LSM 510) or the Opera Phenix Highthroughput imaging system (PerkinElmer) and analysed using ZEN LE Digital Imaging 2009, ImageJ or Columbus software (PerkinElmer). Analysis of images from the Opera Phenix Highthroughput imaging system was performed using the automated Columbus software, while analysis of confocal imaging was performed manually using ImageJ. Where manual quantification of immunofluorescence staining was performed, an experimenter was blinded to the treatment for each culture selecting at least five images per condition.

2.7 Western blotting

Western blots were carried out on either mouse tissues or homogenates of cultured cells. Brains and spinal cords of 40, 70, 75, 105 and 110 day old adult female WT and $SOD1^{G93A}$ mice were dissected and snap frozen in liquid nitrogen. Tissue was lysed in 30% w/v radioimmunoprecipitation (RIPA) buffer (50 mM Tris pH 7.5, 150 mM NaCl, 1% NP40, 0.5% sodium deoxycholate, 1 mM egtazic acid (EGTA), 1 mM EDTA and protease inhibitors and homogenised using an electronic homogeniser tool until an even homogenate was obtained. Samples were centrifuged at 15,000 *g* for 20 minutes and the supernatant was stored at -80°C. For an estimation of protein concentration, samples were diluted 1:10-30 and protein concentration was measured according to manufacturer's instructions (Biorad DC protein assay) with absorbance measured using a spectrophotometer at 750 nm.

Cells were washed with PBS and then lysed on ice with RIPA buffer. Samples were subsequently diluted to equal concentrations in RIPA buffer and then added 4:1 in sample buffer (Laemmli buffer, 10% β-mercaptoethanol) and heated at 95°C for 10 minutes to denature proteins. Samples were stored at -80°C until needed.

Protein samples were loaded onto precast 4-12% NuPage Bis-Tris gels and run in NuPage MES SDS running buffer at 160 V for 1 hour. Protein was then transferred onto nitrocellulose membranes (Amersham Biosciences) for 1 hour at 100 V in transfer buffer (National Diagnostics) containing 20% methanol. A Ponceau S stain was used to confirm efficient protein transfer before membranes

were blocked in 5% BSA in TBS 0.1% Tween 20 (TBST) for 1 hour. Membranes were then probed with primary antibodies (Table. 2.2) diluted in blocking solution on a shaker overnight at 4°C.

The following day membranes were washed in TBST and then incubated with secondary antibody (Table. 2.2) for 2 hours at room temperature. After another set of TBST washes, proteins were visualised using Luminata Crescendo chemiluminescence reagent. Images were taken using a Biorad imaging system and bands were quantified using ImageLab software (Biorad). Relative changes in protein expression were measured and normalised to housekeeping protein β-actin, α-tubulin or GAPDH.

2.8 Antibodies

Antibody	Species	Supplier	Dilution (Application)
Primary antibodies			
ALDH1L1	Rabbit	Abcam ab87117	1:100 (IF)
α-tubulin	Mouse	Thermo Fisher Scientific A11126	1:1000 (WB)
β-actin	Mouse	Abcam ab8226	1:40,000 (WB)
CD11b	Rat	Tonbo 25-0112	1:1000 (FACS)
EAAT2	Rabbit	Abcam ab41621	1:100 (IF)
F4/80	Rat	Abcam ab6640	1:100 (IF)
GAPDH	Mouse	Millipore AB2302	1:5000 (WB)
GFAP	Rabbit	Abcam ab7260	1:1000 (IF), 1:10,000 (WB)
GFAP	Chicken	Abcam ab4674	1:5000 (IF)
GFAP	Mouse	Sigma-Aldrich C9205	1:1000 (FACS)
GFP	Chicken	Aves Labs GFP-1010	1:1000 (IF), 1:10,000 (WB)
HA	Rat	Sigma-Aldrich 3F10	1:500 (IF)
Hsp27	Goat	SantaCruz M20 sc-1049	1:300 (IF), 1:3000 (WB)
Hsp60	Goat	SantaCruz N20 sc-1052	1:100 (IF), 1:1000 (WB)
Hsp70	Mouse	SantaCruz W27 sc-24	1:1000 (WB)
Hsp90	Rabbit	SantaCruz H114 sc-7947	1:1000 (WB)
iNOS	Rabbit	Abcam ab178945	1:100 (IF), 1:1000 (WB)
NF-κB	Rabbit	Cell Signaling D14E12	1:400 (IF)

p-NF-κB	Rabbit	Cell Signaling 93H1	1:1000 (WB)
NKX6.1	Goat	R&D Systems AF5857	1:500 (IF)
OLIG2	Rabbit	Abcam ab136253	1:100 (IF)
OTX2	Goat	R&D Systems AF1979	1:500 (IF)
OXPHOS	Mouse	Abcam ab110413	1:500 (WB)
TOM20	Mouse	Abcam ab56783	1:500 (IF)
TRAP1	Rabbit	St. John STJ25957	1:100 (IF), 1:1000 (WB)
TUJ1	Mouse	BioLegend 801202	1:500 (IF)
TUJ1	Rabbit	BioLegend 802001	1:500 (IF)
Secondary antibodies (fluorophore conjugated)			
All species	N/A	Invitrogen	1:1000 (IF)
Secondary antibodies (HRP-conjugated)			
Mouse IgG	Rabbit	Dako P0260	1:5000 (WB)
Rabbit IgG	Swine	Dako P0217	1:5000 (WB)
Goat IgG	Rabbit	Dako P0449	1:5000 (WB)

Table 2.2. Antibodies used for immunofluorescence (IF), western blotting (WB) and fluorescence-activated cell sorting (FACS).

2.9 Statistical analysis

Results are presented as the mean ± SEM. Differences between the means were assessed by t-test, two-way or one-way ANOVA with Tukey or Bonferroni post-hoc comparisons tests or Mann-Whitney U test or a Kruskal-Wallis test with post-hoc Dunn's tests when appropriate using GraphPad Prism Version 7.0 software. Where data sets were too small to display a Gaussian distribution, or data did not pass a Shapiro-Wilk normality test, a non-parametric test was used or a statistical test was not performed. P-values are as indicated or marked as either *≤0.05, **≤0.01, ***≤0.001 or ****≤0.0001.

Chapter 3: Regional differences in glial inflammatory responses: implications for ALS pathogenesis

3.1 Introduction

3.1.1 Glial heterogeneity and implications for ALS

Although once thought of as a homogenous population, it is now clear that glia from different regions of the CNS differ greatly in their morphology (Oberheim et al., 2012; Stowell et al., 2018), protein expression, physiology and function (Bachoo et al., 2004; Bayraktar et al., 2015; Khakh and Sofroniew, 2015; Farmer and Murai, 2017). Regional differences in glia are likely to reflect the fine-tuned support these cells provide to functionally diverse neuronal populations. Glial heterogeneity therefore may have important implications for neurological diseases, such as ALS, where glia play a role in neuronal death.

Several studies have shown that astrocytes from different regions of the CNS display distinct markers and occupy specific domains (Hochstim et al., 2008; Tsai et al., 2012; Martin et al., 2015; Chai et al., 2017). Specification of astrocytes to these regional domains is thought to be the result of a combination of spatiotemporal patterning, determined by certain transcription factors during development and local cues from neurons (Ben Haim and Rowitch, 2017). Interestingly, following focal stab injury in adult mice, spinal cord astrocytes from regionally different areas do not migrate to occupy the injury site in adjacent regions, suggesting that astrocytes strictly maintain their regional position (Tsai et al., 2012).

Although not from the neuroepithelium, microglia have also been found to exist as different subpopulations within the CNS (Grabert et al., 2016; Soreq et al., 2017; Stowell et al., 2018). By comparing microglia and macrophages transplanted into the mouse CNS, it has been suggested that microglial identity is also determined by a combination of their origin and signals from the CNS microenvironment (Bennett et al., 2018).

Regional differences in glia have important implications for neuronal function and survival. Different neuronal populations have been shown to develop better when co-cultured with astrocytes from the same region (Leroux and Reh, 1994; Song et al., 2002; Morel et al., 2017). Differential protein expression of regionally

distinct astrocytes resulting in a differential level of support to neurons may underlie these differences. For example, spinal cord astrocytes have been shown to express up to 10-fold less of the glutamate transporter EAAT2 than hippocampal astrocytes (Regan et al., 2007), and therefore have a reduced ability to uptake glutamate. Furthermore, ventral spinal cord astrocytes express higher levels of Sem3a than dorsal astrocytes (Molofsky et al., 2014). Knockout of *Sem3a* specifically in astrocytes was detrimental to motor neuron survival, suggesting that enrichment of Sem3a specifically in ventral horn astrocytes is critical for motor neuron survival (Molofsky et al., 2014). In addition, the potassium channel Kir4.1 was enriched in astrocytes that surround fast firing alpha motor neurons in the ventral horn of the spinal cord (Kelley et al., 2018). Kir4.1 is likely to have an important influence on the development of fast firing alpha motor neuron size as knockout of the Kir4.1 encoding gene *KCNJ10* in astrocytes results in a reduction in cell size and aberrant electrophysiological properties, specifically in fast firing alpha motor neurons.

Glia from different regions of the CNS also respond differently to inflammatory stimuli. Both astrocytes and microglia are able to undergo widespread changes in gene expression in response to cues from their microenvironment in response to injury or disease (Zamanian et al., 2012; Grabert et al., 2016). This dynamic and likely transient change in gene expression has been termed reactivity, which can have either beneficial or detrimental effects on neurons (Anderson et al., 2016; Hara et al., 2017; Liddelow et al., 2017). Interestingly, glia from the spinal cord have been shown to exhibit a larger inflammatory response than cortical glia following a mechanical lesion (Schnell et al., 1999; Batchelor et al., 2008). Furthermore, microglia from the cerebellum display a stronger upregulation of pro-inflammatory genes in response to LPS than other brain regions (Grabert et al., 2016). Therefore, in addition to their intrinsic regionally determined differences, glia from different regions may also differ in the magnitude of their response to inflammatory stimuli and/or may have different thresholds for the activation of inflammatory pathways.

Regional differences in glial reactivity may play important roles in neurodegenerative diseases such as ALS. For example, neuroinflammatory damage occurs earlier and is more prominent in the lumbar spinal cord when compared with the brain in $SOD1^{G93A}$ mice (Leichsenring et al., 2006; Chiu et al.,

2008). Furthermore, spinal cord microglia, but not cortical microglia, from late-stage SOD1^{G93A} mice, have been reported to display blunted inflammatory responses to LPS (Nikodemova et al., 2014). Transcriptomic microarray analysis of astrocytes from the cortex and spinal cord of symptomatic and late stage SOD1^{G93A} mice has revealed that many genes are differentially expressed, both in terms of genotype between SOD1^{G93A} and WT mice and regionally between the cortex and spinal cord of SOD1^{G93A} mice, although a fully age-matched study has yet to be performed (Miller et al., 2018).

Interestingly, it seems that unlike motor neurons, astrocytes and microglia undergo large changes in gene expression during ageing, becoming more reactive and partially losing their regional identity (Soreq et al., 2017; Clarke et al., 2018). This may have important implications for ALS, where age is a key risk factor (Niccoli et al., 2017). Therefore, differences in the threshold and magnitude of glial inflammatory responses may contribute to the specific pattern of motor neuron death in ALS.

3.1.2 The nitric oxide pathway in motor neuron death in ALS

Although both astrocytes and microglia have been demonstrated to become dysfunctional and contribute to motor neuron death in ALS, the precise mechanism that underlies this toxicity remains poorly understood. As discussed previously, there is evidence for both the toxic release of factors and the loss of supportive functions of astrocytes and microglia being detrimental to motor neuron survival.

Among several toxic factors that are implicated in non-cell autonomous motor neuron death is the small molecule, nitric oxide (NO). NO has several physiological roles such as maintaining motor neuron survival through cGMP synthesis, regulating blood flow as a vasodilator and acting as a retrograde signalling molecule, modulating neuronal transmission and synaptic plasticity (Calabrese et al., 2007). However, production of NO can also be pathological through its reaction with superoxide ($O_2^{\cdot -}$) to produce the highly toxic molecule peroxynitrite ($ONOO^-$), resulting in mitochondrial dysfunction and neuronal death (Brookes et al., 1999; Bal-Price and Brown, 2001; Cassina et al., 2008). Several studies have shown that excessive NO production promotes motor neuron death *in vitro* (Cassina et al., 2002; Pehar et al., 2004; Zhao et al., 2004). Moreover,

mSOD1 motor neurons are more susceptible to death induced by NO (Raoul et al., 2002).

NO can be produced by several enzymes as a product of the oxidisation of arginine to citrulline. Neuronal nitric oxide synthase (nNOS) and endothelial nitric oxide synthase (eNOS) are both calcium-dependent enzymes that are constitutively expressed, primarily in neurons and endothelial cells, and play important roles in synaptic plasticity and vasodilation (Zhou and Zhu, 2009). Inducible nitric oxide synthase (iNOS) however, is a calcium-independent enzyme that is constantly in an active state producing NO, which is upregulated following activation of pro-inflammatory pathways primarily in immune cells (Forstermann and Sessa, 2012).

iNOS is upregulated in response to immune activation in ALS models. Increased iNOS mRNA expression and activity has been observed in the spinal cords of early symptomatic $SOD1^{G93A}$ mice (Almer et al., 1999; Lee et al., 2009). Furthermore, $SOD1^{G93A}$ mixed glial cultures have been reported to express more iNOS and produce more NO in response to a combination of TNF-α and IFN-γ (Hensley et al., 2006), while human embryonic stem cell $SOD1^{G37R}$ astrocytes have been shown to express more iNOS and produce more NO under basal conditions (Marchetto et al., 2008). In addition, $SOD1^{G93A}$ microglial cultures have been shown to produce more NO than WT microglia both under basal conditions and following LPS treatment (Beers et al., 2006). Knockdown of iNOS gene *NOS2*, or treatment with the iNOS specific inhibitor, 1400W, significantly extends the lifespan of $SOD1^{G93A}$ mice (Martin et al., 2007; Chen et al., 2010), indicating that NO production by iNOS contributes towards disease progression in $SOD1^{G93A}$ mice.

The NF-κB complex is a master regulator of inflammatory signalling, which is able to induce iNOS expression when activated (Xie et al., 1994) (Diagram 3.1). Upon activation, the NF-κB complex is released from inhibitory IκB proteins following phosphorylation of these inhibitory proteins by IκB kinases (IKK) (Zhang et al., 2017). NF-κB subunits p65 and p50 then translocate to the nucleus where they increase the transcription of many inflammatory mediators, including iNOS.

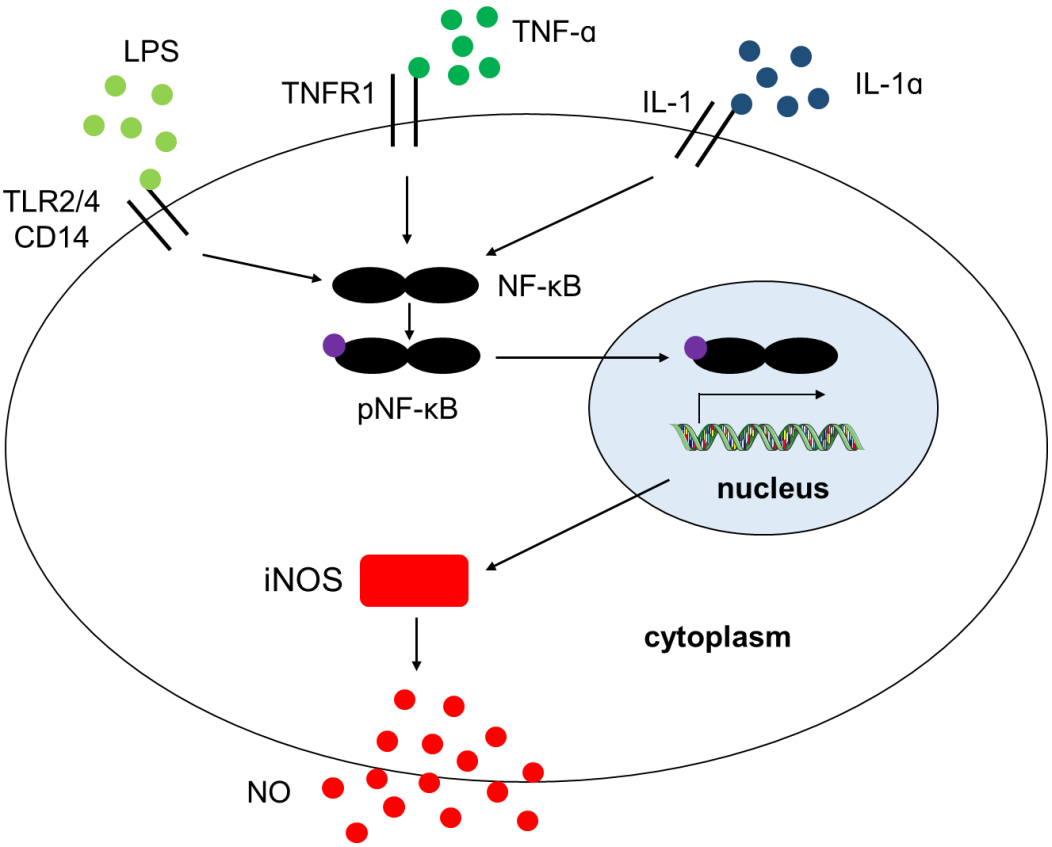

Diagram 3.1. NO-iNOS-NF-κB signalling pathway. Simplified diagram illustrating the pathways involved in the activation of NO production by iNOS.

Activation of NF-κB has been shown to occur in mSOD1 models (Casciati et al., 2002; Frakes et al., 2014) and ALS patient tissue (Migheli et al., 1997; Sako et al., 2012). However, the exact role of NF-κB in ALS remains uncertain. Both NF-κB activation (Ikiz et al., 2015) and deficiency have been reported to result in motor neuron death in ALS (Sulejczak et al., 2015). Previous reports have implicated microglial NF-κB activation as important in modulating disease progression in mSOD1 models (Frakes et al., 2014), with astrocytic activation of NF-κB having no role in disease (Crosio et al., 2011). However, a recent study has suggested that astrocytic NF-κB signalling plays a more subtle and complicated role in mSOD1 models, whereby activation of NF-κB is beneficial at early disease stages but becomes detrimental at the later stages of disease (Ouali Alami et al., 2018). Therefore, both microglial and astrocytic NF-κB signalling are likely to be important in non-cell autonomous motor neuron death in ALS.

3.1.3 Glial models of ALS

Mouse models of ALS have been crucial in understanding the contribution of glia to non-cell autonomous mechanisms of motor neuron death in ALS. By restricting or deleting expression of mSOD1 in specific cell types, the importance of glia in the disease progression of mSOD1 mice has been elucidated (Gong et al., 2000; Boillee et al., 2006; Yamanaka et al., 2008). The advantage of *in vivo* mouse models of ALS is that the effect of ALS-causing mutations can be determined *in situ*, replicating the complex interactions of different cell types as the disease progresses. This enables longitudional sampling of tissue at different stages of disease. However, this model system is not optimal for the dissection of biochemical pathways as it is more difficult to make causative conclusions.

This disadvantage can be addressed with *in vitro* primary cultures from mice carrying ALS-causing mutations. Primary glial cultures, typically obtained from post-natal mice, have been a useful model for studying different pathways involved in ALS pathomechanisms (Nagai et al., 2007; Bilsland et al., 2008; Ferraiuolo et al., 2011). This reductive model can be useful for the study of glia in the absence of other cell types, providing a platform for the study of glial responses to different stressors or mediators of inflammation.

3.1.3.1 iPSC-derived astrocyte models of ALS

It has been suggested that human astrocytes are far more complex than their murine counterparts, and this complexity is partly responsible for more integrated neural circuits and higher cognitive functions (Oberheim et al., 2012). These differences are reflected at the level of the transcriptome, with over 600 genes enriched in human astrocytes compared to mouse astrocytes (Zhang et al., 2016).

Advances in induced pluripotent stem cell (iPSC) technology have enabled the study of highly enriched populations of human astrocytes from ALS patients (Tyzack et al., 2016). The molecular identity of neuralised iPSCs can be directed to different regions of the CNS by the application of specific morphogens before terminal differentiation into astrocytes (Krencik et al., 2011). Gradients of these morphogens along the rostrocaudal and dorsoventral axes established during development can be recapitulated *in vitro* to obtain neural precursor cell (NPC) populations from different regions of the CNS (Patani, 2016). Cervical and

brachial ventral spinal cord progenitors can be obtained using a combination of inhibition of GSK3β signalling to prime cells to caudalising and ventralising cues retinoic acid and Sonic hedgehog, respectively (Patani et al., 2011; Hall et al., 2017). Meanwhile, rostral NPCs can be obtained from neuralisation and the absence of patterning factors (Li et al., 2009; Shi et al., 2012).

By promoting gliogenesis and inhibiting neurogensis, NPCs patterned to different regions can be converted to glial precursor cells (GPCs). A crucial factor governing this gliogenic switch is Notch signalling, which promotes gliogenesis by activating STAT signalling while simultaneously inhibiting neurogenesis by inhibiting proneural basic loop helix loop helix factors (Morrison et al., 2000; Kamakura et al., 2004). Over time in culture, NPCs spontaneously lose their neurogenic potential and become more gliogenic (Krencik et al., 2011). GPCs can then be terminally differentiated into astrocytes through further promotion of STAT signalling by bone morphogenetic proteins (BMPs) and members of the interleukin-6 family including leukocyte inhibitory factor (LIF) (Nakashima et al., 1999; Yanagisawa et al., 2001).

While only a developmental model, iPSC-derived astrocytes from SOD1-ALS patients have been shown to share several pathological hallmarks with mouse astrocyte ALS models and post-mortem ALS tissue. Like primary mouse astrocytes, human iPSC-derived astrocytes are able to become reactive when stimulated with cytokines such as IL-6 and TNF-α (Perriot et al., 2018). Furthermore, astrocytes from $SOD1^{D90A}$ iPSCs differentially express thousands of genes (Tyzack et al., 2017). Transplantation of these astrocytes into the spinal cords of mice results in motor neuron death and motor deficits (Chen et al., 2015a). While the effects of mSOD1 iPSC-derived astrocytes on motor neurons in co-culture have not been performed, astrocytes obtained from the transdifferentiation of $SOD1^{A4V}$ patient fibroblasts are toxic to motor neurons in co-culture (Meyer et al., 2014). Therefore, mSOD1 iPSC-derived astrocytes at least partially recapitulate findings from ALS post-mortem tissue and mSOD1 mouse models.

3.1.4 Aims

Since regional differences in glial inflammatory responses may play a role in ALS, the NO-iNOS-NF-κB inflammatory responses of primary glial cultures from the cortex and spinal cord of WT and $SOD1^{G93A}$ mice were assessed in terms of their responses to different inflammatory inducers. In order to verify findings in human cells, $SOD1^{D90A}$ and control human iPSC-derived astrocytes patterned to the cortex and spinal cord were generated and exposed to different inflammatory inducers in order to explore the NO-iNOS-NF-κB inflammatory pathway.

The specific aims of this Chapter are to:

1) Assess whether regional differences in the NO-iNOS-NF-κB inflammatory response exist between cortical and spinal cord glia of WT mice;
2) Determine whether any regional differences in the NO-iNOS-NF-κB inflammatory response are affected by ALS-causing mSOD1 mutations.

Note: Some of the experiments described in this Chapter were undertaken in collaboration with Jing Yip and Rebecca San Gil, PhD students in the Greensmith lab. The experiments undertaken by these colleagues are indicated in the relevant figure legends.

3.2 Methods

For a full description of the methods applied in this Chapter, see Chapter 2: General methods. Methods specifically used in this Chapter are described below.

3.2.1 NO production measurements

Release of NO was indirectly measured using a Griess assay. This assay measures the stable final product of the NO pathway, nitrite (NO_2^-). Nitrite reacts with the Griess reagent to form an azo dye agent that gives off fluorescence, which can be detected at 540nm. Media from cultures was collected 24 hours after treatments and mixed in a 1:1 ratio with modified Griess reagent. Sodium nitrite standards ($NaNO_2$) were prepared in feeding media (see 2.3) and absorbances were measured using a spectrophotometer at 540 nm. For primary glial cultures, total protein levels were then measured (Biorad DC protein assay) using a spectrophotometer at 750 nm and nitrite levels were normalised to protein concentration.

3.2.2 Fluorescence-activated cell sorting analysis

Fluorescence-activated cell sorting (FACS) analysis was carried out by Rebecca San Gil, a visiting PhD student. Primary glial cultures were detached using 0.025% trypsin and washed with PBS. Cells were incubated with primary antibodies GFAP and CD11b (see 2.8) in 3% BSA in PBS overnight at 4°C. Cells were then centrifuged at 400g for 5 minutes and washed with PBS before being analysed using an LSRII Flow Cytometer (BD Biosciences). The percentage of cells above an arbitrary threshold were designated as astrocytes or microglia.

3.2.3 Isolated microglia

Glial cultures were tapped vigorously to detach microglia and then replated on poly-D-lysine coated plates. Immunofluorescence was performed to ensure that an enriched microglial culture had been obtained. Cells were treated with 80 µg/ml LPS 24 hours later and then assessed by Griess assay 24 hours after.

3.3 Results

3.3.1 Characterisation of glial cultures from the cortex and spinal cord

In order to compare regional differences in glial inflammatory responses, primary mixed glial cultures were obtained from the cortex and spinal cord of post-natal day 2-3 wildtype (WT) mice. qPCR of regional markers orthodenticle homeobox 2 (OTX2) (forebrain/midbrain) and NK6 homeobox 1 (NKX6.1) (ventral spinal cord) revealed that glial cultures from the cortex and spinal cord of WT mice maintained their regional identity at DIV 12 (Fig. 3.1).

The cellular compositions of cortical and spinal cord glial cultures were then characterised. This was performed to ensure that any differences found between the inflammatory responses of cortical and spinal cord glial cultures were due to differences in the responses of glia, rather than a difference in the composition of cells in each culture from these two regions.

Glial cultures from the cortex and spinal cord were found to contain similar numbers of astrocytes and microglia, identified by immunofluorescence and FACS analysis (Fig. 3.2-3). The majority of cells in glial cultures from the cortex and the spinal cord were identified as astrocytes (~70-90%), using the astrocyte specific markers GFAP, ALDH1L1 and GLT-1 (Fig. 3.2 A-C, F). Meanwhile microglia accounted for ~10% of cells in both cortical and spinal cord glial cultures, identified by the microglial marker, F4/80 (Fig. 3.2 D, F). GFAP negative, OLIG2 positive cells identifying neurons, oligodendrocyte precursor cells or oligodendrocytes accounted for only ~2% cells in both cortical and spinal cord glial cultures (Fig. 3.2 E, F). FACS analysis for GFAP and CD11b further validated the similar proportion of astrocytes and microglia in glial cultures from the cortex and spinal cord (Fig. 3.3).

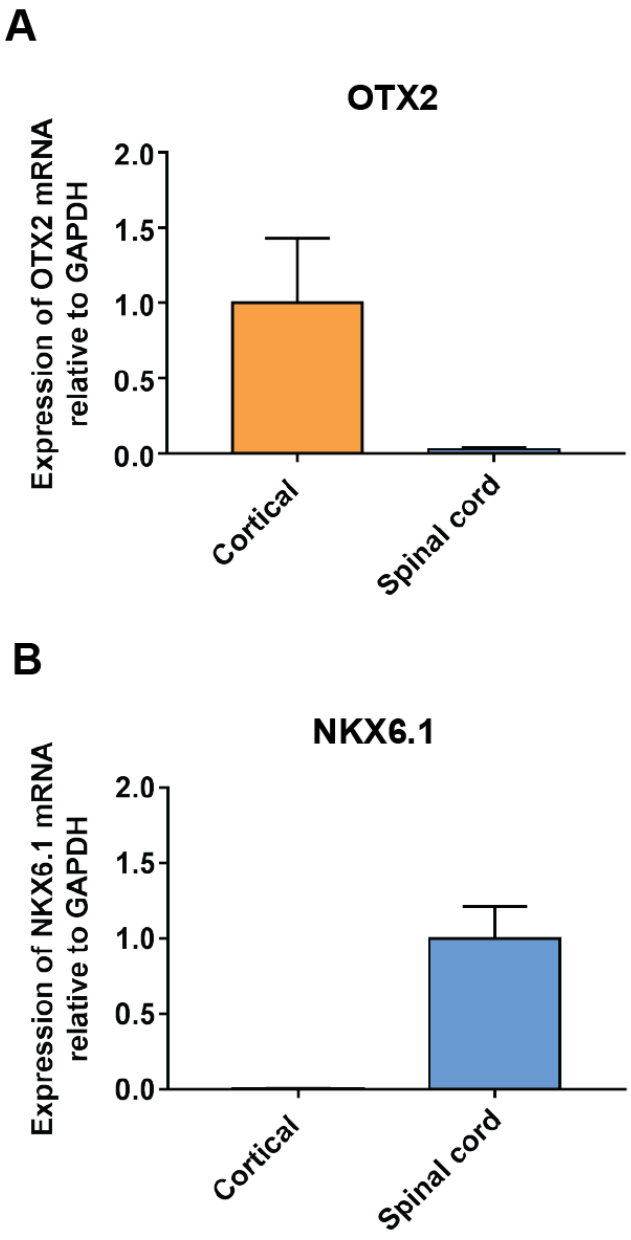

Figure 3.1. Specific expression of regional markers in glial cultures from the cortex and spinal cord. qPCR analysis for OTX2 **(A)** and NKX6.1 **(B)** in cortical and spinal cord glial cultures. Data are expressed as the mean ± SEM. A Mann-Whitney U test was used for statistical comparison. N=3.

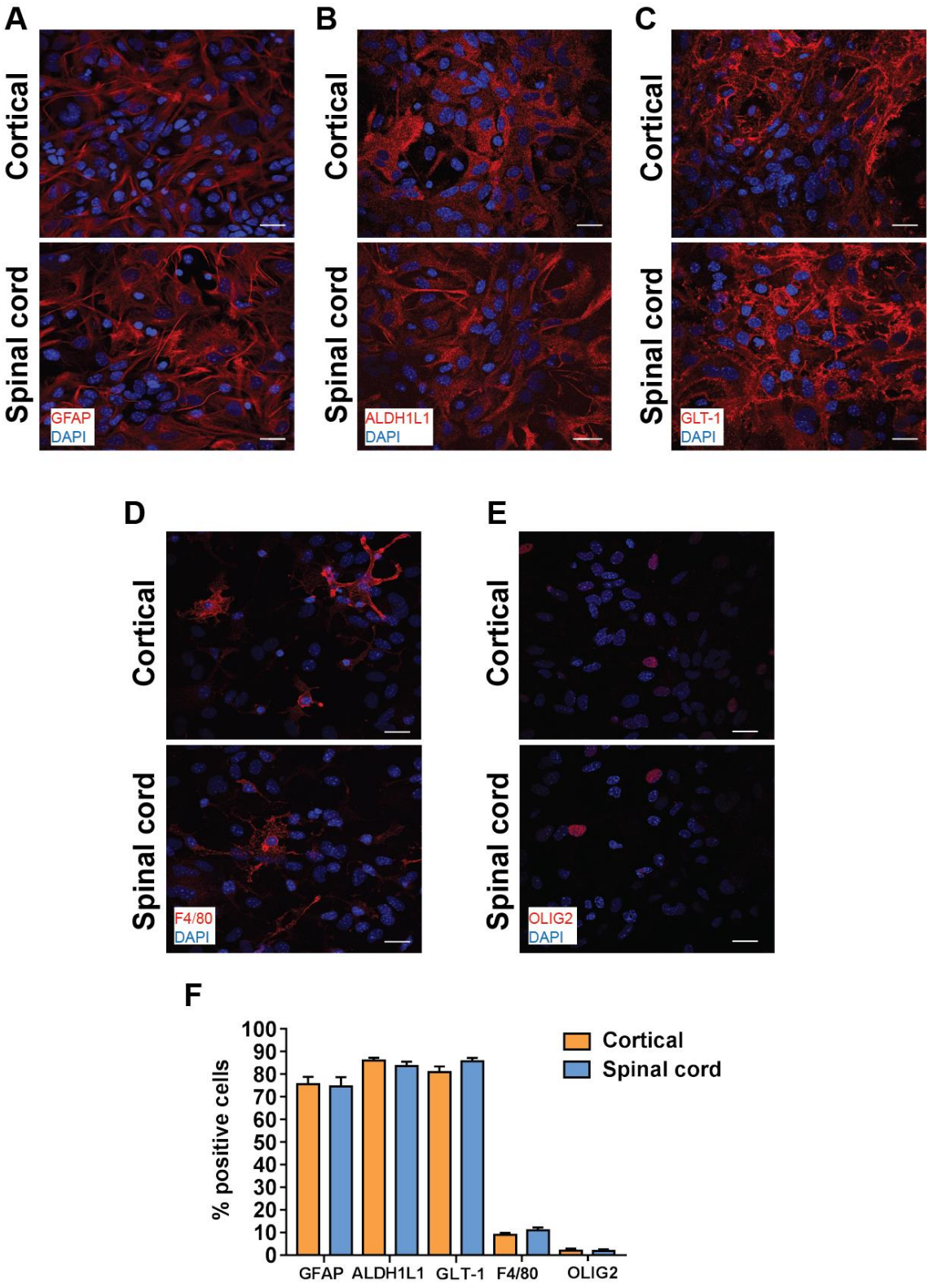

Figure 3.2. Characterisation of glial cultures from the cortex and spinal cord for markers of glial subtypes. Representative images for immunofluorescence staining for **(A)** GFAP, **(B)** ALDH1L1, **(C)** GLT-1, **(D)** F4/80 and **(E)** OLIG2 (all red) and **(F)** quantification. Data are expressed as the mean ± SEM. A Mann-Whitney U test was used for statistical comparison. Scale bar: 20 µm. N=3.

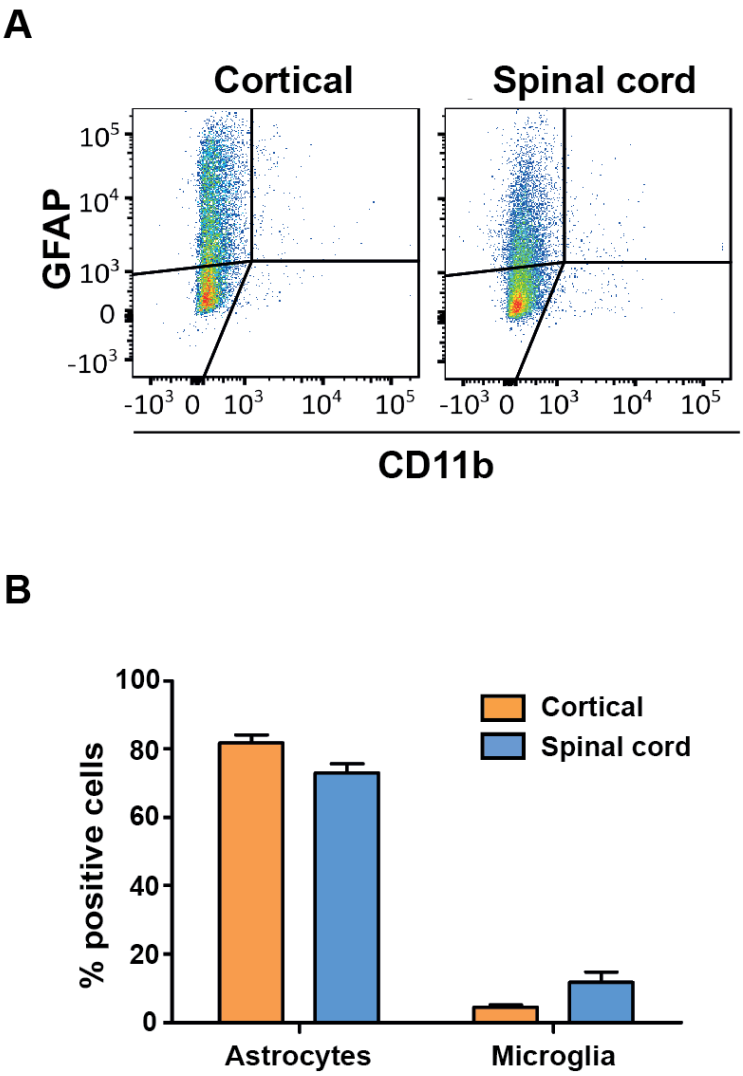

Figure 3.3. FACS analysis of glial cultures from the cortex and spinal cord. **(A)** Representative images and **(B)** quantification for FACS analysis of cortical and spinal cord glial cultures for GFAP (astrocytes) and CD11b (microglia). Data are expressed as the mean ± SEM. A two-way ANOVA with Tukey post-hoc tests was used for statistical comparison. N=3. (Data collected by Rebecca San Gil).

3.3.2 Regional differences in the NO pathway in cortical and spinal cord glial cultures

To compare the level of activation of the NO-iNOS-NF-κB inflammatory pathway in cortical and spinal cord glia in WT mice, glial cultures from these regions were treated with inducers of inflammation, LPS and TNF-α (Fig. 3.4). Griess assays were performed to indirectly measure NO production by measuring the levels of nitrite in the media.

NO was produced at significantly higher levels in glial cultures from the spinal cord compared with cortical cultures following 24 hour exposure to increasing concentrations of LPS or TNF-α (Fig. 3.4 A, B). Production of NO has been attributed to three enzymes: neuronal nNOS, eNOS and iNOS. The specific inhibitor of iNOS, 1400W, almost completely ablated NO production in both cortical and spinal cord glia following exposure to LPS or TNF-α (Fig. 3.4 C, D), suggesting that iNOS was responsible for the majority of NO production in both cortical and spinal cord glial cultures.

Analysis of western blots showed that glial cultures from the spinal cord upregulated iNOS protein expression more than cortical cultures following treatment with 80 µg/ml LPS (Fig. 3.5 A, B). Treatment with 100 ng/ml TNF-α did not result in any detectable iNOS by western blot. In line with increased expression of iNOS in spinal cord glial cultures compared with cortical cultures, there were more iNOS positive cells in spinal cord glial cultures than cortical cultures following treatment with LPS, determined by immunofluorescence (Fig. 3.5 C, D).

3.3.3 Localisation of iNOS expression in cortical and spinal cord glial cultures following LPS treatment

Previous studies have suggested that only microglia express iNOS following LPS treatment and astrocytic iNOS is only produced following exposure to a combination of LPS and IFN-γ (Saura et al., 2005; Hamby et al., 2006). To identify the specific cell type expression of iNOS following LPS treatment, cortical and spinal cord glial cultures treated with LPS were co-stained with iNOS and the markers of astrocytes and microglia, GFAP and F4/80, respectively.

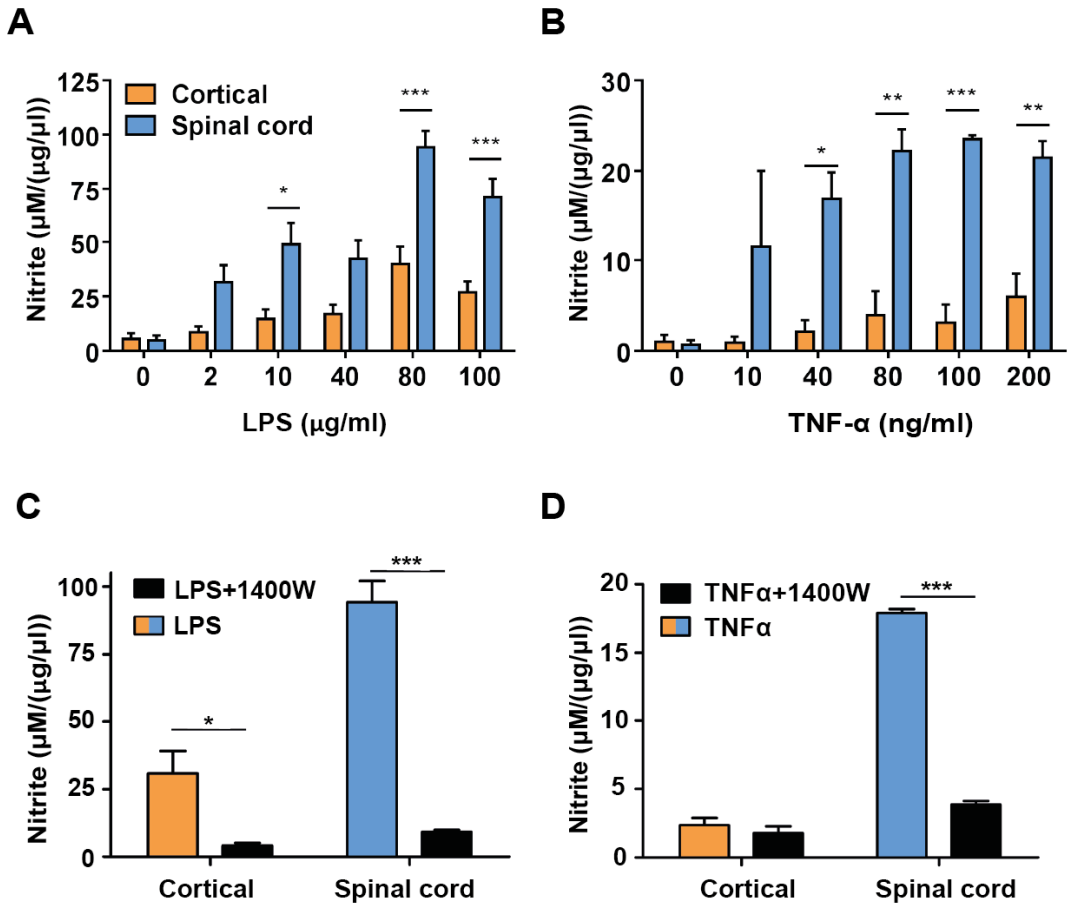

Figure 3.4. Production of NO in cortical and spinal cord glial cultures following exposure to inflammatory mediators. Nitrite production of cortical and spinal cord glial cultures exposed to increasing concentrations of **(A)** LPS or **(B)** TNF-α, and **(C, D)** the iNOS inhibitor, 1400W, measured by Griess assay. 80 µg/ml LPS and 100 ng/ml TNF-α concentrations were chosen for **(C)** and **(D)**. Data are expressed as the mean ± SEM. P=*≤0.05, **≤0.01, ***≤0.001. A two-way ANOVA with Tukey post-hoc tests was used for statistical comparison. N=3 (Data collected by Jing Yip).

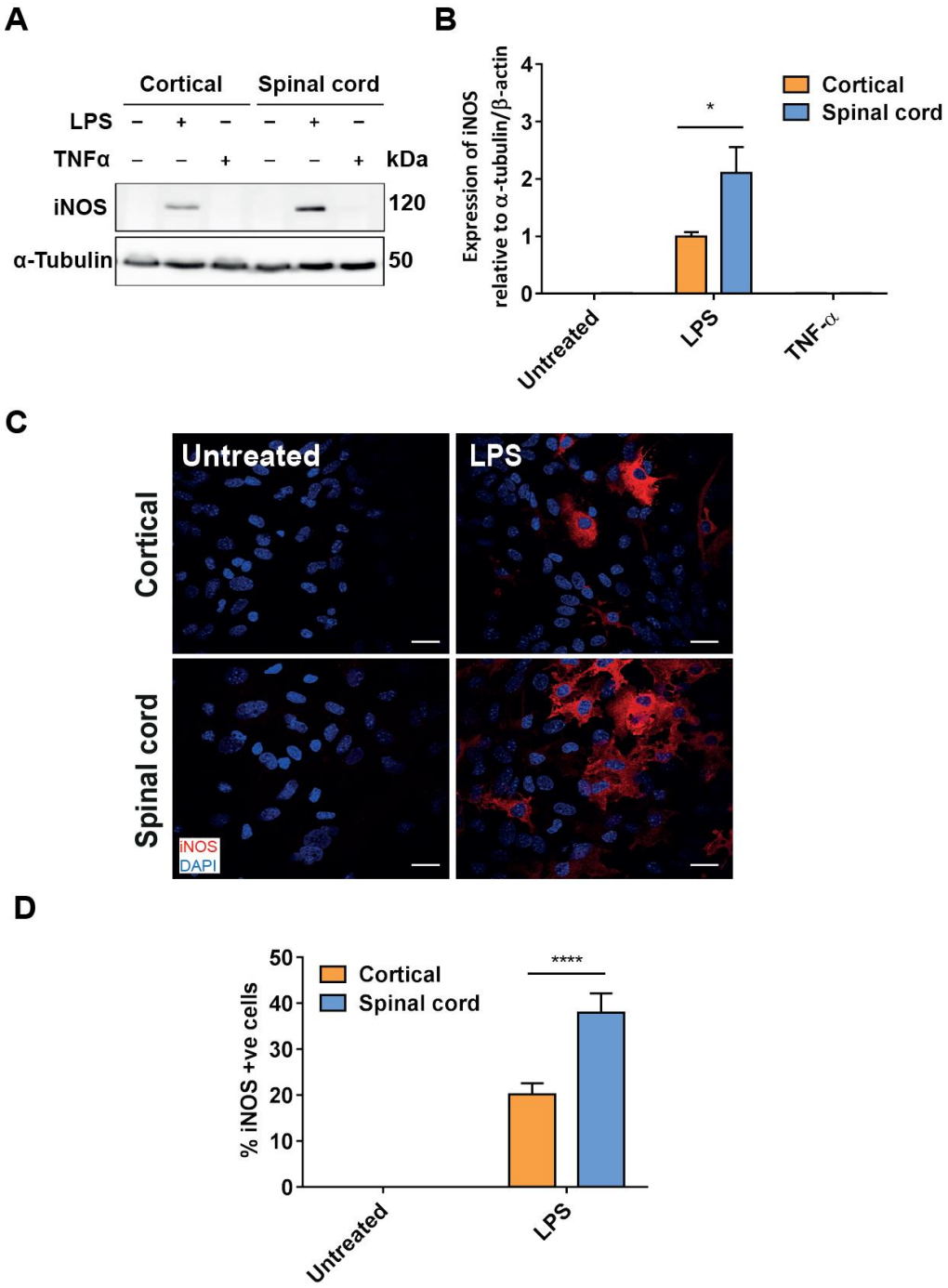

Figure 3.5. Expression of iNOS in cortical and spinal cord glial cultures following exposure to inflammatory mediators. (A, B) Western blots for iNOS expression in cortical and spinal cord glial cultures exposed to 80 µg/ml LPS or 100 ng/ml TNF-α. N=3-8. **(C)** Representative images and **(D)** quantification of immunofluorescence staining for iNOS (red) in cortical and spinal cord glial cultures treated with LPS. N=4. Data are expressed as the mean ± SEM. P=*≤0.05, ****≤0.0001. A two-way ANOVA with Bonferroni post-hoc tests was used for statistical comparison. Scale bar 20 µm. (Data for Fig. 3.5 A collected by Rebecca San Gil).

A subset of astrocytes from both cortical and spinal cord glial cultures expressed iNOS following treatment with LPS (Fig. 3.6). Although there were no differences in the number of astrocytes in cortical or spinal cord glial cultures following LPS treatment (Fig. 3.6 C), there was an increase in the proportion of astrocytes that expressed iNOS in spinal cord glial cultures compared to cortical cultures (Fig. 3.6 D).

A subset of microglia from both cortical and spinal cord glial cultures also expressed iNOS following treatment with LPS (Fig. 3.7). While there were no differences in the proportion of microglia that expressed iNOS between cortical and spinal cord glial cultures, there was a significant increase in the proportion of microglia in glial cultures from the spinal cord, but not the cortex, following treatment with LPS. This suggests that there was a region specific proliferation of microglia following LPS treatment in spinal cord glial cultures (Fig. 3.7 C, D).

3.3.4 Production of NO and expression of iNOS in SOD1^{G93A} expressing glial cultures

Since NO production by iNOS is known to contribute to motor neuron death in SOD1^{G93A} mice (Chen et al., 2010; Frakes et al., 2014), the production of NO and iNOS expression was next compared in cortical and spinal cord glial cultures from WT and SOD1^{G93A} mice following treatment with LPS. SOD1^{G93A} glia produced similar levels of NO to WT glia following treatment with LPS, with a trend towards reduced NO production in SOD1^{G93A} cultures (Fig. 3.8 A). NO production in SOD1^{G93A} glia was again almost completely prevented by the iNOS specific inhibitor 1400W, indicating that, similar to WT glial cultures, NO production in SOD1^{G93A} cultures is predominately produced by iNOS (Fig. 3.8 B).

Levels of iNOS expression were also similar between SOD1^{G93A} and WT glia following treatment with LPS. Both expression levels, measured by western blot (Fig. 3.9), and the proportion of iNOS positive cells, measured by immunofluorescence (Fig. 3.10), were similar in SOD1^{G93A} and WT glial cultures from the cortex and spinal cord treated with LPS. Finally, there was no difference in the proportion of cells that were positive for nuclear translocation of NF-κB (Fig. 3.11), indicative of activation of the NF-κB pathway, between SOD1^{G93A} and WT glial cultures from both the cortex and spinal cord.

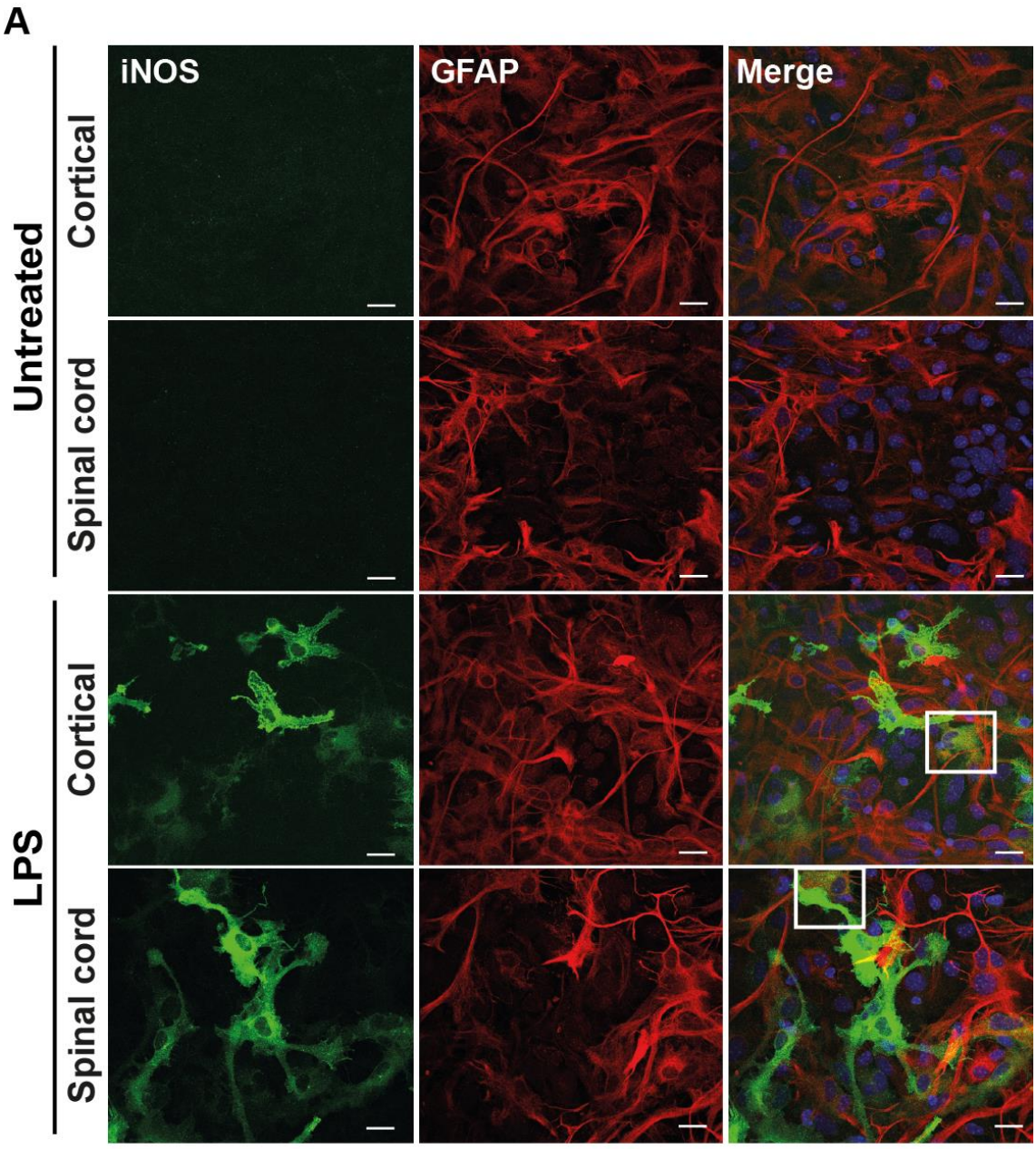
A
iNOS
GFAP
Merge
Untreated
Cortical
Spinal cord
LPS
Cortical
Spinal cord
B
Cortical
Spinal cord
LPS
iNOS
GFAP
DAPI

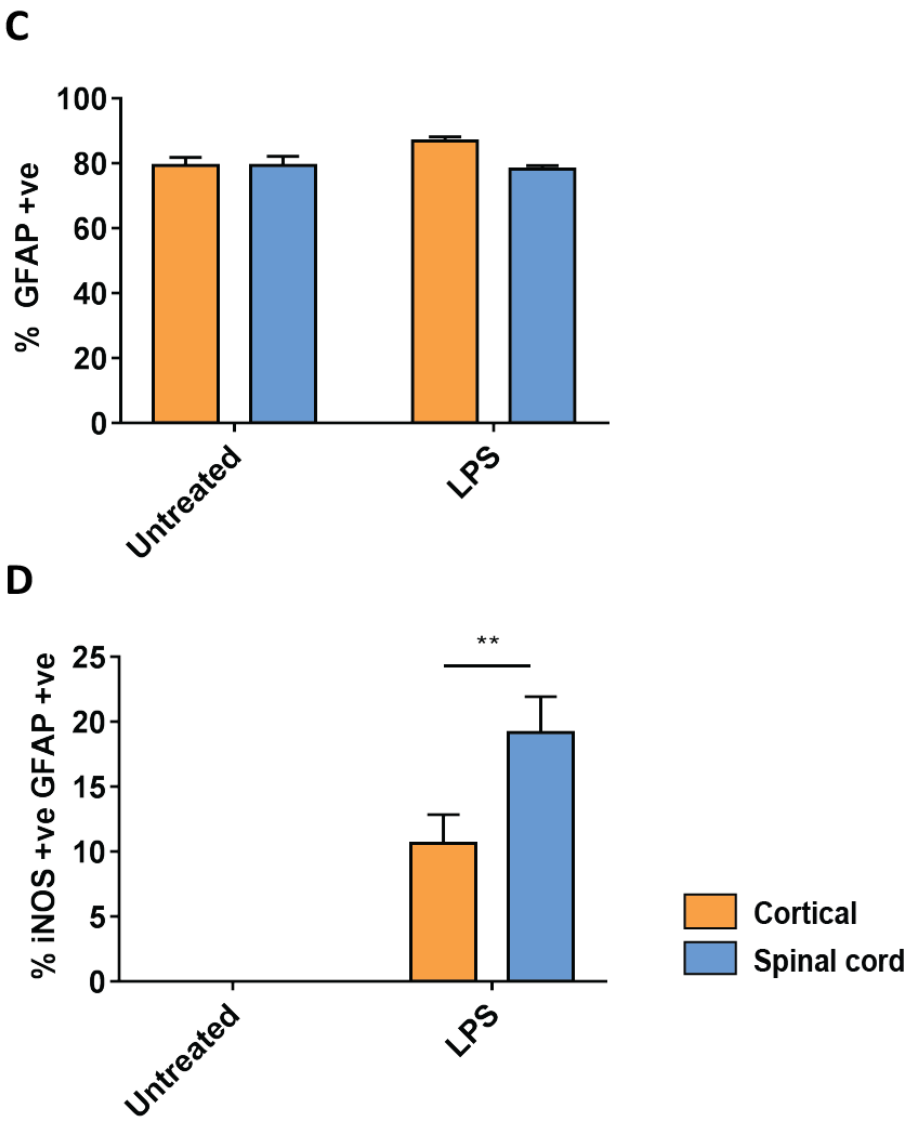

Figure 3.6. Localisation of iNOS in astrocytes from cortical and spinal cord glial cultures following treatment with LPS. (A) Representative and **(B)** enlarged images of cortical and spinal cord glial cultures treated with LPS and stained for iNOS (green), GFAP (red) and DAPI (blue). Quantification of **(C)** the proportion of GFAP positive cells and **(D)** the proportion of iNOS positive and GFAP positive cells. Data are expressed as the mean ± SEM. P=**≤0.01. A two-way ANOVA with Tukey post-hoc tests was used for statistical comparison. Scale bar: 20 µm. N=3.

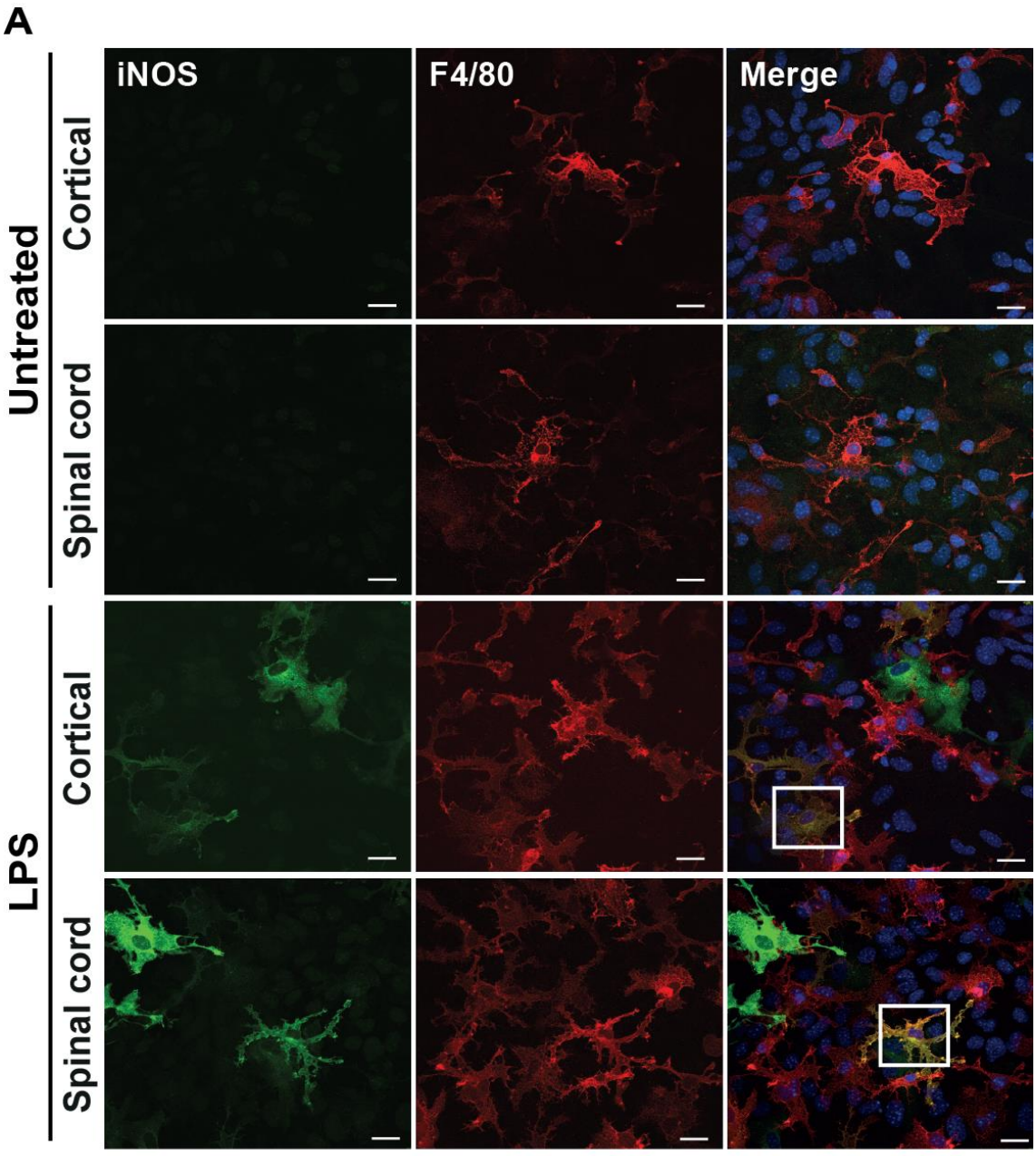
A
iNOS
F4/80
Merge
Untreated
Cortical
Spinal cord
LPS
Cortical
Spinal cord

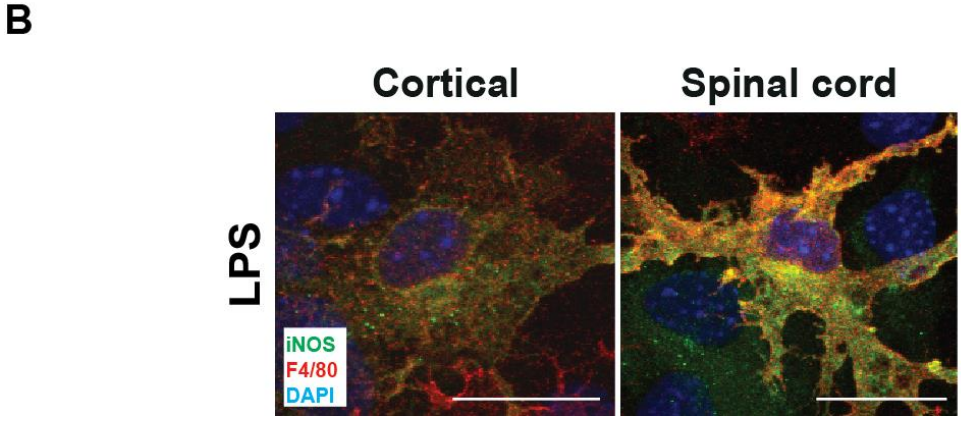
B
Cortical
Spinal cord
LPS
iNOS
F4/80
DAPI

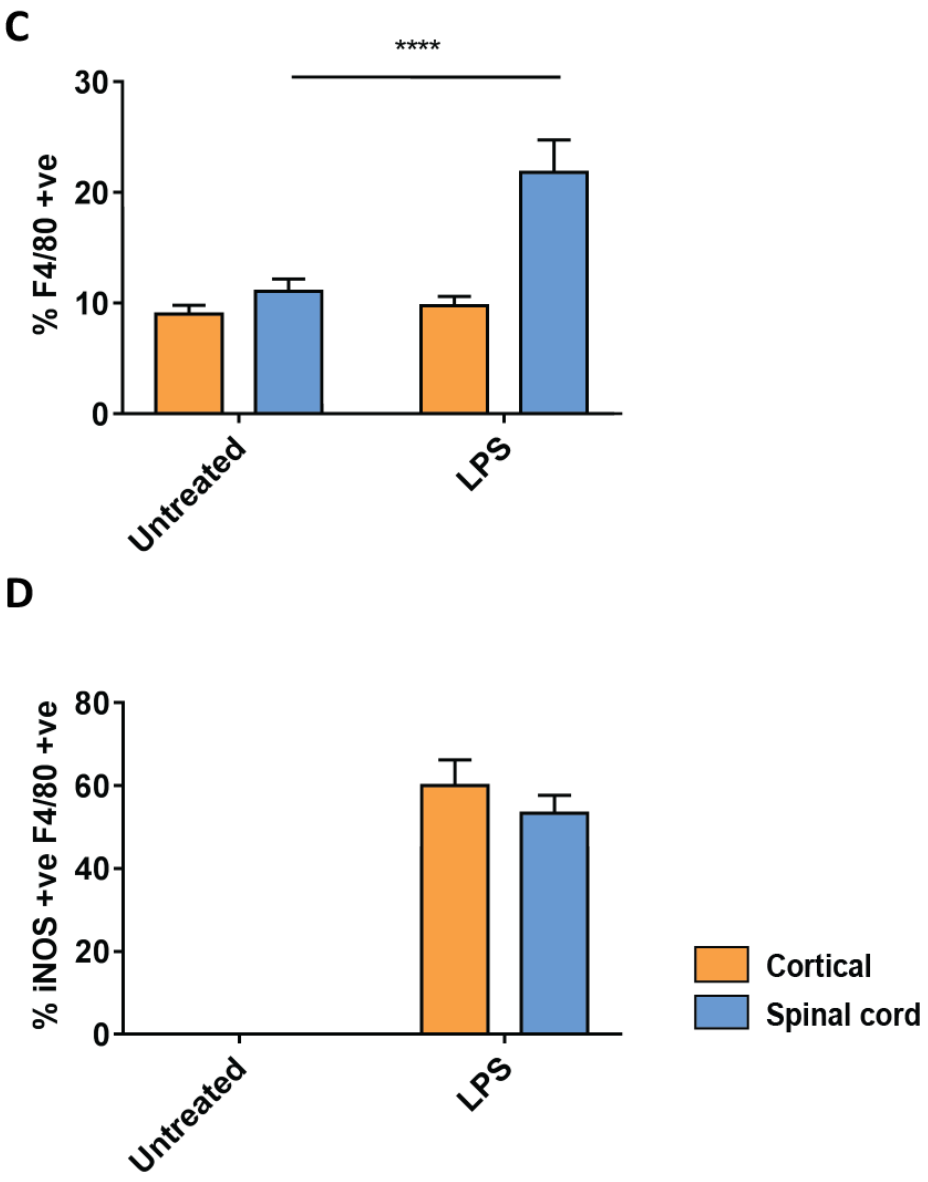

Figure 3.7. Localisation of iNOS in microglia from cortical and spinal cord glial cultures following treatment with LPS. (A) Representative and **(B)** enlarged images of cortical and spinal cord glial cultures treated with LPS and stained for iNOS (green), F4/80 (red) and DAPI (blue). Quantification of **(C)** the proportion of F4/80 positive cells and **(D)** the proportion of iNOS positive and F4/80 positive cells. Data are expressed as the mean ± SEM. P=****≤0.0001. A two-way ANOVA with Tukey post-hoc tests was used for statistical comparison. Scale bar: 20 µm. N=3.

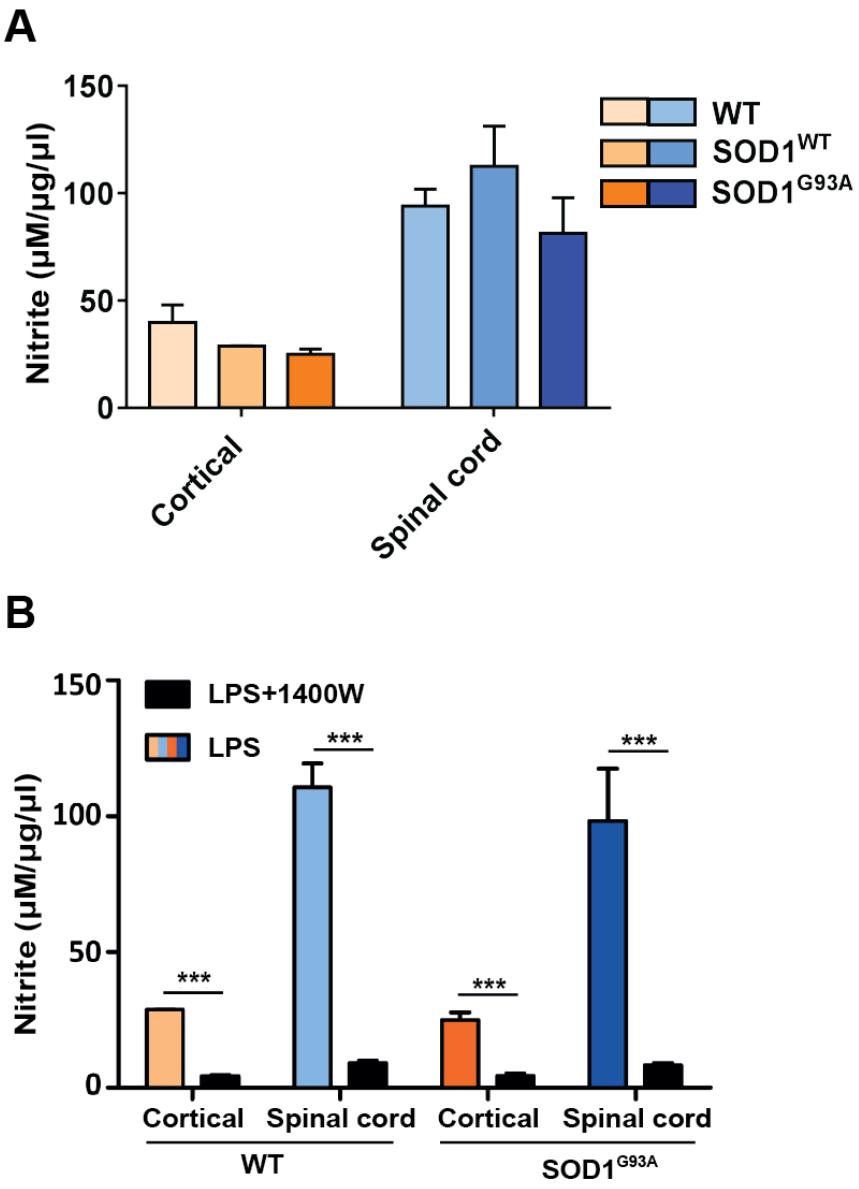

Figure 3.8. NO production in SOD1^{G93A} cortical and spinal cord glial cultures following treatment with LPS. (A) Nitrite production of wildtype (WT), SOD1^{WT} and SOD1^{G93A} glial cultures from the cortex and spinal cord following treatment with 80 µg/ml LPS and/or **(B)** 1400W**.** Data are expressed as the mean ± SEM. A two-way ANOVA with Tukey post-hoc tests was used for statistical comparison. P=***≤0.001. N=3-4. (Data for Fig. 3.8 collected by Jing Yip).

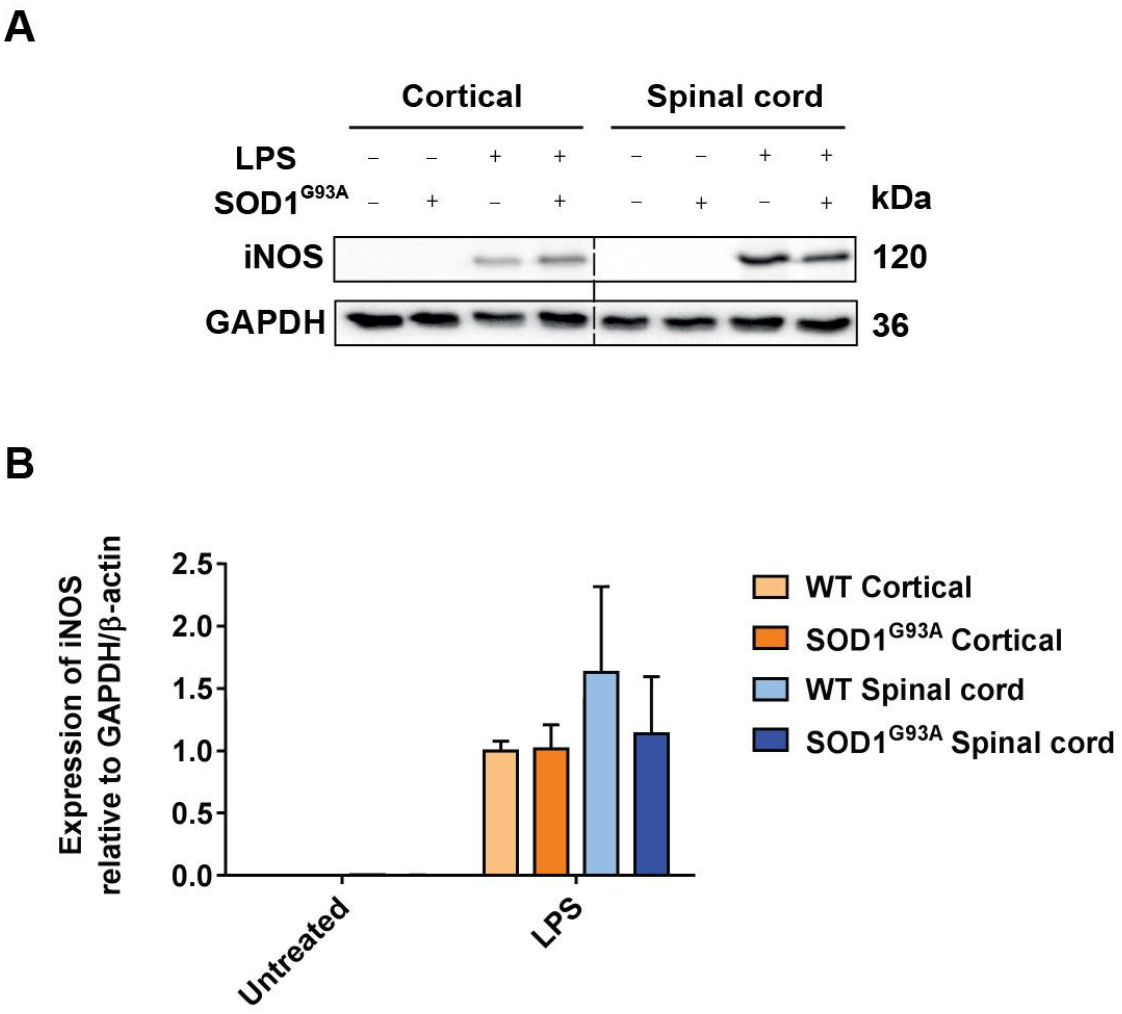

Figure 3.9. iNOS expression in SOD1^{G93A} cortical and spinal cord glial cultures following treatment with LPS. (A) Immunoblotting and **(B)** quantification for iNOS in SOD1^{G93A} and wildtype (WT) cortical and spinal cord glial cultures treated with LPS. Data are expressed as the mean ± SEM. A two-way ANOVA with Tukey post-hoc tests was used for statistical comparison. N=4.

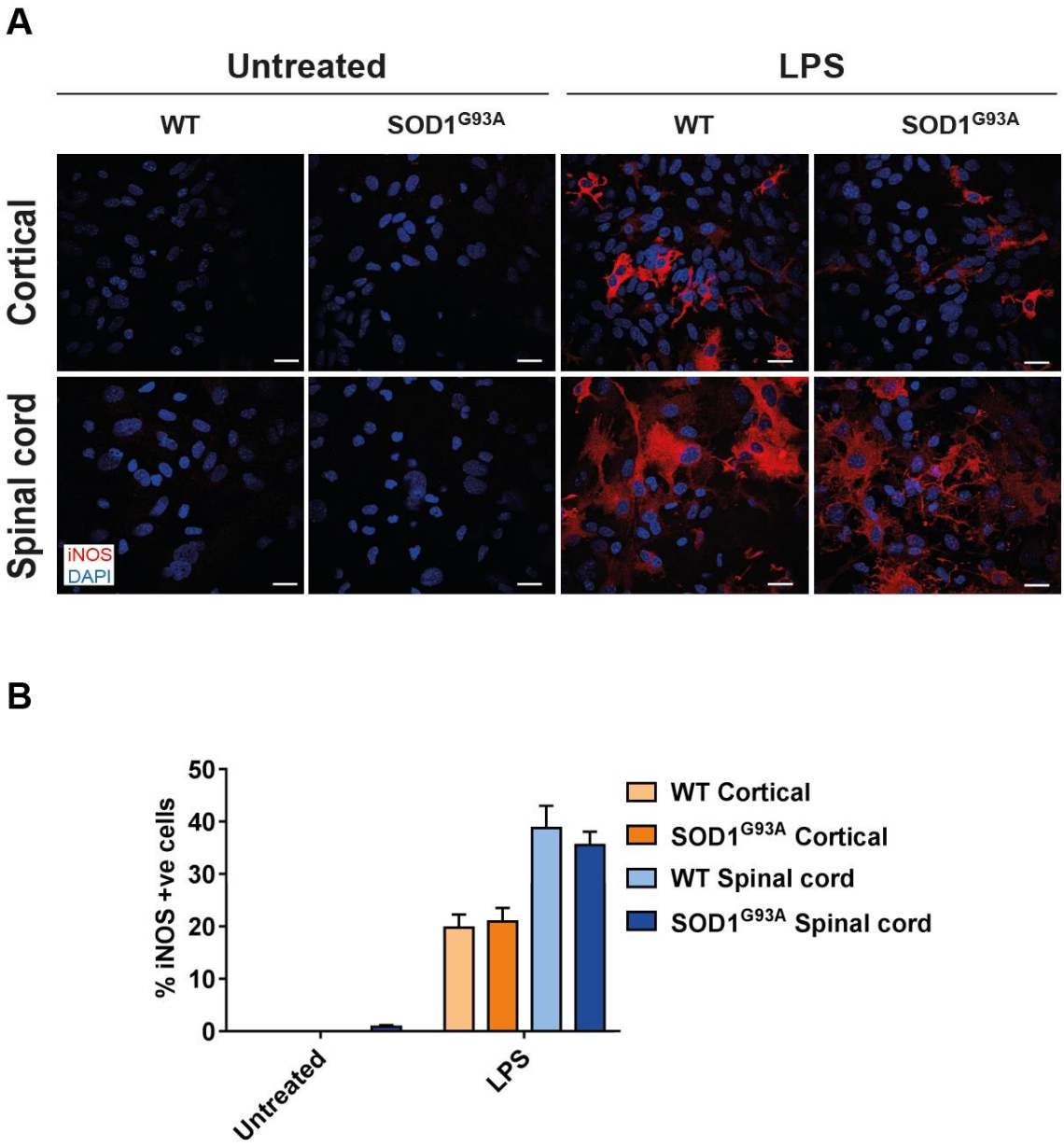

Figure 3.10. iNOS expression in SOD1^{G93A} cortical and spinal cord glial cultures following treatment with LPS. (A) Representative images and **(B)** quantification of immunostaining for iNOS (red) in SOD1^{G93A} and wildtype (WT) cortical and spinal cord glial cultures treated with LPS. Data are expressed as the mean ± SEM. A two-way ANOVA with Bonferroni post-hoc tests was used for statistical comparison. Scale bar: 20 µm. N=3-4.

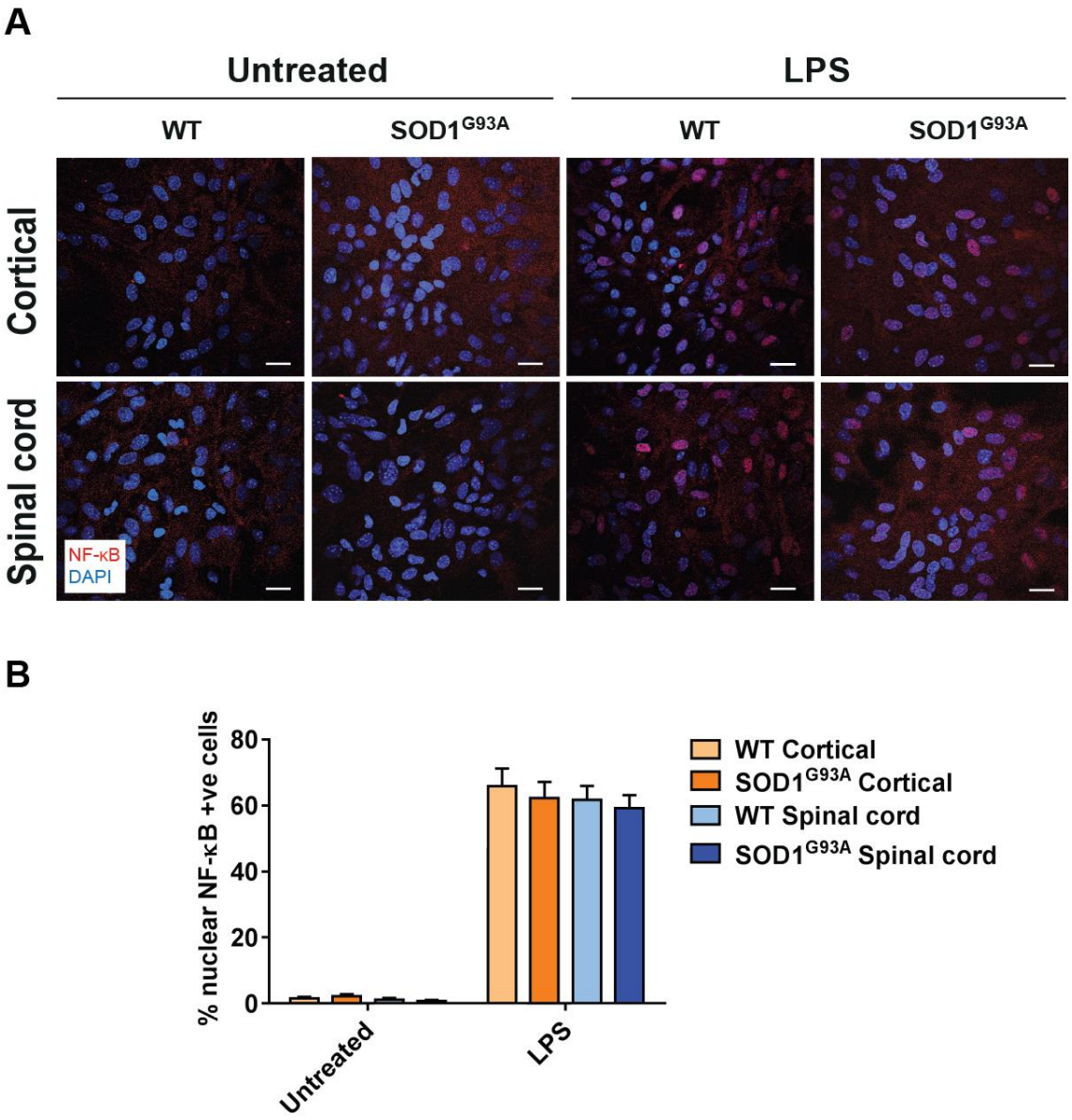

Figure 3.11. NF-κB expression in SOD1^{G93A} cortical and spinal cord glial cultures following treatment with LPS. (A) Representative images and **(B)** quantification of immunofluorescence staining for the proportion of cells with nuclear NF-κB (red) in SOD1^{G93A} and wildtype (WT) cortical and spinal cord glial cultures treated with LPS. Data are expressed as the mean ± SEM. A two-way ANOVA with Tukey post-hoc tests was used for statistical comparison. Scale bar: 20 µm. N=3.

Finally, there was also no difference in NO production between SOD1^{G93A} and WT microglia isolated from cortical and spinal cord glial cultures treated with LPS (Fig. 3.12 C). However, there was a trend towards increased production of NO in spinal cord microglia compared with cortical microglia.

3.3.5 Characterisation of human iPSC-derived cortical and spinal cord astrocytes

To study regional differences in a human model of astrocytes, human iPSCs were patterned to the cortex and spinal cord and subsequently differentiated into highly enriched populations of astrocytes, adapting previously described protocols to direct neural progenitors to different regions of the CNS (Shi et al., 2012; Hall et al., 2017).

In order to characterise the regional position of astrocytes patterned to the cortex and spinal cord, NPCs patterned to these regions were characterised for regional markers. qPCR analysis revealed that OTX2 and forebrain marker forkhead box protein G1 (FOXG1) were expressed in cortical, but not spinal cord, NPCs (Fig. 3.13). Furthermore, spinal cord, but not cortical, NPCs expressed spinal cord markers NKX6.1 and homeobox A4 (HOXA4). Immunostaining revealed that NPCs patterned to the cortex, but not the spinal cord, were positive for forebrain/midbrain marker OTX2 (Fig. 3.14 A, B). Conversely, NPCs patterned to the spinal cord, but not the cortex, were positive for ventral spinal cord marker NKX6.1 (Fig. 3.14 C, D).

Astrocytes differentiated from cortical and spinal cord NPCs both expressed astrocytic markers GFAP and ALDH1L1 (Fig. 3.15). Furthermore, mature astrocytes partially maintained the expression of regional markers at the mRNA (Fig. 3.16) and protein level (Fig. 3.17), albeit with variability between different lines.

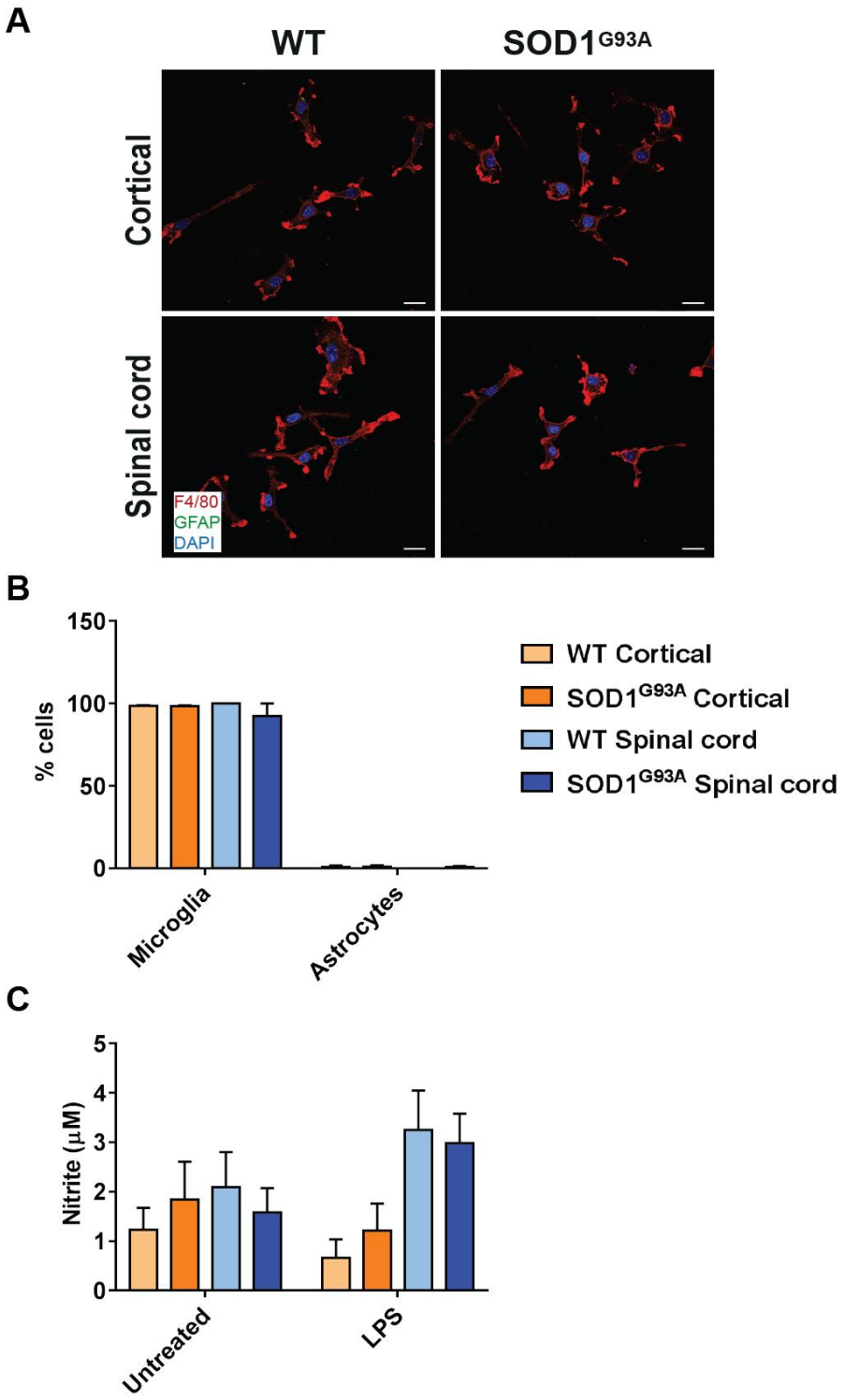

Figure 3.12. NO production in SOD1^{G93A} cortical and spinal cord isolated microglia following LPS treatment. (A) Representative images and **(B)** quantification of SOD1^{G93A} and wildtype (WT) microglia isolated from cortical and spinal cord glial cultures. **(C)** Nitrite production of wildtype (WT) and SOD1^{G93A} isolated microglia from the cortex and spinal cord following treatment with LPS. Data are expressed as the mean ± SEM. A statistical test was not performed due to low n numbers. Scale bar: 20 µm. N=2-3.

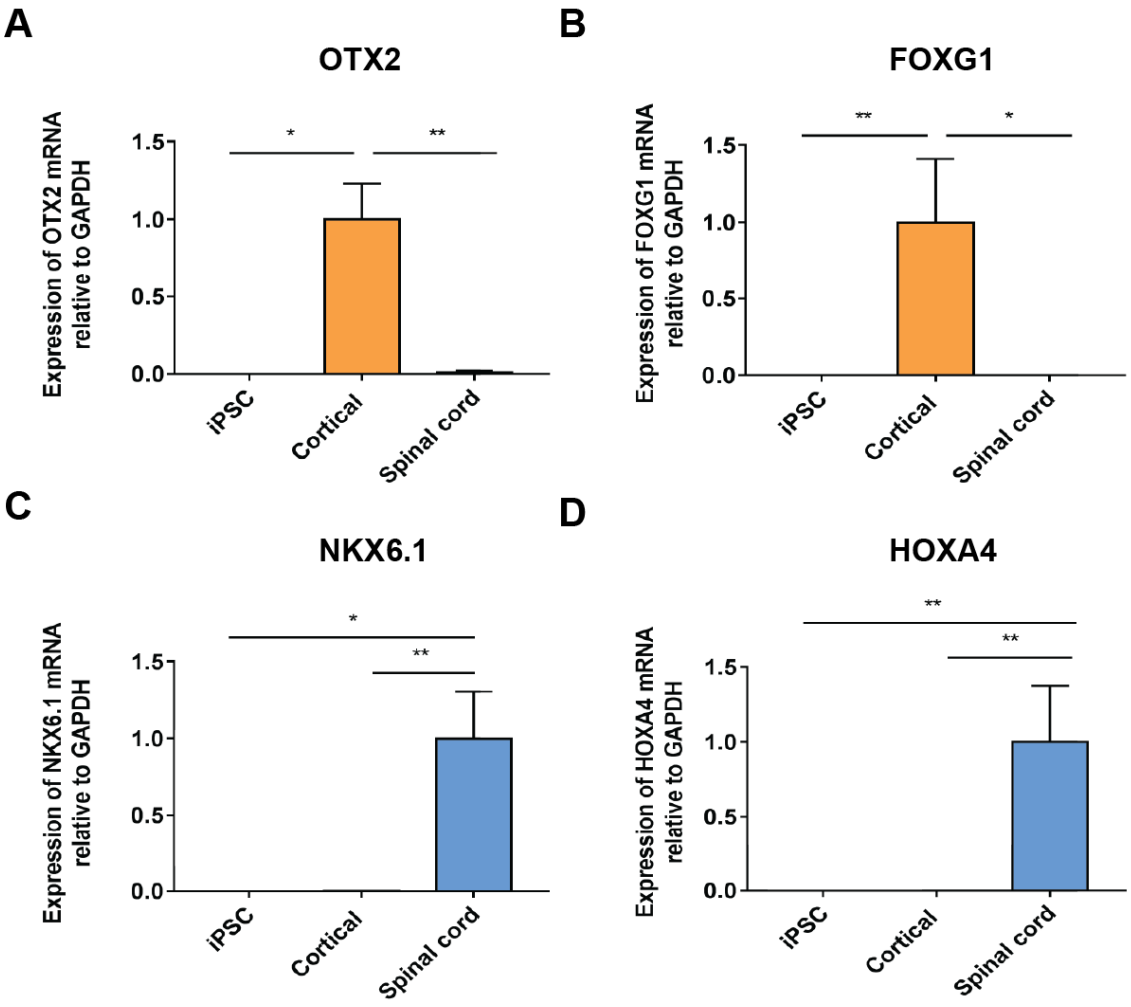

Figure 3.13. Expression of region-specific markers of human NPCs patterned to the cortex and spinal cord. qPCR analysis for forebrain markers **(A)** OTX2 and **(B)** FOXG1 and spinal cord markers **(C)** NKX6.1 and **(D)** HOXA4. Data are expressed as the mean ± SEM. A one-way ANOVA with Tukey post-hoc tests or a Kruskal-Wallis test with post-hoc Dunn's tests was used for statistical comparison. P=*≤0.05, **≤0.01. N=3.

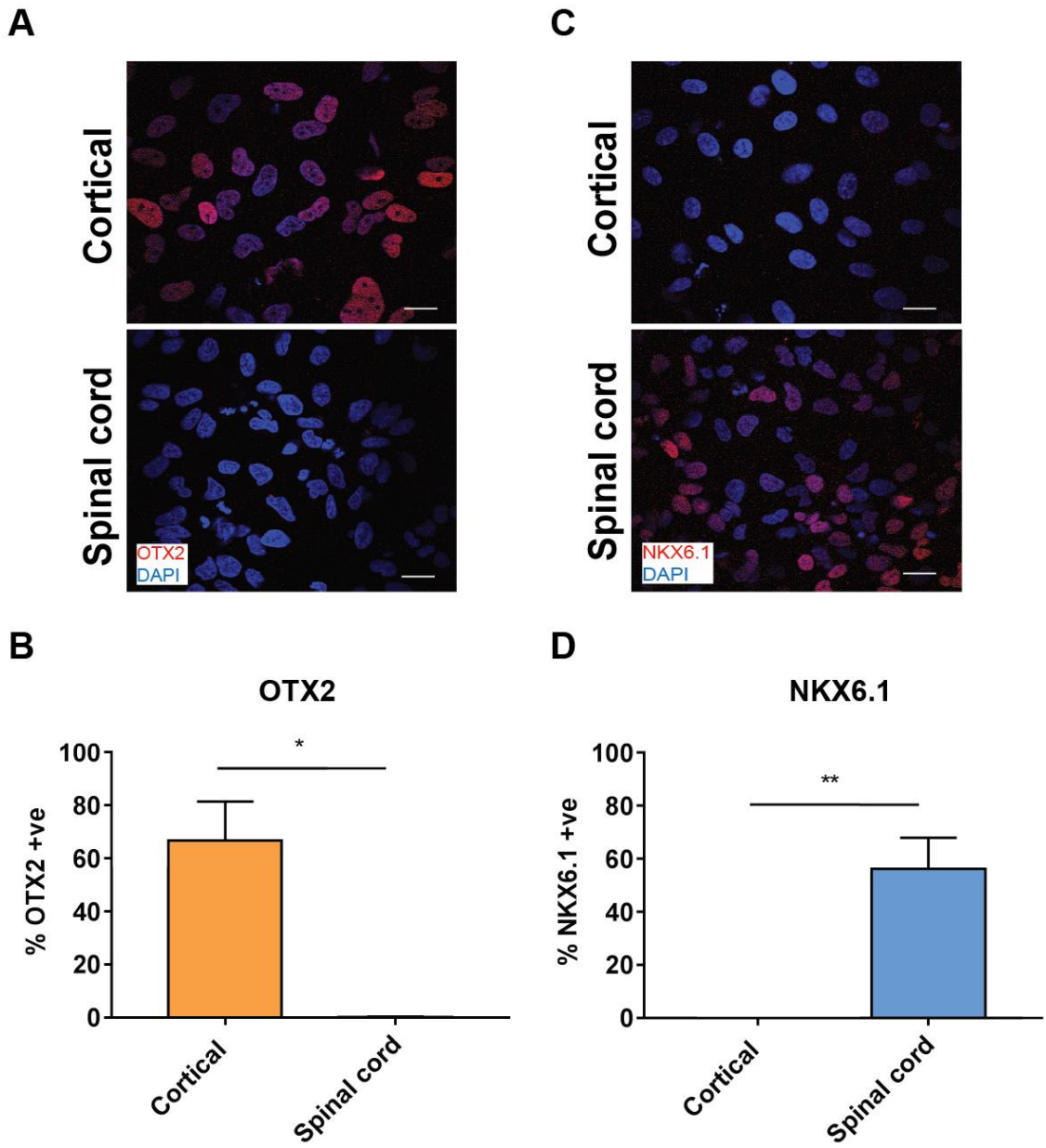

Figure 3.14. Expression of region-specific markers of human NPCs patterned to the cortex and spinal cord. Representative images and quantification of immunofluorescence staining for **(A, B)** OTX2 and **(C, D)** NKX6.1 (both red) in NPCs from D15 and D40 after neural induction, patterned to the cortex and spinal cord. Data are expressed as the mean ± SEM. A Mann-Whitney U test was used for statistical comparison. P=*≤0.05, **≤0.01. Scale bar: 20 µm. N=3.

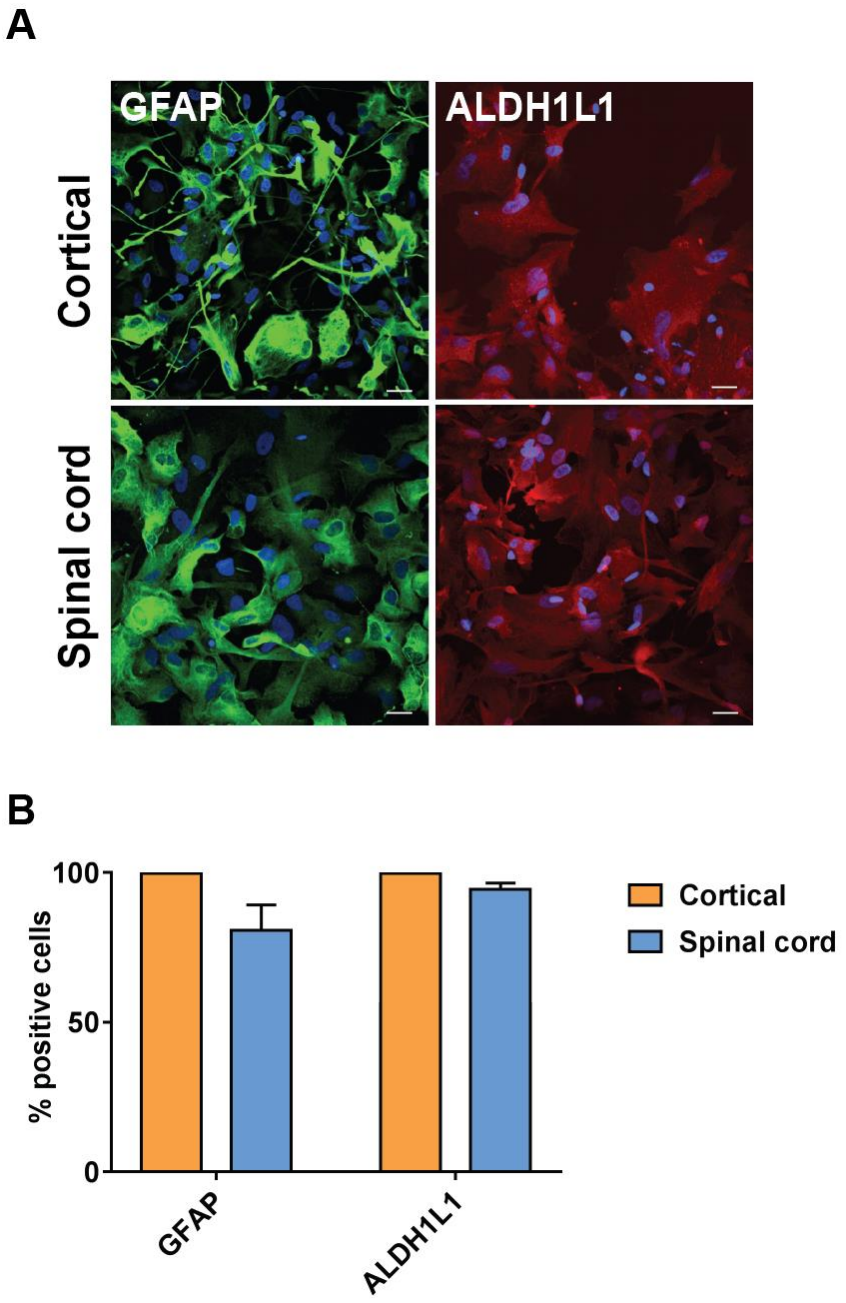

Figure 3.15. Expression of markers of astrocytes in human iPSC-derived astrocytes patterned to the cortex and spinal cord. (A) Representative images and **(B)** quantification of terminally differentiated iPSC-derived astrocytes for astrocytic markers GFAP (green) and ALDH1L1 (red). Data are expressed as the mean ± SEM. A statistical test was not performed due to low n numbers. Scale bar: 20 µm. N=2-3.

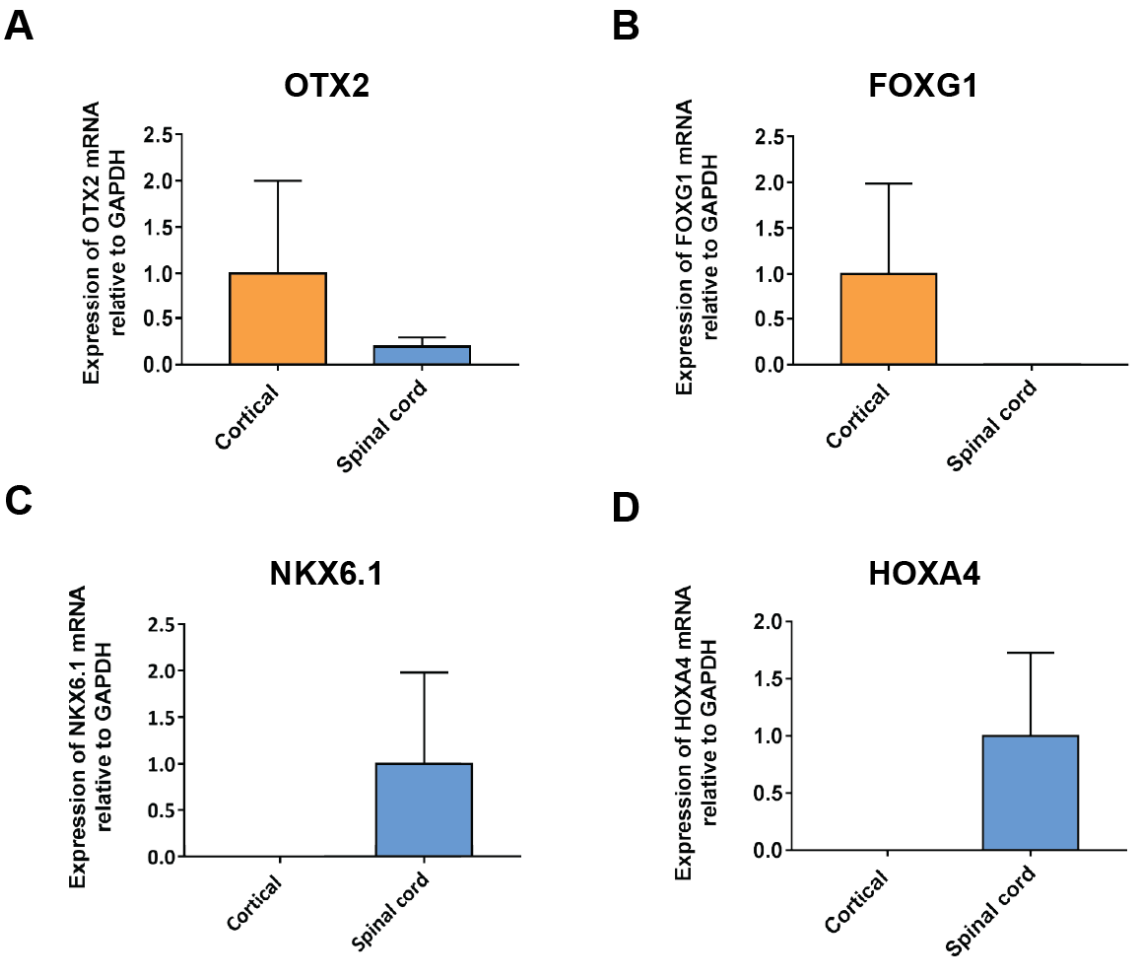

Figure 3.16. Expression of region-specific markers in human iPSC-derived astrocytes patterned to the cortex and spinal cord. qPCR analysis for forebrain markers **(A)** OTX2 and **(B)** FOXG1 and spinal cord markers **(C)** NKX6.1 and **(D)** HOXA4 in human iPSC-derived cortical and spinal cord astrocytes. Data are expressed as the mean ± SEM. A statistical test was not performed due to low n numbers. Scale bar: 20 µm. N=2.

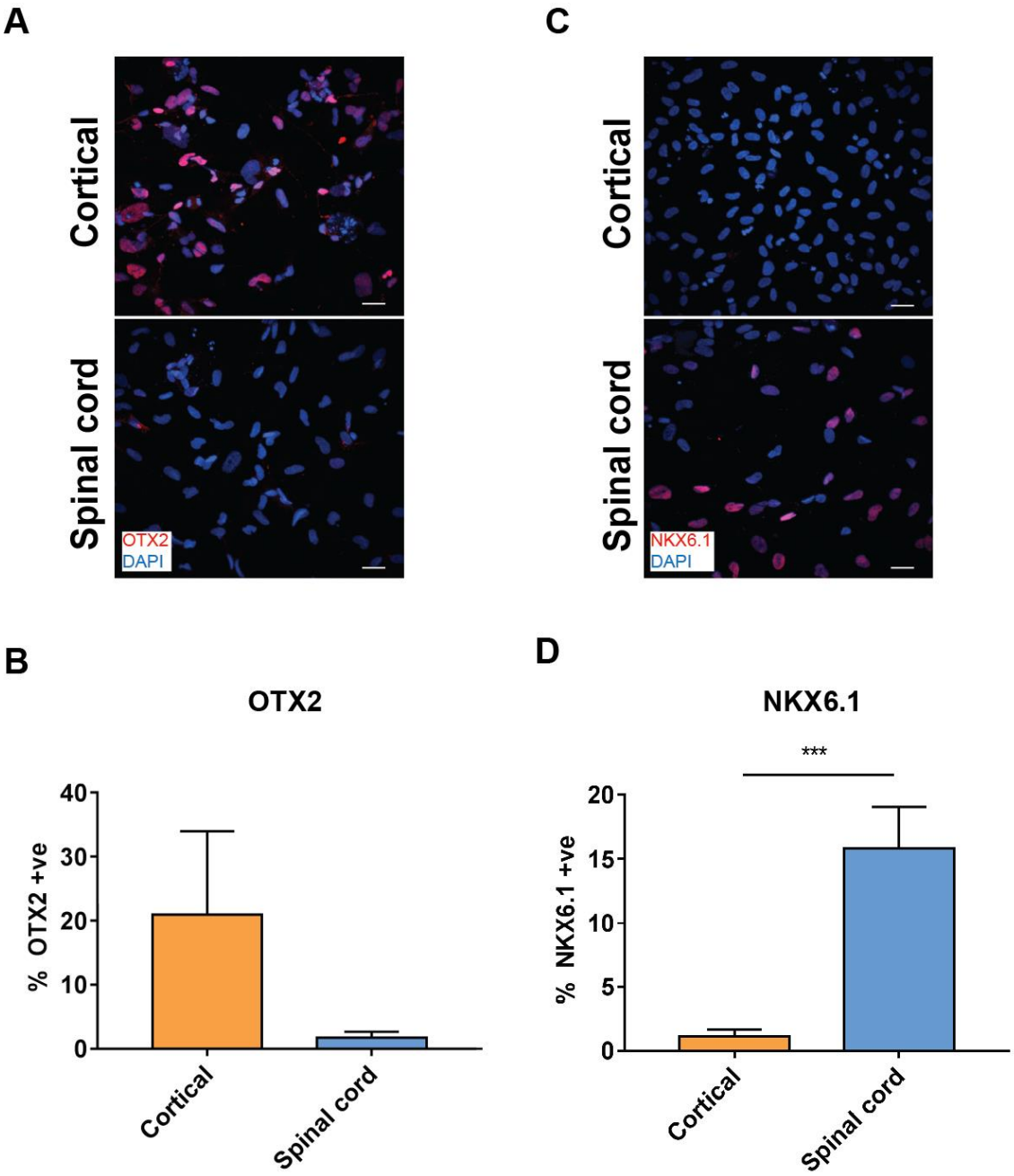

Figure 3.17. Expression of region-specific markers in human iPSC-derived astrocytes patterned to the cortex and spinal cord. Representative images and quantification for regional markers **(A, B)** OTX2 and **(C, D)** NKX6.1 (both red) in human iPSC-derived cortical and spinal cord astrocytes. Data are expressed as the mean ± SEM. P=***≤0.001. A Mann-Whitney U test was used for statistical comparison. Scale bar: 20 µm. N=2-3.

3.3.6 Regional differences in the NO-iNOS-NF-κB pathway in human iPSC-derived cortical and spinal cord astrocytes

It has been recently shown that LPS treatment induces a pro-inflammatory phenotype in astrocytes, but only in the presence of microglia (Liddelow et al., 2017). This response was not observed in microglial knockout (*csfr1*$^{-/-}$) mice, suggesting that microglia were crucial for directing astrocytes to a pro-inflammatory state, at least following LPS treatment. Therefore, in order to study the inflammatory responses of human iPSC-derived astrocytes, the cultures were exposed to a combination of TNF-α, IL-1α and C1q in parallel with LPS. These pro-inflammatory cytokines are known to be released from microglia and when administered together have been shown to partially recapitulate the pro-inflammatory state of astrocytes observed following LPS treatment (Liddelow et al., 2017).

Treatment of human iPSC-derived astrocytes patterned to the cortex and spinal cord with LPS did not result in NO production (Fig. 3.18 A). However, treatment with a combination of TNF-α, IL-1α and C1q did result in a small increase in NO production (Fig. 3.18 B). In agreement with findings in mouse primary glial cultures, there was a trend towards a higher production of NO in human iPSC-derived spinal cord patterned astrocytes compared with cortical patterned astrocytes. Notably, NO production was lower and took longer to induce in human iPSC-derived astrocytes than in mouse glial cultures.

No change in iNOS expression was detected by western blot or immunofluorescence in human iPSC-derived astrocytes following treatment with either LPS or TNF-α, IL-1α and C1q (data not shown as no signal was detected). However, increased nuclear NF-κB translocation was observed in human iPSC-derived astrocytes following treatment with TNF-α, IL-1α and C1q, but not LPS, with a trend towards an increased proportion of NF-κB positive cells in spinal cord patterned astrocytes compared to cortical patterned astrocytes (Fig. 3.19). Although results from this experiment did not reach significance, spinal cord glia consistently displayed a higher level of activation of the NO-iNOS-NF-κB inflammatory pathway in both mouse primary glial cultures and human iPSC-derived astrocytes.

Next, human SOD1^{D90A} iPSCs and a SOD1^{D90D} isogenic control line were differentiated into highly enriched astrocyte populations (Fig. 3.20). Human astrocytes from SOD1^{D90A} iPSCs displayed a trend towards decreased nuclear NF-κB translocation (Fig. 3.21 A, B) and reduced phosphorylation of the p65 subunit of NF-κB (Fig. 3.22 A-C) in response to TNF-α, IL-1α and C1q compared with astrocytes from control iPSC lines. Phosphorylation of the p65 subunit of NF-κB is required for activation of the complex (Hayden and Ghosh, 2008). Furthermore, there was a trend towards decreased NO production in SOD1^{G93A} mouse primary glial cultures treated with TNF-α, IL-1α and C1q or LPS compared to WT cultures (Fig. 3.22 D). Thus, inflammatory signalling in iPSC-derived astrocytes expressing SOD1^{D90A} was not significantly different from control lines. These results are in line with findings from the mouse primary glial cultures.

3.4 Discussion

The aims of this Chapter were to i) determine whether regional differences in the inflammatory responses of glia exist between the cortex and spinal cord and ii) if regional differences in inflammatory responses were altered in mSOD1 glial models of ALS. The results of this Chapter show that normal, WT spinal cord glia elicit a stronger inflammatory response than cortical glia in response to inflammatory induction. Furthermore, glial inflammatory responses are not significantly affected by the expression of SOD1 mutations in either mouse or human models, although there were trends across multiple different assays that inflammatory responses were reduced in mSOD1 glia.

3.4.1 Spinal cord glia increase production of NO more than cortical glia when treated with inflammatory mediators

It is well established that both astrocytes and microglia contribute to the death of motor neurons in ALS (Boillee et al., 2006; Yamanaka et al., 2008). Regional heterogeneity in the inflammatory responses of these glial cells may account for the specific pattern of damage in mutant SOD1 models of ALS. While both the cortex and spinal cord experience degeneration in SOD1^{G93A} mice, motor neurons in the spinal cord are more significantly affected (Leichsenring et al., 2006).

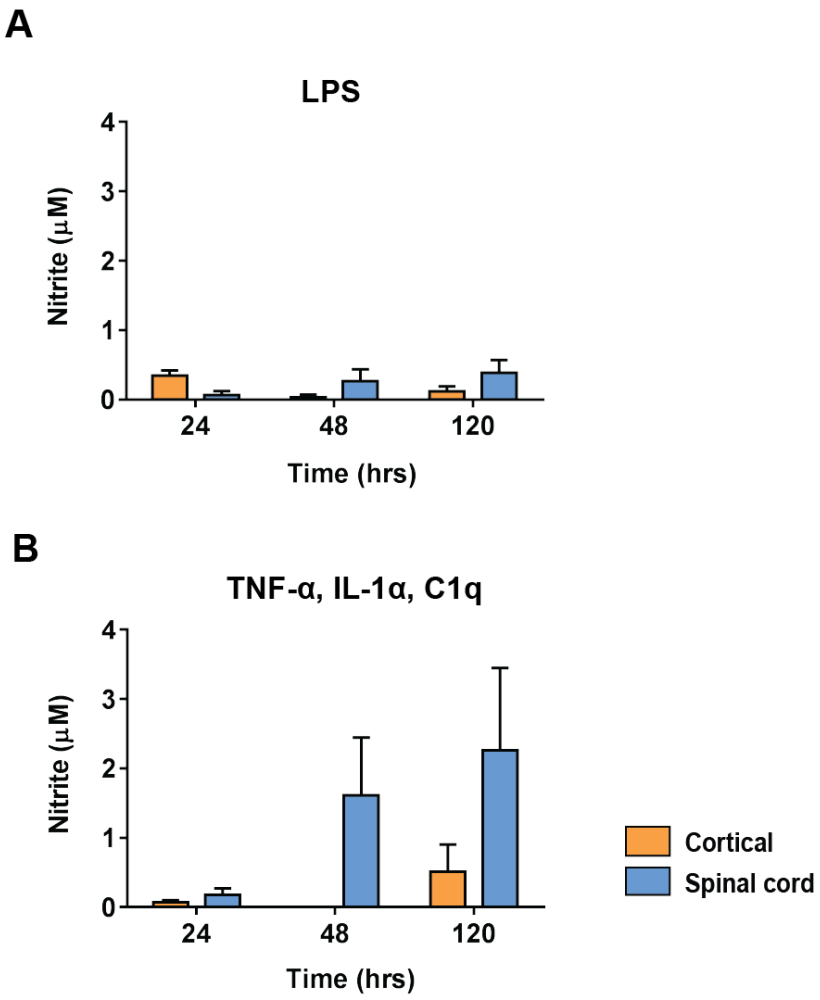

Figure 3.18. NO production in human iPSC-derived astrocytes patterned to the cortex and spinal cord treated with inducers of inflammation. Nitrite production of cortical and spinal cord patterned human iPSC-derived astrocytes exposed to **(A)** 80 µg/ml LPS or **(B)** 100 ng/ml TNF-α, 100ng/ml IL-1α and 1000 ng/ml C1q measured by Griess assay at 24, 48 and 120 hours following initial treatment and normalised to the levels of nitrite from untreated cells at each timepoint. Data are expressed as the mean ± SEM. A mixed model ANOVA with Tukey post hoc tests was used for statistical comparison. N=3.

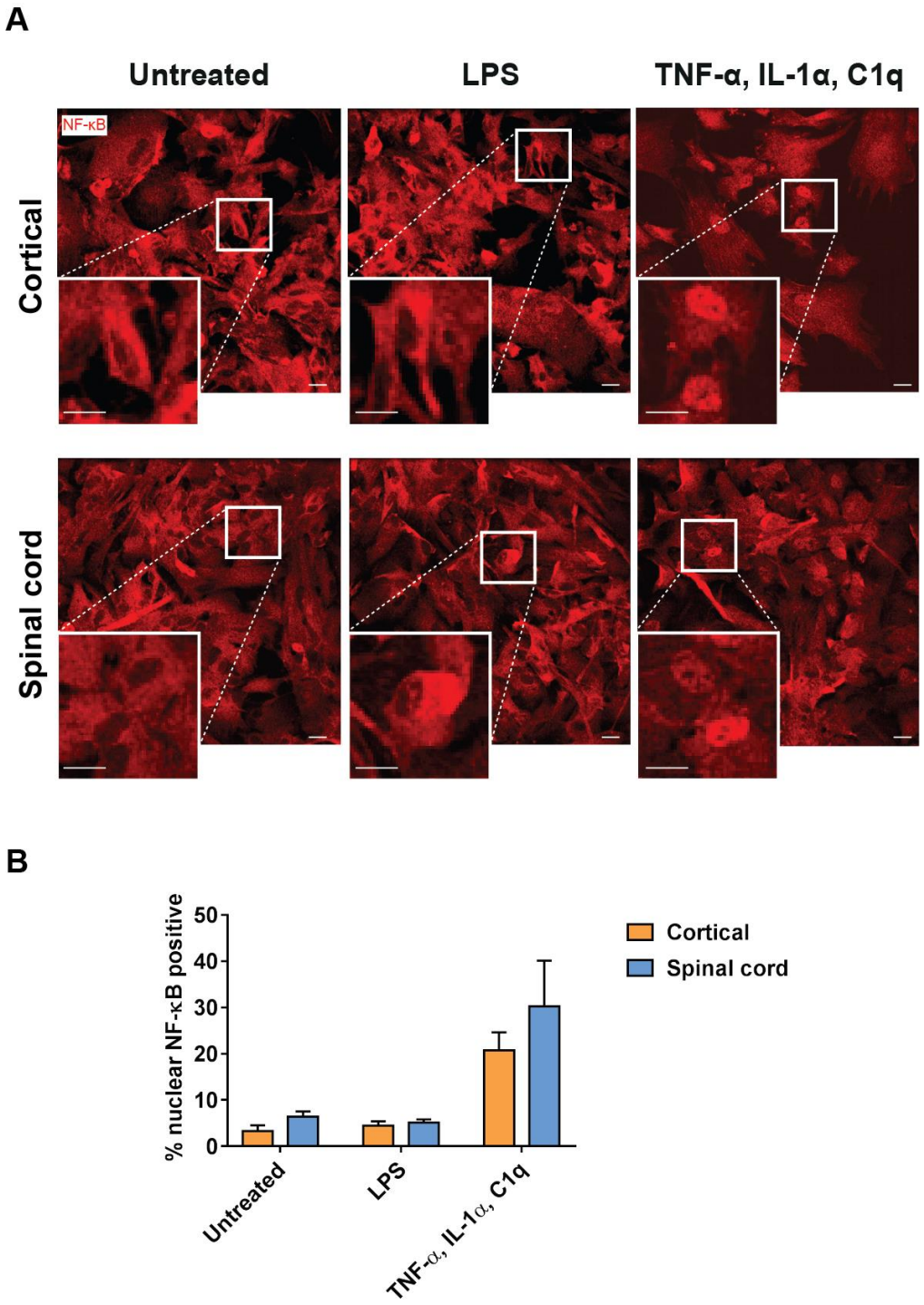

Figure 3.19. NF-κB localisation in cortical and spinal cord patterned human iPSC-derived astrocytes following exposure to inflammatory mediators. (A) Representative images of NF-κB immunostaining (red) and **(B)** quantification of the % nuclear NF-κB positive cells in human iPSC-derived cortical and spinal cord patterned astrocyte cultures treated with 80 µg/ml LPS or 100 ng/ml TNF-α, 100 ng/ml IL-1α and 1000 ng/ml C1q. Data are expressed as the mean ± SEM. A two-way ANOVA with post-hoc Tukey tests was used for statistical comparison. Scale bar: 20 µm. N=3.

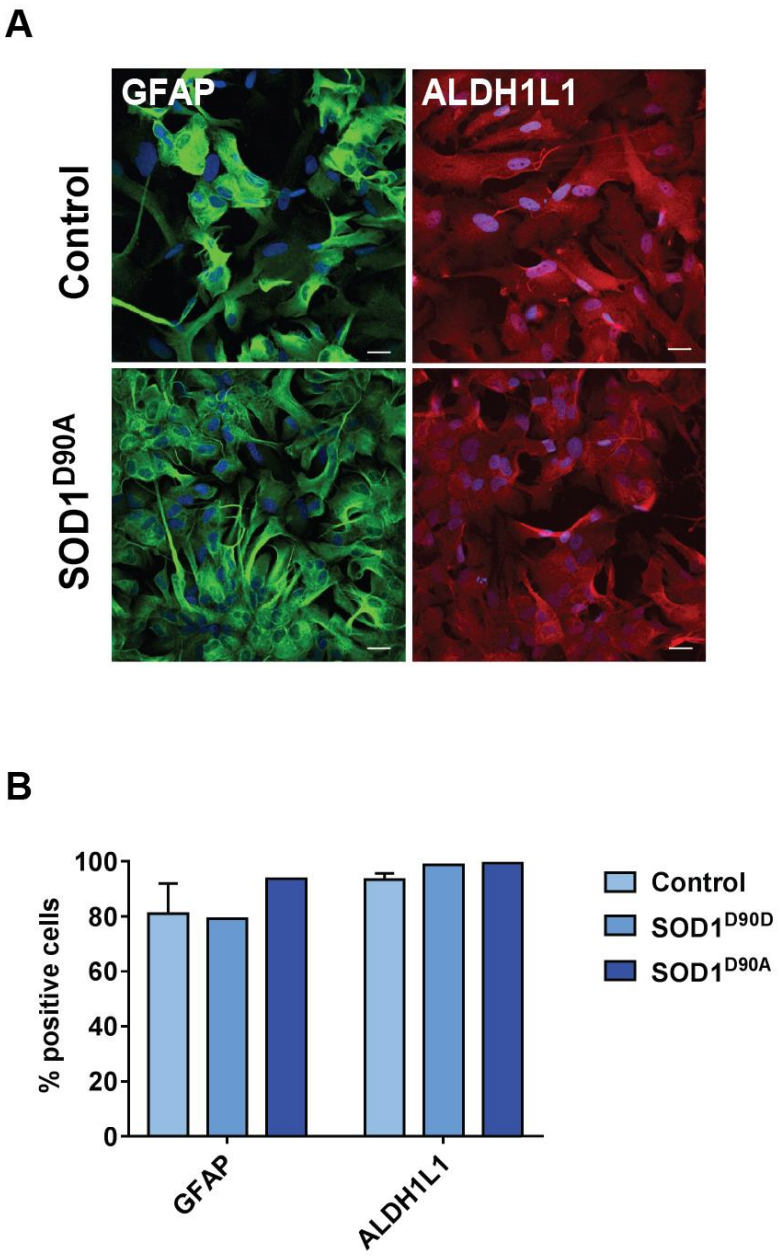

Figure 3.20. Expression of astrocytic markers in ALS patient iPSC-derived SOD1^{D90A} astrocyte cultures. (A) Representative images and **(B)** quantification of astrocytic markers GFAP (green) and ALDH1L1 (red) in human iPSC-derived control, an isogenic SOD1^{D90D} control line and SOD1^{D90A} astrocyte cultures. Data are expressed as the mean ± SEM. A statistical test was not performed due to low n numbers. Scale bar: 20 µm. N=2-3.

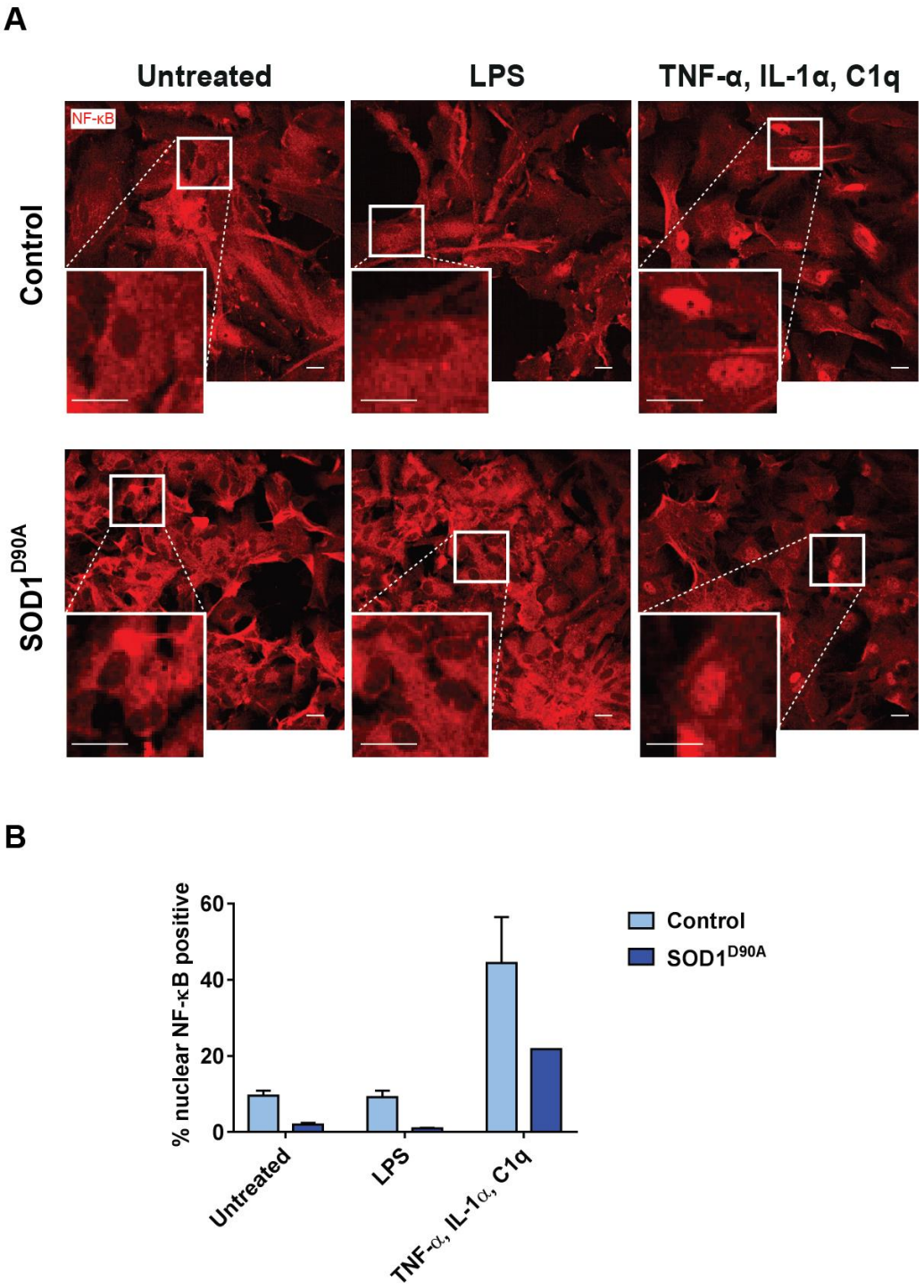

Figure 3.21. NF-κB localisation in SOD1^{D90A} ALS patient iPSC-derived astrocytes following exposure to inflammatory mediators. (A) Representative images of NF-κB immunostaining (red) and **(B)** quantification of human iPSC-derived control and SOD1^{D90A} astrocyte cultures for the % nuclear NF-κB positive cells treated with 80 µg/ml LPS or 100 ng/ml TNF-α, 100 ng/ml IL-1α and 1000 ng/ml C1q. Data are expressed as the mean ± SEM. A statistical test was not performed due to low n numbers. Scale bar: 20 µm. N=2-3.

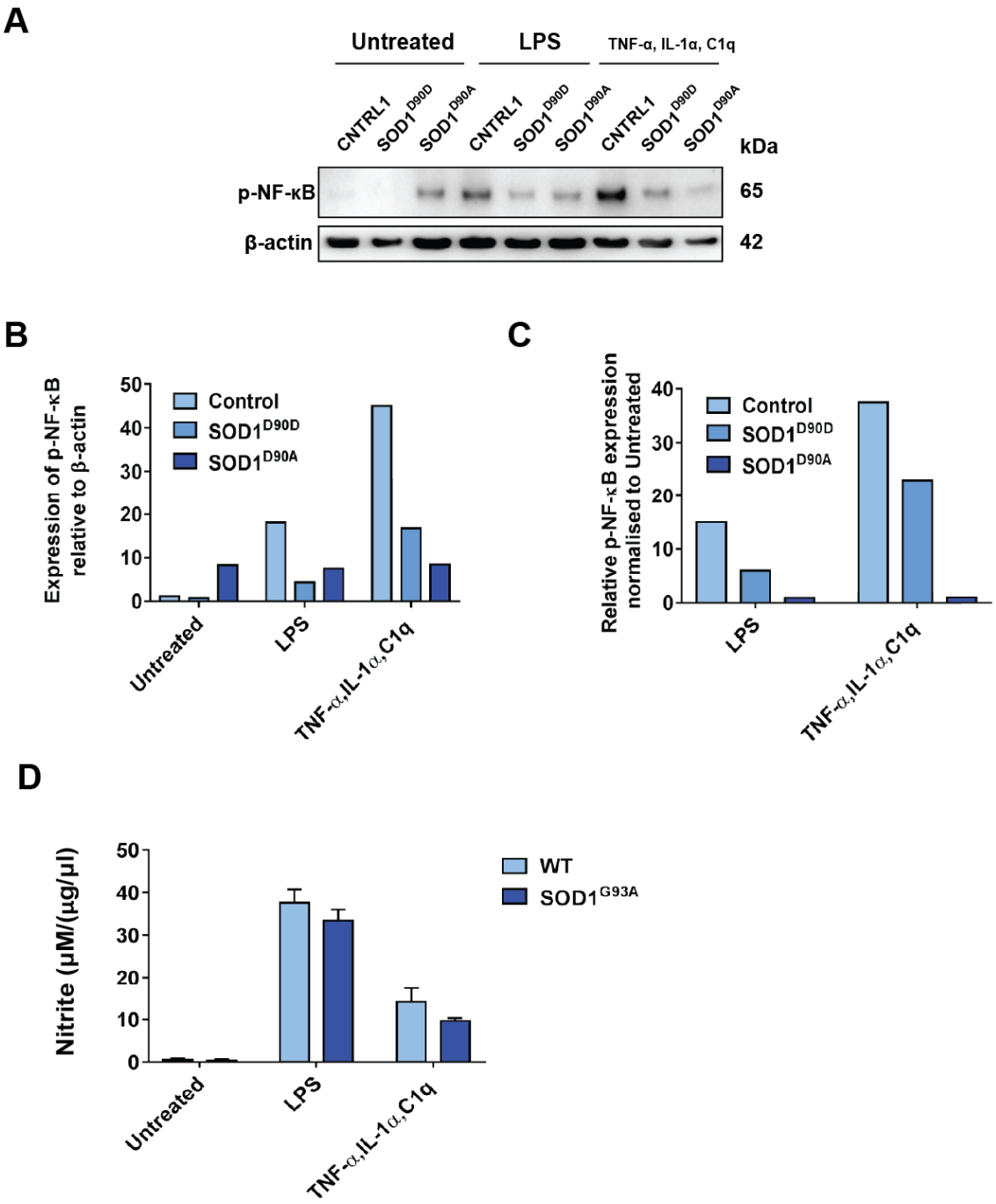

Figure 3.22. NF-κB expression and NO production in mouse and human mSOD1 glia following treatment with TNF-α, IL-1α and C1q. (A) Western blot and quantification **(B, C)** of human iPSC-derived astrocytes: i) a control (CNTRL) line, ii) isogenic SOD1^{D90D} control line and iii) a mutant SOD1^{D90A} line treated with 80 µg/ml LPS or 100 ng/ml TNF-α, 100 ng/ml IL-1α and 1000 ng/ml C1q. N=1-2. **(D)** Nitrite production of wildtype (WT) and SOD1^{G93A} mouse primary glial cultures treated with 80 µg/ml LPS or 100 ng/ml TNF-α, 100 ng/ml IL-1α and 1000 ng/ml C1q. Data are expressed as the mean ± SEM. A two-way ANOVA with post-hoc Tukey tests was used for statistical comparison. N=3.

Mouse primary glial cultures were obtained from the cortex and spinal cord. These cultures displayed similar proportions of astrocytes and microglia, identified by immunofluorescence staining using cell-specific markers. Since manual counting of these cultures is difficult to accurately quantify, FACS analysis was also performed, confirming that cultures from the cortex and spinal cord contained similar proportions of astrocytes and microglia.

In order to study inflammatory responses of glia, the pro-inflammatory signalling molecule NO was first measured in cultures exposed to TNF-α or LPS, two widely used inducers of inflammation (Zamanian et al., 2012; Perriot et al., 2018). Spinal cord glia were found to produce more NO than cortical glia following exposure to inflammatory mediators. Increased iNOS expression was observed following LPS treatment in spinal cord glia by western blot and immunofluorescence. Increased production of pro-inflammatory signalling molecules such as NO in spinal cord glia may contribute to the greater vulnerability of spinal motor neurons to death in mSOD1 mice compared to cortical neurons.

3.4.2 iNOS is responsible for NO production in primary glial cultures following exposure to inflammatory mediators

NO production was almost completely ablated by treatment of glial cultures with the iNOS specific inhibitor 1400W, suggesting that this enzyme was responsible for the vast majority of NO production observed. Blocking NO production with 1400W has been shown to extend the lifespan of $SOD1^{G93A}$ mice (Chen et al., 2010). 1400W has also been shown to be beneficial in other pathological conditions, including ischaemia (Chen et al., 2012), traumatic brain injury (Jafarian-Tehrani et al., 2005) and neuropathic pain (Staunton et al., 2018).

3.4.3 iNOS is differentially expressed between cortical and spinal cord astrocytes and microglia following exposure to inflammatory mediators

These results show that both astrocytes and microglia induce iNOS expression following induction of inflammation. Several studies have identified microglia as the main cell type responsible for increased iNOS expression following treatment with LPS (Kong et al., 1996; Noack et al., 2000; Saura et al., 2005). Furthermore, microglia have been demonstrated to be critical in directing astrocytes to a pro-inflammatory phenotype (Holm et al., 2012; Chen et al., 2015b; Liddelow et al., 2017). However, astrocytes have also been reported to express iNOS following

induction of inflammation (Hamby et al., 2006) and even enhance microglial nitrite production (Sola et al., 2002). Here, LPS caused an increase in the proportion of microglia in mouse primary spinal cord glial cultures, but not in cortical cultures, indicating that there is a region-specific enhanced response of spinal cord microglia to induction of inflammation. To support this possibility, spinal cord microglial cultures, obtained by shaking mixed glial cultures, showed increased NO production compared to cortical cultures, although this experiment was limited by the low yield of microglia obtained.

Previous studies have suggested that iNOS expression is largely restricted to microglia and only very few astrocytes (Saura et al., 2005; Hamby et al., 2006; Saura, 2007). In this study, a significant proportion of astrocytes were found to express iNOS following LPS treatment. This may be due to a higher LPS concentration used in these experiments compared to previous studies. Interestingly, an increased proportion of iNOS positive astrocytes were observed in spinal cord cultures compared to cortical cultures. This effect may be due to the proliferation of microglia in spinal cord cultures following LPS treatment, but may also be due to an elevated intrinsic ability of spinal cord astrocytes to respond to inflammatory stimuli. Therefore, regional differences between cortical and spinal cord glial inflammatory responses may be due to differences in both astrocytes and microglia.

3.4.4 Similar levels of induction of inflammation in WT and SOD1^{G93A} glia

While a regional difference in NO production and iNOS expression was observed following induction of inflammation, no clear differences were found between WT and SOD1^{G93A} glia from either the cortex or spinal cord. Previously, SOD1^{G93A} glial cultures have been reported to produce more NO and express more iNOS than WT cultures (Hensley et al., 2006). Furthermore, increased NO production has been observed in mSOD1 microglial cultures from neonatal and adult mice (Weydt et al., 2004; Xiao et al., 2007; Liao et al., 2012). Differential iNOS expression and NO production may be due to different inflammatory inducers used in these studies. In addition, the ages of the mice at which cultures were taken may account for these differences in results, as both astrocytes and microglia have been shown to undergo large changes in their transcriptome with age, becoming more reactive (Soreq et al., 2017; Clarke et al., 2018).

Several different model systems, including primary mouse mixed glial cultures, have suggested that mSOD1 glia exhibit a non-cell autonomous phenotype when co-cultured with motor neurons (Nagai et al., 2007; Marchetto et al., 2008; Haidet-Phillips et al., 2011; Meyer et al., 2014). However, in this study no differences were observed in the production of NO under basal conditions between $SOD1^{G93A}$ and WT glia. Therefore, excessive NO production may not be responsible for this non-cell autonomous effect observed *in vitro*. Nevertheless, NO may still be an important factor in ALS, since *NOS2* knockout or pharmacological inhibition both extend lifespan of $SOD1^{G93A}$ mice (Martin et al., 2007; Chen et al., 2010). Although there were no differences in the magnitude of NO production between $SOD1^{G93A}$ and WT cultures, regional differences in NO signalling between the cortex and spinal cord may only become apparent under inflammatory conditions, such as those that occur in the $SOD1^{G93A}$ mouse.

iNOS expression can be induced by activation of the NF-κB complex (Xie et al., 1994). NF-κB activation increases over the lifespan of $SOD1^{G93A}$ mice, and in co-culture, inhibition of NF-κB rescues motor neuron death and ablates NO production in $SOD1^{G93A}$ microglia (Frakes et al., 2014). In this Chapter, LPS treatment activated NF-κB signalling in primary mouse glial cultures, measured by the translocation of NF-κB to the nucleus. Although a regional difference in iNOS expression was observed between cortical and spinal cord glial cultures following LPS treatment, there were no differences in the number of nuclear NF-κB positive cells. Furthermore, there were no differences in the number of nuclear NF-κB positive cells between WT and $SOD1^{G93A}$ glia following LPS treatment. The relatively high proportion of cells that were positive for NF-κB translocation (~60%) suggests that many cells were affected by LPS treatment, but only a minority of these cells express iNOS in cortical cultures. This may be due to regionally different mechanisms of transcriptional suppression of NF-κB in the nucleus or additional NF-κB independent mechanisms regulating iNOS expression. Several other transcription factors including signal transducer and activator of transcription 1 alpha (STAT-1α) and interferon regulatory factor-1 (IRF-1) have been implicated in regulating iNOS expression following LPS treatment (Kleinert et al., 2004), which may be responsible for the differences between cortical and spinal cord glia observed in these experiments.

3.4.5 Astrocytes patterned to the cortex and spinal cord can be obtained from human iPSCs

In order to further explore regional differences in the inflammatory responses of glia, human iPSC-derived astrocytes patterned to the cortex and spinal cord were obtained by adapting previously described protocols (Shi et al., 2012; Hall et al., 2017). Using these protocols, NPCs were directed to the forebrain/midbrain and ventral spinal cord, albeit with significant line to line variability. Contrary to a previous study there was reduced expression of regional markers as NPCs were differentiated into astrocytes (Krencik et al., 2011). Astrocytes may downregulate regional markers expressed during development and differences with the aforementioned study may be explained by a lack of multiple lines used. Alternatively, FGF used to promote gliogenesis may cause caudalisation of progenitors, reducing the expression of rostral markers such as OTX2 and FOXG1. Patterning factors may require longer periods of administration to maintain the positional identity of NPCs and astrocytes *in vitro*.

3.4.6 Human iPSC-derived astrocytes patterned to the spinal cord may elicit a stronger inflammatory response than cortical astrocytes

In this study, iPSC-derived astrocytes did not produce significant levels of NO in response to LPS treatment. This may be due to the lack of microglia present in the culture (Liddelow et al., 2017) or differences between mouse and human astrocytes (Tarassishin et al., 2014). While LPS treatment did not result in NO production, a combination of pro-inflammatory cytokines TNF-α, IL-1α and C1q induced the production of NO and translocation of NF-κB to the nucleus. TNF-α, IL-1α and C1q were previously discovered to induce a pro-inflammatory state in astrocytes that mimics LPS treatment (Liddelow et al., 2017). However, no increase in iNOS expression was detected by western blot or immunofluorescence following treatment with TNF-α, IL-1α and C1q (data not shown), likely because of the low levels of NO production resulting from this treatment.

While NO production was low and there was high variability between different iPSC lines, a trend towards increased production of NO in spinal cord patterned astrocytes was observed, in agreement with the findings from primary glial cultures from the cortex and spinal cord. Furthermore, there was a trend towards

an increase in the number of cells that were positive for translocation of NF-κB to the nucleus in spinal cord patterned astrocytes compared to cortical astrocytes.

3.4.7 ALS patient iPSC-derived SOD1^{D90A} astrocytes may elicit reduced inflammatory responses compared to control astrocytes

In agreement with results from SOD1^{G93A} glial cultures, inflammatory responses of SOD1^{D90A} human iPSC-derived astrocytes were not significantly different to control astrocytes, but did display a trend towards a reduced response to inflammatory induction measured by western blot for the phosphorylation of NF-κB subunit p65 and by immunofluorescence for the nuclear translocation of NF-κB. These experiments need to be repeated in order to confirm these results.

Potential differences between SOD1^{G93A} primary glial cultures and SOD1^{D90A} human iPSC-derived astrocytes may be due to interspecies differences, the overexpression of mutant protein in mouse primary glial cultures or differences in the site of SOD1 mutation. Alternatively, serum present in the media of primary glial cultures, which has been shown to induce a reactive phenotype in glia, may affect subsequent responses to inflammatory stimuli (Foo et al., 2011; Perriot et al., 2018). Furthermore, factors used to pattern or promote the differentiation of human iPSC-derived astrocytes may also affect the reactivity state of the resulting astrocytes obtained (Noble et al., 2011; Sirko et al., 2013). A reduced NF-κB response in mSOD1 astrocytes could be detrimental as astrocytic NF-κB has been shown to be beneficial in the early stages of disease in SOD1^{G93A} mice (Ouali Alami et al., 2018).

In conclusion, the results of this Chapter demonstrate that spinal cord glia display increased sensitivity to pro-inflammatory stimuli, even though this effect was more prominent in glial cultures and not significant in iPSC-derived astrocytes. Thus, spinal cord glia produce more NO and express more iNOS than cultures from the cortex. While SOD1^{G93A} glial cultures were not different to WT cultures in this respect, the increased ability of spinal cord glia to elicit an inflammatory response compared to cortical glia may contribute to the pattern of damage observed in mSOD1 models of ALS, where motor neurons in the spinal cord are more affected than motor neurons in the cortex. Finally, mSOD1 astrocytes may display a reduced response to inflammatory inducers, which may increase the susceptibility of motor neurons to death in the early disease phase of ALS.

Chapter 4: Regulatory role of the glial heat shock response in inflammatory signalling in models of ALS.

4.1 Introduction

4.1.1 The HSR in glia

As previously discussed, the HSR is a cytoprotective response to stressful conditions involving the upregulation of Hsps to maintain protein homeostasis and inhibit the apoptotic machinery. It is now clear that different cell types vary in their induction threshold and the strength of their HSR (Tsvetkov et al., 2013; Sala et al., 2017). For example, motor neurons have a surprisingly high threshold for the induction of the HSR and are therefore unable to upregulate Hsps under stressful conditions, which may confer motor neuron-specific vulnerability in ALS (Batulan et al., 2003). Conversely, astrocytes are able to robustly upregulate Hsps in response to stress (Nishimura et al., 1991; Marcuccilli et al., 1996; Kalmar et al., 2002).

It has been hypothesised that astrocytes may supplement motor neurons with Hsps as part of their supportive role (Kalmar and Greensmith, 2017; San Gil et al., 2017). Astrocytes release Hsps into the extracellular milieu (Guzhova et al., 2001) and motor neurons are able to take up exogenously applied Hsps from their surroundings (Robinson et al., 2005). Therefore, motor neurons may rely on surrounding astrocytes for the supply of Hsps under proteotoxic stress conditions, such as those that occur in ALS.

Astrocytes are known to activate neuroprotective mechanisms in response to a number of stressful conditions, which can become compromised in disease. For example, a previous study has shown that mSOD1 astrocytes lose their ability to provide a stress-dependent STAT3-mediated neuroprotective mechanism (Tyzack et al., 2017). Loss of other neuroprotective pathways such as the HSR may also occur in mSOD1 astrocytes. In ALS tissues and models, aggregates containing Hsps are found in glia as well as motor neurons (Bruijn et al., 1997; Watanabe et al., 2001). Sequestration of Hsps in astrocytes may lead to a loss of Hsp supplementation to motor neurons, possibly contributing to motor neuron death in ALS.

4.1.2 Effects of the HSR on inflammatory responses

In addition to aiding protein homeostasis, Hsps have also been linked to anti-inflammatory effects that act to counterbalance the overactivation of the NO-iNOS-NF-κB inflammatory pathway. An early indication that the HSR is involved in inflammatory signalling came from a study that showed that increased cytokine production occurred in HSF-$1^{-/-}$ mice compared with HSF-$1^{+/-}$ mice following treatment with LPS (Xiao et al., 1999). Furthermore, preconditioning rats with hyperthermia reduced NF-κB activation following intracerebral injection of LPS (Heneka et al., 2000).

Mice overexpressing the potent anti-aggregation Hsp, Hsp70, have been shown to be less vulnerable to ischaemic damage, experiencing reduced neurological deficits and inflammation compared with WT mice following cerebral artery occlusion (Zheng et al., 2008; Barreto et al., 2012). Furthermore, knockdown of Hsp70 using antisense oligonucleotides partially abolished the inhibitory effects of heat stress on iNOS expression in primary glial cultures following treatment with LPS (Feinstein et al., 1996). Together, these findings suggest that Hsp70 plays an important role in the anti-inflammatory effects of the HSR.

The mechanism by which the HSR reduces inflammatory signalling remains unclear. Hsp70 has been shown to inhibit pro-inflammatory NF-κB signalling at several different levels of the NF-κB signalling pathway. Hsp70 has been reported to inhibit NF-κB both through direct interaction with the complex (Guzhova et al., 1997) and indirectly through inhibition of the NF-κB activators, TRAF6 (Chen et al., 2006) or IKK-γ (Ran et al., 2004). Alternatively, Hsp70 may reduce the degradation of the NF-κB inhibitor, IκB (Wong et al., 1997) or reduce the expression of the NF-κB p65 subunit (Sheppard et al., 2014).

In addition to Hsp70, there is evidence that other Hsps also play roles in NF-κB-mediated inflammatory processes. The small Hsp, Hsp27, has been shown to inhibit IKK-β, reducing NF-κB activation (Park et al., 2003). Furthermore, Hsp27 has been shown to enhance the degradation of the NF-κB activator, TRAF6 (Wu et al., 2009). Conversely, Hsp90 has also been implicated in NF-κB signalling as an activator of IKKs (Chen et al., 2002), through an interaction with IKK-α (Park et al., 2003). Therefore, Hsp27 and Hsp90 may have opposing actions in NF-κB signalling.

4.1.3 Aims

Since Hsps are known to have neuroprotective properties, they may therefore represent a promising therapeutic target in neurodegenerative diseases such as ALS. Glial Hsps in particular may be interesting in the context of ALS, as Hsps can be transferred from glia to neurons under stressful conditions to aid protein homeostasis and inhibit apoptosis. Furthermore, inducible Hsps have anti-inflammatory effects that may be beneficial in reducing non-cell autonomous mechanisms of motor neuron death observed in ALS. Regional differences in inflammatory signalling between cortical and spinal cord glia described in Chapter 3 of this Thesis may be partly explained by a differential HSR of glia from these regions. To investigate the regional differences in the glial HSR in ALS, cortical and spinal cord $SOD1^{G93A}$ glial cultures and ALS patient iPSC-derived $SOD1^{D90A}$ astrocytes patterned to the cortex and spinal cord were exposed to heat stress to induce the HSR and inducible Hsps; the expression levels of Hsp70, Hsp27 and Hsp90 were then measured. Furthermore, the effects of the glial HSR on inflammatory signalling were assessed by combining the inflammatory inducer LPS with exposure to heat stress.

The specific aims of this Chapter are to:

1) Assess whether regional differences in the HSR exist between cortical and spinal cord glia;
2) Determine whether any regional differences in the HSR are affected by ALS-causing mSOD1 mutations;
3) Evaluate whether regional differences in the NO-iNOS-NF-κB inflammatory response are affected by induction of the HSR;
4) Determine the effects of mSOD1 on the ability of the HSR to affect glial inflammatory responses.

Note: Some of the experiments described in this Chapter were undertaken in collaboration with Rebecca San Gil, a PhD student in the Greensmith lab. These experiments are indicated in the relevant figure legends.

4.2. Results

4.2.1 Hsp70 expression levels in mSOD1 models of glia

In order to assess the HSR in glia, mouse primary glial cultures were initially exposed to heat stress and Hsp70 expression levels were measured (Fig. 4.1). Glial cultures exposed to heat stress upregulated and maintained Hsp70 for at least 24 hours following heat stress (Fig. 4.1 A, B). Next, heat stress-induced expression of Hsp70 was measured in $SOD1^{G93A}$ and WT glial cultures from the cortex and spinal cord. While no differences were observed between glial cultures from the cortex and spinal cord, Hsp70 expression levels in $SOD1^{G93A}$ glia were consistently lower than WT glia following heat stress, although due to experimental variability this did not reach statistical significance (Fig. 4.1 C, D). Expression of inducible Hsp70 mRNA was significantly reduced in $SOD1^{G93A}$ glia compared with WT glia following heat stress, supporting data from western blots (Fig. 4.1 E). LPS treatment did not induce Hsp70 expression.

Next, Hsp70 expression was assessed in control and $SOD1^{D90A}$ ALS patient iPSC-derived astrocytes after heat stress. Unlike primary mouse glial cultures, iPSC-derived astrocytes did not upregulate Hsp70 after heat stress (42°C for 30 minutes), but required a prolonged stress (42°C for 2 hours) for Hsp70 induction (Fig. 4.2). The duration of Hsp70 induction was not as persistent in iPSC-derived astrocytes as in primary glial cultures, with a decrease in Hsp70 after 24 hours compared to 4 hours following heat stress. Hsp70 expression was variable between control and $SOD1^{D90A}$ lines, however, when Hsp70 expression following heat shock was compared to pre-heat shock levels for each line, there was a clear trend of decreased expression of Hsp70 in $SOD1^{D90A}$ astrocytes compared with control astrocytes (Fig. 4.3 A-C). Furthermore, a $SOD1^{D90A}$ line expressed ~50% of the Hsp70 expression of its isogenic-paired control (Fig. 4.3 D).

In order to examine whether the results obtained *in vitro* are relevant to *in vivo* expression levels, Hsp70 expression levels in the brain and spinal cord were compared between $SOD1^{G93A}$ and WT mice at different stages of disease. Hsp70 levels were decreased at presymptomatic (day 40) and symptomatic (day 75) ages in the $SOD1^{G93A}$ brain (Fig. 4.4 A, B). Conversely, there was a trend towards an increase in Hsp70 levels with disease progression in the $SOD1^{G93A}$ spinal cord. (Fig. 4.4 C, D).

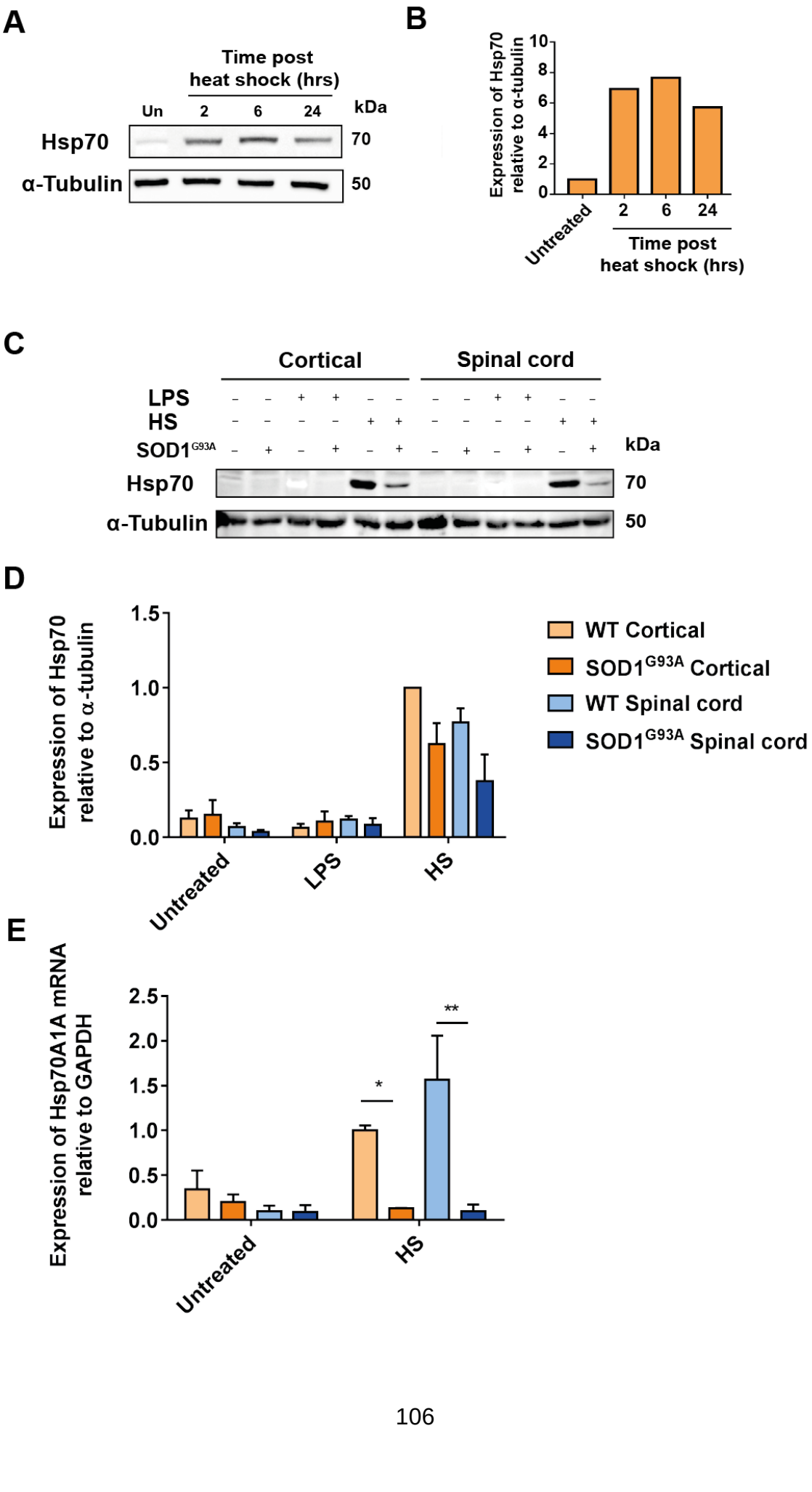
A
Time post heat shock (hrs)
Un
2
6
24
kDa
Hsp70
70
α-Tubulin
50
B
Expression of Hsp70 relative to α-tubulin
10
8
6
4
2
0
Untreated
2
6
24
Time post heat shock (hrs)
C
Cortical
Spinal cord
LPS
HS
SOD1G93A
kDa
Hsp70
70
α-Tubulin
50
D
Expression of Hsp70 relative to α-tubulin
1.5
1.0
0.5
0.0
Untreated
LPS
HS
WT Cortical
SOD1G93A Cortical
WT Spinal cord
SOD1G93A Spinal cord
E
Expression of Hsp70A1A mRNA relative to GAPDH
2.5
2.0
1.5
1.0
0.5
0.0
*
**
Untreated
HS

Figure 4.1. Hsp70 expression levels in SOD1^{G93A} cortical and spinal cord glial cultures following heat stress. Western blot **(A)** and quantification **(B)** of Hsp70 protein expression in cortical glial cultures following heat shock of 42°C for 30 minutes and collected 2, 6 or 24 hours later. N=1. Western blot **(C)** and quantification **(D)** of Hsp70 protein expression in SOD1^{G93A} and wildtype (WT) cortical and spinal cord glial cultures exposed to 80 µg/ml LPS or heat stress (HS) of 42 °C for 30 minutes and collected 24 hours later. N=4. **(E)** qPCR quantification of Hsp70A1A mRNA from wildtype (WT) and SOD1^{G93A} cortical and spinal cord glial cultures exposed to heat stress (HS) at 42°C for 30 minutes and collected 24 hours later. N=2-3. Data are expressed as the mean ± SEM. A two-way ANOVA with post-hoc Bonferroni tests was used for statistical comparison. P=*≤0.05, **≤0.01. (Data for Fig. 4.1 A, B collected by Rebecca San Gil).

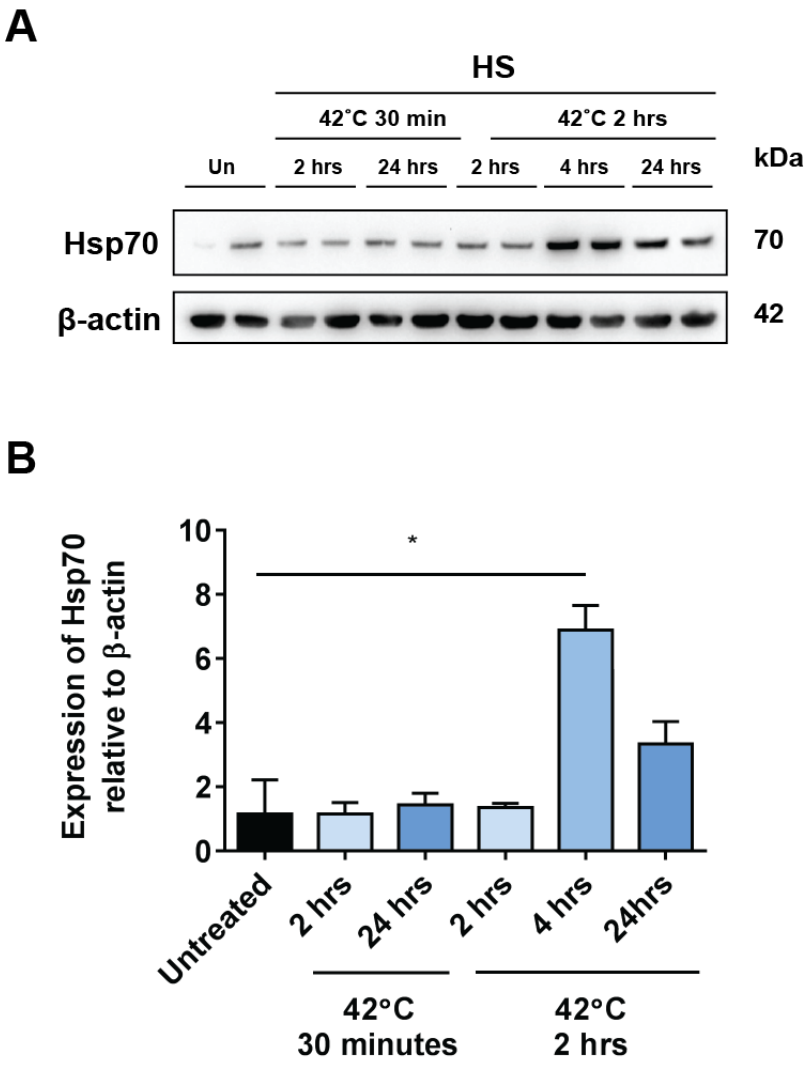

Figure 4.2. Hsp70 expression levels in human iPSC-derived astrocytes following heat stress. Western blot **(A)** and quantification **(B)** of Hsp70 protein expression levels in human iPSC-derived astrocytes exposed to heat stress (HS) (42°C for 30 minutes or 2 hours) and collected 2, 4 or 24 hours later. Data are expressed as the mean ± SEM. A one-way ANOVA with post-hoc Tukey tests was used for statistical comparison. P=*≤0.05. N=2.

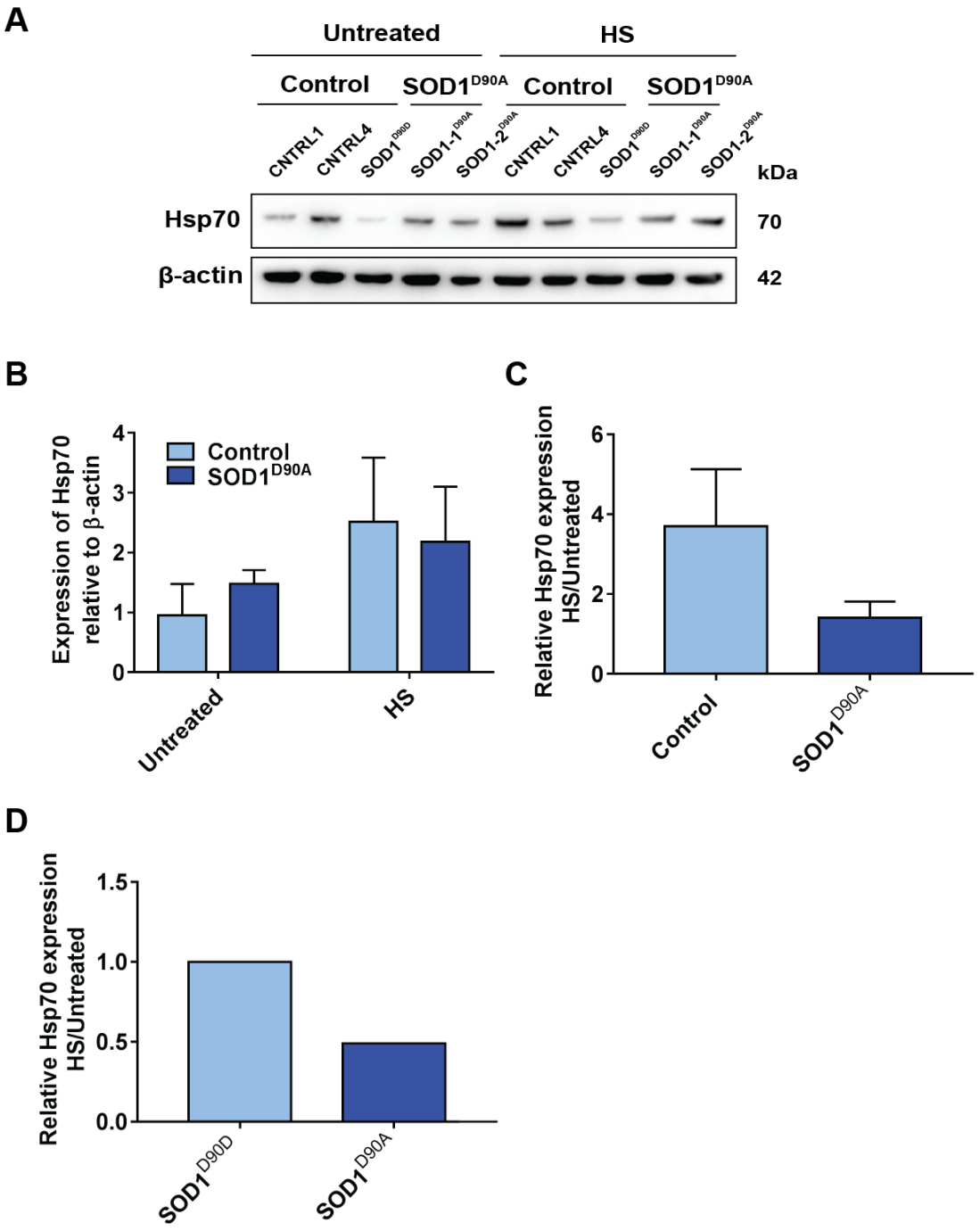

Figure 4.3. Hsp70 expression levels in ALS patient iPSC-derived SOD1^{D90A} astrocytes following heat stress. Western blot **(A)** and quantification **(B-D)** of Hsp70 protein levels in SOD1^{D90A} and control human iPSC-derived astrocytes, including an SOD1^{D90D} isogenic control line, exposed to heat stress (HS) of 42°C for 2 hours and then collected 4 hours later. Data are expressed as the mean ± SEM. A statistical test was not performed due to low n numbers. N=2-3.

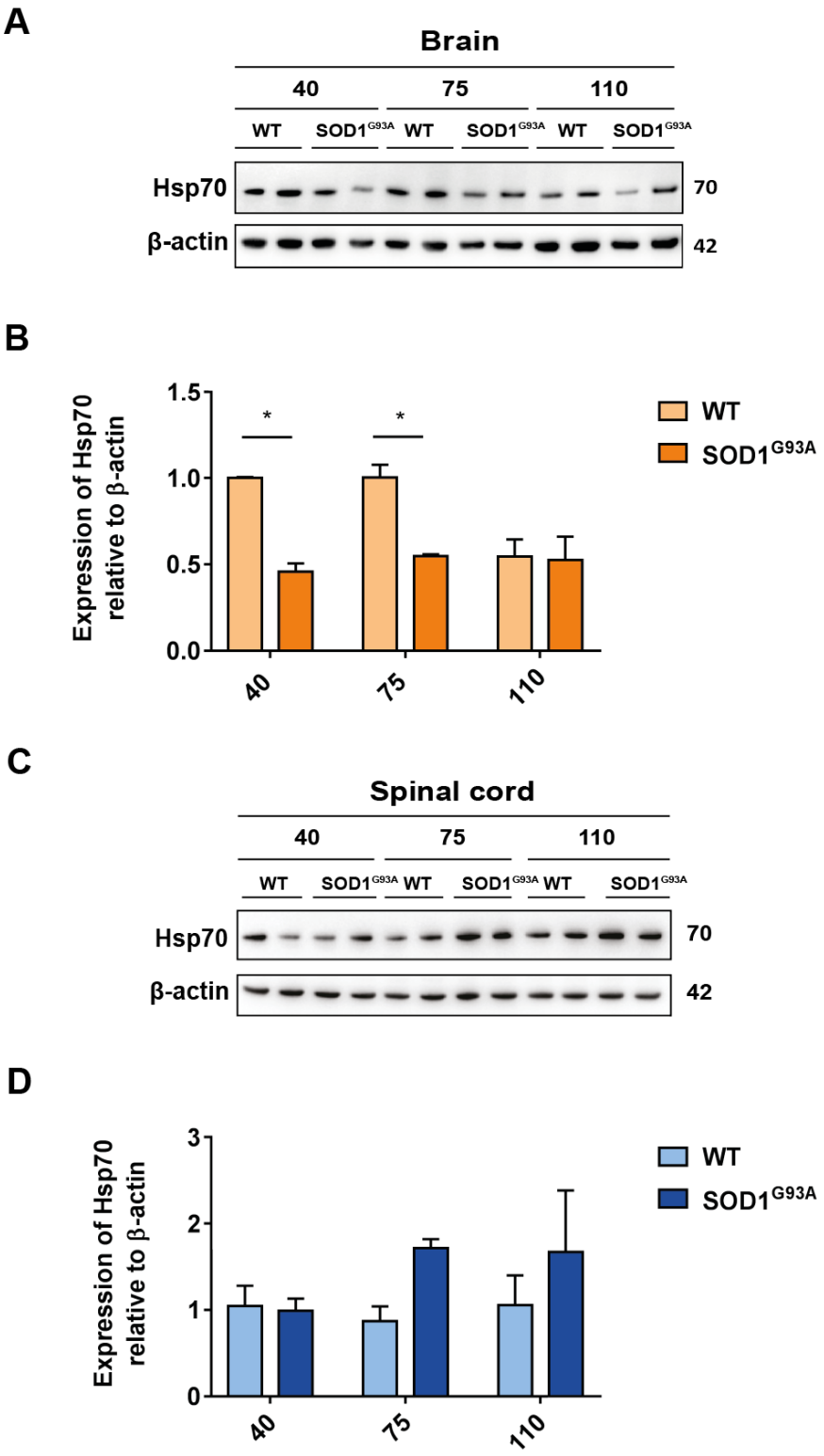

Figure 4.4. Hsp70 expression levels in the brain and spinal cord of adult SOD1^{G93A} mice. Western blot and quantification of Hsp70 expression in brain **(A, B)** and spinal cord **(C, D)** lysates from 40, 75 and 110 day old wildtype (WT) and SOD1^{G93A} mice. P=*≤0.05. Data are expressed as the mean ± SEM. A two-way ANOVA with post-hoc Bonferroni tests was used for statistical comparison. N=2-5.

4.2.2 Hsp27 and Hsp90 expression levels in mSOD1 models of glia

Although Hsp70 is the most widely studied Hsp, several other Hsps are also upregulated following induction of the HSR. Hsp27, or the mouse ortholog Hsp25, is an inducible small Hsp, which has previously been shown to reduce NF-κB activation (Park et al., 2003).

However, in these experiments, levels of Hsp25 were unaltered following treatment with either LPS or heat stress in either cortical or spinal cord glial cultures. Interestingly, spinal cord glia expressed Hsp25 at higher levels when compared with cortical glia under basal conditions (Fig. 4.5 A, B). Using immunofluorescence, increased expression of Hsp25 in spinal cord cultures was found in GFAP-positive astrocytes (Fig. 4.6). Next, immunostaining for Hsp25 in sections of WT and 90 day old (symptomatic) $SOD1^{G93A}$ spinal cord and brain revealed that Hsp25 levels were higher in the spinal cord and were particularly enriched in motor neurons (Fig. 4.7 A). Hsp25 expression partially correlated with increases in GFAP expression in the $SOD1^{G93A}$ spinal cord at presymptomatic (day 40), symptomatic (day 70) and late stages (day 105) of disease (Fig. 4.7 B-D).

While increased expression of Hsp25 was observed in spinal cord glial cultures compared with cortical cultures, only a trend of increased expression of Hsp27 was observed in human iPSC-derived spinal cord astrocytes, compared with iPSC-derived cortical astrocytes (Fig. 4.8 A, B). Furthermore, in agreement with findings from mouse primary glial cultures, there were no differences in Hsp27 expression between control and $SOD1^{D90A}$ human iPSC-derived astrocytes (Fig. 4.9).

Hsp90 is another cytosolic Hsp that has been reported to be inducible under conditions of cellular stress (Vigh et al., 1997). Hsp90 binds to and stabilises HSF-1 in the cytoplasm and thus Hsp90 inhibitors have been used to induce Hsps and inhibit inflammation (Dello Russo et al., 2006). In this study, Hsp90 was not induced by LPS or heat stress in primary glial cultures from either the cortex or the spinal cord (Fig 4.10). Furthermore, there was no difference in the expression of Hsp90 between $SOD1^{G93A}$ and WT glial cultures.

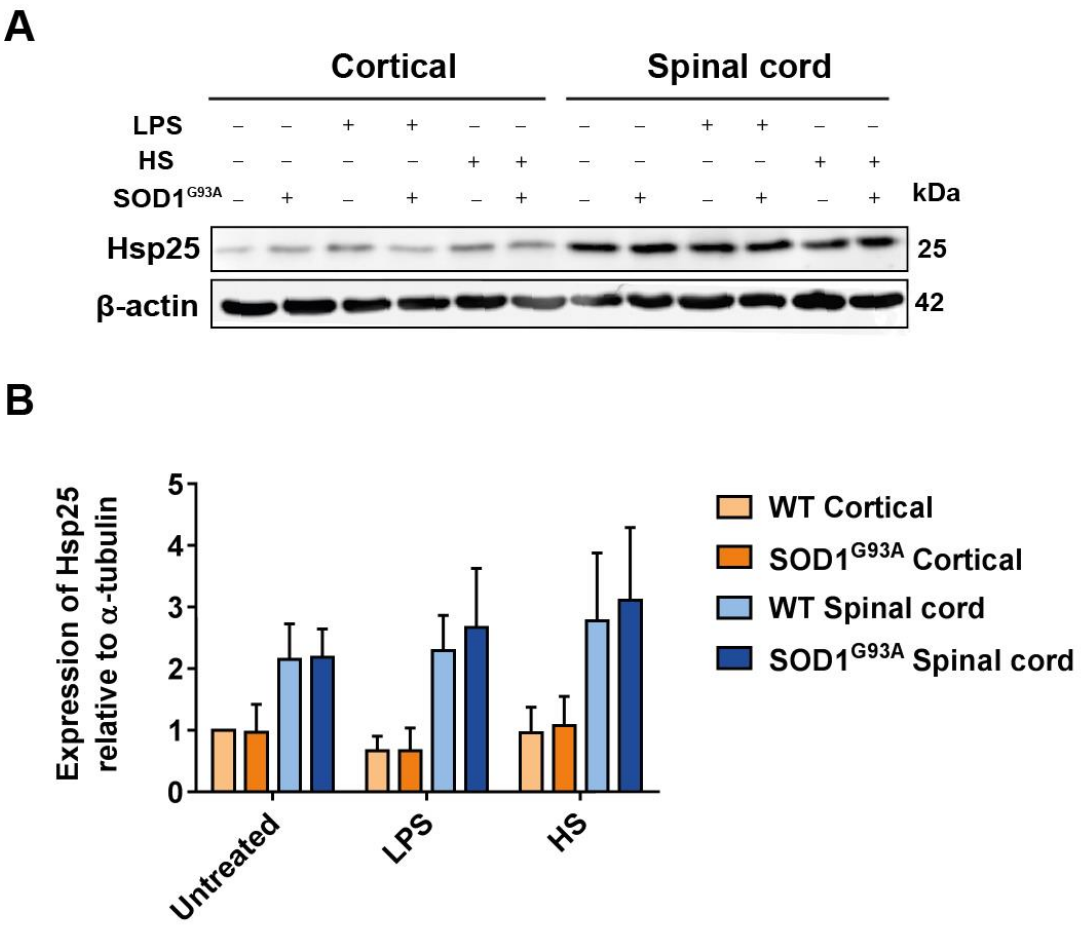

Figure 4.5. Hsp25 expression levels in SOD1^{G93A} cortical and spinal cord glial cultures following treatment with LPS or heat stress. Western blot **(A)** and quantification **(B)** for Hsp25 of wildtype (WT) and SOD1^{G93A} cortical and spinal cord glial cultures treated with 80 µg/ml LPS or heat stress of 42°C for 30 minutes. Data are expressed as the mean ± SEM. A two-way ANOVA with post-hoc Tukey tests was used for statistical comparison. N=3.

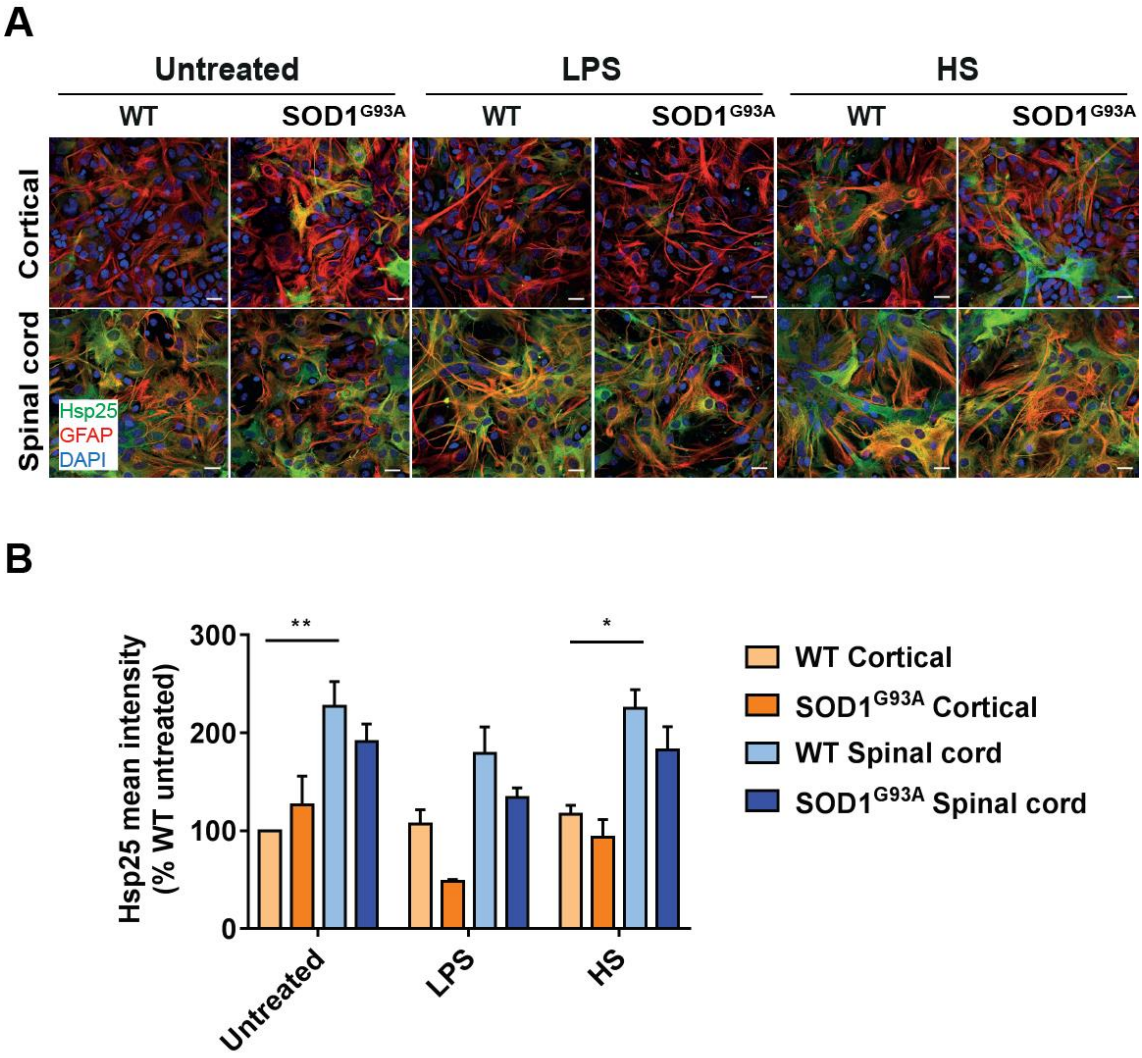

Figure 4.6. Hsp25 expression levels in SOD1^{G93A} cortical and spinal cord glial cultures following treatment with LPS or heat stress. (A) Representative images and **(B)** quantification for Hsp25 of wildtype (WT) and SOD1^{G93A} cortical and spinal cord glial cultures treated with 80 µg/ml LPS or heat stress of 42°C for 30 minutes. Data are expressed as the mean ± SEM. A two-way ANOVA with post-hoc Tukey tests was used for statistical comparison. P=*≤0.05, **≤0.01. Scale bar: 20µm. N=3.

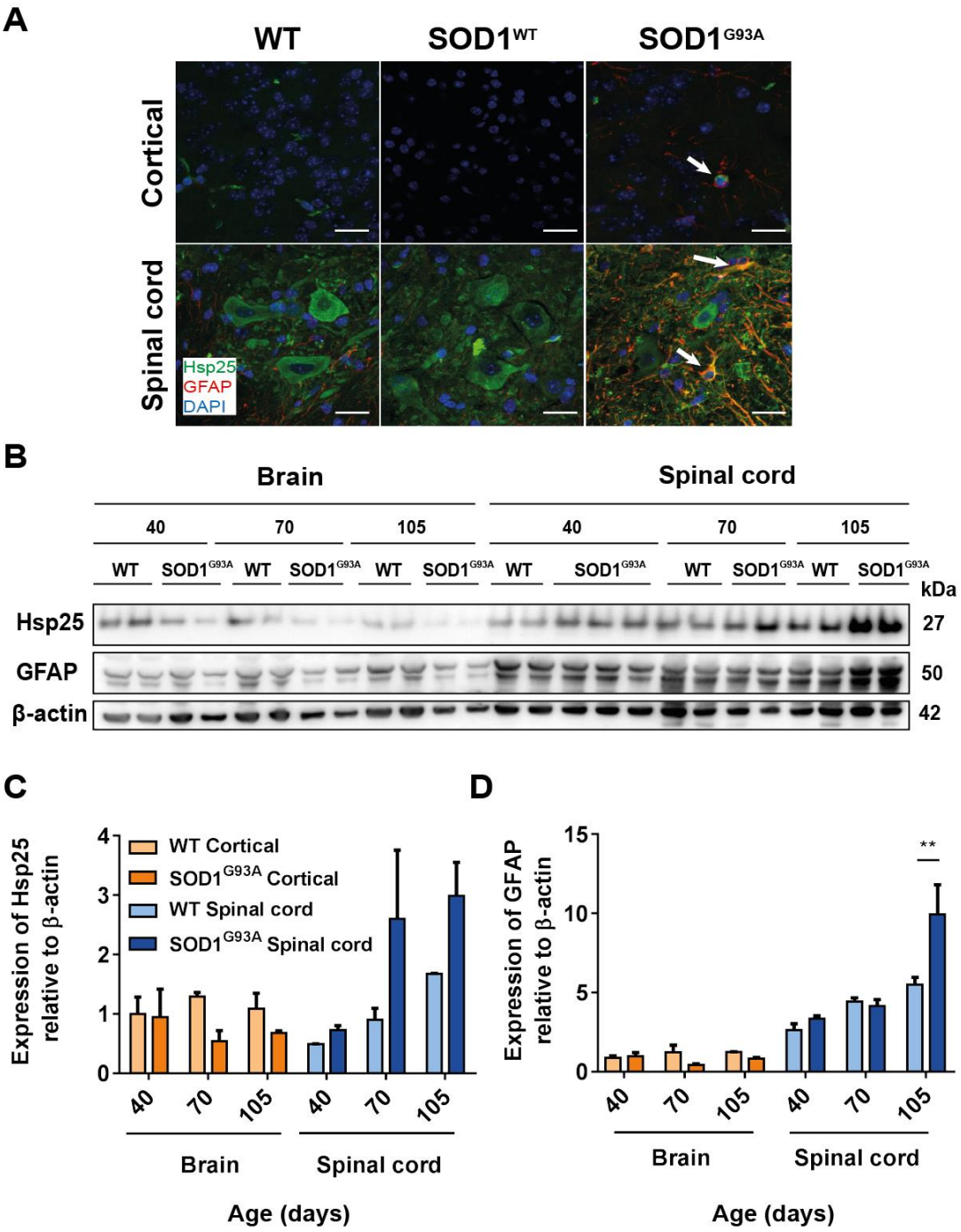

Figure 4.7. Hsp25 expression in the cortex and spinal cord of adult SOD1^{G93A} mice. (A) Immunofluorescence for Hsp25 and GFAP in layer V of the motor cortex and spinal cord of 90 day old wildtype (WT), SOD1^{WT} and SOD1^{G93A} mice. **(B)** Western blot and quantification **(C, D)** of Hsp25 and GFAP in brain and spinal cord lysates from 40, 70 and 105 day old wildtype (WT) and SOD1^{G93A} mice. Data are expressed as the mean ± SEM. A two-way ANOVA with post-hoc Tukey tests was used for statistical comparison. P=**≤0.01. Scale bar: 20µm. N=2-3.

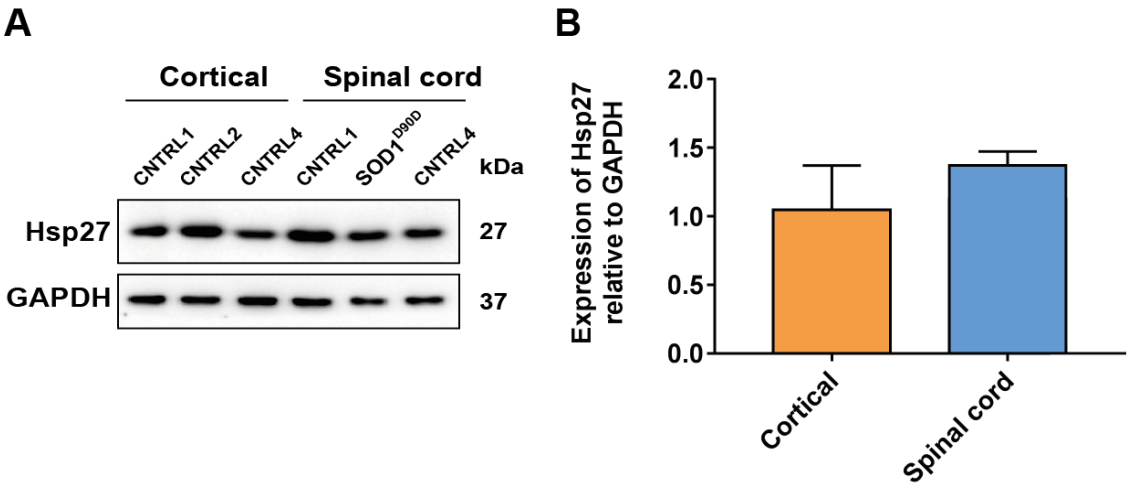

Figure 4.8. Hsp27 levels in human iPSC-derived astrocytes patterned to the cortex and spinal cord. (A) Western blot and quantification **(B)** for Hsp27 in human iPSC-derived astrocytes patterned to the cortex and spinal cord. Data are expressed as the mean ± SEM. A Mann-Whitney U test was used for statistical comparison. N=3.

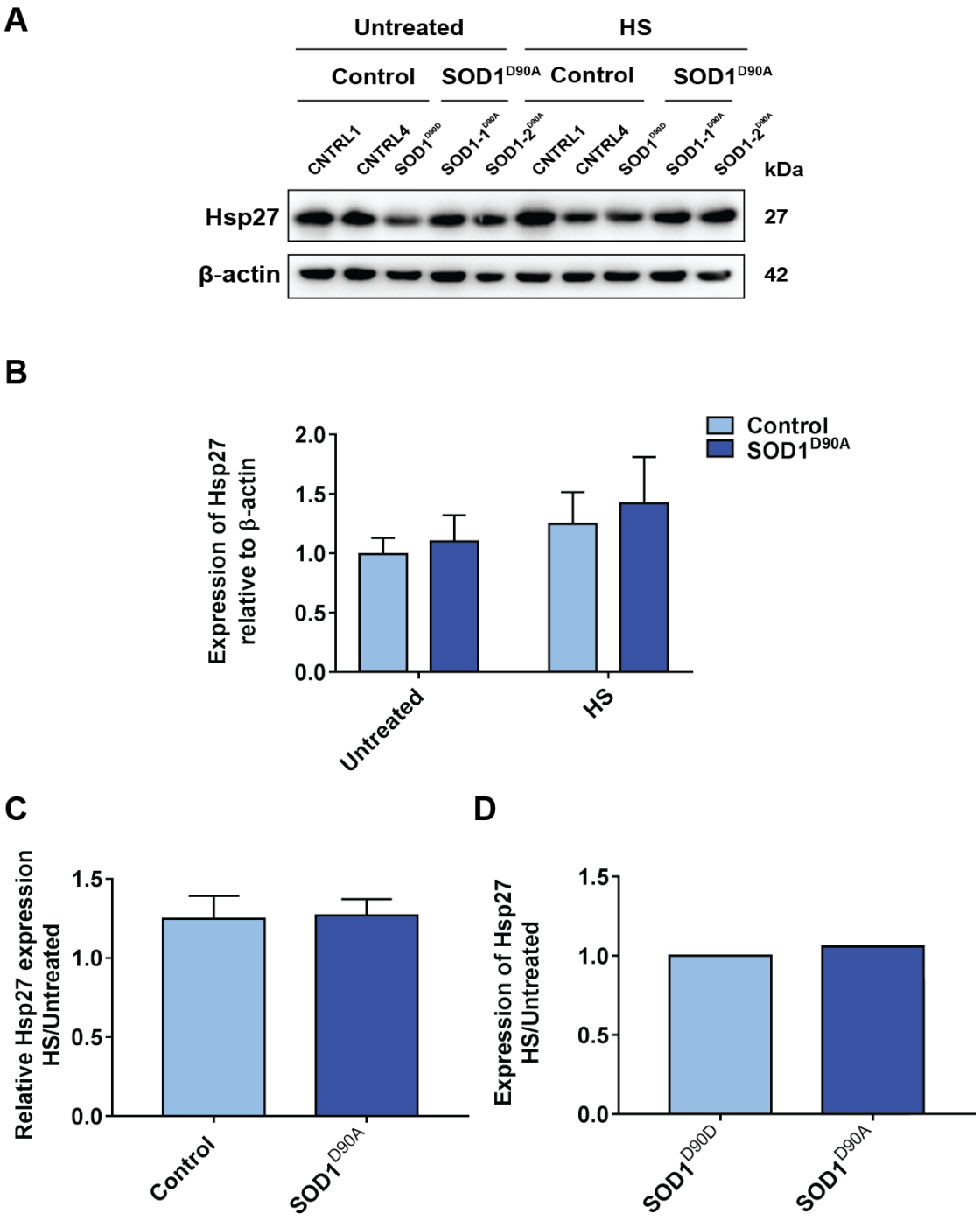

Figure 4.9. Hsp27 levels in control and SOD1^{D90A} ALS patient iPSC-derived astrocytes. (A) Western blot and quantification **(B-D)** for Hsp27 of control, an isogenic SOD1^{D90D} control line and SOD1^{D90A} human iPSC-derived astrocytes exposed to heat stress. Data are expressed as the mean ± SEM. A statistical test was not performed due to low n numbers. N=2-3.

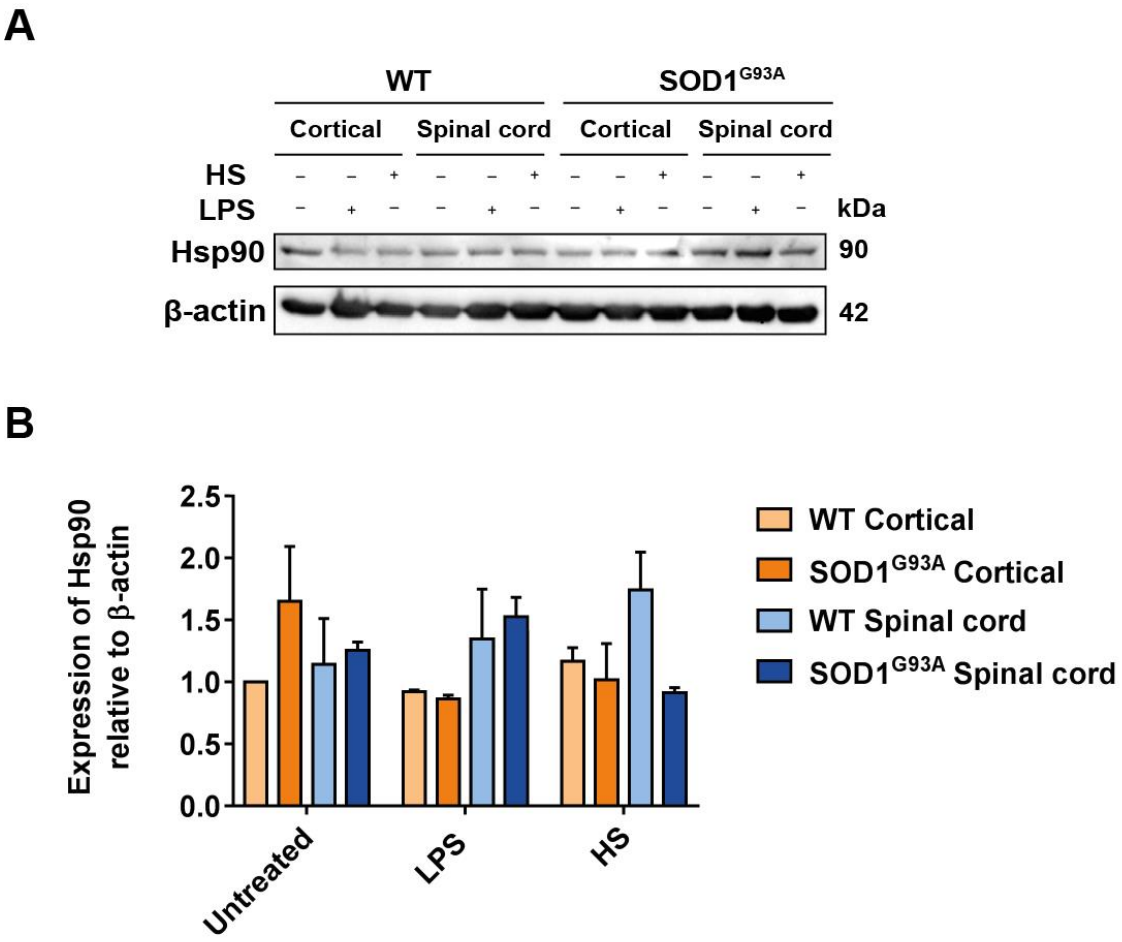

Figure 4.10. Hsp90 expression levels in SOD1^{G93A} cortical and spinal cord glial cultures exposed to LPS or heat stress. (A) Western blot and quantification **(B)** for Hsp90 in cortical and spinal cord glial cultures from wildtype (WT) and SOD1^{G93A} mice exposed to LPS and HS. Data are expressed as the mean ± SEM. A statistical test was not performed due to low n numbers. N=2.

4.2.3 Effects of heat stress on inflammatory signalling

To investigate whether the HSR affects inflammatory signalling in glial cultures, cortical and spinal cord glial cultures were co-treated with both LPS and heat stress (Fig. 4.11). Activation of inflammatory pathways was assessed by measuring the expression levels of iNOS and both phosphorylation and nuclear translocation of NF-κB. Heat stress reduced the expression of iNOS and the levels of phosphorylation of the NF-κB subunit, p65, in spinal cord glial cultures (Fig. 4.11 A-C). Phosphorylation of the p65 subunit of the NF-κB complex is required for activation of downstream NF-κB signalling (Hayden and Ghosh, 2008). Therefore, heat stress inhibited the NF-κB and iNOS signalling pathway.

In agreement with these findings, heat stress reduced the proportion of iNOS positive cells in LPS treated cultures (Fig. 4.12) as well as the number of cells that were positive for nuclear NF-κB translocation induced by LPS treatment (Fig. 4.13). Interestingly, both cortical and spinal cord glial cultures expressing $SOD1^{G93A}$ expressed more iNOS positive cells (Fig. 4.14) and nuclear NF-κB positive cells (Fig. 4.15) than WT cultures exposed to both heat stress and LPS. Therefore, heat stress did not reduce inflammatory activation as effectively in $SOD1^{G93A}$ glial cultures than in WT cultures, suggesting that dysregulation of the HSR in $SOD1^{G93A}$ glia may lead to overactivation of inflammatory signalling.

4.3 Discussion

The aims of this Chapter were to assess the HSR of cortical and spinal cord mSOD1 glia and determine whether differences in the glial HSR affect inflammatory signalling. The results of this Chapter suggest that mSOD1 glia are unable to effectively upregulate Hsp70 in response to stress. Furthermore, the glial HSR of mSOD1 is unable to limit inflammatory signalling as effectively as WT glia, possibly due to reduced Hsp70 expression. Intriguingly, levels of Hsp27 and Hsp90, previously reported to be inducible Hsps, were unchanged in glia following exposure to heat stress. Instead, Hsp27 levels were found to be higher in spinal cord glia than cortical glia under basal conditions.

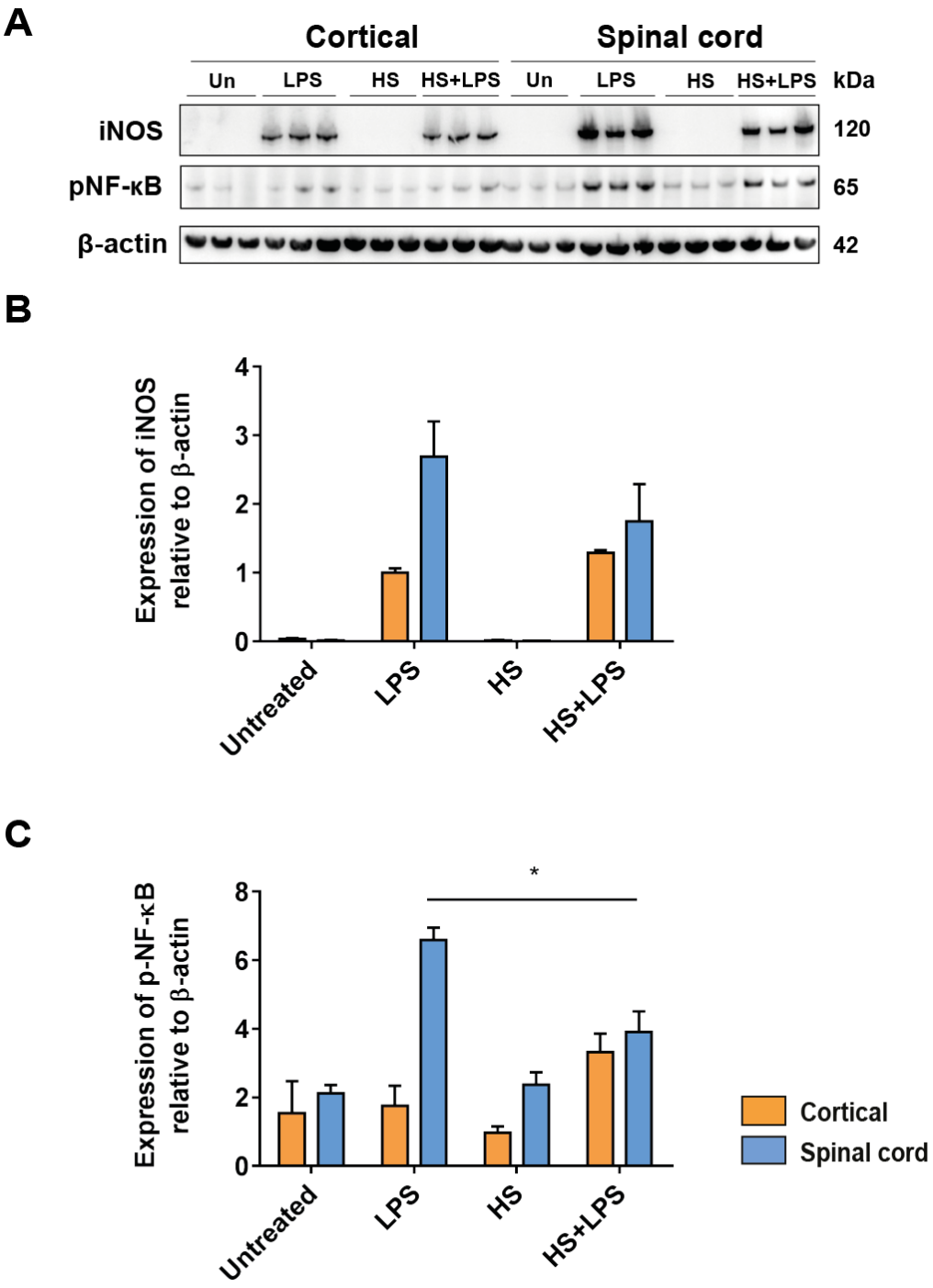

Figure 4.11. iNOS and pNF-κB expression in cortical and spinal cord glial cultures treated with LPS and heat stress. Western blot **(A)** and quantification of iNOS **(B)** and p-NF-κB **(C)** protein expression levels in cortical and spinal cord glial cultures exposed to combination treatment of 80 µg/ml LPS and/or heat stress of 42°C for 30 minutes. Data are expressed as the mean ± SEM. P=*≤0.05. A two-way ANOVA with post-hoc Bonferroni tests was used for statistical comparison. N=3-4.

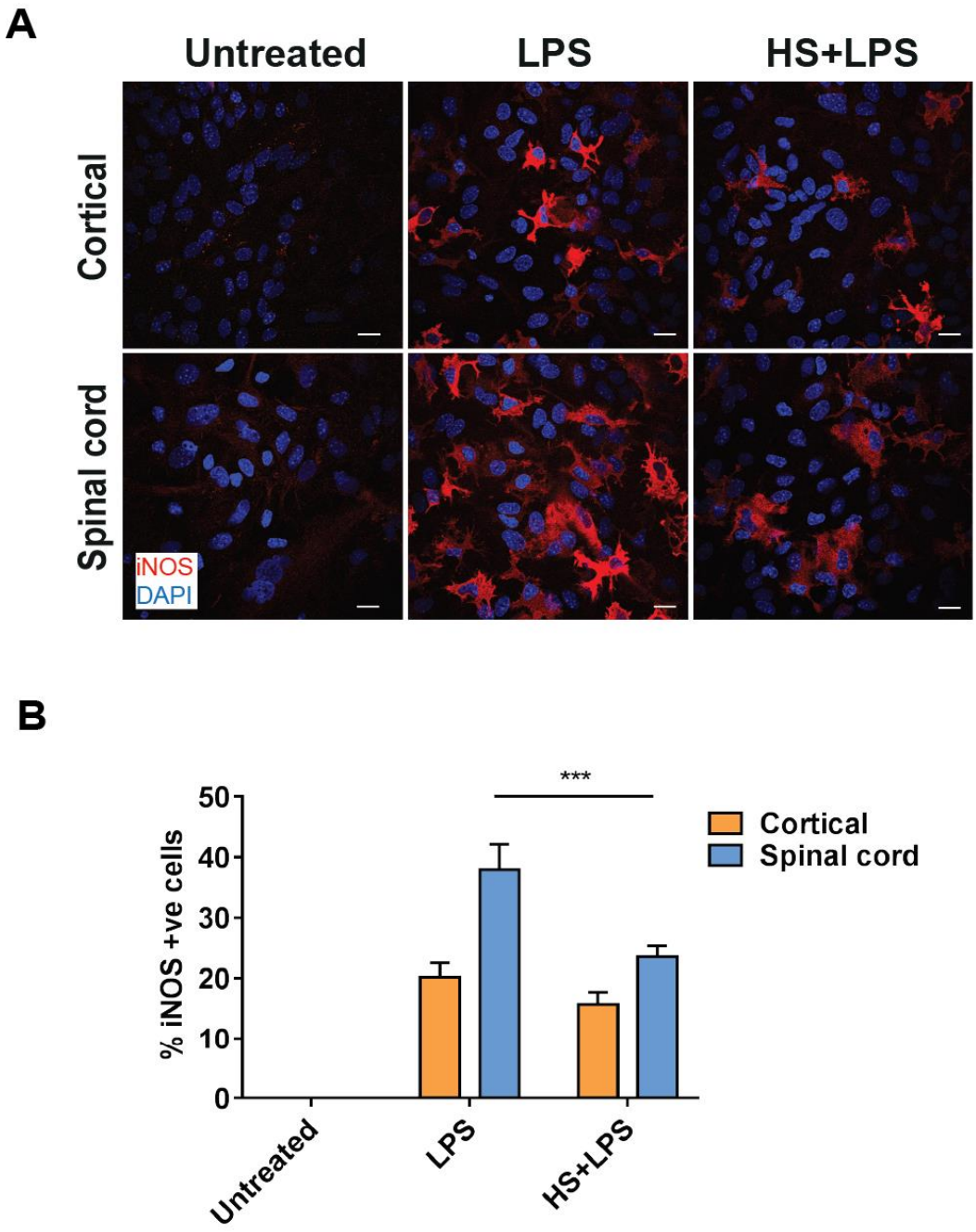

Figure 4.12. iNOS expression in cortical and spinal cord glial cultures treated with LPS and heat stress. (A) Representative images and **(B)** quantification of immunofluorescence staining for iNOS (red) in cortical and spinal cord glial cultures treated with 80 µg/ml LPS and/or heat stress (42°C for 30 minutes and collected 24 hours later). Data are expressed as the mean ± SEM. P=***≤0.001. A two-way ANOVA with post-hoc Tukey tests was used for statistical comparison. Scale bar: 20µm. N=4.

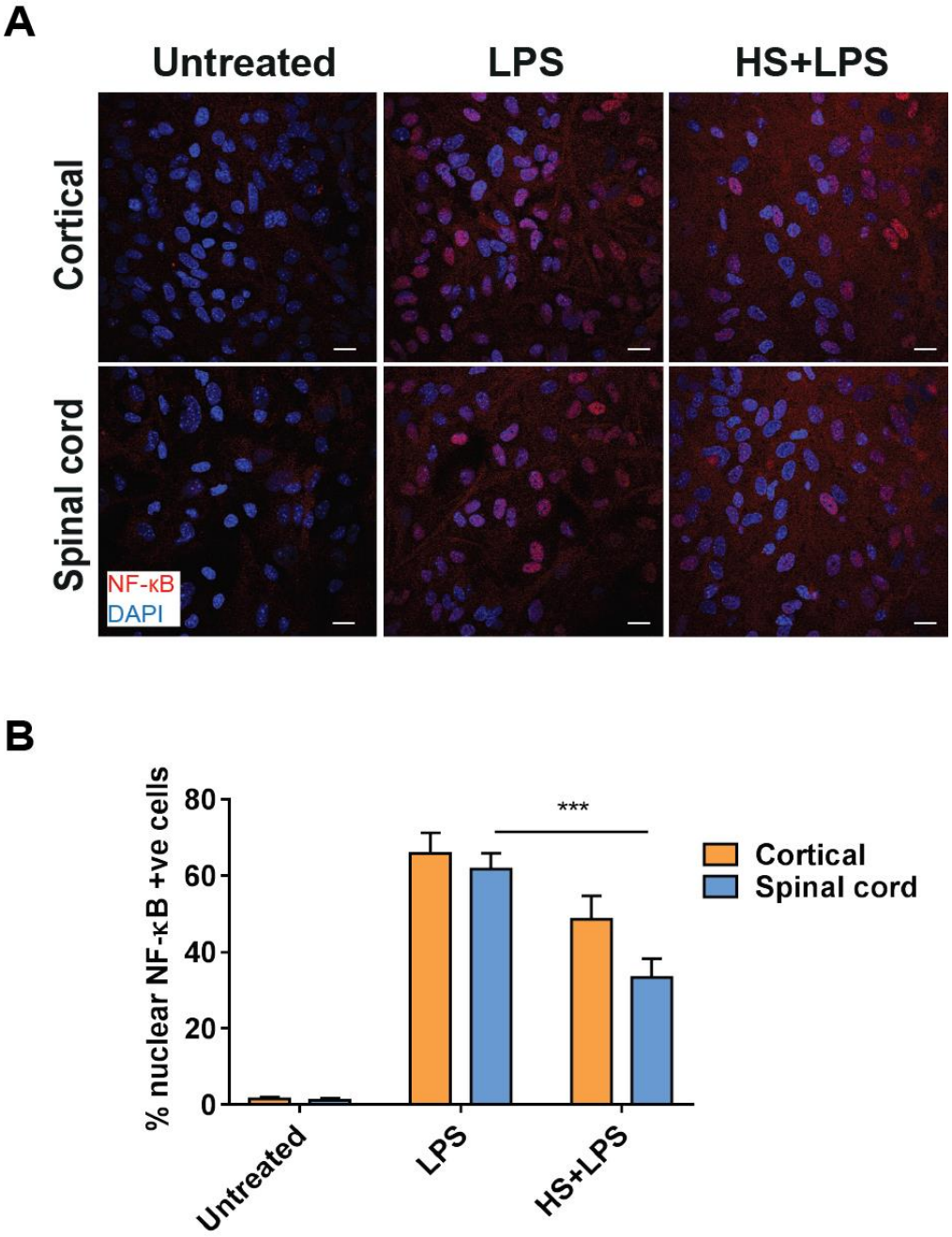

Figure 4.13. NF-κB expression in cortical and spinal cord glial cultures treated with LPS and heat stress. Representative images **(A)** and quantification **(B)** of immunofluorescence staining for NF-κB (red) in cortical and spinal cord glial cultures treated with 80 µg/ml LPS and/or heat stress (42°C for 30 minutes and collected 24 hours later). Data are expressed as the mean ± SEM. P=***≤0.001. A two-way ANOVA with post-hoc Tukey tests was used for statistical comparison. Scale bar: 20µm. N=3.

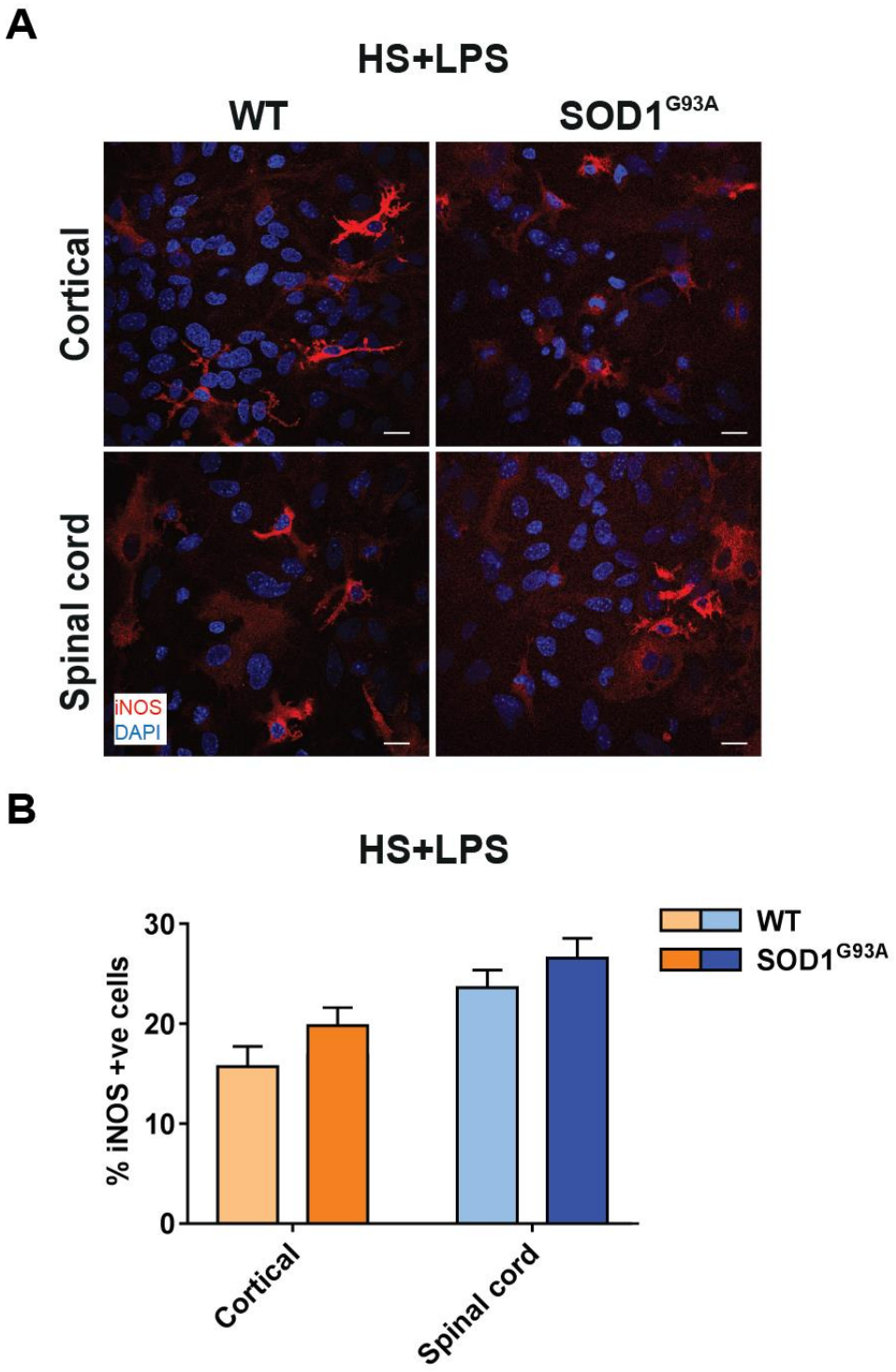

Figure 4.14. iNOS expression in SOD1^{G93A} cortical and spinal cord glial cultures treated with LPS and heat stress. Representative images **(A)** and quantification **(B)** of immunofluorescence staining for iNOS (red) in wildtype (WT) and SOD1^{G93A} cortical and spinal cord glial cultures treated with 80 µg/ml LPS and heat stress (42°C for 30 minutes and collected 24 hours later). Data are expressed as the mean ± SEM. A two-way ANOVA with post-hoc Bonferroni tests was used for statistical comparison. Scale bar: 20µm. N=2-3.

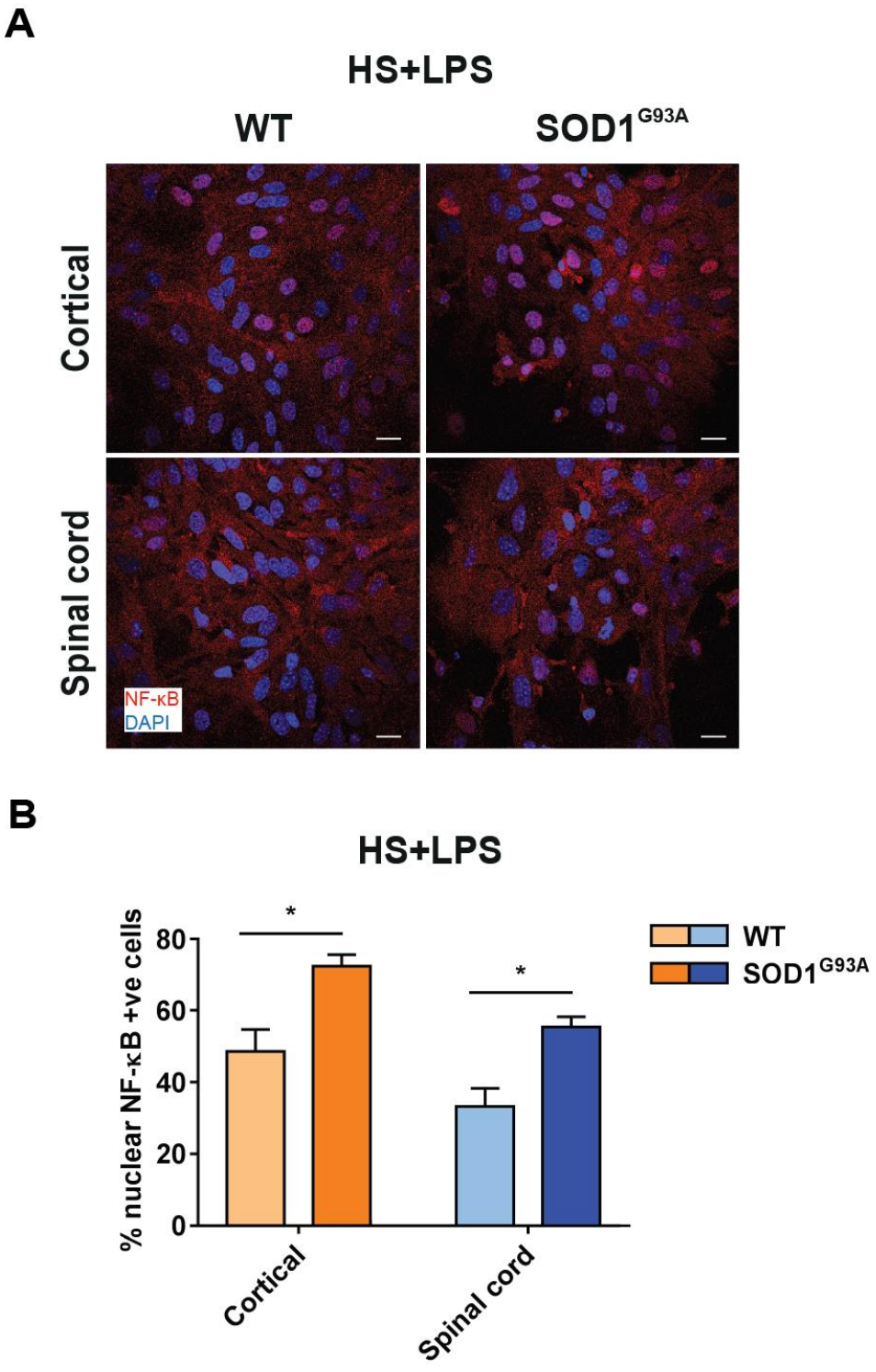

Figure 4.15. NF-κB expression in SOD1^{G93A} cortical and spinal cord glial cultures treated with LPS and heat stress. Representative images **(A)** and quantification **(B)** of immunofluorescence staining for NF-κB (red) in wildtype (WT) and SOD1^{G93A} cortical and spinal cord glial cultures treated with 80 µg/ml LPS and heat stress (42°C for 30 minutes and collected 24 hours later). Data are expressed as the mean ± SEM. P=*≤0.05. A two-way ANOVA with post-hoc Bonferroni tests was used for statistical comparison. Scale bar: 20µm. N=2-3.

4.3.1 Dysfunction in the glial HSR may contribute to motor neuron death in ALS

The results presented in this Chapter suggest that the glial HSR may be reduced in ALS, contributing towards motor neuron death. Motor neurons possess a high threshold for the induction of the HSR, due to an inability to activate HSF-1 (Batulan et al., 2003). However, glia are normally able to activate the HSR well and robustly upregulate Hsps in response to stressful conditions (Nishimura et al., 1991; Kalmar et al., 2002). Here, Hsp70, a major cytoprotective Hsp, was upregulated following heat stress in both cortical and spinal cord glial cultures. Interestingly, both $SOD1^{G93A}$ mouse primary glial cultures and $SOD1^{D90A}$ ALS patient iPSC-derived astrocytes from either region were unable to express Hsp70 as highly as WT/healthy control cultures following heat stress, suggesting that mSOD1 astrocytes are unable to effectively induce the HSR. Since astrocytes may provide motor neurons with cytoprotective Hsps under stressful conditions, any reduction or loss of the HSR in astrocytes may have detrimental consequences to motor neurons and may contribute towards their death in ALS.

Differential changes in Hsp70 levels were observed in the brain and spinal cord of $SOD1^{G93A}$ mice during disease progression. $SOD1^{G93A}$ mouse brains expressed less Hsp70 than age-matched WT mice at presymptomatic (day 40) and symptomatic (day 75) stages of disease. However, there were no clear differences in the expression of Hsp70 in the spinal cord between $SOD1^{G93A}$ and age-matched WT mice at any age studied, with a trend towards an increase in $SOD1^{G93A}$ at symptomatic (day 75) and end stages of disease (day 110). These findings are supported by a study that observed increased levels of Hsp70 in the spinal cord of $SOD1^{G93A}$ mice at later stages of the disease (Yamashita et al., 2007). However, another study has reported that Hsp70 levels are decreased in the $SOD1^{G93A}$ spinal cord at 3 months of age (Liu et al., 2005). Changes in Hsp70 expression of $SOD1^{G93A}$ mice with ageing may be due to the dramatic changes in cell populations during disease progression, with the proliferation of glial cells and loss of motor neurons.

4.3.2 Hsp27 is differentially expressed in cortical and spinal cord glia

Hsp27, also known by the mouse ortholog Hsp25, is another Hsp that has been reported to be inducible (Chang et al., 2013). Hsp27 has numerous cytoprotective

functions including protein handling (Yerbury et al., 2013), inhibition of apoptotic pathways (Havasi et al., 2008) and anti-oxidant effects (Preville et al., 1999). Overexpression of Hsp27 has been shown to improve motor neuron survival in SOD1^{G93A} mice, but has no effect on lifespan (Sharp et al., 2008). Although it has previously been demonstrated that Hsp27 mRNA is increased in post-mortem human astrocytes following treatment with a mixture of pro-inflammatory cytokines (Bajramovic et al., 2000), in the present study there were no differences in the expression of Hsp25 following treatment with LPS. There was also no change in Hsp25 levels after glia were exposed to heat stress, suggesting that in astrocytes, Hsp25 may not be under the control of HSF-1. This finding is in agreement with a previous study that found no change in Hsp27 expression following heat shock in human astrocytes (Satoh and Kim, 1995). Furthermore, no differences in Hsp25/Hsp27 were found between mSOD1 and WT/control glia. A recent study showed that Hsp27 mRNA was increased in SOD1^{D90A} human iPSC-derived astrocytes (Tyzack et al., 2017). However, no differences were found in Hsp27 expression at the protein level, which may be due to regulatory translational or post-translational mechanisms.

Hsp25 has been previously reported to be increased in SOD1^{G93A} mice during disease progression (Vleminckx et al., 2002). Here, Hsp25 positive astrocytes were found in the SOD1^{G93A} ventral spinal cord and GFAP expression correlated with Hsp25 expression in SOD1^{G93A} mice as the disease progressed. This suggests that increased Hsp25 in the spinal cord may be due to gliosis that occurs during disease progression in the SOD1^{G93A} mouse.

Interestingly, basal Hsp25 levels were higher in spinal cord astrocytes than cortical astrocytes in mouse primary glial cultures. A slight increase in Hsp27 expression was observed in human iPSC-derived astrocytes patterned to the spinal cord compared to the cortex. A lack of a significant effect in this model could be reconciled by a lack of efficient patterning of these cells to these regions. In a recent study, increased Hsp27 was observed in human spinal cord astrocytes compared to cortical astrocytes (Gorter et al., 2018). The authors suggest that differences in astrocytic Hsp27 expression may be due to differences in the cytoskeleton of these two astrocyte populations. Hsp27 binds to both actin and GFAP and has been proposed to protect the cytoskeleton under stressful conditions (Perng et al., 1999; Mounier and Arrigo, 2002). Here, increased GFAP

expression was observed in the adult mouse spinal cord compared to the cortex. Therefore, differences in the expression of components of the cytoskeleton between cortical and spinal cord astrocytes may account for differences in Hsp27 expression.

4.3.3 Hsp90 expression is not induced by stress in glia

Hsp90 is another previously reported heat-inducible chaperone (Vigh et al., 1997). However, no increased expression in Hsp90 was observed following heat stress in mouse primary glial cultures. Furthermore, induction of inflammatory signalling by LPS treatment did not affect Hsp90 expression levels. There were also no differences in the expression of Hsp90 between $SOD1^{G93A}$ and WT glial cultures.

4.3.4 Dysfunction in the HSR exacerbates pro-inflammatory signalling in $SOD1^{G93A}$ glia

Increased phosphorylation of NF-κB was observed in spinal cord glial cultures compared with cortical cultures following exposure to LPS, but no regional difference was found in the proportion of cells that were positive for the nuclear translocation of NF-κB. Therefore, regional differences in the inflammatory responses of glia from these two regions may be due to the amount of phosphorylation of the NF-κB complex, rather than the localisation of NF-κB following inflammatory induction.

Heat stress reduced pro-inflammatory signalling, demonstrated by both a reduction in LPS-induced iNOS expression and phosphorylation and translocation of NF-κB to the nucleus, indicative of reduced activation of the NF-κB pathway. This data is in agreement with previous studies that show that the HSR can limit the extent of inflammatory responses of glia (Feinstein et al., 1996; Ialenti et al., 2005).

Although not all of these effects can be attributed to increased Hsp70 expression, Hsp70 expression inversely correlated with a reduction in inflammatory signalling. It has previously been shown that knockdown of Hsp70 partially rescues reduction of NO production of LPS and IFN-γ treated glial cultures by heat stress (Feinstein et al., 1996). Furthermore, this study also showed that overexpression of Hsp70 reduced NO production when glia were treated with LPS and IFN-γ.

Therefore, Hsp70 may be responsible for the effects of the HSR on NF-κB mediated pro-inflammatory responses.

Interestingly, heat stress did not reduce LPS-induced NF-κB signalling as strongly in $SOD1^{G93A}$ glia compared to WT glia. This finding supports the hypothesis that reduced Hsp70 upregulation by $SOD1^{G93A}$ glia is responsible for a reduced inhibition of inflammatory signalling. Therefore, a dysfunctional HSR in $SOD1^{G93A}$ may result in a lack of pro-inflammatory signalling in glia, possibly exacerbating inflammatory damage in ALS.

In conclusion, the results of this Chapter demonstrate that mSOD1 glia are unable to effectively upregulate Hsp70 as strongly as WT glia, possibly reducing the level of glial support to motor neurons and thus limiting neuronal protein chaperoning. This lack of effective induction of the HSR in mSOD1 glia may also result in an inability to limit pro-inflammatory NF-κB signalling. Therefore, a reduced ability of glia to induce the HSR in ALS may result in reduced protein homeostasis and an exacerbated pro-inflammatory response, both contributing to motor neuron death.

Chapter 5: Mitochondrial heat shock proteins in motor neurons and their role in oxidative stress

5.1 Introduction

The vast majority of studies investigating the HSR have focused on Hsps located in the cytosol. However, certain Hsps reside in other cellular compartments including the endoplasmic reticulum and mitochondria (Kleizen and Braakman, 2004; Tatsuta, 2009). Indeed, several Hsps have been found to specifically reside in mitochondria including mtHsp70, Hsp60 and TNF-receptor associated protein 1 (TRAP1), as well as mitochondria-specific co-chaperones Tid-1, TIMM14, Hsc20 and Hsp10 (Voos, 2013). Hsps located within mitochondria (mitochondrial Hsps; mtHsps) play important roles in mitochondrial protein import, folding and maintenance, alongside mitochondrial proteases (Moehle et al., 2019). mtHsps may not only play an important role in maintaining mitochondrial protein homeostasis under normal physiological conditions, but also in responding to stressful conditions to protect mitochondrial functions.

At one point in evolution, mitochondria were separate organisms that were then incorporated into the cell to form a symbiotic relationship. As a result, mitochondria contain their own DNA (mtDNA), consisting of 37 genes. These genes encode proteins that comprise of some of the components of the electron transport chain or aid in its assembly (Anderson et al., 1981). Therefore, mtDNA encodes proteins that account for only a small proportion of the more than 1000 proteins that make up the mitochondrial proteome (Pagliarini et al., 2008). The vast majority of mitochondrial proteins are nuclear encoded and therefore are synthesised in the cytosol and must be subsequently imported into mitochondria. This process involves the unfolding and refolding of proteins when crossing mitochondrial membranes, requiring the chaperone functions of mtHsps (Chacinska et al., 2009). Thus, mtHsps play an important role in maintaining mitochondrial function.

mtHsps are not only important in the process of refolding imported proteins once inside mitochondria, but also in maintaining the correct conformation of mitochondrial proteins, their transport to the correct destination within mitochondria and directing damaged proteins to mitochondrial proteases for degradation (Bender et al., 2011). The presence of misfolded ALS-proteins

accumulating at the outer membrane, intermembrane space and matrix of mitochondria in ALS models (Vande Velde et al., 2011; Wang et al., 2016) suggests that mtHsps are unable to respond effectively to protein misfolding in ALS. As mitochondria are a major source of ROS, mtHsps are important in maintaining the correct conformation of mitochondrial proteins that may become misfolded by oxidation.

5.1.1 TRAP1

TRAP1 is a mtHsp that has been proposed to have numerous pro-survival roles. Although it was first found to associate with the TNF-α receptor (Song et al., 1995), subsequent studies have shown that TRAP1 localises specifically to the intermembrane space and matrix of mitochondria (Cechetto et al., 2000; Pridgeon et al., 2007). TRAP1 is a member of the Hsp90 family of Hsps but shares only around 60% sequence homology with Hsp90 and does not bind to the Hsp90 co-chaperones p23 or Hop, although importantly it does retain chaperoning activity (Kang, 2012; Felts et al., 2000).

TRAP1 has been of interest in the field of cancer research as altered levels have been observed in several different cancer lines (Kang et al., 2007). Knockdown of TRAP1 reduced proliferation and mitochondrial membrane potential in lung cancer cell lines (Agorreta et al., 2014). Liver tissue from *Trap1* knockout mice displayed dramatic changes in mitochondrial respiratory chain subunit expression, suggesting that TRAP1 is important in regulating bioenergetic pathways (Lisanti et al., 2014). Furthermore, overexpression of TRAP1 protected melanoma cells against cell death induced by complex I inhibition, while TRAP1 knockdown exacerbated ROS production and cell death (Basit et al., 2017).

TRAP1 has also been implicated as a pro-survival protein in neurons from studies into Parkinson's disease (PD). Mitochondrial dysfunction has been heavily implicated as an important pathomechanism in PD as the mitochondrial toxin MPTP causes parkinsonian symptoms, complex I activity is reduced in PD post-mortem tissue and mutations in mitochondria-associated genes such as *PINK1* are associated with the disease (Schapira et al., 1989; Plun-Favreau et al., 2008). Under normal conditions PINK1 enters mitochondria, however, when the mitochondrial membrane becomes depolarised, PINK1 accumulates on the outer

mitochondrial membrane and recruits the E3 ubiquitin ligase parkin, initiating degradation of the mitochondrion through mitophagy (Pickrell and Youle, 2015).

Interestingly, PINK1 has been shown to phosphorylate and thereby activate TRAP1, a process that is reduced in PD-causing PINK1 mutant expressing cells (Pridgeon et al., 2007). In this study, reduced phosphorylation of TRAP1 in *PINK1* knockout cells or *PINK1* mutants correlated with increased oxidative stress-induced cell death. PINK1 has also been shown to phosphorylate HtrA2, another gene linked to PD (Plun-Favreau et al., 2007). Recently, TRAP1 has also been implicated as a protective downstream effector of HtrA2 (Fitzgerald et al., 2017). Therefore, TRAP1 activation by PINK1 or HtrA2 may be neuroprotective and loss of TRAP1 activation may therefore contribute to neurodegeneration, at least in PD.

5.1.2 Hsp60

Hsp60, encoded by the *HSPD1* gene, resides in the mitochondrial matrix and has an important role as a mitochondrial chaperone, folding both nascent and misfolded proteins (Ostermann et al., 1989; Hartl et al., 2011). Hsp60 forms two back-to-back tetradecameric rings that surround client proteins in an ATP-dependent manner (Okamoto et al., 2015). Hsp60 performs its chaperoning role in conjunction with the co-chaperone, Hsp10, which acts as a “lid” to the Hsp60-Hsp10 complex, trapping proteins and therefore allowing Hsp60 to refold the client protein into the correct conformation.

Hsp60 is vital for life as knockout of *Hspd1* in mice is embryonically lethal at embryonic day 6.5-7.5 (Christensen et al., 2010). Knockdown of Hsp60 in glioblastoma cells exacerbated H_2O_2-induced cell death, with cells producing higher levels of ROS (Tang et al., 2016). In this study, knockdown of Hsp60 was also associated with a reduction in the production of several proteins that make up mitochondrial complex I. Interestingly, rare mutations in *HSPD1* have been linked to the motor neuropathy hereditary spastic paraplegia (Hansen et al., 2002). The disease is thought to manifest through a loss of Hsp60 chaperoning activity (Bross et al., 2008). Heterozygous Hsp60 knockout mice display late onset motor symptoms, decreased ATP synthesis in the brain and spinal cord and altered levels of complex III, but do not display motor neuron degeneration (Magnoni et al., 2013).

5.1.3 mtHsps as stress responsive chaperones

Mitochondria have a unique adaptive mechanism in response to stress called the mitochondrial unfolded protein response (mtUPR) (Zhao et al., 2002; Haynes and Ron, 2010). Activation of the mtUPR transiently inhibits protein translation and increases the levels of mitochondrial protein chaperones, proteases and anti-oxidant enzymes to restore protein homeostasis (Munch and Harper, 2016).

mtUPR activation has been induced using transfection of mutant ornithine transcarbamylase (ΔOTC) (Zhao et al., 2002; Horibe and Hoogenraad, 2007) or depletion of mtDNA by ethidium bromide (Martinus et al., 1996). Furthermore, a more physiologically relevant oxidative stressor, H_2O_2, has previously been shown to induce the mtUPR in HeLa cells (Guyton et al., 1996). Interestingly, loss of mitochondrial protein homeostasis and activation of the mtUPR can be induced by the TRAP1 inhibitor gamitrinib-triphenylphosphonium (GTPP) (Kang et al., 2009; Siegelin et al., 2011; Kim et al., 2016). The transcription factors C/EBP homologous protein (CHOP) and ATF5 have been implicated as important initiating factors of the mtUPR (Fiorese et al., 2016; Munch and Harper, 2016). Loss of protein homeostasis in mitochondria results in the translocation of these transcription factors to the nucleus resulting in the upregulation of several chaperones, including Hsp60, mitochondrial proteases and antioxidant enzymes (Zhao et al., 2002; Aldridge et al., 2007; Munch and Harper, 2016).

It is poorly understood whether mtHsp expression increases following exposure to cellular stress. There is some evidence suggesting that Hsp60 levels increase under conditions of oxidative stress (Mitsumoto et al., 2002; Runkel et al., 2013) or in the hippocampus of a rat model of epilepsy (Marino Gammazza et al., 2015). However, while levels of Hsp60 have been reported to increase in response to certain stressful conditions, no studies have shown that TRAP1 expression levels change in response to cellular stress.

5.1.4 Possible role for mtHsps in ALS

As previously discussed, mitochondrial dysfunction is common to several neurodegenerative diseases, including ALS (Magrane and Manfredi, 2009; Kiskinis et al., 2014). Mutant ALS proteins including SOD1, TDP-43 and FUS are known to be recruited to mitochondria and cause mitochondrial dysfunction (Liu et al., 2004; Deng et al., 2015; Wang et al., 2016). Deficits in mitochondrial

functions including reduced mitochondrial membrane potential (Nguyen et al., 2009) and reduced complex I expression (Li et al., 2010) have been observed in mSOD1 models. Furthermore, mitochondrial dysfunction in mSOD1 models leads to increased oxidative stress and lipid peroxidation (Liu et al., 1999). Decreased mtHsp expression may lead to mitochondrial dysfunction through a loss of protein homeostasis. Increasing levels of mtHsps may therefore be beneficial to mitochondrial function in response to increased protein misfolding and oxidative stress that occur in ALS.

5.1.5 Aims

mtHsps TRAP1 and Hsp60 have been suggested to play important roles in maintaining mitochondrial function in health and disease. However, research on mtHsps has been limited to the fields of either cancer or, in case of neurodegenerative conditions, Parkinson's disease. In this Chapter, the role of these mtHsps in the maintenance of motor neurons was investigated. Firstly, to establish the possible involvement of mtHsps in disease, the expression levels of mtHsps were evaluated in $SOD1^{G93A}$ mice and under stressful conditions. In order to elucidate the exact role of Hsp60 and TRAP1 in the protection of motor neurons mitochondria under stress conditions, the levels of these proteins were then manipulated in motor neurons using lentiviral overexpression or shRNA knockdown. The effects of manipulating the levels of these proteins on mitochondrial functions were measured using assays for mitochondrial membrane potential, oxidative stress, lipid peroxidation and cell survival, under basal conditions and following treatment with the oxidative stressor, H_2O_2.

The specific aims of this Chapter are to:

1) Investigate whether expression levels of mtHsps Hsp60 and TRAP1 are affected by disease at different stages of motor neuron degeneration in the $SOD1^{G93A}$ mouse model of ALS;
2) Investigate the expression of mtHsps TRAP1 and Hsp60 under oxidative stress conditions;
3) Investigate whether overexpression of mtHsps TRAP1 or Hsp60 protects motor neuron mitochondrial function from oxidative stress;
4) Explore the effects of knockdown of TRAP1 or Hsp60 on mitochondrial function in motor neurons under basal and oxidative stress conditions.

5.2 Methods

For a full description of the methods applied in this Chapter, see Chapter 2: General methods. Methods specifically used in this Chapter are described below.

5.2.1 Primary motor neuron cultures

To obtain motor neuron cultures, the ventral spinal cord was dissected from 12.5-13.5 day old C57BL/6J x SJL (Charles River) embryonic mice based on a previously described protocol (Camu and Henderson, 1992). Pregnant female mice were humanely culled by intraperitoneal injection of euthanol and confirmation of death was obtained by cervical dislocation. A laparotomy was performed and embryos were removed from their amniotic sacs and placed in chilled HBSS containing 1% Penicillin/Streptomycin. Embryonic spinal cords were excised from the body by removing the head, tail and skin off the back of the embryo. Once the spinal cord was isolated, the ventral horn was obtained by removal of the dorsal root ganglia, meninges and dorsal horn.

Ventral horn preparations were then dissociated in HBSS containing 0.025% trypsin for 10 minutes. Tissue was transferred to L15 media supplemented with 0.1 mg/ml deoxyribonuclease (DNase) and 0.4% BSA. After 4 repeated gentle triturations supernatant was removed and the spinal cords were triturated another 10 times in L15 media containing 0.4% BSA and 20 µg/ml DNase. Supernatants were combined from both rounds of trituration and then centrifuged at 380 *g* for 5 minutes in a falcon tube containing 1 ml BSA cushion (4% w/v in L15 media). Cells were counted using a haemocytometer and plated at 30,000 cells/well onto µ-Slide 8 well imaging slides (Ibidi) for live cell imaging or onto 24 well plates at 50,000 cells/well for immunofluorescence and western blotting. All wells were precoated with 3 µg/ml poly-L-orthinine overnight and then for 2 hours with 5 µg/ml laminin. Cells were cultured in motor neuron media (2% B-27 supplement (Gibco), 2% horse serum (Gibco), 10 µg/ml BDNF (Peprotech), 10 µg/ml GDNF (Peprotech), 5 µg/ml CTNF (Peprotech), 1% Penicillin-Streptomycin (Gibco), 1x Glutamax (Gibco) and 0.1 mM β-mercaptoethanol in neurobasal media (Gibco)).

Resulting motor neuron cultures consisted of several different cell types. Motor neurons were distinguished from other cells using criteria established by a previous study: focal plane, cell body size (at least > 15 μm^2) and minimum of three neuritic processes (Bilsland et al., 2008).

5.2.1.1 Treatment of primary motor neuron cultures

Primary motor neuron cultures were treated at DIV 5-8. Cells were treated with 100-500 µM H_2O_2 (VWR), 1 µM rotenone or subjected to heat shock at 42°C for 30 minutes. Cells were then processed for immunoblotting or used in live cell imaging studies 30 minutes or 24 hours later.

5.2.2 mtHsp expression construct design

Human *TRAP1* and *HSPD1* constructs were purchased from Genewiz and cloned into a pUltra plasmid flanked by EcoRV and Xba1 restriction sites. These constructs were then inserted into a construct previously used in the Greensmith lab, a gift from Malcolm Moore (Addgene plasmid #24129) (Lou et al., 2012). The resulting plasmid was driven by a single UbC promoter, containing a self-cleaving P2A sequence between the eGFP and mtHsp gene with an HA tag (Diagram 5.1). This resulted in the production of two separate protein products, theoretically in equal amounts.

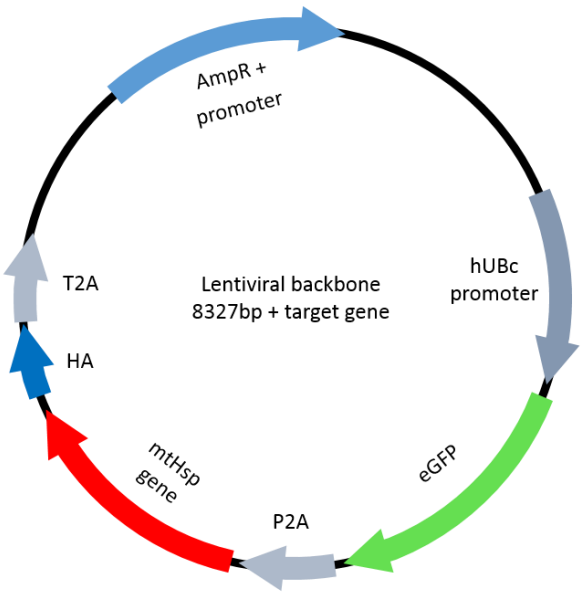

Diagram 5.1 mtHsp expression construct design.

5.2.3 shRNA construct design

shRNA constructs were purchased from Geneocopia. shRNA constructs were designed to silence the *Trap1* and *Hspd1* mouse genes and contained a GFP reporter to identify the presence of successful expression of the plasmid in cells (Diagram 5.2). shRNA constructs were first screened in N2A neuroblastoma cells.

Cells were cultured in 10 cm^2 dishes in maintenance media (DMEM containing 10% FBS and 1x glutamax). Only N2A cells that had been passaged less than 20 times were used for experiments. N2A cells were treated with shRNA constructs using lipofectamine 2000 according to manufacturer's instructions. Media was changed 6 hours after treatment with shRNAs and then cells were lysed in RIPA buffer 24 hours later for immunoblot analysis.

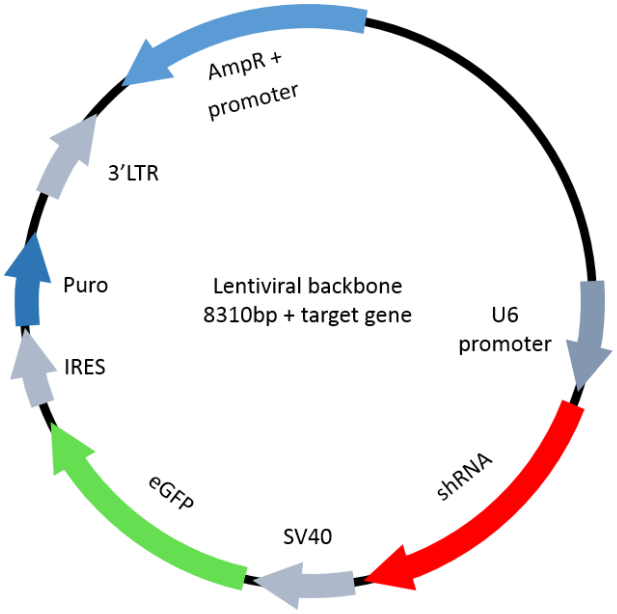

Diagram 5.2 mtHsp shRNA construct design.

Name	#Catalogue	shRNA sequence
trap1-1	MSH034436-31-LVRU6GP	GGTTGAAGTCTATTCTCGATC
trap1-2	MSH034436-32-LVRU6GP	GGTAACAAAGTACAGTAACTT
trap1-3	MSH034436-33-LVRU6GP	GGATGTTCTACAACAGAGATT
trap1-4	MSH034436-34-LVRU6GP	GCTGAACATTCACCCTATTAC
Hspd1-1	MSH029408-31-LVRU6GP	GCTAAACTTGTTCAGGACGTT
Hspd1-2	MSH029408-32-LVRU6GP	GCTAGAAATTATTGAAGGCAT
Hspd1-3	MSH029408-33-LVRU6GP	CCTATGTCTTGTTGAGTGAAA
Hspd1-4	MSH029408-34-LVRU6GP	GCCTTGGATTCATTAAAGCCT
Scrambled control	CSHCTR001-LVRU6GP	GCTTCGCGCCGTAGTCTTA

Table 5.1. mtHsp shRNA construct sequences. shRNA sequences for knockdown of mouse *Trap1* and *Hspd1* genes.

5.2.4 Generation of viral vectors for gene delivery

mtHsp expression or shRNA plasmids were amplified in Top10 *Escherichia coli* (*e.coli*, Thermo Fisher Scientific) on ampicillin containing agar plates overnight at 37°C. DNA was extracted using a Mini-prep or Hispeed Plasmid Maxi prep kit (Qiagen), according to manufacturer's instructions. All plasmids were sequenced to verify that they were correct. EGFP_C_F primer (Source Bioscience), sequence: CAT GGT CCT GCT GGA GTT CGT G, was used to sequence each plasmid.

LentiHEK cells were cultured in 10 cm^2 or 15 cm^2 dishes in DMEM, 10% FBS and 1x glutamax under standard cell culture conditions. Cells were split once they reached 70-80% confluency. For shRNA constructs, a 2nd generation lentivirus was used consisting of pCMVdeltaR8.74 and pMD.G.2 (both Addgene) packaging and envelope plasmids respectively. Cells were transfected with 11.75 µg of shRNA construct, 11.75 µg pCMVdeltaR8.74 and 7.8µg pMD.G.2 plasmids (both Addgene) using Lipofectamine 3000, according to manufacturer's instructions. For overexpression constructs, a 3rd generation lentivirus was used. Packaging genes (pMDLg/pRRE and pRSV-Rev) and the envelope gene (pMD2.G) were all obtained from Addgene. Cells were transfected with 30 µg of transfer plasmid, 9 µg pMDLg/pRRE, 5 µg pRSV-Rev and 6 µg pMD2.G using Lipofectamine 2000. Media was collected at 48 and 72-hour timepoints after transfection. Media was centrifuged at 500 *g* for 10 minutes at 4°C to remove cell debris and supernatant was then combined 3:1 with Lenti-X concentrator (Clontech). After 1 hour at 4°C the resulting solution was centrifuged at 1500 *g* for 45 minutes at 4°C. The viral pellet was resuspended in 200 µl Optimem media, aliquoted, and stored at -80°C.

Primary motor neuron cultures were treated with 1:250 lentiviral constructs at DIV1 and then media was replaced with fresh media the following day. Live imaging, immunoblotting and immunofluorescence experiments were performed between DIV5-8.

5.2.5 Live cell imaging experiments

5.2.5.1 Mitochondrial membrane potential recordings

Primary motor neuron cultures were loaded with 20 nM tetramethylrhodamine methyl ester (TMRM) in recording media (156 mM NaCl, 10 mM HEPES, 10 mM D-glucose, 3 mM KCl, 2 mM $MgSO_4$, 2 mM $CaCl_2$, 1.25 mM KH_2PO_4, pH 7.35) with 0.005% pluronic acid for 30 minutes at room temperature. 500 µM H_2O_2 was added to appropriate wells in conjunction with TMRM for acute treatments. For chronic treatments, cultures were treated for 6 hours with 100 µM H_2O_2. Neurons were identified using calcein blue and 4 z-stacks were taken on the 63x objective of a 510 Zeiss confocal microscope per condition. TMRM intensities and mitochondrial area measurements were recorded from the cell bodies of neurons using ImageJ. For groups treated with lentiviruses, only GFP-positive neurons were included in the analysis.

5.2.5.2 ROS production measurements

Cells were loaded with 5 µM dihydroethidium (DHE) in recording media and cells were treated with 500µM H_2O_2 for 30 minutes at room temperature. Neurons were identified using calcein blue or GFP and 4 z stacks were taken per condition on the 63x objective of a 510 Zeiss confocal microscope. DHE intensities were recorded from the nuclei of neurons using ImageJ. For groups treated with lentiviruses, only GFP-positive cells were included in the analysis.

5.2.5.3 Lipid peroxidation measurements

Cells were loaded with 2 µM Bodipy 581/591 C11 in recording media and cells were treated with 500 µM H_2O_2 for 30 minutes at room temperature. Neurons were identified using calcein blue or GFP. 4 z stacks were taken per condition on the 63x objective of a 510 Zeiss confocal microscope. The intensity of Bodipy 581/591 C11 fluorescence was measured in the cytoplasm of neurons using ImageJ.

5.2.5.4 Cell viability assay

Cells were treated for 24 hours with 100 µM H_2O_2 and then loaded with 1 µM calcein blue. At least 8 images were obtained using the 63x objective of a LSM510 confocal microscope for each condition. The total number of GFP positive neurons was counted using ImageJ to assess cell death.

5.3 Results

5.3.1 Expression of mtHsps in models of ALS

In order to investigate whether the expression of mtHsps are affected in ALS, the expression of TRAP1 and Hsp60 were assessed in the $SOD1^{G93A}$ mouse model of ALS. Comparison of the expression of TRAP1 and Hsp60 levels in the spinal cord of $SOD1^{G93A}$ and WT mice showed that there was no differences at presymptomatic (day 40), symptomatic (day 75) and late stages (day 110) of disease (Fig. 5.1).

However, since analysis of the whole spinal cord does not give an accurate representation of protein expression specifically in motor neurons, due to the presence of non-neuronal cell types and the changing cellular architecture during $SOD1^{G93A}$ disease progression, the intensity of TRAP1 and Hsp60 staining of motor neurons was next examined in symptomatic (day 90) $SOD1^{G93A}$ and age-matched WT mice. At this time, there is almost a 50% loss of motor neurons in the ventral horn of the spinal cord (Bilsland et al., 2010). A decreased intensity of both TRAP1 and Hsp60 immunostaining was observed in $SOD1^{G93A}$ neurons from the ventral horn of the spinal cord (Fig. 5.2).

Next, changes in the levels of TRAP1 and Hsp60 were assessed in primary motor neuron cultures in response to different stressful conditions modelling ALS. Oxidative stress resulting from H_2O_2 treatment, mitochondrial stress resulting from complex I inhibition by rotenone treatment and HSR induction by heat shock all failed to alter the levels of TRAP1 or Hsp60 in primary motor neuron cultures (Fig. 5.3 A-C), while heat shock was able to increase levels of Hsp70 indicating activation of the HSR (Fig. 5.3 D, E). Thus, the expression levels of TRAP1 and Hsp60 are not induced by oxidative stress or the HSR.

5.3.2 Characterisation of lentiviral vectors overexpressing mtHsps

In order to study the role of mtHsps in motor neurons, expression constructs for human TRAP1 and Hsp60 were synthesised (see 5.2.2). Briefly, this construct contained a ubiquitin promoter, a HA tag attached to the mtHsp gene of interest and a GFP sequence.

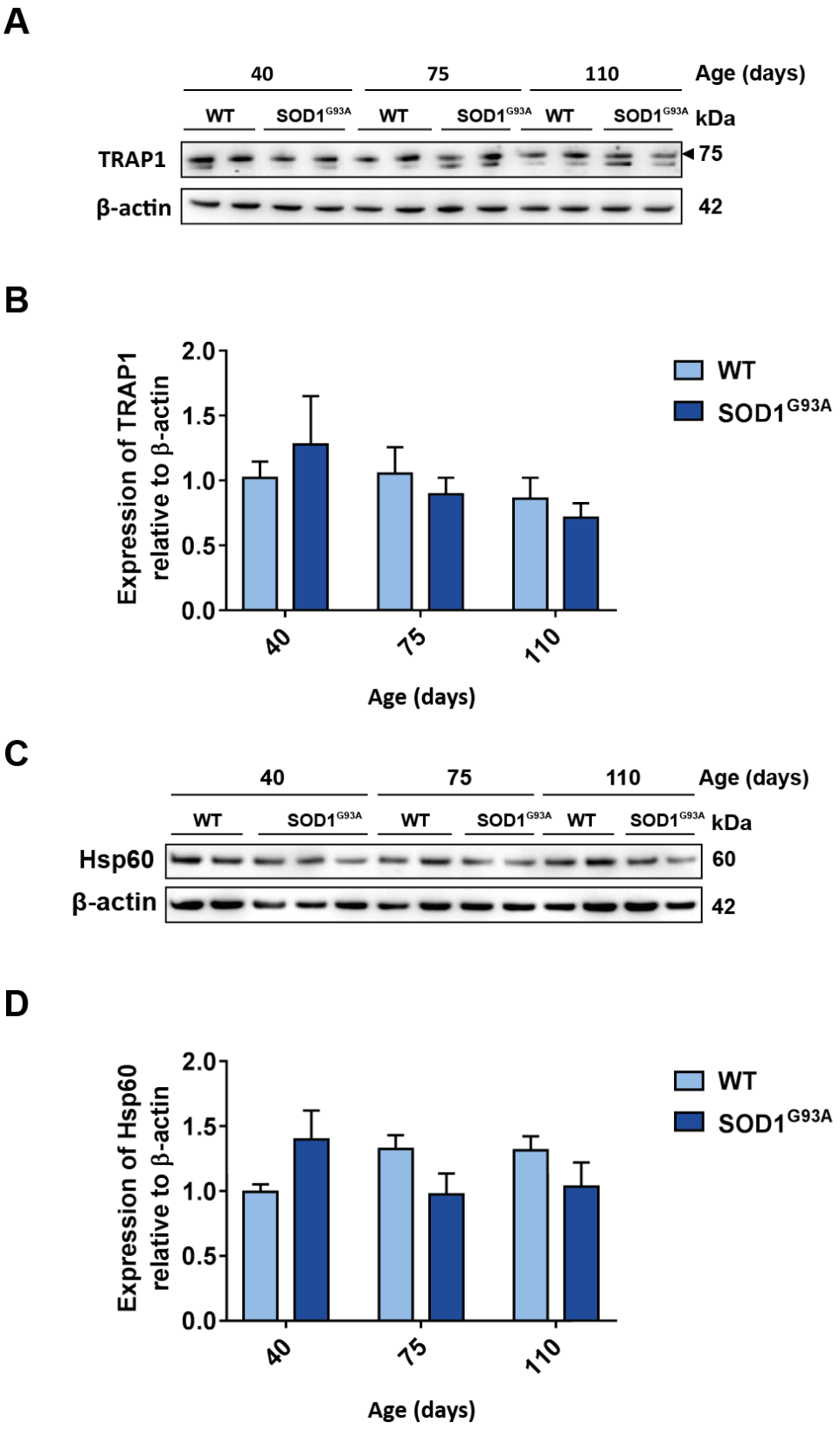

Figure 5.1. mtHsp expression in aged SOD1^{G93A} mouse spinal cord. (A) Western blot and quantification **(B, C)** of TRAP1 and Hsp60 in the spinal cord of 40, 75 and 110 day old wildtype (WT) and SOD1^{G93A} mice. Data are expressed as the mean ± SEM. A two-way ANOVA with post-hoc Bonferroni tests was used for statistical comparison. N=4-5.

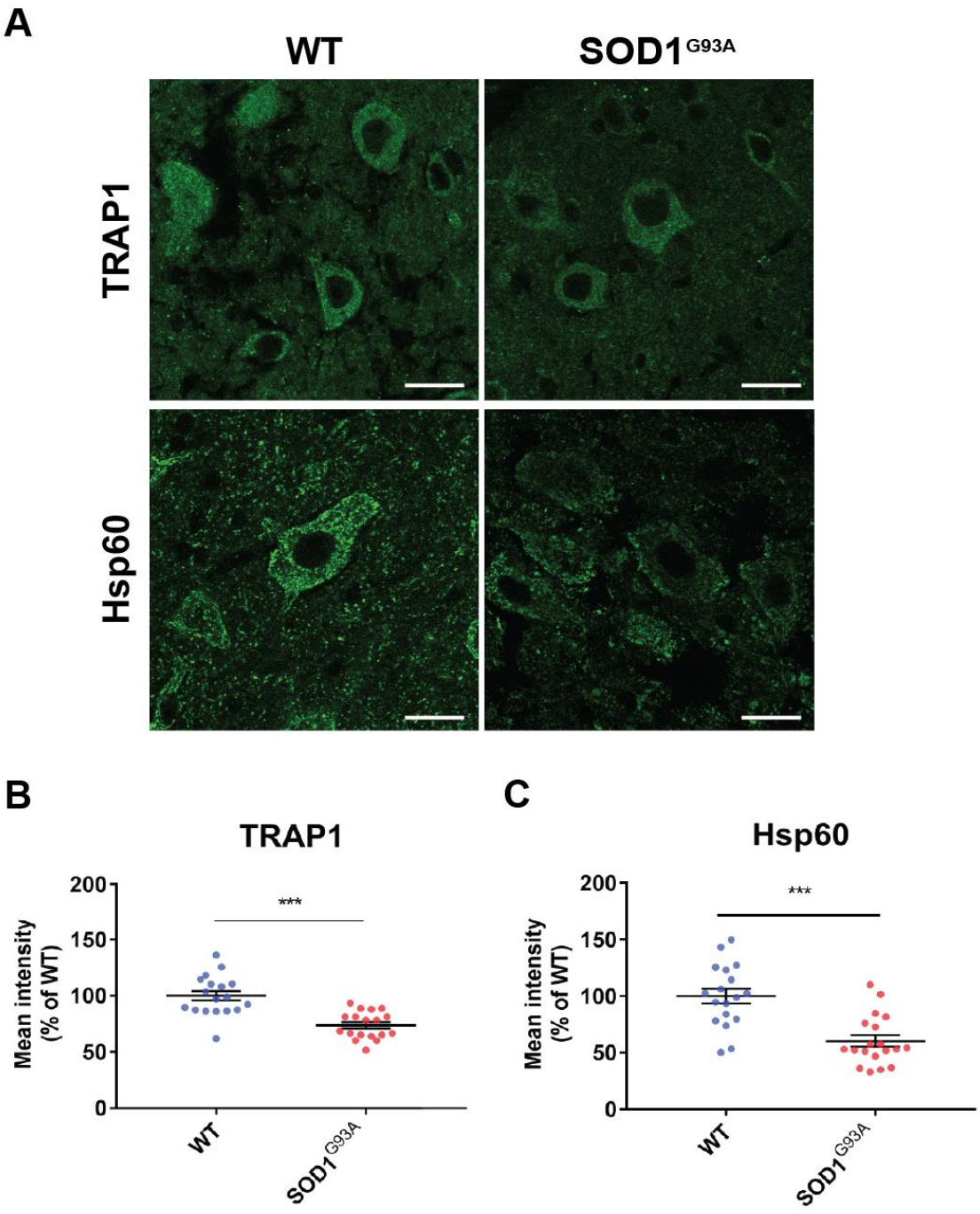

Figure 5.2. Immunofluorescence staining for TRAP1 and Hsp60 in symptomatic SOD1^{G93A} neurons from the ventral horn of the spinal cord. (A) Immunofluorescence staining for TRAP1 and Hsp60 in the ventral horn of the spinal cord from 90-day-old wildtype (WT) and SOD1^{G93A} mice. Quantification of average intensities of neuronal cell bodies in the ventral horn of the spinal cord for **(B)** TRAP1 and **(C)** Hsp60. Data are expressed as the mean ± SEM. A Mann-Whitney U test was used for statistical comparison. P= ***≤0.001. Scale bar: 20µm. N=2-3 mice per group, 18-19 neurons assessed per condition.

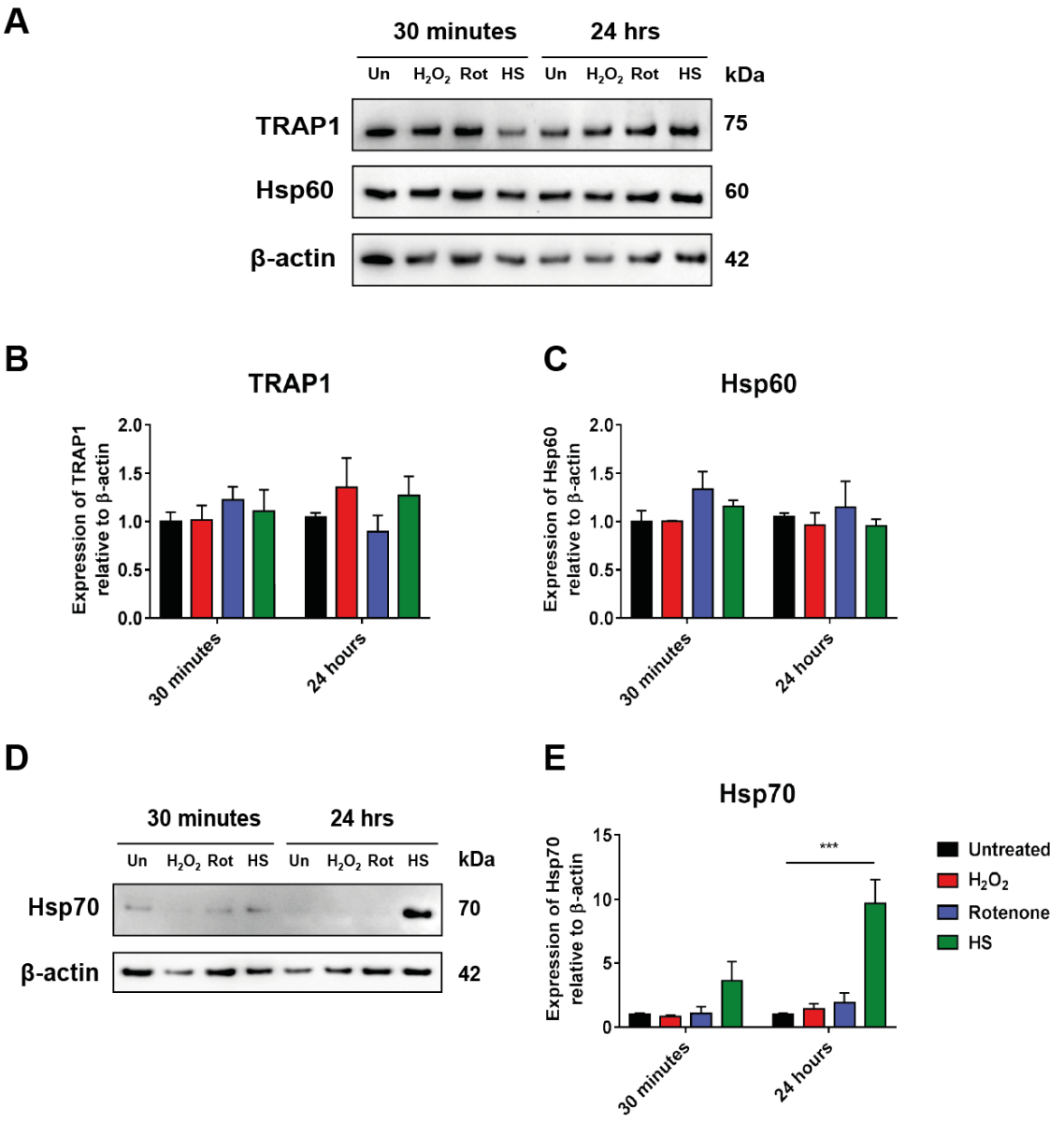

Figure 5.3. Expression of mtHsps in primary motor neuron cultures following treatment with H_2O_2, rotenone or heat stress. (A) Western blot of primary motor neuron cultures for TRAP1 and Hsp60 (Un: Untreated, Rot: rotenone, HS: heat shock). Quantification of western blots for **(B)** TRAP1 and **(C)** Hsp60. **(D)** Western blot for cytosolic heat shock protein Hsp70 in primary motor neuron cultures. **(E)** Quantification of western blots for Hsp70 in primary motor neuron cultures. Data are expressed as the mean ± SEM. A two-way ANOVA with post-hoc Bonferroni tests was used for statistical comparison. P=***≤0.001. N=2-4.

Lentiviruses for TRAP1 and Hsp60 expression constructs, as well as an empty construct not containing a mtHsp gene, successfully transduced primary motor neuron cultures, demonstrated by both the expression of HA at the correct molecular weight and GFP expression (Fig. 5.4 A). At a concentration of 1:250 of the lentivirus for the TRAP1 construct there was a significantly higher expression of TRAP1 protein, on average ~6 times levels expressed in untransduced cultures or cultures transduced with empty vector (Fig. 5.4 B, C). Although there was successful expression of the lentivirus for the Hsp60 construct, identified by the second higher band of transduced Hsp60 protein, even at high viral titres it was not possible to overexpress this protein (Fig. 5.4 D, E).

Using immunofluorescence the expression of GFP and the HA tag confirmed that TRAP1 and Hsp60 lentiviral constructs successfully transduced neurons (Fig. 5.5 A, B). Furthermore, the expression of the HA tag for both of these constructs appeared to be in a pattern typically associated with mitochondria. Further investigation by performing colocalisation by immunofluorescence of the HA tag with TRAP1 or Hsp60 (Fig. 5.6), or with the mitochondrial marker TOM20 (Fig. 5.7), confirmed that the constructs for TRAP1 and Hsp60 resulted in mitochondrial expression of these proteins.

5.3.3 Overexpression of TRAP1 protects neurons from oxidative stress

Since lentiviruses successfully expressed human TRAP1 and Hsp60 in primary motor neuron cultures, the effects of the expression of these proteins on mitochondrial functions following exposure to stressful conditions were evaluated next. First, the effects of the expression of TRAP1 and Hsp60 on mitochondrial membrane potential in response to oxidative stress was examined. TMRM is a cationic dye that localises to mitochondria and can be used as a measure of mitochondrial membrane potential, an indicator of mitochondrial health. When cells are incubated with concentrations of TMRM of less than 50nM, a drop in the fluorescence from mitochondria is observed when there is a reduction in mitochondrial membrane potential, as the dye exits mitochondria (Perry et al., 2011).

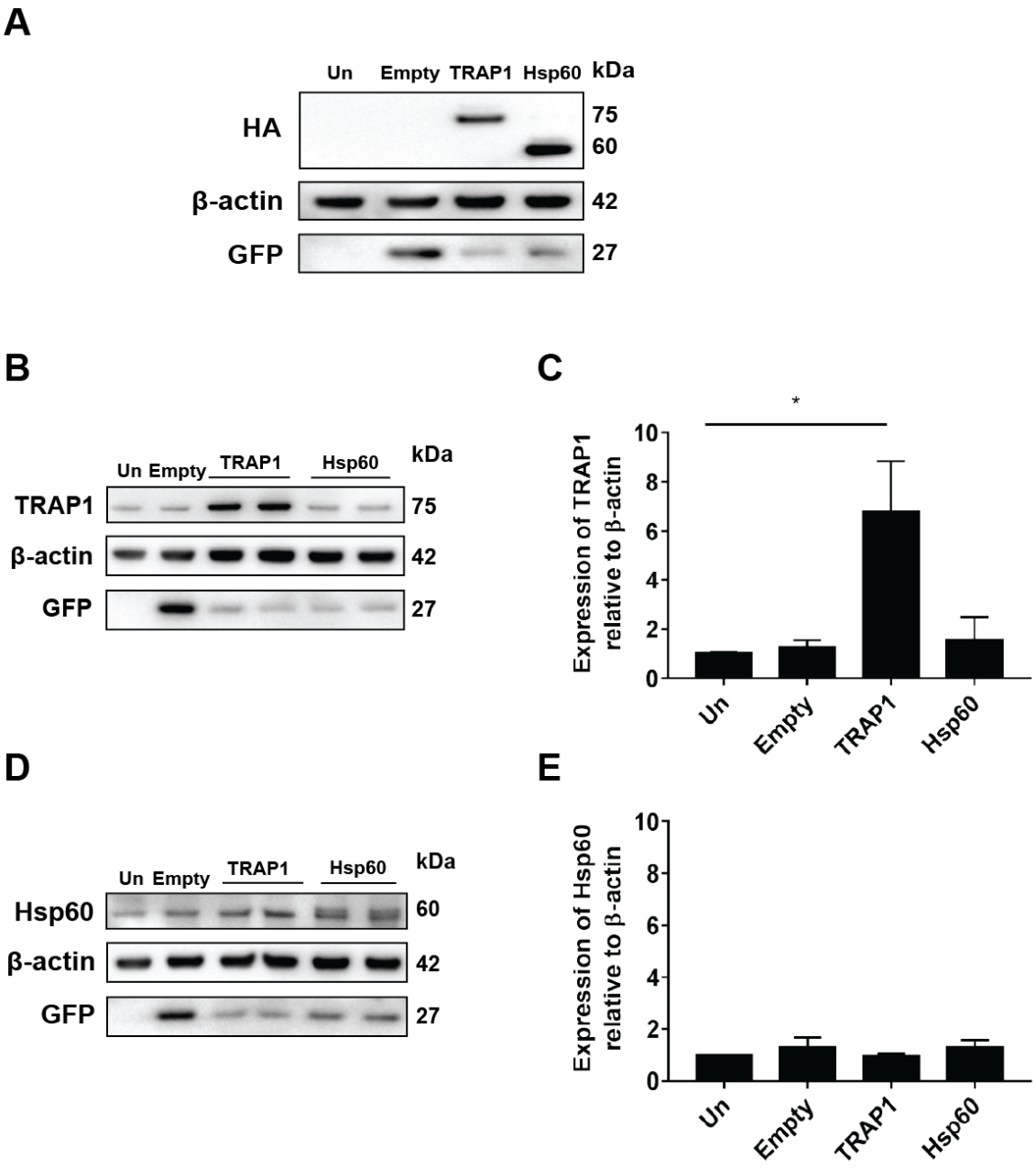

Figure 5.4. Expression of TRAP1 and Hsp60 using lentivirally transduced expression constructs. Western blot **(A)** for HA and GFP of primary motor neuron cultures either untransduced (Un) or transduced with lentiviruses containing expression constructs for TRAP1, Hsp60 or an empty construct. Western blot **(B)** and quantification **(C)** for TRAP1 and GFP of transduced primary motor neuron cultures. Western blot **(D)** and quantification **(E)** for Hsp60 and GFP of transduced primary motor neuron cultures. Data are expressed as the mean ± SEM. A Kruskal-Wallis test with post-hoc Dunn's tests was used for statistical comparison. P=*≤0.05. N=3.

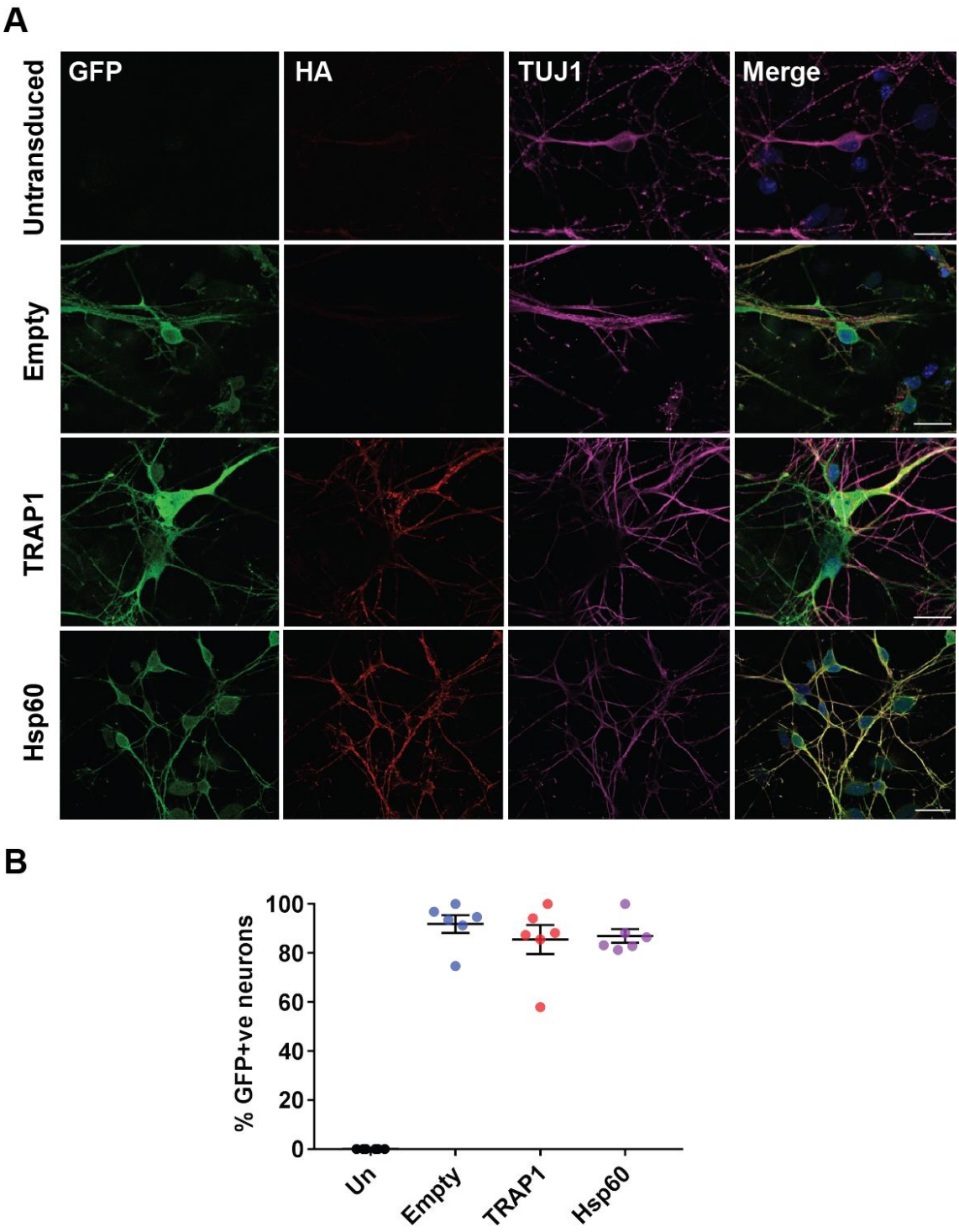

Figure 5.5. Immunofluorescence of neurons transduced with lentiviral vectors for TRAP1 or Hsp60. (A) Immunofluorescence for GFP (green), HA (red) and TUJ1 (magenta) in primary motor neuron cultures either untransduced (Un) or transduced with Empty, TRAP1 or Hsp60 lentiviruses. **(B)** Quantification of GFP positive neurons in primary motor neuron cultures transduced with Empty, TRAP1 or Hsp60 lentiviruses. Data are expressed as the mean ± SEM. Scale bar: 20µm. N=6.

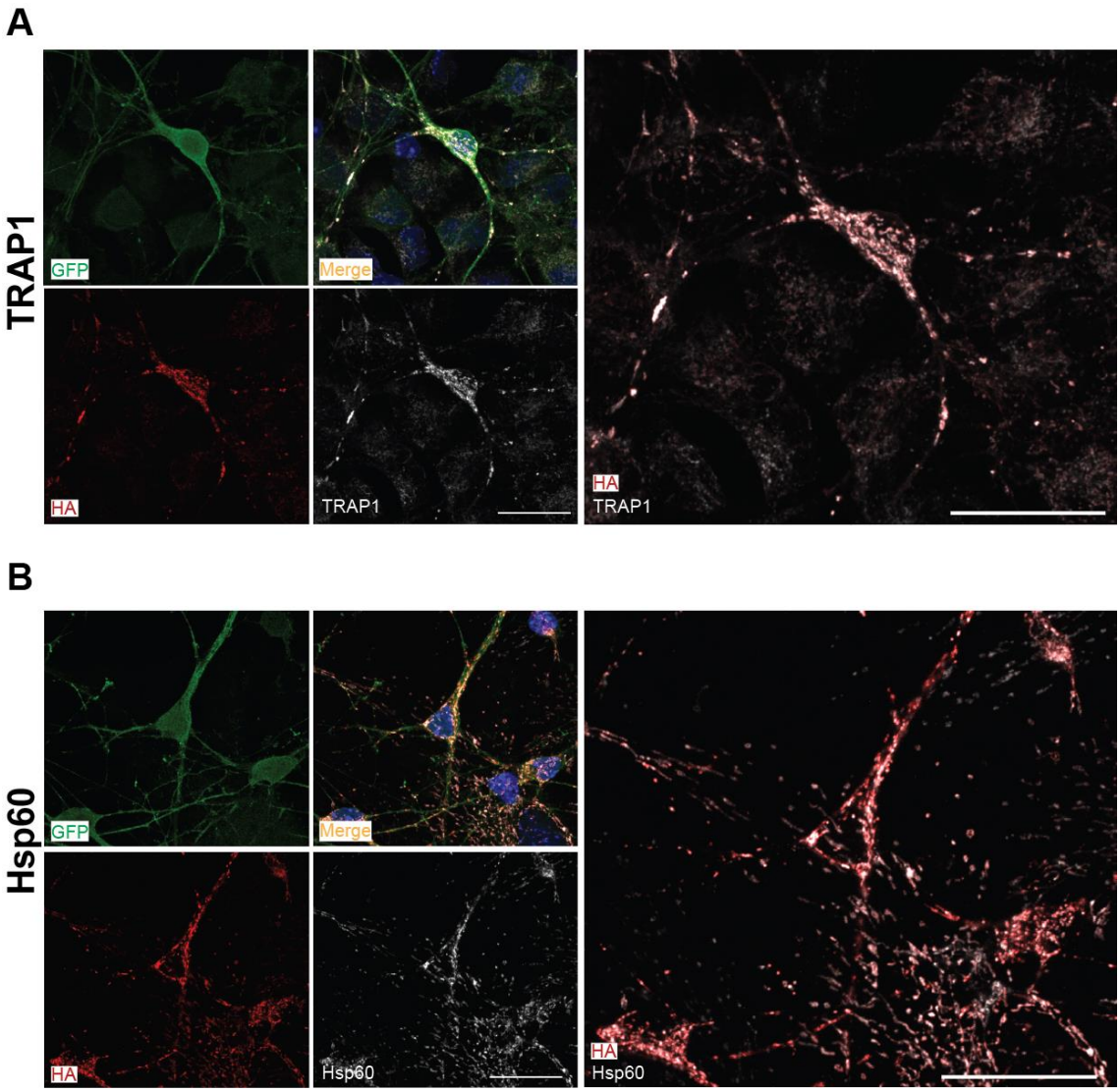

Figure 5.6. Colocalisation of HA tag and either TRAP1 or Hsp60 in lentivirally transduced neurons. Immunofluorescence staining for GFP (green), HA (red), TRAP1 or Hsp60 (white) in primary motor neuron cultures transduced with TRAP1 **(A)** or Hsp60 **(B)** lentiviruses. Scale bar: 20µm.

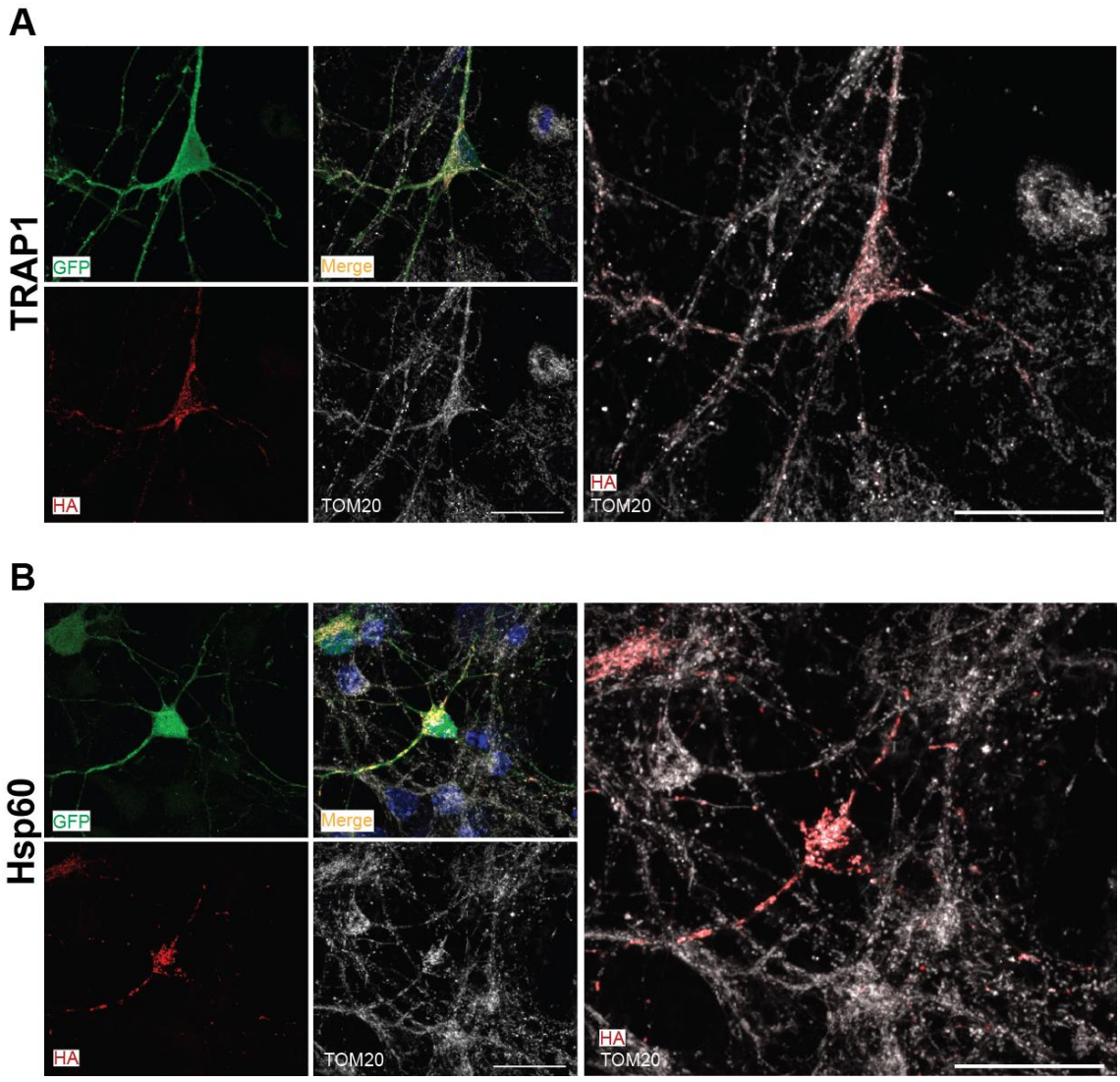

Figure 5.7. Colocalisation of HA tag and TOM20 in lentivirally transduced neurons. Immunofluorescence staining for GFP (green), HA (red) and TOM20 (white) in primary motor neuron cultures transduced with TRAP1 **(A)** and Hsp60 **(B)** lentiviruses. Scale bar: 20µm.

H_2O_2 is a commonly used oxidative stressor. Treatment of cells with H_2O_2 results in the production of superoxide, which is damaging to mitochondria and initiates apoptotic pathways (Gille and Joenje, 1992).

Treatment of primary motor neuron cultures with H_2O_2 for 30 minutes resulted in a decrease in TMRM intensity from neuronal cell bodies (Fig. 5.8 A). The largest drop in TMRM intensity was observed following treatment with 500 µM H_2O_2 and therefore this concentration was selected for further experiments (Fig. 5.8 B). In addition, a chronic H_2O_2 treatment (100 µM for 6 hours) resulted in a similar drop in TMRM intensity as the acute treatment, however, this chronic treatment had a more variable effect on neuronal TMRM intensity (Fig. 5.8 C).

Transduction of neurons with the TRAP1 lentivirus resulted in a partial rescue of TMRM intensity following either acute or chronic treatments with H_2O_2, indicating that overexpression of TRAP1 protects mitochondrial membrane potential from oxidative stress (Fig. 5.8 D, E). Mitochondrial area was unaffected by H_2O_2 treatment or expression of lentiviral constructs (Fig. 5.8 F, G). Although H_2O_2 treatment resulted in a reduction in mitochondrial membrane potential, the expression levels of proteins that are part of the mitochondrial electron transport chain were unaffected (Fig. 5.9), indicating that within the time frame of these experiments there was no loss of mitochondrial complexes that could have led to the loss of mitochondrial membrane potential. Furthermore, expression of TRAP1 or Hsp60 had no effect on the levels of these proteins.

Next, the effects of expression of mtHsps on the production of superoxide resulting from oxidative stress was assessed in neurons. To study this, DHE was used as a marker of superoxide accumulation (Fig. 5.10). Increased levels of superoxide oxidises DHE, converting it to ethidium, which in turn binds to DNA in the nucleus of cell staining it fluorescent red. H_2O_2 treatment of primary motor neuron cultures increased superoxide in neurons and the intensity of nuclear DHE staining was measured. Neurons transduced with the TRAP1 construct elicited a significantly lower level of nuclear fluorescence than neurons transduced with the Hsp60 lentivirus, the empty lentivirus or untransduced cells following treatment with H_2O_2 (Fig. 5.10). This suggests that overexpression of TRAP1 reduces the levels of superoxide production in neurons following exposure to oxidative stress.

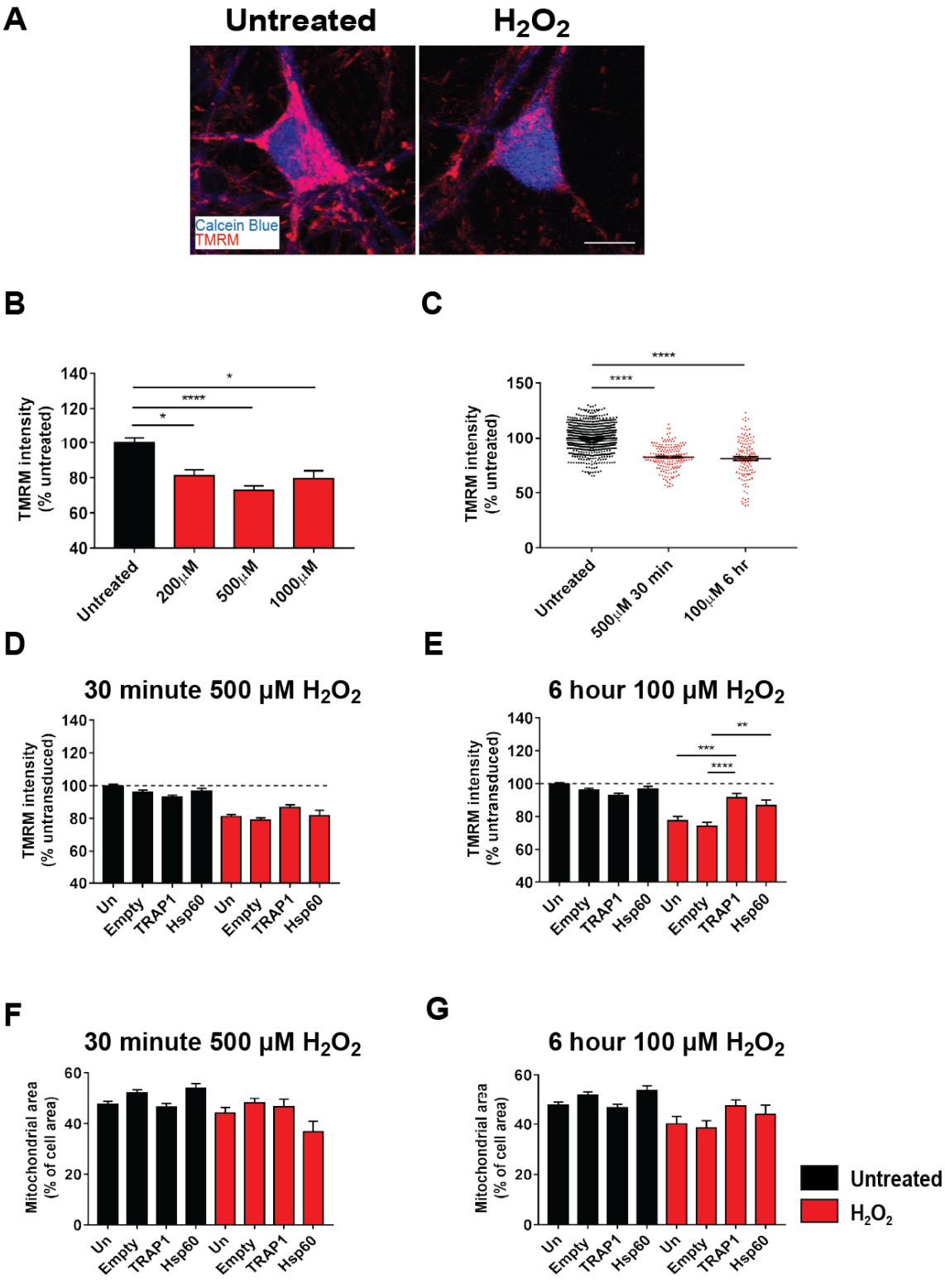
A
Untreated
H2O2
Calcein Blue
TMRM
B
TMRM intensity
(% untreated)
140
120
100
80
60
40
*
****
*
Untreated
200μM
500μM
1000μM
C
TMRM intensity
(% untreated)
150
100
50
0
****
****
Untreated
500μM 30 min
100μM 6 hr
D
30 minute 500 μM H2O2
TMRM intensity
(% untransduced)
140
120
100
80
60
40
Un
Empty
TRAP1
Hsp60
Un
Empty
TRAP1
Hsp60
E
6 hour 100 μM H2O2
TMRM intensity
(% untransduced)
140
120
100
80
60
40
**
***
****
Un
Empty
TRAP1
Hsp60
Un
Empty
TRAP1
Hsp60
F
30 minute 500 μM H2O2
Mitochondrial area
(% of cell area)
60
40
20
0
Un
Empty
TRAP1
Hsp60
Un
Empty
TRAP1
Hsp60
G
6 hour 100 μM H2O2
Mitochondrial area
(% of cell area)
60
40
20
0
Un
Empty
TRAP1
Hsp60
Un
Empty
TRAP1
Hsp60
Untreated
H2O2

Figure 5.8. Mitochondrial membrane potential measurements from lentivirally transduced neurons exposed to oxidative stress. TMRM intensity was used as a measure of mitochondrial membrane potential from the cell bodies of lentivirally transduced neurons treated with/without 500µM H_2O_2 for 30 minutes. **(A)** Representative images of neurons loaded with Calcein Blue and TMRM. **(B)** TMRM intensity measurements from neuronal cell bodies treated with increasing concentrations of H_2O_2. N=1, 18-48 neurons. **(C)** TMRM intensity measurements from neuronal cell bodies treated with an acute or chronic treatment of H_2O_2. N=3-6, 122-809 neurons. TMRM intensity measurements from cell bodies of lentivirally transduced neurons treated with an acute **(D)** or chronic **(E)** treatment of H_2O_2. N=3-6, 24-252 neurons. Mitochondrial area displayed as a % of the neuronal soma of lentivirally transduced neurons treated with an acute **(F)** or chronic **(G)** treatment of H_2O_2 N=3-6, 24-252 neurons. Data are displayed as a percentage of the average intensity measurements from control cells and expressed as the mean ± SEM. A Kruskal-Wallis test with post-hoc Dunn's tests or two-way ANOVA with post-hoc Bonferroni tests was used for statistical comparison. P=*≤0.05, **≤0.01, ***≤0.001, ****≤0.0001. Scale bar: 10µm.

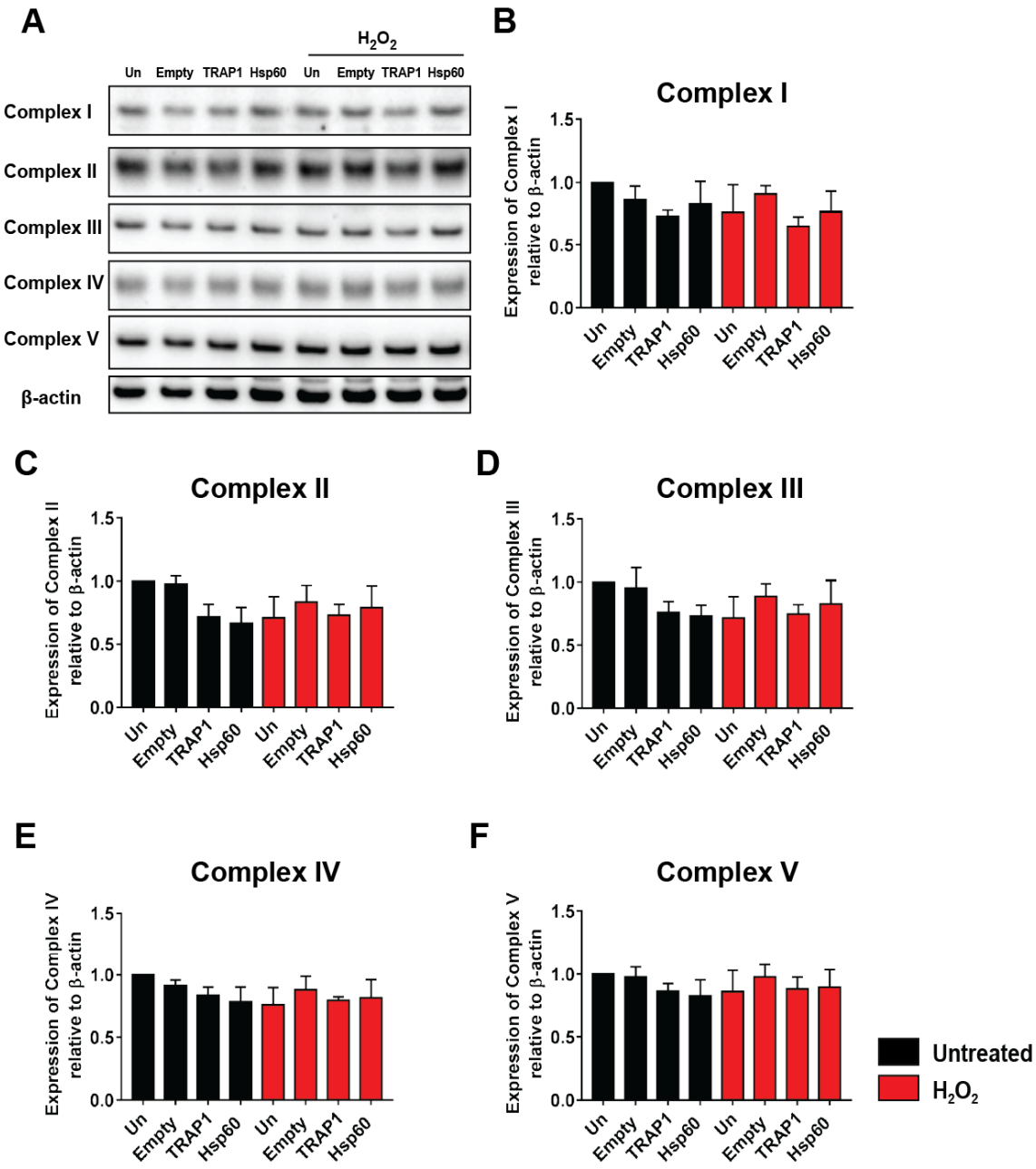

Figure 5.9. Expression of OXPHOS components in lentivirally transduced neurons exposed to oxidative stress. (A) Western blot for OXPHOS subunits of lentivirally transduced motor neuron cultures exposed to 500μM H_2O_2 for 30 minutes. Quantification of blots for complex I **(B)**, complex II **(C)**, complex III **(D)**, complex IV **(E)** and complex V **(F)**. Data are expressed as the mean ± SEM. A two-way ANOVA with post-hoc Tukey tests was used for statistical comparison. N=3.

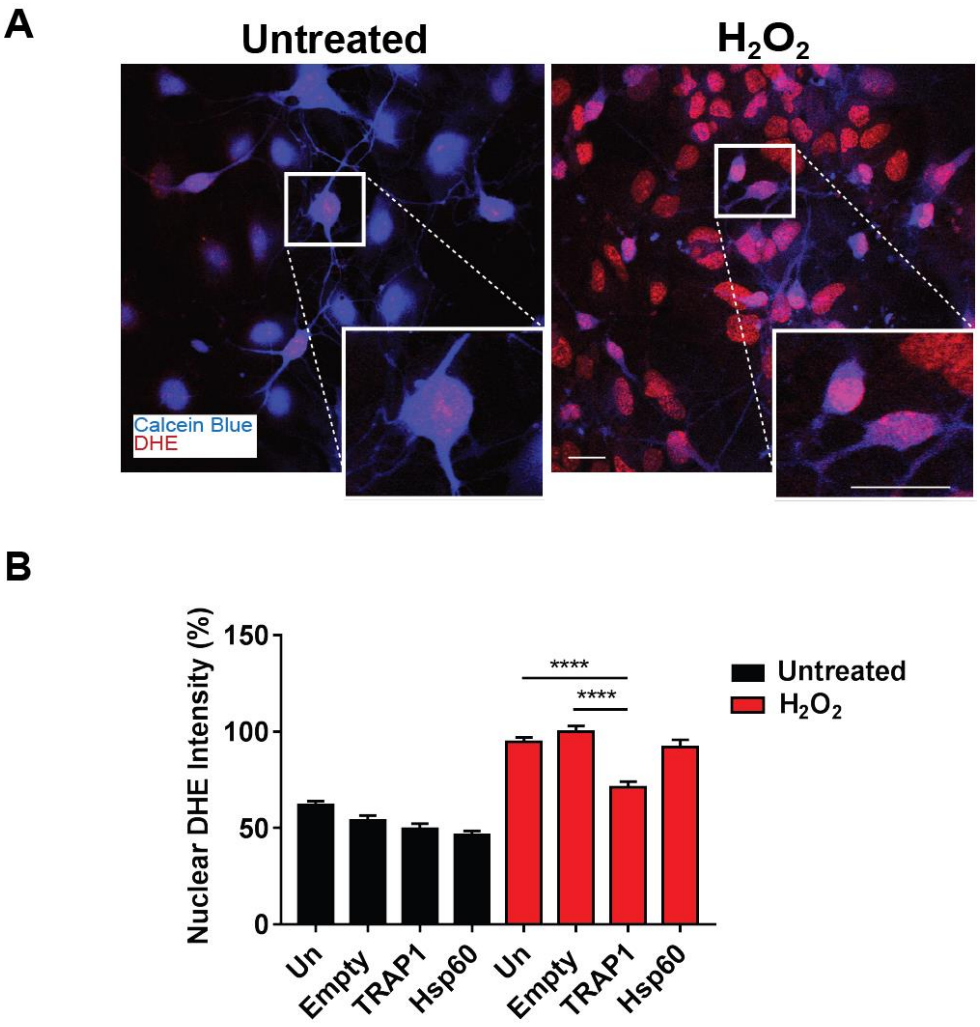

Figure 5.10. Nuclear DHE intensity measurements from lentivirally transduced neurons exposed to oxidative stress. (A) Representative images of neurons loaded with Calcein Blue and DHE. **(B)** DHE intensity measurements from the nuclei of lentivirally transduced neurons treated with/without 500µM H_2O_2 for 30 minutes. Data are expressed as the mean ± SEM. A two-way ANOVA with post-hoc Tukey tests was used for statistical comparison. P=****≤0.0001. Scale bar: 20µm. N=3-4, 95-167 neurons.

Lipid peroxidation was measured using the dye Bodipy 581/591 C11. This dye intercalates in the cell membrane and shifts fluorescence from 590 nm to 510 nm when oxidised. 500 µM H_2O_2 treatment for 30 minutes did not significantly alter the fluorescence of the Bodipy dye in primary motor neuron cultures. Therefore, under these experimental conditions no change in lipid peroxidation was detected (Fig. 5.11).

The effects of lentiviral expression of TRAP1 and Hsp60 on oxidative stress-induced cell death were next assessed. Neurons transduced with lentiviral constructs were counted using Calcein Blue, a dye that becomes fluorescent after cleavage by cellular esterases, giving an estimation of the number of live neurons in the culture. Calcein Blue and GFP-positive cells were counted following a 24 hour treatment with 100 µM H_2O_2. The extent of cell death following H_2O_2 treatment was variable between different experiments, however, there was a clear trend of increased neuronal survival in neurons transduced with the TRAP1 lentivirus (Fig. 5.12). Conversely, the expression of Hsp60 had no effect on oxidative stress-induced neuronal cell death.

5.3.4 Lentiviral vectors containing shRNAs successfully knockdown expression of TRAP1 and Hsp60

Next, shRNAs were used to study the effects of reducing expression of TRAP1 and Hsp60. Candidate shRNA constructs were obtained from Genecopia and first transfected into neuroblastoma N2A cells to identify the shRNAs that would effectively reduce the levels of TRAP1 or Hsp60. All four commercially obtained constructs for each mtHsp, as well as a scrambled shRNA control construct, successfully transfected N2A cells as indicated by positive GFP reporter expression (Fig. 5.13 A). Of these constructs, two shRNA constructs for each mtHsp that reduced their expression by around 50% or more were selected for lentiviral transduction. For TRAP1 these were shRNAs 1 and 3, while for Hsp60 shRNAs 1 and 2 were chosen (Fig. 5.13 B-E).

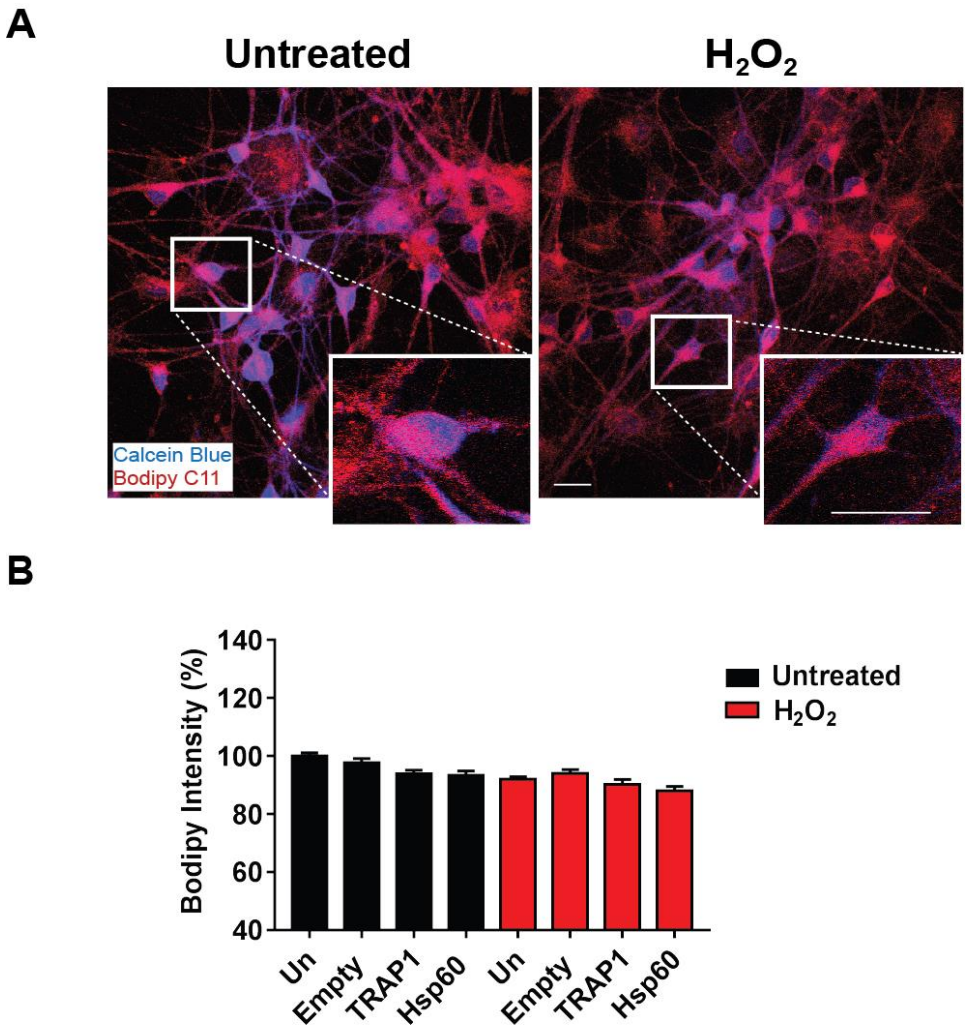

Figure 5.11. Bodipy 581/591 C11 intensity measurements from lentivirally transduced neurons exposed to oxidative stress. (A) Representative images of neurons loaded with Calcein Blue and Bodipy 581/591 C11. **(B)** Bodipy 581/591 C11 intensity measurements from the cell bodies of lentivirally transduced neurons treated with/without 500µM H_2O_2 for 30 minutes. Data are expressed as the mean ± SEM. A two-way ANOVA with post-hoc Bonferroni tests was used for statistical comparison. Scale bar: 20µm. N=3-4, 94-168 neurons.

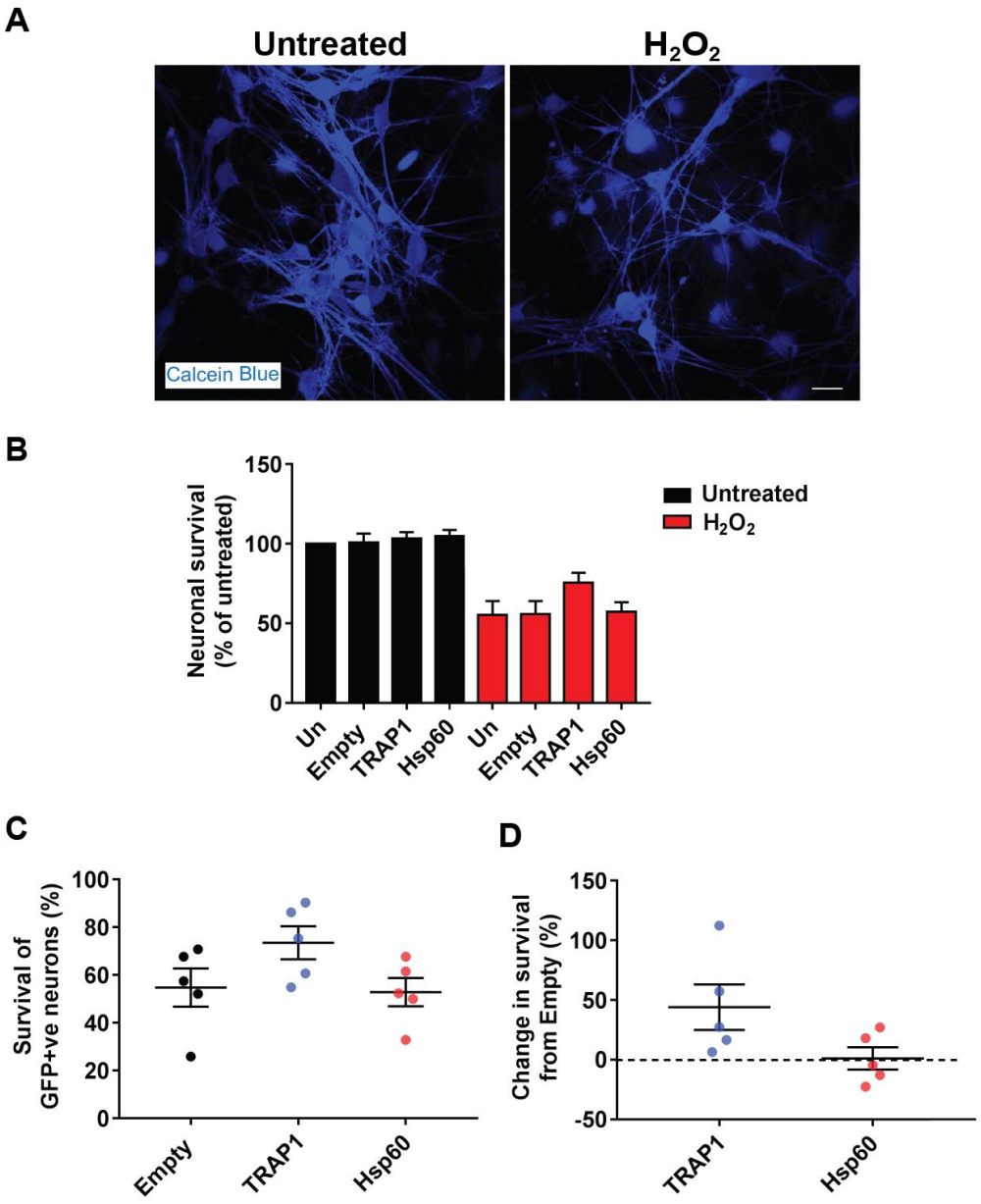

Figure 5.12. Neuronal survival following H_2O_2 treatment in lentivirally transduced motor neuron cultures. (A) Representative images of primary motor neuron cultures treated with 100 µM H_2O_2 and loaded with Calcein Blue to identify neurons. **(B)** The survival of GFP-positive neurons transduced with lentiviral expression constructs treated with 100 µM H_2O_2 for 24 hours. **(C)** The survival of GFP-positive neurons treated with 100 µM H_2O_2, expressed as a percentage of GFP-positive neurons in untreated cultures. **(D)** Survival of GFP-positive transduced neurons treated with 100 µM H_2O_2, expressed as the fold change of the number of GFP-positive neurons expressing the empty construct for each experiment. Data are expressed as the mean ± SEM. A Kruskal-Wallis test with post-hoc Dunn's tests or Mann-Whitney U test was used for statistical comparison. Scale bar: 20µm. N=3-5.

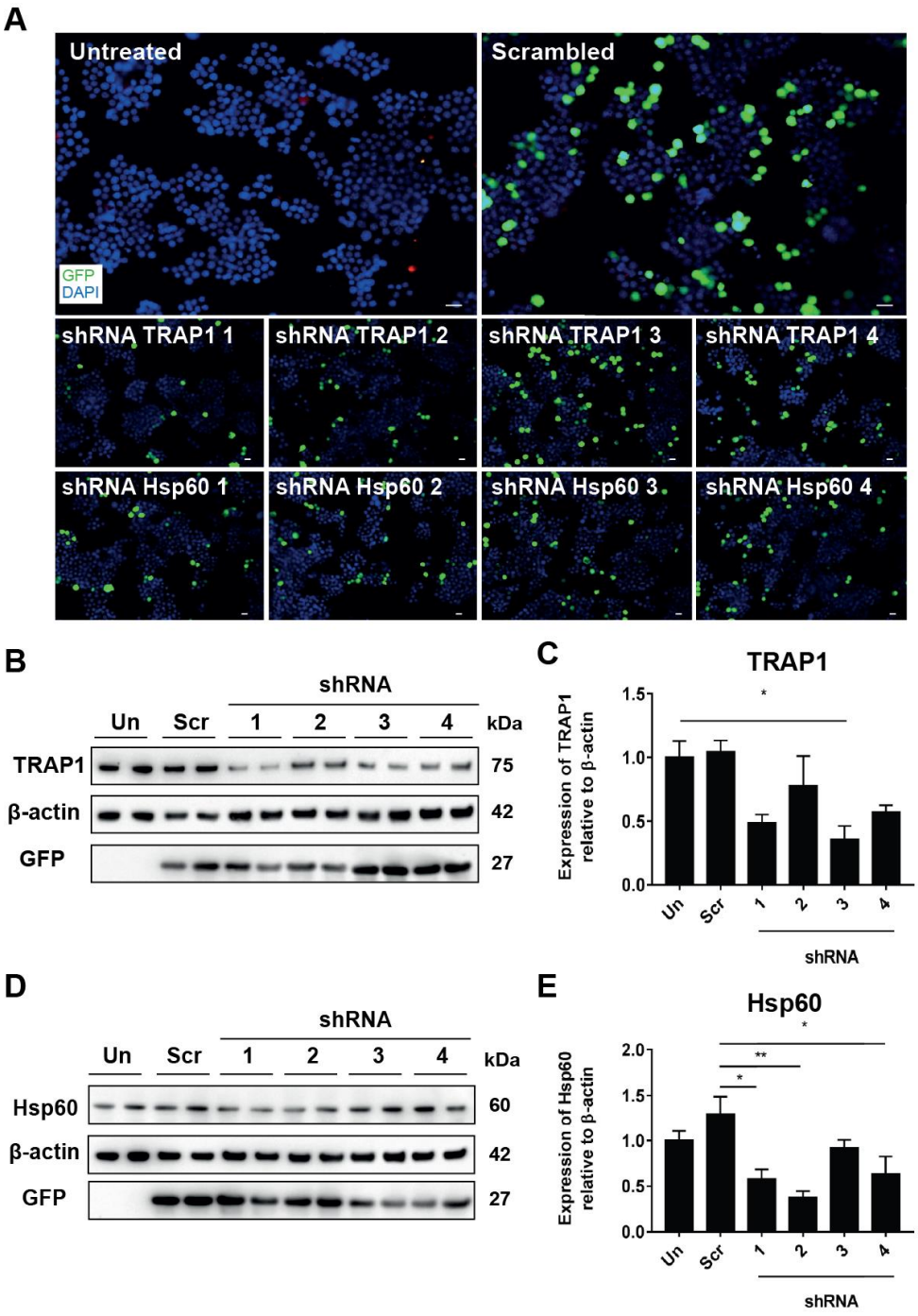

Figure 5.13. shRNA knockdown of TRAP1 and Hsp60 in N2A cells. (A) Immunofluorescence for GFP in N2A cells transfected with 500 ng of scrambled (Scr), TRAP1 or Hsp60 shRNA plasmids using Lipofectamine 2000. **(B)** Western blot and **(C)** quantification for TRAP1 and GFP in cells treated with 4 shRNA constructs for TRAP1. **(D)** Western blot and **(E)** quantification for Hsp60 and GFP in cells treated with 4 shRNA constructs for Hsp60. Data are expressed as the mean ± SEM. P=*≤0.05, **≤0.01. A one-way ANOVA with post-hoc Tukey tests was used for statistical comparison. Scale bar: 20µm. N=2 (with 2 technical replicates per biological replicate).

Next, lentiviruses containing shRNAs designed to knockdown TRAP1 or Hsp60 mRNA were used to transduce primary motor neuron cultures. Both lentiviruses designed for TRAP1 achieved a 50% knockdown or more of this protein and expressed GFP (Fig. 5.14 A, B). Lentivirus 1 designed to target Hsp60 was also able to achieve at least a 50% knockdown, however, lentivirus 2 for Hsp60 did not knockdown Hsp60 (Fig. 5.14 C, D). Therefore, lentivirus 3 for TRAP1 and lentivirus 1 for Hsp60 were chosen for experiments assessing the effects of knockdown of mtHsps on mitochondrial functions.

Since primary motor neuron cultures contain several non-neuronal cell types, the ability of shRNA lentiviruses to specifically knockdown the expression of mtHsps in motor neurons was assessed by immunofluorescence. shRNA lentiviruses for both TRAP1 and Hsp60 were able to transduce neurons, although a higher expression of GFP was seen in non-neuronal cells (Fig. 5.15 A, B). Nevertheless, on average over 50% of neurons were transduced, albeit with a high amount of variability between different cultures (Fig. 5.15 C). Furthermore, the intensity of TRAP1 and Hsp60 was lower in GFP-positive neuronal cell bodies, identified by the pan-neuronal marker TUJ1, transduced with corresponding lentiviral shRNA constructs (Fig. 5.15 D, E). For measurements of Hsp60 intensity, scrambled shRNA treated cultures displayed lower signal than untransduced cultures, suggesting that viral transduction had some effect on Hsp60 levels.

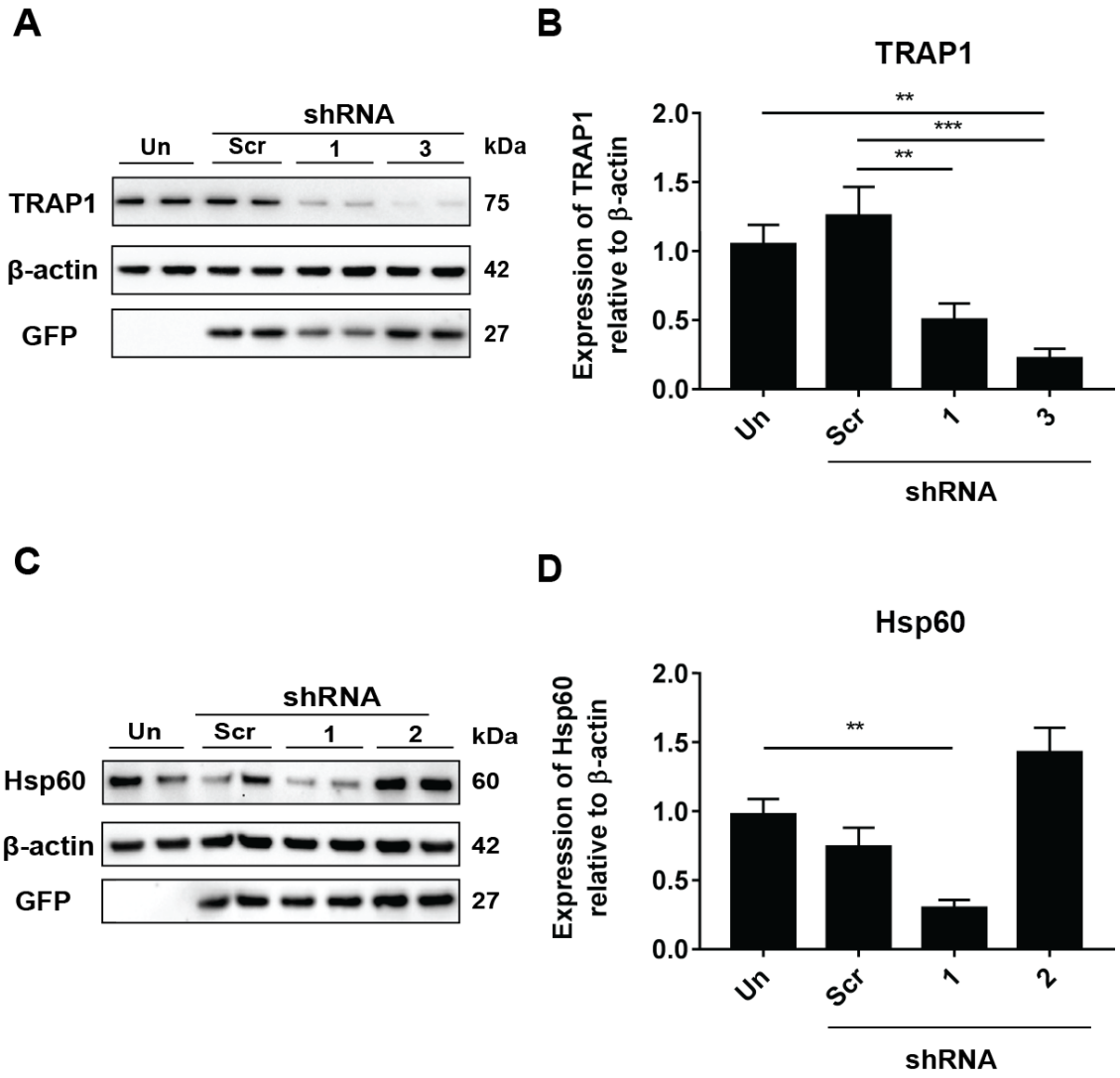

Figure 5.14. Lentiviral shRNA knockdown of TRAP1 or Hsp60 in motor neuron cultures. Western blot **(A)** and quantification **(B)** for TRAP1 of primary motor neuron cultures treated with lentiviruses containing shRNAs for TRAP1. Western blot **(C)** and quantification **(D)** for Hsp60 of primary motor neuron cultures treated with lentiviruses containing shRNAs for Hsp60. Data are expressed as the mean ± SEM. A one-way ANOVA with post-hoc Tukey tests was used for statistical comparison. P=**≤0.01, ***≤0.001. N=3 (with 2 technical replicates per biological replicate).

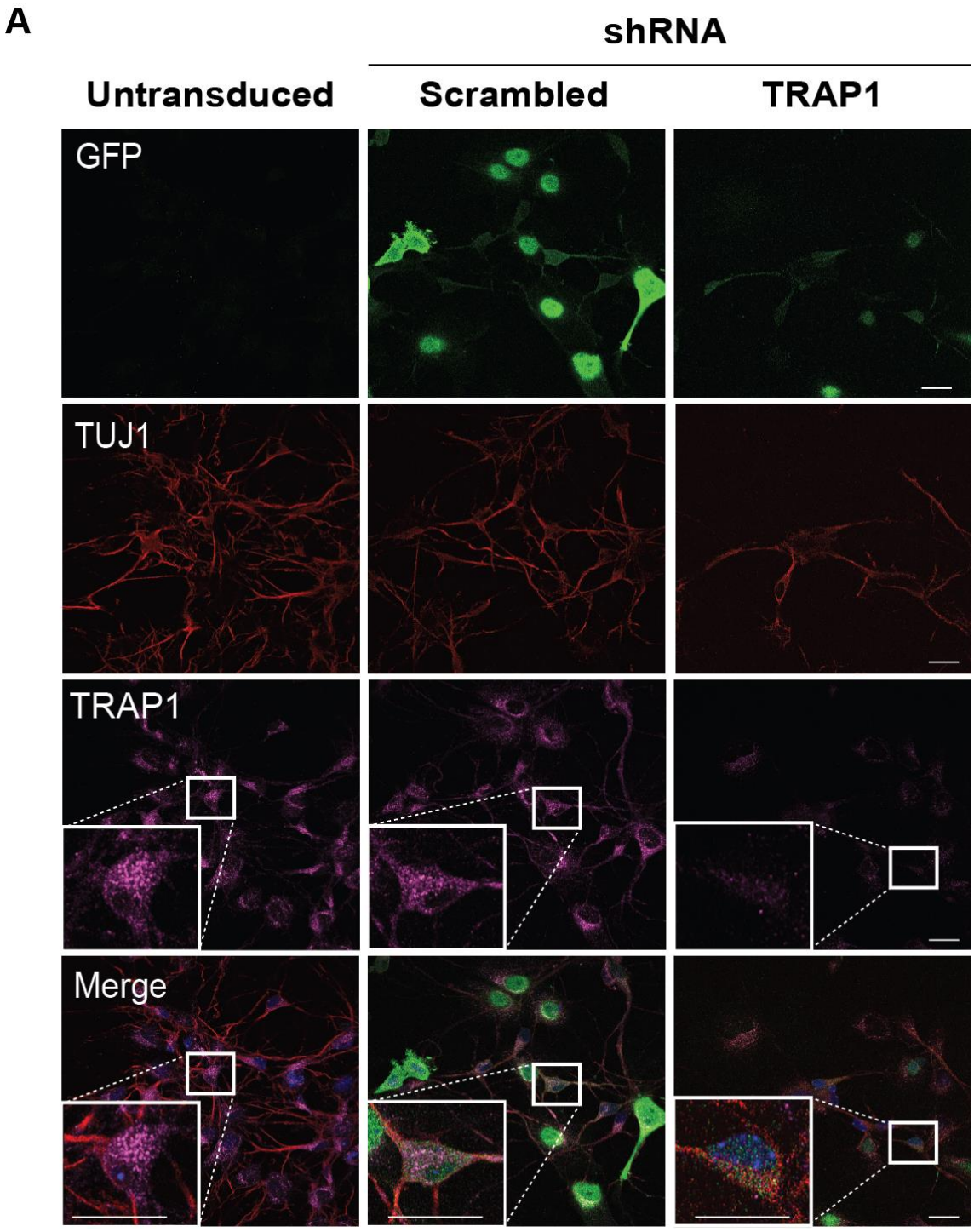
A
shRNA
Untransduced
Scrambled
TRAP1
GFP
TUJ1
TRAP1
Merge

B

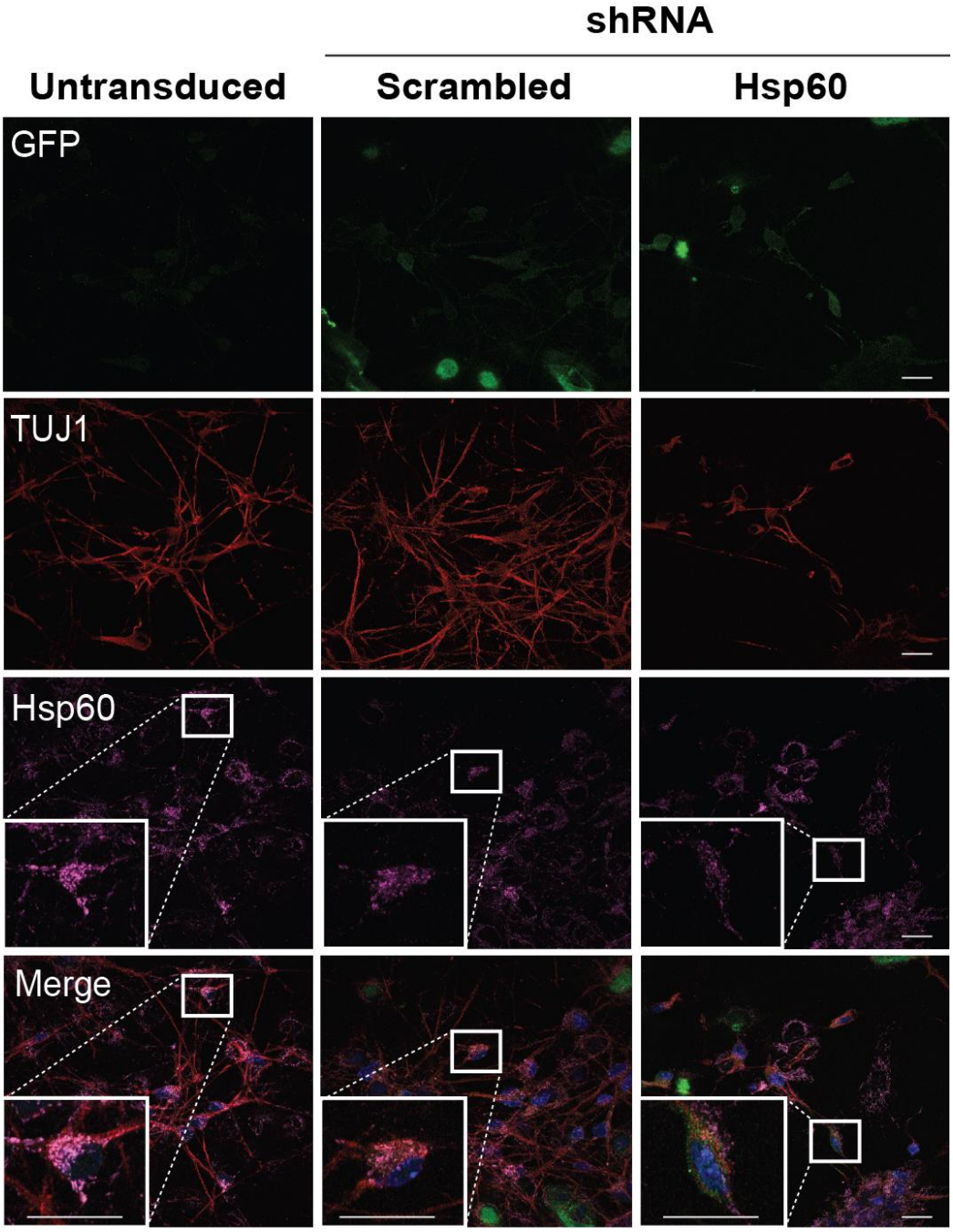

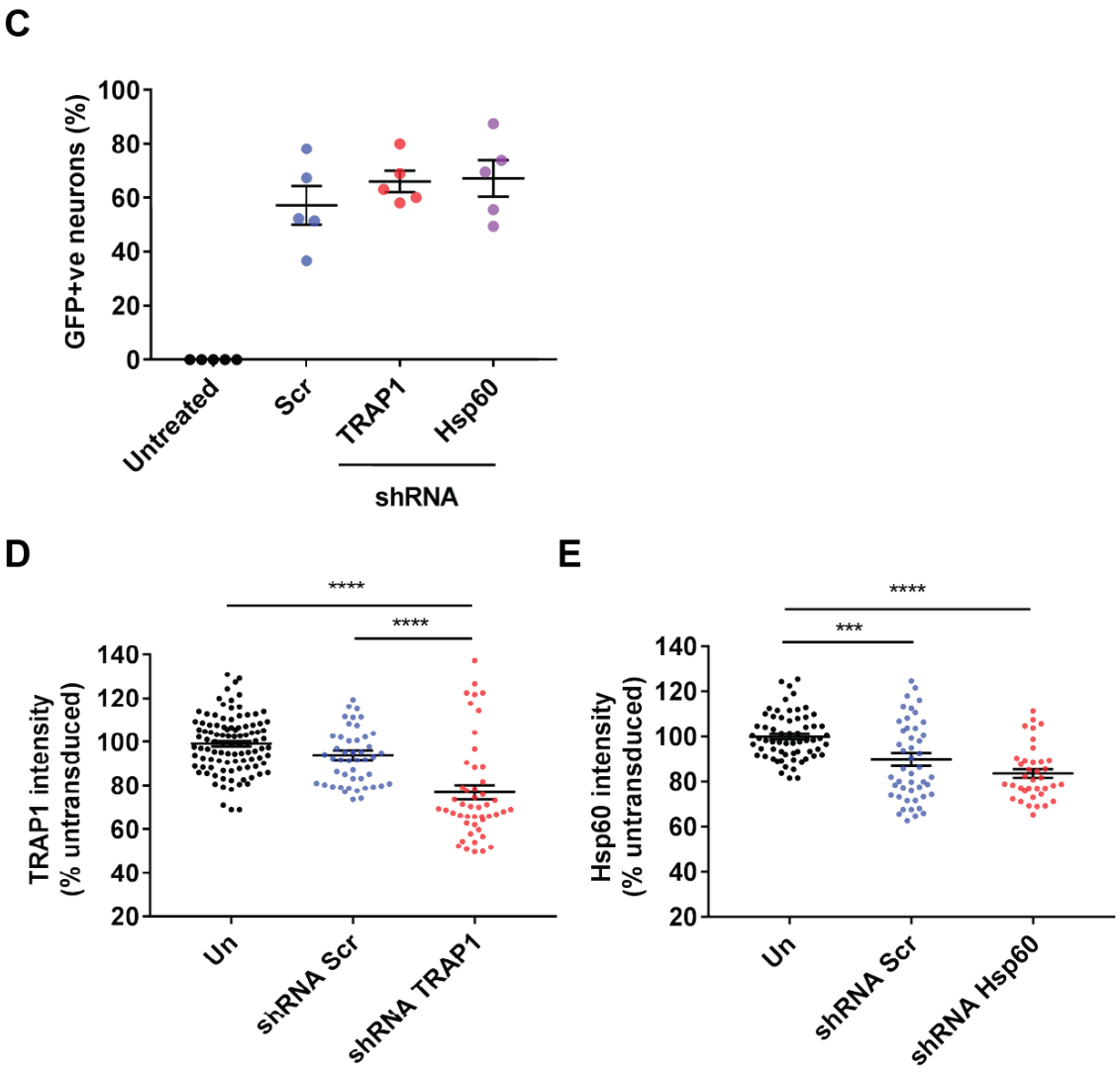

Figure 5.15. Lentiviral shRNA knockdown of TRAP1 or Hsp60 in motor neuron cultures. Immunofluorescence **(A, B)** for GFP (green), TRAP1/Hsp60 (magenta) and TUJ1 (red) of motor neuron cultures transduced with lentiviruses containing shRNAs for **(A)** TRAP1 and **(B)** Hsp60. **(C)** Quantification of GFP-positive neurons in shRNA transduced motor neuron cultures. N=5. Quantification of intensity of TRAP1 **(D)** and Hsp60 **(E)** in neuronal cell bodies of motor neuron cultures treated with shRNA lentiviruses. Data are expressed as the mean ± SEM. A Kruskal-Wallis test with post-hoc Dunn's tests was used for statistical comparison. P=***≤0.001, ****≤0.0001. Scale bar: 20µm. N=3, 37-101 neurons.

5.3.5 Effect of reducing TRAP1 or Hsp60 expression levels on mitochondrial functions under conditions of oxidative stress in motor neurons

Next, lentiviral shRNA knockdown was used to assess the effect of reducing the levels of TRAP1 or Hsp60 on mitochondrial function. Under basal conditions, reduced TMRM intensity was observed in neurons treated with a shRNA lentivirus targeting TRAP1 (Fig. 5.16 A). However, there were no significant differences in TMRM intensity between neurons treated with an Hsp60 shRNA lentivirus and untreated cells. The effects of TRAP1 or Hsp60 knockdown were also observed following treatment with the oxidative stressor, H_2O_2. Acute treatment did not exacerbate the decrease in TMRM intensity caused by reduced TRAP1 levels in motor neurons (Fig. 5.16 C). Furthermore, chronic treatment did not result in a further drop in TMRM intensity, which may reflect the high levels of variability in responses to H_2O_2 using this condition (Fig. 5.16 D). Mitochondrial area was unaffected by H_2O_2 or expression of lentiviral constructs (Fig. 5.16 E, F).

As acute treatment with H_2O_2 caused a drop in mitochondrial membrane potential, the effect of this treatment on the expression of proteins involved in the mitochondrial electron transport chain was next evaluated. Neither H_2O_2 treatment nor treatment of primary motor neuron cultures with shRNA containing lentiviruses affected the expression of proteins in each of the complexes that form the electron transport chain (Fig. 5.17).

The effects of knockdown of TRAP1 or Hsp60 on ROS production were next evaluated in primary motor neuron cultures. Increased ROS production was found in neurons following treatment with H_2O_2, indicated by an increase in intensity of neuronal nuclear DHE intensity (Fig. 5.18 A). Knockdown of TRAP1 or Hsp60, did not affect the basal production of ROS, but may exacerbate the production of ROS following treatment with H_2O_2 (Fig. 5.18 B).

Although reduced TRAP1 or Hsp60 levels did not affect ROS production in the presence or absence of stress, reduced TRAP1 levels caused a significant increase in lipid peroxidation, as measured by a reduction Bodipy 581/591 C11 intensity (Fig 5.19). Furthermore, while Hsp60 knockdown did not affect lipid peroxidation under basal conditions, reduced Hsp60 increased lipid peroxidation under oxidative stress conditions.

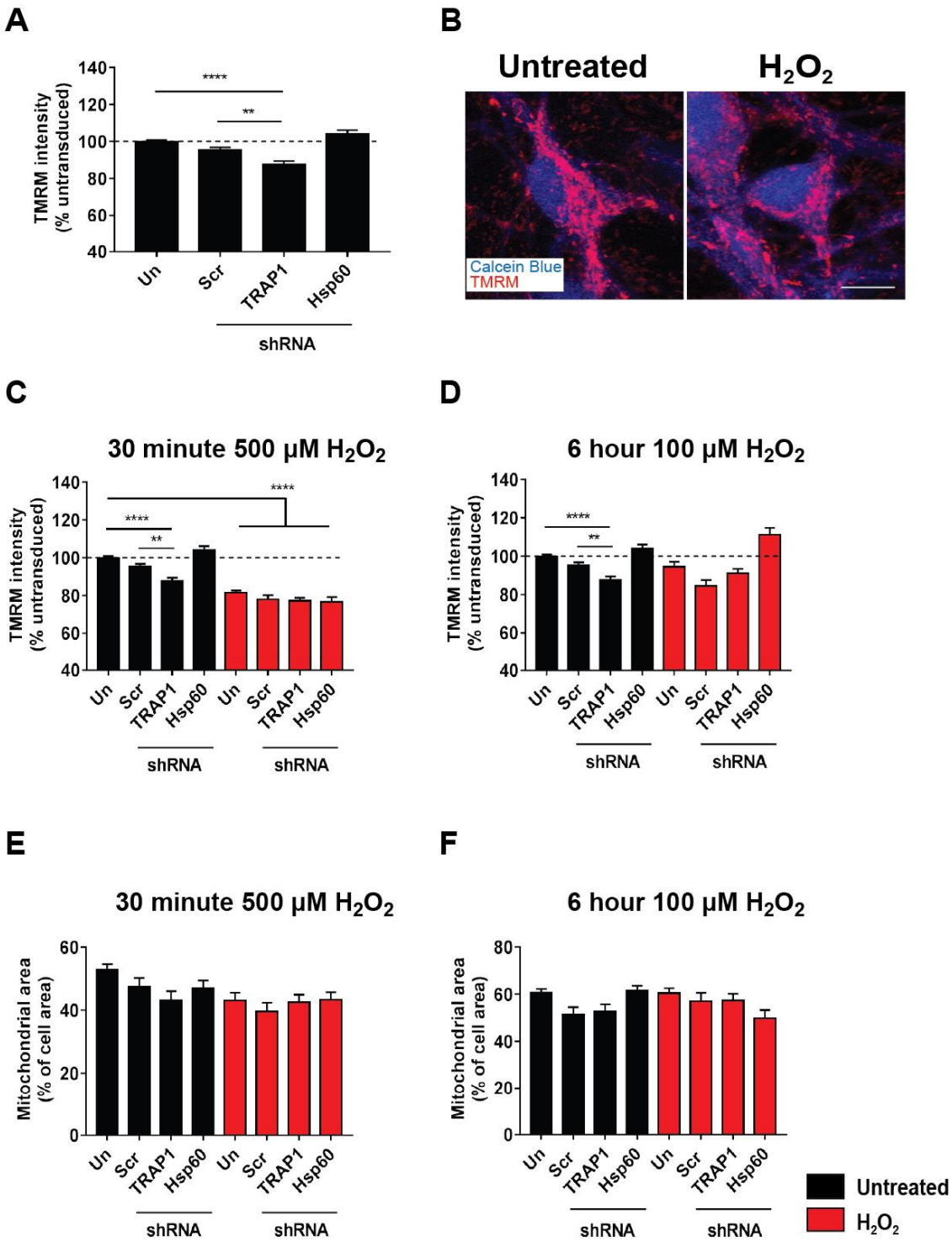
A
TMRM intensity (% untransduced)
140
120
100
80
60
40
****
**
Un
Scr
TRAP1
Hsp60
shRNA
B
Untreated
H2O2
Calcein Blue
TMRM
C
30 minute 500 µM H2O2
TMRM intensity (% untransduced)
****
****
**
Un
Scr
TRAP1
Hsp60
shRNA
shRNA
D
6 hour 100 µM H2O2
TMRM intensity (% untransduced)
****
**
shRNA
shRNA
E
30 minute 500 µM H2O2
Mitochondrial area (% of cell area)
60
40
20
0
shRNA
shRNA
F
6 hour 100 µM H2O2
Mitochondrial area (% of cell area)
80
60
40
20
0
shRNA
shRNA
Untreated
H2O2

Figure 5.16. Mitochondrial membrane potential measurements from lentivirally transduced neurons treated with H_2O_2. (A) Quantification of TMRM intensity from the cell bodies of neurons of cultures treated with lentiviruses containing shRNAs targeting TRAP1 or Hsp60. N=8-9, 95-237 neurons. **(B)** Representative images of neurons loaded with Calcein Blue (blue) and TMRM (red) treated with H_2O_2. **(C)** Quantification of TMRM intensity in transduced neurons exposed to 500 µM H_2O_2 for 30 minutes. N=5. Quantification of TMRM intensity **(D)** in DIV8 transduced neurons exposed to 100 µM H_2O_2 for 6 hours. Mitochondrial area expressed as a % of neuronal soma for lentivirally treated neurons exposed to acute **(E)** or chronic **(F)** treatments of H_2O_2. Data are expressed as the mean ± SEM. P=**≤0.01, ****≤0.0001. A Kruskal-Wallis test with post-hoc Dunn's tests or two-way ANOVA with post-hoc Bonferroni tests was used for statistical comparison. Scale bar: 20µm. N=4, 40-237 neurons.

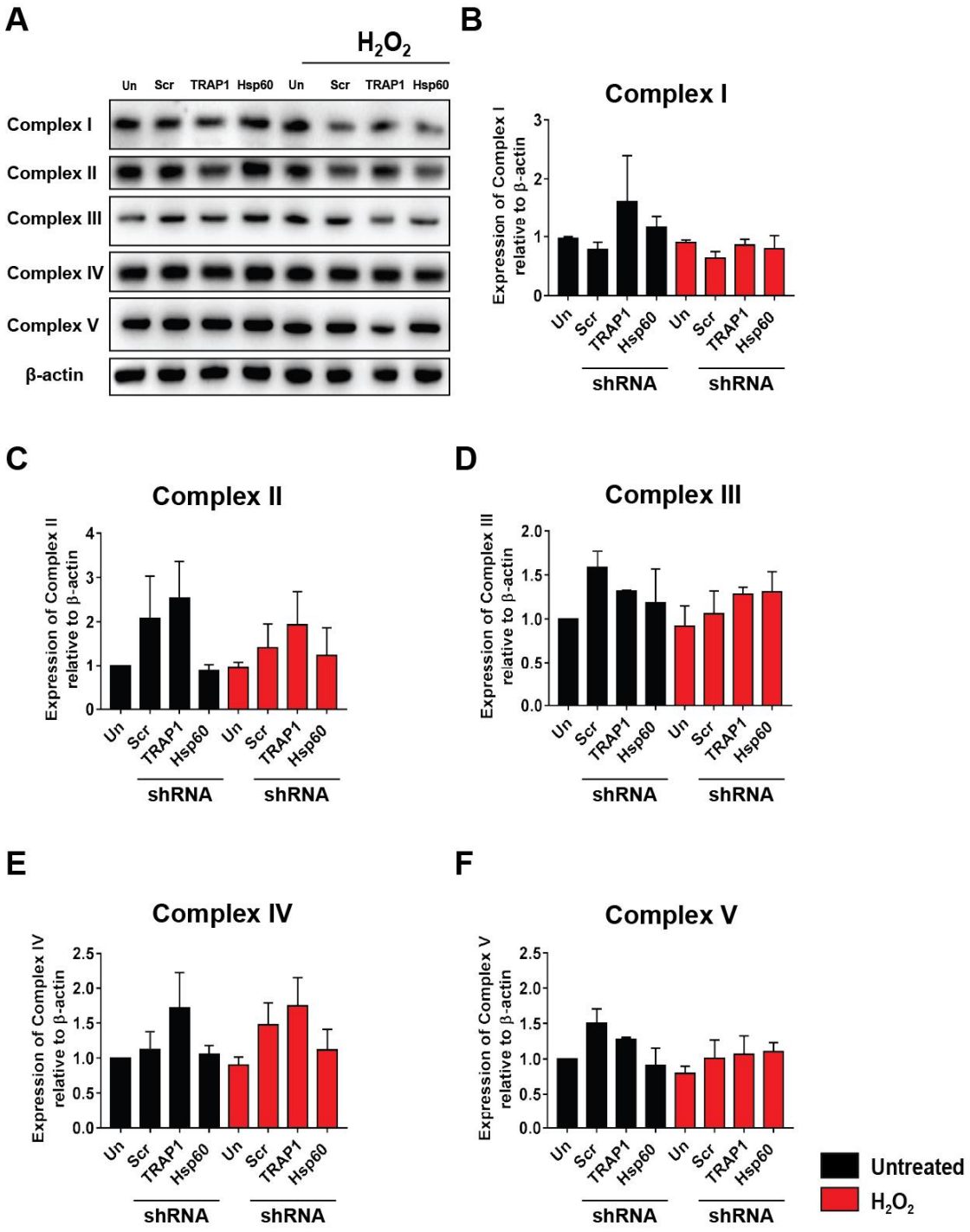

Figure 5.17. Expression of OXPHOS components in motor neuron cultures exposed to oxidative stress. (A) Western blot for OXPHOS subunits of lentivirally transduced motor neuron cultures exposed to 500µM H_2O_2 for 30 minutes. Quantification of blots for complex I **(B)**, complex II **(C)**, complex III **(D)**, complex IV **(E)** and complex V **(F)**. Data are expressed as the mean ± SEM. A two-way ANOVA with post-hoc Tukey tests was used for statistical comparison N=3.

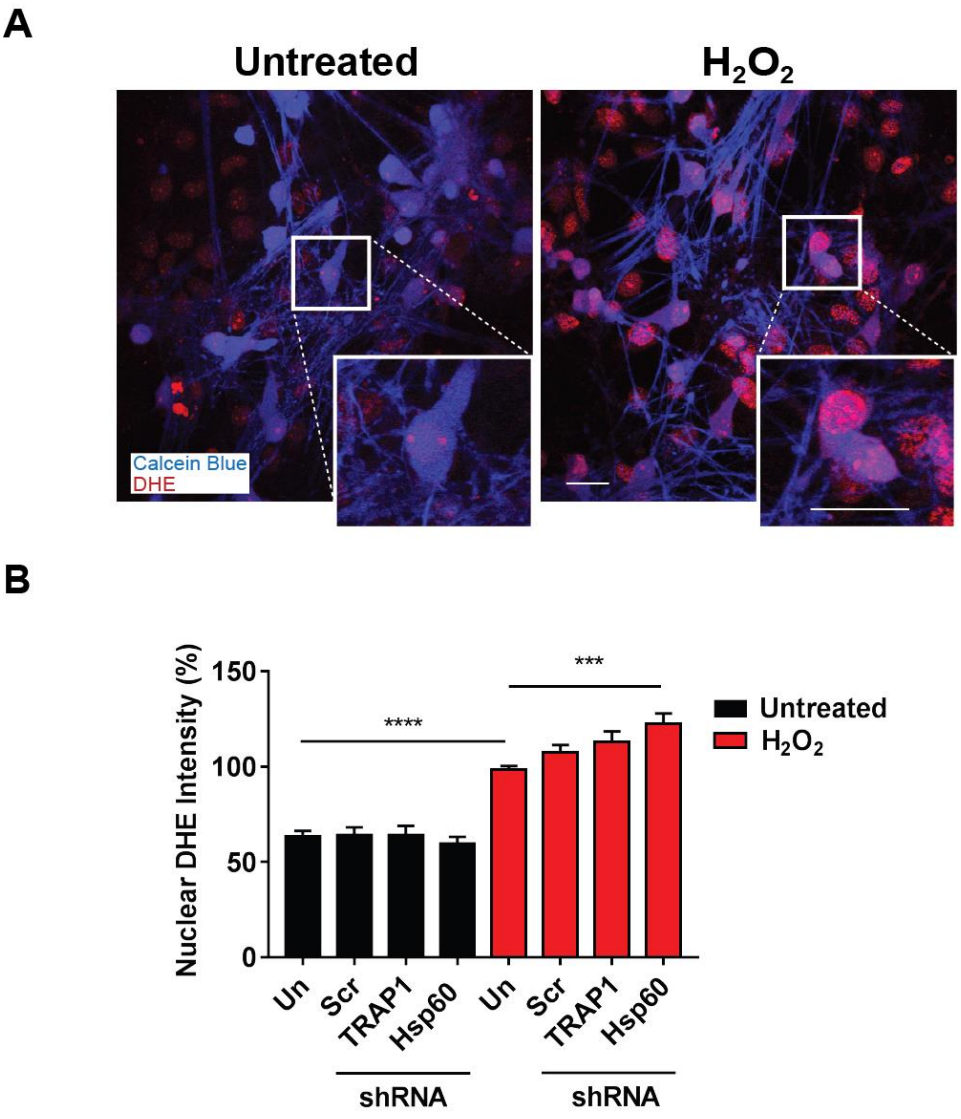

Figure 5.18. DHE intensity measurements from lentivirally transduced neurons treated with H_2O_2. (A) Representative images of neurons loaded with Calcein Blue (blue) and DHE (red) treated with H_2O_2. **(B)** Quantification of lentivirally transduced neurons treated with 500 µM H_2O_2 for 30 minutes. Data are expressed as the mean ± SEM. P=****≤0.0001. A two-way ANOVA with post-hoc Bonferroni tests was used for statistical comparison. Scale bar: 20 µm. N=3-4, 65-169 neurons.

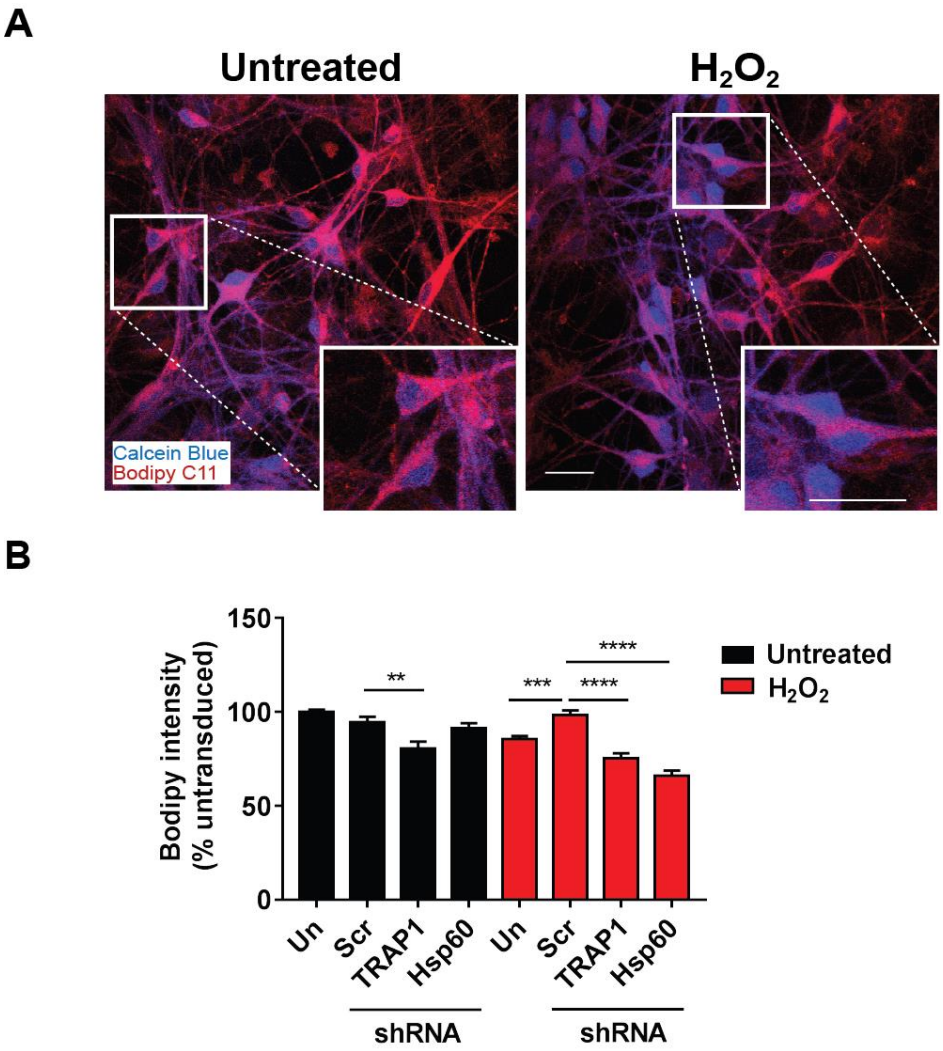

Figure 5.19. Bodipy 581/591 C11 intensity measurements from lentivirally transduced neurons treated with H_2O_2. (A) Representative images of neurons loaded with Calcein Blue (blue) and Bodipy 581/591 C11 (red) treated with H_2O_2. **(B)** Quantification of lentivirally transduced neurons treated with 500 µM H_2O_2 for 30 minutes. Data are expressed as the mean ± SEM. A two-way ANOVA with post-hoc Bonferroni tests was used for statistical comparison. P=**≤0.01, ***≤0.001, ****≤0.0001. Scale bar: 20 µm. N=3-4, 70-225 neurons.

Finally, the effects of TRAP1 and Hsp60 knockdown on cell survival in primary motor neuron cultures were investigated. While treatment of 100 µM H_2O_2 for 24 hours resulted in ~50% loss of neurons, lentiviral shRNA knockdown of TRAP1 or Hsp60 had no effect on neuronal survival under basal conditions or following exposure to oxidative stress (Fig. 5.20).

5.4 Discussion

The aim of this Chapter was to investigate the roles of mtHsps TRAP1 and Hsp60 in motor neurons under basal and stress conditions modelling ALS. The results of this Chapter suggest that TRAP1 and Hsp60 may be downregulated in motor neurons of $SOD1^{G93A}$ mice. To elucidate further the role of mtHsps in promoting resistance of motor neurons to stress conditions, TRAP1 and Hsp60 were genetically manipulated in primary motor neurons. TRAP1 overexpression protected motor neurons against oxidative stress-induced reduction of mitochondrial membrane potential, production of ROS and neuronal cell death. In turn, reduction of TRAP1 expression reduced mitochondrial membrane potential and increased lipid peroxidation, but this effect was not sufficient to lead to measurable increases in ROS production or neuronal death. Exogenous expression of Hsp60 partially rescued mitochondrial membrane potential following exposure to oxidative stress, but had no effect on ROS production, lipid peroxidation or cell survival. Reduction of Hsp60 expression did not affect mitochondrial membrane potential, ROS production, lipid peroxidation or cell survival under basal conditions, but exacerbated ROS production and lipid peroxidation under oxidative stress conditions.

There were no significant differences in the expression of TRAP1 or Hsp60 in the spinal cord at different ages of the $SOD1^{G93A}$ mouse, as determined by western blots. This is in agreement with a previous study that found no differences in Hsp60 expression in mSOD1 rats (Li et al., 2010). However, there was a decreased expression of these proteins specifically in motor neurons from the ventral horn of the spinal cord, identified by immunofluorescence. A lack of any observable difference from western blots of the $SOD1^{G93A}$ spinal cord may be explained by the presence of non-neuronal cells present in the spinal cord.

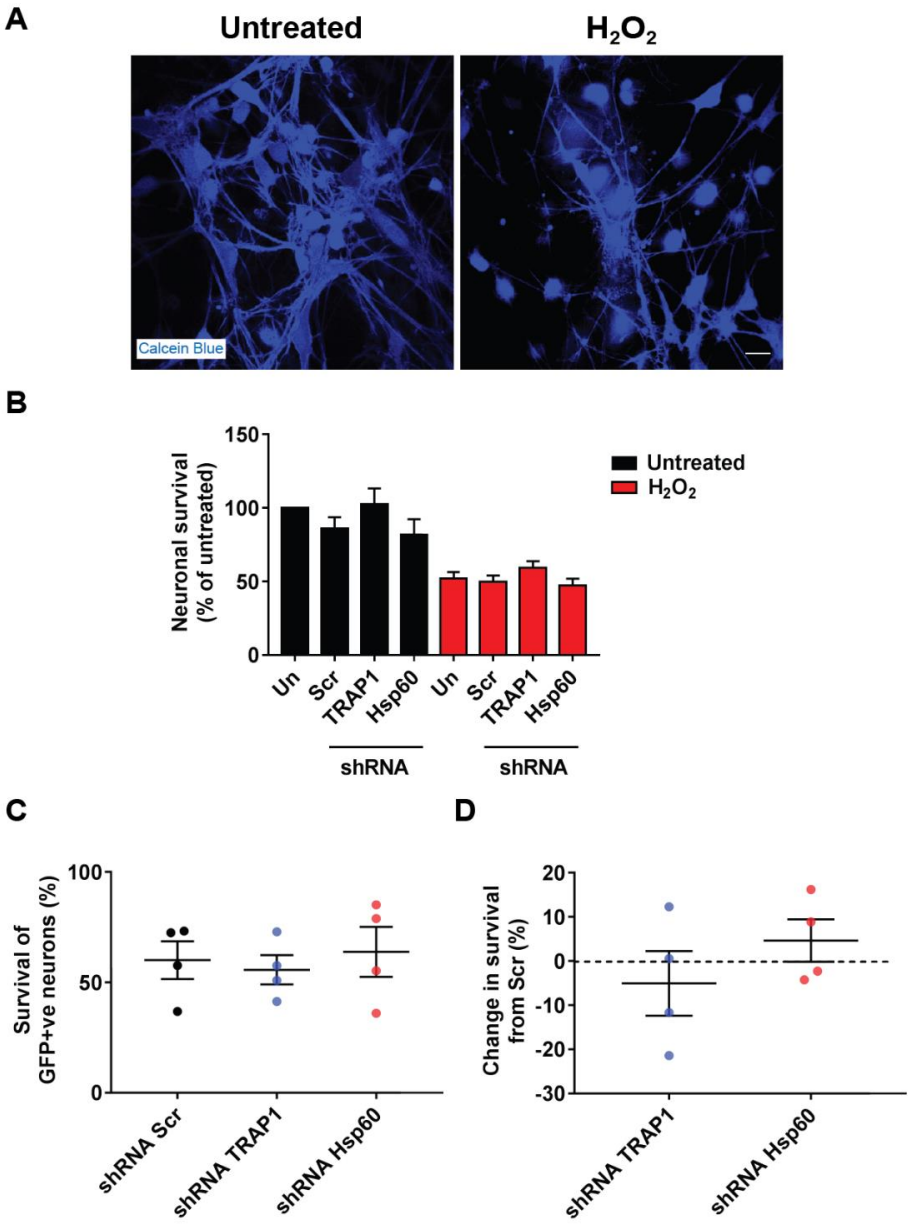

Figure 5.20. Neuronal survival following H_2O_2 treatment in lentivirally transduced motor neuron cultures. (A) Representative images of primary motor neuron cultures treated with 100 µM H_2O_2 and loaded with Calcein Blue to identify neurons. **(B)** The survival of GFP positive neurons transduced with lentiviral shRNA constructs treated with 100 µM H_2O_2 for 24 hours. **(C)** The survival of GFP positive neurons expressed as a percentage of untreated transduced cultures. **(D)** The survival of GFP positive transduced neurons treated with 100 µM H_2O_2, expressed as the fold change from the number of GFP positive neurons transduced with the scrambled shRNA construct for each experiment. Data are expressed as the mean ± SEM. A Kruskal-Wallis test with post-hoc Dunn's tests or Mann-Whitney U test was used for statistical comparison. Scale bar: 20 µm. N=3-4.

Furthermore, as western blotting is a semi-quantitative technique, performing laser capture microdissection of motor neurons followed by qPCR may provide more sensitivity in quantifying levels of TRAP1 and Hsp60 in the $SOD1^{G93A}$ spinal cord.

The expression levels of TRAP1 and Hsp60 did not change in response to stressful conditions in motor neuron cultures. While the HSR was induced in these cultures, as determined by increased Hsp70 expression following heat shock, no change in TRAP1 or Hsp60 expression was observed. These results suggest that unlike Hsp70, TRAP1 and Hsp60 are not under the control of HSF-1.

Since Hsp60 has been shown previously to be upregulated following induction of the mtUPR, these results also suggest that the mtUPR is not activated in primary motor neuron cultures following H_2O_2, rotenone or heat stress treatment. More stressors such as expression of misfolded protein ΔOTC should be evaluated in future studies. Furthermore, although the overall levels of TRAP1 and Hsp60 may not change, post translational modifications or a change in the localisation of these proteins may occur during or following stress. The phosphorylation state of TRAP1 has been suggested to be involved in the pro-survival effects of this protein (Pridgeon et al., 2007). Moreover, TRAP1 has been shown to be released from mitochondria when treated with the oxidative stressor and PD model oxidopamine (6-OHDA) (Shin and Oh, 2014).

As motor neurons have been previously shown to be poor at inducing the HSR (Batulan et al., 2003), it may be that motor neurons are also unable to activate mitochondrial stress responses. Alternatively, since mitochondria are dynamic organelles, mitochondria in motor neurons may instead rely on fission/fusion processes or mitophagy to combat stressful conditions rather than increasing mitochondrial protein chaperones.

TRAP1 has previously been implicated as a pro-survival protein. While overexpression of TRAP1 is able to rescue mitochondrial function and prevent cell death, knockdown of TRAP1 exacerbates mitochondrial dysfunction and cell death (Zhang et al., 2013; Baqri et al., 2014; Basit et al., 2017; Fitzgerald et al., 2017). In support of these studies, in this study TRAP1 overexpression rescued loss of mitochondrial membrane potential in neurons induced by oxidative stress.

Meanwhile, TRAP1 knockdown reduced mitochondrial membrane potential under basal conditions. In agreement with this result, the TRAP1 inhibitor GTPP has also been shown to reduce mitochondrial membrane potential in HeLa cells (Kang et al., 2009).

TRAP1 overexpression also reduced ROS production after oxidative stress, but knockdown of TRAP1 did not exacerbate ROS production. A previous study has reported that increased ROS production was observed in *Trap1* knockout *Drosophila* brains (Baqri et al., 2014). A lack of an observable phenotype here in primary motor neuron cultures after TRAP1 knockdown may be due to lack of a complete knockdown of TRAP1, or perhaps the timing of H_2O_2 treatment may have caused a maximal production of ROS, masking any further effect of TRAP1 knockdown.

While no observable effects of TRAP1 overexpression were detected in lipid peroxidation after exposure to oxidative stress, knockdown of TRAP1 increased lipid peroxidation under basal conditions. Fibroblasts from *Trap1* knockout mice also showed increased lipid peroxidation under basal conditions (Yoshida et al., 2013). H_2O_2 did not affect lipid peroxidation following 30 minutes of treatment even though ROS production was high at this timepoint. Lipid peroxidation may manifest later in this model system and therefore later timepoints or longitudinal imaging could be performed to investigate the effects of mtHsp manipulation on lipid peroxidation under conditions of oxidative stress. Alternatively, although TRAP1 is an important factor in protecting cells against oxidative stress, its effects might be mild, making it difficult to measure using fluorescent probes.

TRAP1 overexpression was able to reduce neuronal death in primary motor neuron cultures following H_2O_2 treatment. These findings are in agreement with a previous study that demonstrated that TRAP1 overexpression was protective to cortical neurons (Butler et al., 2012). However, the aforementioned study was limited as there was no quantification of TRAP1 overexpression levels or repeated experiments in independent cultures. Here, cell death was assessed in at least 4 independent cultures. Although the amount of cell death from different cultures was variable, overexpression of TRAP1 consistently resulted in increased neuronal survival following treatment with H_2O_2 compared to cultures transduced with an empty vector.

Knockdown of TRAP1 has previously been reported to sensitise melanoma cells to apoptotic cell death following complex I inhibition (Basit et al., 2017). However, in this study, knockdown of TRAP1 had no effect on cell death under basal or oxidative stress conditions. This may be due to ineffective complete knockdown of TRAP1 expression in neurons. Further experiments using a number of different concentrations of H_2O_2 in combination with longitudinal imaging may be able to uncover any effect of TRAP1 knockdown on neuronal cell death induced by oxidative stress. Furthermore, TRAP1 inhibitors such as GTPP could be used in parallel with shRNA knockdown (Siegelin et al., 2011; Park et al., 2017).

Exactly how TRAP1 mediates its pro-survival effects is unclear. Interactors of TRAP1 have been poorly characterised with no known co-chaperones and contradictory interacting partners identified, which may reflect different TRAP1 interactors in different cell types. TRAP1 has been suggested to primarily interact with other mitochondrial chaperones Hsp60 and mtHsp70, but also with several mitochondrial respiratory subunits (Joshi, bioRxiv 2019). It is also possible that TRAP1 has a direct effect on increasing antioxidant systems present in mitochondria, such as the glutathione reductase system (Montesano Gesualdi et al., 2007). However, the interactome of TRAP1 has not been established in neurons.

TRAP1 may have additional pro-survival functions beyond its chaperone function. Restoration of oxygen consumption rate by TRAP1 overexpression did not require the ATPase domain, suggesting that TRAP1 chaperoning activity is not required for its protective effects (Joshi, bioRxiv 2019). However, other studies found that a functional TRAP1 ATPase domain was required to rescue fragmentation of the mitochondrial network, ATP production and cell survival following overexpression of α-synuclein and/or rotenone (Butler et al., 2012; Zhang et al., 2013). It is important to consider that truncation of TRAP1 or mutation of crucial targeting sequences may affect the localisation of TRAP1, thus confounding effects of TRAP1 manipulation. Studies modifying the structure of TRAP1 usually do not characterise the subcompartmental localisation of the modified protein, even though specific sequences are very important localising mitochondrial proteins to different compartments (Chacinska et al., 2009). This aside, it seems that a combination of TRAP1 chaperoning and non-chaperoning functions are likely to contribute to TRAP1-mediated neuroprotection.

TRAP1 has been suggested to inhibit the activity of mitochondrial complexes (Sciacovelli et al., 2013; Yoshida et al., 2013). Inhibition of mitochondrial complexes would theoretically reduce ROS production and therefore reduce cellular damage (Masgras et al., 2017). Overexpression or knockdown of TRAP1 had no effect on the expression levels of mitochondrial complexes, but may have still had an effect on the activity of these complexes. Therefore, the neuroprotective effects of TRAP1 may be due to an inhibition of the activity of mitochondrial complexes. Further experiments should investigate whether inhibition of mitochondrial complexes using pharmacological inhibitors affects the protective effects of TRAP1 overexpression.

While overexpression and knockdown of TRAP1 affected mitochondrial functions under stressful and basal conditions, expression of Hsp60 only mildly protected against H_2O_2 induced mitochondrial membrane potential loss. This may be due to insufficient overexpression of Hsp60. Meanwhile, knockdown of Hsp60 exacerbated lipid peroxidation under oxidative stress conditions but did not have any effect on mitochondrial membrane potential, ROS production or neuronal survival. Hsp60 is a crucial protein chaperone as *Hspd1* knockout mice do not live past birth (Christensen et al., 2010). Heterozygous *Hspd1* knockout mice are viable and only develop a late onset motor neuropathy (Magnoni et al., 2013), and therefore partial knockdown may not be sufficient to induce a phenotype in primary motor neuron cultures.

In conclusion, these results show that strategies that aim to increase the levels of mtHsps TRAP1 and Hsp60 may be beneficial in ALS. These results suggest that TRAP1 and Hsp60 have important protective properties in motor neurons under conditions of oxidative stress. Targeting mtHsps TRAP1 and Hsp60 could therefore be therapeutically beneficial, particularly as part of a combination therapy targeting several ALS pathomechanisms.

Chapter 6: General discussion

In this Thesis, stress responses and their role in the neurodegenerative disease ALS were examined. The ability of neurons and glia to activate stress responsive pathways is crucial for limiting damage in injury and disease. Regional differences in the abilities of motor neurons and glia to respond to stressful stimuli may, at least in part, explain the specific pattern of damage observed in ALS. Alterations in the stress responses of motor neurons and glia may contribute towards the death of motor neurons in ALS, leading to paralysis and death.

The overall aim of this Thesis was to explore stress responses in both murine and human models of ALS. Primary glial cultures from the cortex and spinal cord of mice were utilised as this model recapitulates regionally distinct cellular populations *in vitro*, enabling the straightforward manipulation of stress responses in a reductive system. Cultures from the $SOD1^{G93A}$ mouse model of ALS were studied since this model partially recapitulates key pathological hallmarks of ALS including progressive adult onset motor neuron death, muscle paralysis and premature death (Gurney et al., 1994). Spinal cord motor neurons are also primarily affected in this model compared to cortical motor neurons (Leichsenring et al., 2006).

To complement findings from mouse models, ALS patient iPSC-derived astrocytes were also studied. This model has the advantage of studying human astrocytes, which are more complex than mouse astrocytes (Oberheim et al., 2012), and importantly, cells express the mutant SOD1 protein at physiological levels. However, since both primary glial cultures and human iPSC-derived astrocytes are developmental models and ALS is an adult-onset disease where age is an important risk factor, where possible findings were validated in adult tissue from $SOD1^{G93A}$ mice at different stages of disease.

The results presented in Chapter 3 suggest that spinal cord glia are more readily activated by pro-inflammatory stimuli than cortical glia. Spinal cord glia produced more NO than cortical glia following treatment with inflammatory mediators. Increased NO production in spinal cord glia was found to be due to increased iNOS expression. Increased phosphorylation of inflammatory transcription factor NF-κB was also observed in spinal cord glia compared with cortical glia, indicating that activation of NF-κB is stronger in spinal cord glia than cortical glia.

Surprisingly, mSOD1 glia were not significantly different to WT/healthy control glia in terms of their regional differences in response to inflammatory stimuli, however, mSOD1 glia appear to have a diminished ability to activate pro-inflammatory pathways. This reduced ability to activate this stress responsive pathway may be detrimental during the early stages of disease, where NF-κB mediated inflammatory processes may be protective (Ouali Alami et al., 2018).

The HSR is a cytoprotective response to stressful conditions which involves the upregulation of Hsps. The results presented in Chapter 4 suggest that the glial HSR may become dysfunctional in ALS. mSOD1 glia were unable to effectively upregulate the major cytoprotective protein, Hsp70, following exposure to heat stress. This indicates that mSOD1 glia have a reduced ability to upregulate Hsp70 in ALS, which would potentially have detrimental effects on motor neurons in ALS through a lack of proteostatic support. Furthermore, reduced Hsp70 in glia may result in an exacerbation of pro-inflammatory signalling. mSOD1 glia expressed increased iNOS and displayed an increased number of nuclear NF-κB positive cells than WT glia when treated with a combination of heat stress and the inflammatory mediator, LPS. This suggests that due to reduced Hsp70, mSOD1 glia are unable to inhibit the activation of inflammatory pathways as strongly as wildtype glia.

In addition to Hsp70, several other Hsps including Hsp27 and Hsp90 have been reported to be inducible following exposure to stressful conditions. However, no differences in the expression of Hsp27 or Hsp90 were observed after glia were exposed to heat stress. Furthermore, no differences in Hsp27 or Hsp90 were found between mSOD1 and WT glia under stress conditions. However, Hsp27 was upregulated under basal conditions in spinal cord glia compared to cortical glia. Regional differences in Hsp27 expression may reflect differences in the cytoskeletal makeup of glia from different anatomical regions, as Hsp27 plays an important role in cytoskeletal maintenance (Gorter et al., 2018).

It is not only cytosolic Hsps which may play an important role in ALS. Certain Hsps are specialised to function in mitochondria. The mtHsps TRAP1 and Hsp60 have been previously reported to be cytoprotective (Tang et al., 2016; Basit et al., 2017), but their role in motor neurons is unknown. Data presented in Chapter 5 demonstrates that expression of mtHsps TRAP1 and Hsp60 are decreased in

motor neurons of symptomatic SOD1^{G93A} mice, suggesting that reduced expression of TRAP1 and Hsp60 may contribute to motor neuron death in ALS.

Expression of TRAP1 and Hsp60 was unaltered after primary motor neuron cultures were subjected to a number of different stress conditions, suggesting that motor neurons do not upregulate TRAP1 or Hsp60 in response to cellular stress. Overexpression or knockdown of TRAP1 and Hsp60 was performed to investigate whether these proteins were protective to motor neurons. Lentiviral expression of TRAP1 or Hsp60 partially rescued mitochondrial function diminished by oxidative stress. Overexpression of TRAP1 also resulted in a partial rescue of oxidative stress-induced motor neuron death. Meanwhile, knockdown of TRAP1 or Hsp60 was broadly detrimental to mitochondrial function under either basal or oxidative stress conditions. These findings therefore support previous studies which show that expression of TRAP1 and Hsp60 are protective under conditions of cellular stress and suggests that increasing expression of these proteins may protect motor neurons and have a beneficial therapeutic effect in ALS.

6.1 Further work

The work presented in this Thesis opens up several avenues for future work. One significant caveat of the work presented in this Thesis is the lack of non-mSOD1 models of ALS. While cell models of mSOD1 were used here due to the relative abundance of understanding on inflammatory signalling and the HSR in these models, mutations in SOD1 only account for only ~2% of all cases of ALS. Since glia expressing mutant ALS-causing proteins including TDP-43 (Tong et al., 2013), FUS (Kia et al., 2018), C9orf72 (Meyer et al., 2014) and VCP (Hall et al., 2017) have all been implicated in non-cell autonomous mechanisms of motor neuron death, studying the stress responses of glia in non-mSOD1 models would determine whether differences in stress responses found in mSOD1 glia are common to other ALS-causing mutations.

Glial cultures from the spinal cord were found to produce higher levels of NO than cortical cultures in response to inflammatory induction, due to increased iNOS expression. Both microglia and astrocytes were found to be positive for iNOS following LPS treatment, with an increased proliferation of spinal cord microglia and an increased proportion of iNOS positive spinal cord astrocytes observed

following inflammatory induction. To understand the contribution of microglial proliferation to this response, mitotic inhibitors such as 5-fluorodeoxyuridine could be used to stop microglial proliferation.

Isolated microglial cultures were obtained by shaking mixed glial cultures. However, this technique was only able to obtain a low yield of microglia. Future work should use alternative methods such as trypsinisation to obtain enriched microglia cultures (Saura et al., 2003). Furthermore, a protocol to obtain microglia from human iPSCs have been recently described (Haenseler et al., 2017). Co-cultures of iPSC-derived astrocytes and microglia would provide a useful model system to study the interaction of these two cell types in a human model. In addition, a greater understanding of the role of microglia in ALS could be gained by generating microglia from iPSCs from ALS patients.

Human iPSC-derived astrocyte cultures did not respond to LPS, but instead elicited an inflammatory response following treatment with a combination of TNF-α, IL-1α and C1q, cytokines which have been shown to be released from microglia and induce a pro-inflammatory state in astrocytes (Liddelow et al., 2017). Since inflammatory responses of glia are stimulus dependent (Zamanian et al., 2012; Perriot et al., 2018), it would be interesting to treat mouse primary cortical and spinal cord glial cultures with TNF-α, IL-1α and C1q in order to examine whether the regional differences observed in cortical and spinal cord glia following LPS treatment extends to other inflammatory inducers. Furthermore, findings from human iPSC-derived astrocytes should be compared to experiments performed in enriched mouse astrocyte cultures, obtained from glial cultures by addition of microglial specific toxin, L-leucine methyl ester. This would allow for a direct comparison of mouse and human astrocytes and enable the study of their ability to induce inflammatory responses in the absence of any microglia.

In order to relate regional differences in inflammatory signalling to neuronal health survival, co-cultures of glia and neurons from different regions could be cultured and then treated with inflammatory inducers to determine whether regional differences in inflammatory responses of glia affect neuronal function and survival. Differences in neuronal survival could be linked to the NO-iNOS-NFκB pathway by using specific inhibitors such as 1400W or genetic modifications used in previous studies to reduce NF-κB signalling (Frakes et al., 2014). In addition,

the protective effects of the HSR could be assessed by co-culturing neurons with astrocytes that had been exposed to heat stress.

In addition to the NO-iNOS-NFκB inflammatory pathway, many other factors have been implicated in non-cell autonomous mechanisms of motor neuron death in ALS. Therefore, unbiased assays such as mass spectroscopy or RNA sequencing of regionally different glial populations treated with different inflammatory inducers would provide a more complete picture of how regional differences in glia affect inflammatory responses and how these responses are affected by ALS-causing mutations. In addition, cytokine array analysis of the media from glial cultures would complement findings from mass spectroscopy or RNA sequencing.

Analysis of media released from glia could also provide information about which Hsps are released from glia. Here, mSOD1 glia were found to produce less Hsp70 than WT glia following exposure to heat stress. It would be interesting to determine whether this change affected the amount of Hsp70 that was released from glia into the media as astrocytes may supplement motor neurons with Hsp70 to aid protein homeostasis, which may be lost in mSOD1 glia, contributing towards motor neuron death.

Hsp70 has been previously implicated as an anti-inflammatory protein through inhibition of NF-κB signalling (Feinstein et al., 1996; Chen et al., 2006). Since heat stress was found to reduce activation of the NO-iNOS-NFκB pathway, it is likely that Hsp70 is at least partly responsible for these effects. This is supported by data showing reduced production of Hsp70 after heat stress in mSOD1 glia compared to WT glia and increased NO-iNOS-NFκB activation in mSOD1 glia compared to WT glia following treatment with a combination of heat stress and LPS. However, further experiments using $SOD1^{WT}$ overexpressing mice should be performed to show that the decrease in Hsp70 expression after heat stress is mutation specific and not simply a result of overexpression of SOD1 protein. Furthermore, in order to more directly implicate Hsp70 in these effects, recombinant Hsp70 could be added to LPS treated mSOD1 glia to determine whether this reduces NO-iNOS-NF-κB activation. By expressing truncated forms of Hsp70, the region of the protein important for regulation of inflammatory signalling could be identified. Furthermore, Hsp70 knockout glia could be treated

with LPS and heat stress and compared to WT glia to further elucidate the contribution of Hsp70 to this anti-inflammatory effect.

Hsp25/Hsp27 has previously been described to be an inducible Hsp (Chang et al., 2013). However, Hsp25 levels were unchanged in glial cultures after exposure to stressful conditions. Although the levels of Hsp25 did not change, post-translational modifications such as phosphorylation state have been reported to be important in Hsp25 function in inflammatory processes (Park et al., 2003). Using phospho-tag gels or radiolabelling would enable the study of the phosphorylation state of Hsp25 under stressful conditions.

mtHsp TRAP1 has also been reported to become phosphorylated when activated (Pridgeon et al., 2007). Since levels of TRAP1 and Hsp60 were also not altered in primary motor neuron cultures, perhaps post-translational modifications may dictate the protective effects of these proteins rather than a change in expression levels. Alternatively, the stressors used in this work may not be sufficient to induce upregulation. Previous studies inducing the mtUPR using ethidium bromide or ΔOTC could induce the expression of TRAP1 and Hsp60 (Martinus et al., 1996; Zhao et al., 2002). How TRAP1 and Hsp60 confer their neuroprotective actions is poorly understood. By combining co-immunoprecipitation with mass spectroscopy of primary motor neuron cultures exposed to different stressors, the interactors of these proteins when exposed to stressful conditions could be elucidated.

TRAP1 and Hsp60 levels were decreased in motor neurons of symptomatic $SOD1^{G93A}$ mice. Further analysis of immunostaining of motor neurons at different stages of $SOD1^{G93A}$ disease, as well as qPCR of motor neurons from symptomatic $SOD1^{G93A}$ obtained by laser capture microdissection and intensity measurements of TRAP1 and Hsp60 in motor neurons from post-mortem ALS tissue should be performed in order to add to this finding.

Overexpression or knockdown of TRAP1 and Hsp60 affected mitochondrial functions in WT primary motor neuron cultures either under basal conditions or after exposure to oxidative stress. To further explore the manipulation of these proteins on mitochondrial protection or dysfunction, maintenance of the mitochondrial membrane potential could be assessed using respiratory chain inhibitors and mitochondrial respiration could be assessed by measuring

NADH/FAD autofluorescence (Plun-Favreau et al., 2012). In addition, further experiments should investigate the effects of TRAP1 and Hsp60 overexpression or knockdown on mitochondrial functions in SOD1^{G93A} primary embryonic motor neurons to determine whether overexpression or knockdown of these proteins affects any mitochondrial phenotypes that occur in this model.

Since increasing the levels of these mtHsps had neuroprotective effects on neurons in primary motor neuron cultures, increasing the expression of TRAP1 or Hsp60 may have beneficial effects on disease progression in the SOD1^{G93A} mouse. To explore further the neuroprotective effects of mtHsps, TRAP1 and Hsp60 could be overexpressed in SOD1^{G93A} mice to see if acute neuroprotective effects observed *in vitro* can be recapitulated in a chronic *in vivo* model. The effects of overexpression of these mtHsps should be assessed by changes in lifespan, motor neuron loss and muscle strength, as detailed in previous studies (Kieran et al., 2004; Kalmar et al., 2008). Furthermore, compounds that increased the levels of these proteins could be screened *in vitro* and validated using the *in vitro* assays detailed in this Thesis before preclinical testing in mSOD1 mice.

6.2 Concluding remarks

The experiments described in this Thesis were designed to study stress responses in models of ALS. This work reflects the diverse mechanisms by which different cell types and mechanisms contribute towards motor neuron death. These results suggest that manipulation of the stress responsive pathways of neurons and glia may be a successful approach to protect motor neurons from death in ALS. Therefore, targeting of these stress responsive pathways in glia and motor neurons may provide a therapeutic benefit to patients living with this devastating disease.

References

Abe, K., M. Aoki, H. Tsuji, Y. Itoyama, G. Sobue, M. Tanaka, K. Nakamura, and A.L.S.S.G. Edaravone. 2017. Safety and efficacy of edaravone in well defined patients with amyotrophic lateral sclerosis: a randomised, double-blind, placebo-controlled trial. *Lancet Neurol*. 16:505-512.

Abe, K., L.H. Pan, M. Watanabe, T. Kato, and Y. Itoyama. 1995. Induction of Nitrotyrosine-Like Immunoreactivity in the Lower Motor-Neuron of Amyotrophic-Lateral-Sclerosis. *Neuroscience Letters*. 199:152-154.

Agorreta, J., J. Hu, D. Liu, D. Delia, H. Turley, D.J. Ferguson, F. Iborra, M.J. Pajares, M. Larrayoz, I. Zudaire, et al. 2014. TRAP1 regulates proliferation, mitochondrial function, and has prognostic significance in NSCLC. *Mol Cancer Res*. 12:660-669.

Al-Chalabi, A., A. Calvo, A. Chio, S. Colville, C.M. Ellis, O. Hardiman, M. Heverin, R.S. Howard, M.H.B. Huisman, N. Keren, et al. 2014. Analysis of amyotrophic lateral sclerosis as a multistep process: a population-based modelling study. *Lancet Neurology*. 13:1108-1113.

Al-Chalabi, A., L.H. van den Berg, and J. Veldink. 2017. Gene discovery in amyotrophic lateral sclerosis: implications for clinical management. *Nat Rev Neurol*. 13:96-104.

Al-Sarraj, S., A. King, C. Troakes, B. Smith, S. Maekawa, I. Bodi, B. Rogelj, A. Al-Chalabi, T. Hortobagyi, and C.E. Shaw. 2011. p62 positive, TDP-43 negative, neuronal cytoplasmic and intranuclear inclusions in the cerebellum and hippocampus define the pathology of C9orf72-linked FTLD and MND/ALS. *Acta Neuropathologica*. 122:691-702.

Al-Tahan, S., E. Al-Obeidi, H. Yoshioka, A. Lakatos, L. Weiss, M. Grafe, J. Palmio, M. Wicklund, Y. Harati, M. Omizo, et al. 2018. Novel valosin-containing protein mutations associated with multisystem proteinopathy. *Neuromuscul Disord*. 28:491-501.

Albo, F., M. Pieri, and C. Zona. 2004. Modulation of AMPA receptors in spinal motor neurons by the neuroprotective agent riluzole. *J Neurosci Res*. 78:200-207.

Aldridge, J.E., T. Horibe, and N.J. Hoogenraad. 2007. Discovery of genes activated by the mitochondrial unfolded protein response (mtUPR) and cognate promoter elements. *PLoS One*. 2:e874.

Alexianu, M.E., B.K. Ho, A.H. Mohamed, V. Labella, R.G. Smith, and S.H. Appel. 1994. The Role of Calcium-Binding Proteins in Selective Motoneuron Vulnerability in Amyotrophic-Lateral-Sclerosis. *Annals of Neurology*. 36:846-858.

Alexianu, M.E., M. Kozovska, and S.H. Appel. 2001. Immune reactivity in a mouse model of familial ALS correlates with disease progression. *Neurology*. 57:1282-1289.

Allen, S.P., B. Hall, L.M. Castelli, L. Francis, R. Woof, A.P. Siskos, E. Kouloura, E. Gray, A.G. Thompson, K. Talbot, et al. 2019. Astrocyte adenosine deaminase loss increases motor neuron toxicity in amyotrophic lateral sclerosis. *Brain*. 142:586-605.

Alliot, F., I. Godin, and B. Pessac. 1999. Microglia derive from progenitors, originating from the yolk sac, and which proliferate in the brain. *Brain Res Dev Brain Res*. 117:145-152.

Almer, G., S. Vukosavic, N. Romero, and S. Przedborski. 1999. Inducible nitric oxide synthase up-regulation in a transgenic mouse model of familial amyotrophic lateral sclerosis. *Journal of Neurochemistry*. 72:2415-2425.

Alonso, A., G. Logroscino, S.S. Jick, and M.A. Hernan. 2009. Incidence and lifetime risk of motor neuron disease in the United Kingdom: a population-based study. *Eur J Neurol*. 16:745-751.

Anderson, M.A., J.E. Burda, Y. Ren, Y. Ao, T.M. O'Shea, R. Kawaguchi, G. Coppola, B.S. Khakh, T.J. Deming, and M.V. Sofroniew. 2016. Astrocyte scar formation aids central nervous system axon regeneration. *Nature*. 532:195-200.

Anderson, S., A.T. Bankier, B.G. Barrell, M.H. de Bruijn, A.R. Coulson, J. Drouin, I.C. Eperon, D.P. Nierlich, B.A. Roe, F. Sanger, et al. 1981. Sequence and organization of the human mitochondrial genome. *Nature*. 290:457-465.

Bachoo, R.M., R.S. Kim, K.L. Ligon, E.A. Maher, C. Brennan, N. Billings, S. Chan, C. Li, D.H. Rowitch, W.H. Wong, et al. 2004. Molecular diversity of astrocytes with implications for neurological disorders. *Proc Natl Acad Sci U S A*. 101:8384-8389.

Bajramovic, J.J., M. Bsibsi, S.B. Geutskens, R. Hassankhan, K.C. Verhulst, G.J. Stege, C.J. de Groot, and J.M. van Noort. 2000. Differential expression of stress proteins in human adult astrocytes in response to cytokines. *J Neuroimmunol*. 106:14-22.

Bal-Price, A., and G.C. Brown. 2001. Inflammatory neurodegeneration mediated by nitric oxide from activated glia-inhibiting neuronal respiration, causing glutamate release and excitotoxicity. *Journal of Neuroscience*. 21:6480-6491.

Balendra, R., and A.M. Isaacs. 2018. C9orf72-mediated ALS and FTD: multiple pathways to disease. *Nat Rev Neurol*. 14:544-558.

Bang, J., S. Spina, and B.L. Miller. 2015. Frontotemporal dementia. *Lancet*. 386:1672-1682.

Bannwarth, S., S. Ait-El-Mkadem, A. Chaussenot, E.C. Genin, S. Lacas-Gervais, K. Fragaki, L. Berg-Alonso, Y. Kageyama, V. Serre, D.G. Moore, et al. 2014. A mitochondrial origin for frontotemporal dementia and amyotrophic lateral sclerosis through CHCHD10 involvement. *Brain*. 137:2329-2345.

Baqri, R.M., A.V. Pietron, R.H. Gokhale, B.A. Turner, L.S. Kaguni, A.W. Shingleton, S. Kunes, and K.E. Miller. 2014. Mitochondrial chaperone TRAP1 activates the mitochondrial UPR and extends healthspan in Drosophila. *Mech Ageing Dev*. 141-142:35-45.

Barber, S.C., and P.J. Shaw. 2010. Oxidative stress in ALS: key role in motor neuron injury and therapeutic target. *Free Radic Biol Med*. 48:629-641.

Baron, D.M., L.J. Kaushansky, C.L. Ward, R.R. Sama, R.J. Chian, K.J. Boggio, A.J. Quaresma, J.A. Nickerson, and D.A. Bosco. 2013. Amyotrophic lateral sclerosis-linked FUS/TLS alters stress granule assembly and dynamics. *Mol Neurodegener*. 8:30.

Barreto, G.E., R.E. White, L.J. Xu, C.J. Palm, and R.G. Giffard. 2012. Effects of heat shock protein 72 (Hsp72) on evolution of astrocyte activation following stroke in the mouse. *Experimental Neurology*. 238:284-296.

Basit, F., L.M. van Oppen, L. Schockel, H.M. Bossenbroek, S.E. van Emst-de Vries, J.C. Hermeling, S. Grefte, C. Kopitz, M. Heroult, P. Hgm Willems, et al. 2017. Mitochondrial complex I inhibition triggers a mitophagy-dependent ROS increase leading to necroptosis and ferroptosis in melanoma cells. *Cell Death Dis*. 8:e2716.

Basso, M., T. Massignan, G. Samengo, C. Cheroni, S. De Biasi, M. Salmona, C. Bendotti, and V. Bonetto. 2006. Insoluble mutant SOD1 is partly oligoubiquitinated in amyotrophic lateral sclerosis mice. *Journal of Biological Chemistry*. 281:33325-33335.

Batchelor, P.E., S. Tan, T.E. Wills, M.J. Porritt, and D.W. Howells. 2008. Comparison of inflammation in the brain and spinal cord following mechanical injury. *J Neurotrauma*. 25:1217-1225.

Batulan, Z., G.A. Shinder, S. Minotti, B.P. He, M.M. Doroudchi, J. Nalbantoglu, M.J. Strong, and H.D. Durham. 2003. High threshold for induction of the stress response in motor neurons is associated with failure to activate HSF1. *J Neurosci*. 23:5789-5798.

Bayraktar, O.A., L.C. Fuentealba, A. Alvarez-Buylla, and D.H. Rowitch. 2015. Astrocyte Development and Heterogeneity. *Csh Perspect Biol*. 7.

Beal, M.F., R.J. Ferrante, S.E. Browne, R.T. Matthews, N.W. Kowall, and R.H. Brown. 1997. Increased 3-nitrotyrosine in both sporadic and familial amyotrophic lateral sclerosis. *Annals of Neurology*. 42:644-654.

Beckman, J.S., M. Carson, C.D. Smith, and W.H. Koppenol. 1993. ALS, SOD and peroxynitrite. *Nature*. 364:584.

Beers, D.R., J.S. Henkel, Q. Xiao, W. Zhao, J. Wang, A.A. Yen, L. Siklos, S.R. McKercher, and S.H. Appel. 2006. Wild-type microglia extend survival in PU.1 knockout mice with familial amyotrophic lateral sclerosis. *Proc Natl Acad Sci U S A*. 103:16021-16026.

Ben Haim, L., and D.H. Rowitch. 2017. Functional diversity of astrocytes in neural circuit regulation. *Nat Rev Neurosci*. 18:31-41.

Benatar, M., J. Wuu, P.M. Andersen, N. Atassi, W. David, M. Cudkowicz, and D. Schoenfeld. 2018. Randomized, double-blind, placebo-controlled trial of arimoclomol in rapidly progressive SOD1 ALS. *Neurology*. 90:E565-E574.

Bender, T., I. Lewrenz, S. Franken, C. Baitzel, and W. Voos. 2011. Mitochondrial enzymes are protected from stress-induced aggregation by mitochondrial chaperones and the Pim1/LON protease. *Mol Biol Cell*. 22:541-554.

Benkler, C., T. Ben-Zur, Y. Barhum, and D. Offen. 2013. Altered astrocytic response to activation in SOD1G93A mice and its implications on amyotrophic lateral sclerosis pathogenesis. *Glia*. 61:312-326.

Bennett, F.C., M.L. Bennett, F. Yaqoob, S.B. Mulinyawe, G.A. Grant, M.H. Gephart, E.D. Plowey, and B. Barres. 2018. A Combination of Ontogeny and CNS Environment Establishes Microglial Identity. *Neuron*. 98:1170-+.

Bi, F., C. Huang, J. Tong, G. Qiu, B. Huang, Q. Wu, F. Li, Z. Xu, R. Bowser, X.G. Xia, et al. 2013. Reactive astrocytes secrete lcn2 to promote neuron death. *Proc Natl Acad Sci U S A*. 110:4069-4074.

Bilsland, L.G., N. Nirmalananthan, J. Yip, L. Greensmith, and M.R. Duchen. 2008. Expression of mutant SOD1 in astrocytes induces functional deficits in motoneuron mitochondria. *J Neurochem*. 107:1271-1283.

Bilsland, L.G., E. Sahai, G. Kelly, M. Golding, L. Greensmith, and G. Schiavo. 2010. Deficits in axonal transport precede ALS symptoms in vivo. *P Natl Acad Sci USA*. 107:20523-20528.

Boeynaems, S., E. Bogaert, D. Kovacs, A. Konijnenberg, E. Timmerman, A. Volkov, M. Guharoy, M. De Decker, T. Jaspers, V.H. Ryan, et al. 2017. Phase Separation of C9orf72 Dipeptide Repeats Perturbs Stress Granule Dynamics. *Mol Cell*. 65:1044-1055 e1045.

Boillee, S., K. Yamanaka, C.S. Lobsiger, N.G. Copeland, N.A. Jenkins, G. Kassiotis, G. Kollias, and D.W. Cleveland. 2006. Onset and progression in

inherited ALS determined by motor neurons and microglia. *Science*. 312:1389-1392.
Boisvert, M.M., G.A. Erikson, M.N. Shokhirev, and N.J. Allen. 2018. The Aging Astrocyte Transcriptome from Multiple Regions of the Mouse Brain. *Cell Reports*. 22:269-285.
Bosco, D.A., G. Morfini, N.M. Karabacak, Y. Song, F. Gros-Louis, P. Pasinelli, H. Goolsby, B.A. Fontaine, N. Lemay, D. McKenna-Yasek, et al. 2010. Wild-type and mutant SOD1 share an aberrant conformation and a common pathogenic pathway in ALS. *Nat Neurosci*. 13:1396-1403.
Braak, H., A.C. Ludolph, M. Neumann, J. Ravits, and K. Del Tredici. 2017. Pathological TDP-43 changes in Betz cells differ from those in bulbar and spinal alpha-motoneurons in sporadic amyotrophic lateral sclerosis. *Acta Neuropathologica*. 133:79-90.
Brehme, M., C. Voisine, T. Rolland, S. Wachi, J.H. Soper, Y. Zhu, K. Orton, A. Villella, D. Garza, M. Vidal, et al. 2014. A chaperome subnetwork safeguards proteostasis in aging and neurodegenerative disease. *Cell Rep*. 9:1135-1150.
Brenner, D., K. Muller, T. Wieland, P. Weydt, S. Bohm, D. Lule, A. Hubers, C. Neuwirth, M. Weber, G. Borck, et al. 2016. NEK1 mutations in familial amyotrophic lateral sclerosis. *Brain*. 139:e28.
Brenner, D., K. Sieverding, C. Bruno, P. Luningschror, E. Buck, S. Mungwa, L. Fischer, S.J. Brockmann, J. Ulmer, C. Bliederhauser, et al. 2019. Heterozygous Tbk1 loss has opposing effects in early and late stages of ALS in mice. *Journal of Experimental Medicine*. 216:267-278.
Brenner, D., R. Yilmaz, K. Muller, T. Grehl, S. Petri, T. Meyer, J. Grosskreutz, P. Weydt, W. Ruf, C. Neuwirth, et al. 2018. Hot-spot KIF5A mutations cause familial ALS. *Brain*. 141:688-697.
Brookes, P.S., J.P. Bolanos, and S.J.R. Heales. 1999. The assumption that nitric oxide inhibits mitochondrial ATP synthesis is correct. *Febs Letters*. 446:261-263.
Bross, P., S. Naundrup, J. Hansen, M.N. Nielsen, J.H. Christensen, M. Kruhoffer, J. Palmfeldt, T.J. Corydon, N. Gregersen, D. Ang, et al. 2008. The Hsp60-(p.V98I) mutation associated with hereditary spastic paraplegia SPG13 compromises chaperonin function both in vitro and in vivo. *Journal of Biological Chemistry*. 283:15694-15700.
Brown, I.R. 2007. Heat shock proteins and protection of the nervous system. *Ann N Y Acad Sci*. 1113:147-158.
Brown, R.H., Jr., and A. Al-Chalabi. 2017. Amyotrophic Lateral Sclerosis. *N Engl J Med*. 377:1602.
Bruening, W., J. Roy, B. Giasson, D.A. Figlewicz, W.E. Mushynski, and H.D. Durham. 1999. Up-regulation of protein chaperones preserves viability of cells expressing toxic Cu/Zn-superoxide dismutase mutants associated with amyotrophic lateral sclerosis. *Journal of Neurochemistry*. 72:693-699.
Bruijn, L.I., M.W. Becher, M.K. Lee, K.L. Anderson, N.A. Jenkins, N.G. Copeland, S.S. Sisodia, J.D. Rothstein, D.R. Borchelt, D.L. Price, et al. 1997. ALS-linked SOD1 mutant G85R mediates damage to astrocytes and promotes rapidly progressive disease with SOD1-containing inclusions. *Neuron*. 18:327-338.
Bruijn, L.I., M.K. Houseweart, S. Kato, K.L. Anderson, S.D. Anderson, E. Ohama, A.G. Reaume, R.W. Scott, and D.W. Cleveland. 1998. Aggregation and motor neuron toxicity of an ALS-linked SOD1 mutant independent from wild-type SOD1. *Science*. 281:1851-1854.

Bunton-Stasyshyn, R.K., R.A. Saccon, P. Fratta, and E.M. Fisher. 2015. SOD1 Function and Its Implications for Amyotrophic Lateral Sclerosis Pathology: New and Renascent Themes. *Neuroscientist*. 21:519-529.

Buratti, E. 2015. Functional Significance of TDP-43 Mutations in Disease. *Adv Genet*. 91:1-53.

Burda, J.E., and M.V. Sofroniew. 2017. Seducing astrocytes to the dark side. *Cell Res*. 27:726-727.

Burstein, S.R., F. Valsecchi, H. Kawamata, M. Bourens, R. Zeng, A. Zuberi, T.A. Milner, S.M. Cloonan, C. Lutz, A. Barrientos, et al. 2018. In vitro and in vivo studies of the ALS-FTLD protein CHCHD10 reveal novel mitochondrial topology and protein interactions. *Human Molecular Genetics*. 27:160-177.

Butler, E.K., A. Voigt, A.K. Lutz, J.P. Toegel, E. Gerhardt, P. Karsten, B. Falkenburger, A. Reinartz, K.F. Winklhofer, and J.B. Schulz. 2012. The mitochondrial chaperone protein TRAP1 mitigates alpha-Synuclein toxicity. *PLoS Genet*. 8:e1002488.

Cady, J., P. Allred, T. Bali, A. Pestronk, A. Goate, T.M. Miller, R.D. Mitra, J. Ravits, M.B. Harms, and R.H. Baloh. 2015. Amyotrophic Lateral Sclerosis Onset Is Influenced by the Burden of Rare Variants in Known Amyotrophic Lateral Sclerosis Genes. *Annals of Neurology*. 77:100-113.

Calabrese, V., C. Mancuso, M. Calvani, E. Rizzarelli, D.A. Butterfield, and A.M.G. Stella. 2007. Nitric oxide in the central nervous system: neuroprotection versus neurotoxicity. *Nature Reviews Neuroscience*. 8:766-775.

Calderwood, S.K., and A. Murshid. 2017. Molecular Chaperone Accumulation in Cancer and Decrease in Alzheimer's Disease: The Potential Roles of HSF1. *Front Neurosci-Switz*. 11.

Camu, W., and C.E. Henderson. 1992. Purification of embryonic rat motoneurons by panning on a monoclonal antibody to the low-affinity NGF receptor. *J Neurosci Methods*. 44:59-70.

Casciati, A., A. Ferri, M. Cozzolino, F. Celsi, M. Nencini, G. Rotilio, and M.T. Carri. 2002. Oxidative modulation of nuclear factor-kappaB in human cells expressing mutant fALS-typical superoxide dismutases. *J Neurochem*. 83:1019-1029.

Cassina, P., A. Cassina, M. Pehar, R. Castellanos, M. Gandelman, A. de Leon, K.M. Robinson, R.P. Mason, J.S. Beckman, L. Barbeito, et al. 2008. Mitochondrial dysfunction in SOD1G93A-bearing astrocytes promotes motor neuron degeneration: prevention by mitochondrial-targeted antioxidants. *J Neurosci*. 28:4115-4122.

Cassina, P., H. Peluffo, M. Pehar, L. Martinez-Palma, A. Ressia, J.S. Beckman, A.G. Estevez, and L. Barbeito. 2002. Peroxynitrite triggers a phenotypic transformation in spinal cord astrocytes that induces motor neuron apoptosis. *Journal of Neuroscience Research*. 67:21-29.

Chacinska, A., C.M. Koehler, D. Milenkovic, T. Lithgow, and N. Pfanner. 2009. Importing mitochondrial proteins: machineries and mechanisms. *Cell*. 138:628-644.

Chai, H., B. Diaz-Castro, E. Shigetomi, E. Monte, J.C. Octeau, X.Z. Yu, W. Cohn, P.S. Rajendran, T.M. Vondriska, J.P. Whitelegge, et al. 2017. Neural Circuit-Specialized Astrocytes: Transcriptomic, Proteomic, Morphological, and Functional Evidence. *Neuron*. 95:531-+.

Chang, H.Y., S.C. Hou, T.D. Way, C.H. Wong, and I.F. Wang. 2013. Heat-shock protein dysregulation is associated with functional and pathological TDP-43 aggregation. *Nature Communications*. 4.

Chen, G., P. Cao, and D.V. Goeddel. 2002. TNF-induced recruitment and activation of the IKK complex require Cdc37 and Hsp90. *Mol Cell*. 9:401-410.

Chen, H., K. Qian, W. Chen, B.Y. Hu, L.W. Blackbourn, Z.W. Du, L.X. Ma, H.S. Liu, K.M. Knobel, M. Ayala, et al. 2015a. Human-derived neural progenitors functionally replace astrocytes in adult mice. *Journal of Clinical Investigation*. 125:1033-1042.

Chen, H.J., J.C. Mitchell, S. Novoselov, J. Miller, A.L. Nishimura, E.L. Scotter, C.A. Vance, M.E. Cheetham, and C.E. Shaw. 2016. The heat shock response plays an important role in TDP-43 clearance: evidence for dysfunction in amyotrophic lateral sclerosis. *Brain*. 139:1417-1432.

Chen, H.Q., Y.F. Wu, Y.Q. Zhang, L.N. Jin, L. Luo, B. Xue, C. Lu, X.R. Zhang, and Z.M. Yin. 2006. Hsp70 inhibits lipopolysaccharide-induced NF-kappa B activation by interacting with TRAF6 and inhibiting its ubiquitination. *Febs Letters*. 580:3145-3152.

Chen, K., F.J. Northington, and L.J. Martin. 2010. Inducible nitric oxide synthase is present in motor neuron mitochondria and Schwann cells and contributes to disease mechanisms in ALS mice. *Brain Struct Funct*. 214:219-234.

Chen, S.H., E.A. Oyarzabal, Y.F. Sung, C.H. Chu, Q. Wang, S.L. Chen, R.B. Lu, and J.S. Hong. 2015b. Microglial regulation of immunological and neuroprotective functions of astroglia. *Glia*. 63:118-131.

Chen, X., T. Guan, C. Li, H. Shang, L. Cui, X.M. Li, and J. Kong. 2012. SOD1 aggregation in astrocytes following ischemia/reperfusion injury: a role of NO-mediated S-nitrosylation of protein disulfide isomerase (PDI). *J Neuroinflammation*. 9:237.

Chen, Y.Z., C.L. Bennett, H.M. Huynh, I.P. Blair, I. Puls, J. Irobi, I. Dierick, A. Abel, M.L. Kennerson, B.A. Rabin, et al. 2004. DNA/RNA helicase gene mutations in a form of juvenile amyotrophic lateral sclerosis (ALS4). *Am J Hum Genet*. 74:1128-1135.

Chia, R., M.H. Tattum, S. Jones, J. Collinge, E.M.C. Fisher, and G.S. Jackson. 2010. Superoxide Dismutase 1 and tgSOD1(G93A) Mouse Spinal Cord Seed Fibrils, Suggesting a Propagative Cell Death Mechanism in Amyotrophic Lateral Sclerosis. *Plos One*. 5.

Chiu, I.M., A. Chen, Y. Zheng, B. Kosaras, S.A. Tsiftsoglou, T.K. Vartanian, R.H. Brown, Jr., and M.C. Carroll. 2008. T lymphocytes potentiate endogenous neuroprotective inflammation in a mouse model of ALS. *Proc Natl Acad Sci U S A*. 105:17913-17918.

Chiu, I.M., E.T. Morimoto, H. Goodarzi, J.T. Liao, S. O'Keeffe, H.P. Phatnani, M. Muratet, M.C. Carroll, S. Levy, S. Tavazoie, et al. 2013. A neurodegeneration-specific gene-expression signature of acutely isolated microglia from an amyotrophic lateral sclerosis mouse model. *Cell Rep*. 4:385-401.

Choi, S.Y., R. Lopez-Gonzalez, G. Krishnan, H.L. Phillips, A.N. Li, W.W. Seeley, W.D. Yao, S. Almeida, and F.B. Gao. 2019. C9ORF72-ALS/FTD-associated poly(GR) binds Atp5a1 and compromises mitochondrial function in vivo. *Nat Neurosci*. 22:851-862.

Chow, C.Y., J.E. Landers, S.K. Bergren, P.C. Sapp, A.E. Grant, J.M. Jones, L. Everett, G.M. Lenk, D.M. McKenna-Yasek, L.S. Weisman, et al. 2009. Deleterious variants of FIG4, a phosphoinositide phosphatase, in patients with ALS. *Am J Hum Genet*. 84:85-88.

Christensen, J.H., M.N. Nielsen, J. Hansen, A. Fuchtbauer, E.M. Fuchtbauer, M. West, T.J. Corydon, N. Gregersen, and P. Bross. 2010. Inactivation of the hereditary spastic paraplegia-associated Hspd1 gene encoding the Hsp60 chaperone results in early embryonic lethality in mice. *Cell Stress Chaperones*. 15:851-863.

Cirulli, E.T., B.N. Lasseigne, S. Petrovski, P.C. Sapp, P.A. Dion, C.S. Leblond, J. Couthouis, Y.F. Lu, Q. Wang, B.J. Krueger, et al. 2015. Exome sequencing in amyotrophic lateral sclerosis identifies risk genes and pathways. *Science*. 347:1436-1441.

Clarke, L.E., S.A. Liddelow, C. Chakraborty, A.E. Munch, M. Heiman, and B.A. Barres. 2018. Normal aging induces A1-like astrocyte reactivity. *Proc Natl Acad Sci U S A*. 115:E1896-E1905.

Clement, A.M., M.D. Nguyen, E.A. Roberts, M.L. Garcia, S. Boillee, M. Rule, A.P. McMahon, W. Doucette, D. Siwek, R.J. Ferrante, et al. 2003. Wild-type nonneuronal cells extend survival of SOD1 mutant motor neurons in ALS mice. *Science*. 302:113-117.

Cohen, T.J., A.W. Hwang, C.R. Restrepo, C.X. Yuan, J.Q. Trojanowski, and V.M. Lee. 2015. An acetylation switch controls TDP-43 function and aggregation propensity. *Nat Commun*. 6:5845.

Conte, A., S. Lattante, M. Zollino, G. Marangi, M. Luigetti, A. Del Grande, S. Servidei, F. Trombetta, and M. Sabatelli. 2012. P525L FUS mutation is consistently associated with a severe form of juvenile Amyotrophic Lateral Sclerosis. *Neuromuscular Disord*. 22:73-75.

Cook, C., and L. Petrucelli. 2019. Genetic Convergence Brings Clarity to the Enigmatic Red Line in ALS. *Neuron*. 101:1057-1069.

Couthouis, J., M.P. Hart, R. Erion, O.D. King, Z. Diaz, T. Nakaya, F. Ibrahim, H.J. Kim, J. Mojsilovic-Petrovic, S. Panossian, et al. 2012. Evaluating the role of the FUS/TLS-related gene EWSR1 in amyotrophic lateral sclerosis. *Hum Mol Genet*. 21:2899-2911.

Couthouis, J., M.P. Hart, J. Shorter, M. DeJesus-Hernandez, R. Erion, R. Oristano, A.X. Liu, D. Ramos, N. Jethava, D. Hosangadi, et al. 2011. A yeast functional screen predicts new candidate ALS disease genes. *P Natl Acad Sci USA*. 108:20881-20890.

Coyne, A.N., I. Lorenzini, C.C. Chou, M. Torvund, R.S. Rogers, A. Starr, B.L. Zaepfel, J. Levy, J. Johannesmeyer, J.C. Schwartz, et al. 2017. Post-transcriptional Inhibition of Hsc70-4/HSPA8 Expression Leads to Synaptic Vesicle Cycling Defects in Multiple Models of ALS. *Cell Reports*. 21:110-125.

Crapo, J.D., T. Oury, C. Rabouille, J.W. Slot, and L.Y. Chang. 1992. Copper,zinc superoxide dismutase is primarily a cytosolic protein in human cells. *Proc Natl Acad Sci U S A*. 89:10405-10409.

Crosio, C., C. Valle, A. Casciati, C. Iaccarino, and M.T. Carri. 2011. Astroglial inhibition of NF-kappaB does not ameliorate disease onset and progression in a mouse model for amyotrophic lateral sclerosis (ALS). *PLoS One*. 6:e17187.

Custer, S.K., M. Neumann, H.B. Lu, A.C. Wright, and J.P. Taylor. 2010. Transgenic mice expressing mutant forms VCP/p97 recapitulate the full spectrum of IBMPFD including degeneration in muscle, brain and bone. *Human Molecular Genetics*. 19:1741-1755.

Da Cruz, S., A. Bui, S. Saberi, S.K. Lee, J. Stauffer, M. McAlonis-Downes, D. Schulte, D.P. Pizzo, P.A. Parone, D.W. Cleveland, et al. 2017. Misfolded

SOD1 is not a primary component of sporadic ALS. *Acta Neuropathologica*. 134:97-111.

Damiano, M., A.A. Starkov, S. Petri, K. Kipiani, M. Kiaei, M. Mattiazzi, M. Flint Beal, and G. Manfredi. 2006. Neural mitochondrial Ca2+ capacity impairment precedes the onset of motor symptoms in G93A Cu/Zn-superoxide dismutase mutant mice. *J Neurochem*. 96:1349-1361.

de Boer, A.S., K. Koszka, E. Kiskinis, N. Suzuki, B.N. Davis-Dusenbery, and K. Eggan. 2014. Genetic validation of a therapeutic target in a mouse model of ALS. *Sci Transl Med*. 6:248ra104.

DeJesus-Hernandez, M., I.R. Mackenzie, B.F. Boeve, A.L. Boxer, M. Baker, N.J. Rutherford, A.M. Nicholson, N.A. Finch, H. Flynn, J. Adamson, et al. 2011. Expanded GGGGCC Hexanucleotide Repeat in Noncoding Region of C9ORF72 Causes Chromosome 9p-Linked FTD and ALS. *Neuron*. 72:245-256.

Dello Russo, C., P.E. Polak, P.R. Mercado, A. Spagnolo, A. Sharp, P. Murphy, A. Kamal, F.J. Burrows, L.C. Fritz, and D.L. Feinstein. 2006. The heat-shock protein 90 inhibitor 17-allylamino-17-demethoxygeldanamycin suppresses glial inflammatory responses and ameliorates experimental autoimmune encephalomyelitis. *Journal of Neurochemistry*. 99:1351-1362.

Deng, H., K. Gao, and J. Jankovic. 2014. The role of FUS gene variants in neurodegenerative diseases. *Nat Rev Neurol*. 10:337-348.

Deng, H.X., W. Chen, S.T. Hong, K.M. Boycott, G.H. Gorrie, N. Siddique, Y. Yang, F. Fecto, Y. Shi, H. Zhai, et al. 2011. Mutations in UBQLN2 cause dominant X-linked juvenile and adult-onset ALS and ALS/dementia. *Nature*. 477:211-215.

Deng, H.X., H. Zhai, E.H. Bigio, J. Yan, F. Fecto, K. Ajroud, M. Mishra, S. Ajroud-Driss, S. Heller, R. Sufit, et al. 2010. FUS-immunoreactive inclusions are a common feature in sporadic and non-SOD1 familial amyotrophic lateral sclerosis. *Ann Neurol*. 67:739-748.

Deng, J., M. Yang, Y. Chen, X. Chen, J. Liu, S. Sun, H. Cheng, Y. Li, E.H. Bigio, M. Mesulam, et al. 2015. FUS Interacts with HSP60 to Promote Mitochondrial Damage. *PLoS Genet*. 11:e1005357.

Dengler, R., A. Konstanzer, G. Kuther, S. Hesse, W. Wolf, and A. Struppler. 1990. Amyotrophic Lateral Sclerosis - Macro-Emg and Twitch Forces of Single Motor Units. *Muscle & Nerve*. 13:545-550.

Devoy, A., B. Kalmar, M. Stewart, H. Park, B. Burke, S.J. Noy, Y. Redhead, J. Humphrey, K. Lo, J. Jaeger, et al. 2017. Humanized mutant FUS drives progressive motor neuron degeneration without aggregation in 'FUSDelta14' knockin mice. *Brain*. 140:2797-2805.

Doble, A. 1996. The pharmacology and mechanism of action of riluzole. *Neurology*. 47:S233-241.

Dokladny, K., M.N. Zuhl, M. Mandell, D. Bhattacharya, S. Schneider, V. Deretic, and P.L. Moseley. 2013. Regulatory Coordination between Two Major Intracellular Homeostatic Systems HEAT SHOCK RESPONSE AND AUTOPHAGY. *Journal of Biological Chemistry*. 288:14959-14972.

Endo, F., O. Komine, N. Fujimori-Tonou, M. Katsuno, S. Jin, S. Watanabe, G. Sobue, M. Dezawa, T. Wyss-Coray, and K. Yamanaka. 2015. Astrocyte-derived TGF-beta1 accelerates disease progression in ALS mice by interfering with the neuroprotective functions of microglia and T cells. *Cell Rep*. 11:592-604.

Estevez, A.G., N. Spear, S.M. Manuel, R. Radi, C.E. Henderson, L. Barbeito, and J.S. Beckman. 1998. Nitric oxide and superoxide contribute to motor neuron apoptosis induced by trophic factor deprivation. *J Neurosci*. 18:923-931.

Ezzi, S.A., M. Urushitani, and J.P. Julien. 2007. Wild-type superoxide dismutase acquires binding and toxic properties of ALS-linked mutant forms through oxidation. *J Neurochem*. 102:170-178.

Farg, M.A., V. Sundaramoorthy, J.M. Sultana, S. Yang, R.A. Atkinson, V. Levina, M.A. Halloran, P.A. Gleeson, I.P. Blair, K.Y. Soo, et al. 2014. C9ORF72, implicated in amytrophic lateral sclerosis and frontotemporal dementia, regulates endosomal trafficking. *Hum Mol Genet*. 23:3579-3595.

Farmer, W.T., and K. Murai. 2017. Resolving Astrocyte Heterogeneity in the CNS. *Front Cell Neurosci*. 11:300.

Fecto, F., J. Yan, S.P. Vemula, E. Liu, Y. Yang, W. Chen, J.G. Zheng, Y. Shi, N. Siddique, H. Arrat, et al. 2011. SQSTM1 mutations in familial and sporadic amyotrophic lateral sclerosis. *Arch Neurol*. 68:1440-1446.

Feinstein, D.L., E. Galea, D.A. Aquino, G.C. Li, H. Xu, and D.J. Reis. 1996. Heat shock protein 70 suppresses astroglial-inducible nitric-oxide synthase expression by decreasing NF kappa B activation. *Journal of Biological Chemistry*. 271:17724-17732.

Ferraiuolo, L., A. Higginbottom, P.R. Heath, S. Barber, D. Greenald, J. Kirby, and P.J. Shaw. 2011. Dysregulation of astrocyte-motoneuron cross-talk in mutant superoxide dismutase 1-related amyotrophic lateral sclerosis. *Brain*. 134:2627-2641.

Ferraiuolo, L., K. Meyer, T.W. Sherwood, J. Vick, S. Likhite, A. Frakes, C.J. Miranda, L. Braun, P.R. Heath, R. Pineda, et al. 2016. Oligodendrocytes contribute to motor neuron death in ALS via SOD1-dependent mechanism. *P Natl Acad Sci USA*. 113:E6496-E6505.

Ferrante, R.J., S.E. Browne, L.A. Shinobu, A.C. Bowling, M.J. Baik, U. MacGarvey, N.W. Kowall, R.H. Brown, and M.F. Beal. 1997. Evidence of increased oxidative damage in both sporadic and familial amyotrophic lateral sclerosis. *Journal of Neurochemistry*. 69:2064-2074.

Finelli, M.J., K.X. Liu, Y. Wu, P.L. Oliver, and K.E. Davies. 2015. Oxr1 improves pathogenic cellular features of ALS-associated FUS and TDP-43 mutations. *Hum Mol Genet*. 24:3529-3544.

Finka, A., and P. Goloubinoff. 2013. Proteomic data from human cell cultures refine mechanisms of chaperone-mediated protein homeostasis. *Cell Stress Chaperones*. 18:591-605.

Fiorese, C.J., A.M. Schulz, Y.F. Lin, N. Rosin, M.W. Pellegrino, and C.M. Haynes. 2016. The Transcription Factor ATF5 Mediates a Mammalian Mitochondrial UPR. *Curr Biol*. 26:2037-2043.

Fischer, L.R., D.G. Culver, P. Tennant, A.A. Davis, M. Wang, A. Castellano-Sanchez, J. Khan, M.A. Polak, and J.D. Glass. 2004. Amyotrophic lateral sclerosis is a distal axonopathy: evidence in mice and man. *Exp Neurol*. 185:232-240.

Fischer, L.R., A. Igoudjil, J. Magrane, Y. Li, J.M. Hansen, G. Manfredi, and J.D. Glass. 2011. SOD1 targeted to the mitochondrial intermembrane space prevents motor neuropathy in the Sod1 knockout mouse. *Brain*. 134:196-209.

Fischer, L.R., Y. Li, S.A. Asress, D.P. Jones, and J.D. Glass. 2012. Absence of SOD1 leads to oxidative stress in peripheral nerve and causes a progressive distal motor axonopathy. *Exp Neurol*. 233:163-171.

Fitzgerald, J.C., A. Zimprich, D.A. Carvajal Berrio, K.M. Schindler, B. Maurer, C. Schulte, C. Bus, A.K. Hauser, M. Kubler, R. Lewin, et al. 2017. Metformin reverses TRAP1 mutation-associated alterations in mitochondrial function in Parkinson's disease. *Brain*. 140:2444-2459.

Foo, L.C., N.J. Allen, E.A. Bushong, P.B. Ventura, W.S. Chung, L. Zhou, J.D. Cahoy, R. Daneman, H. Zong, M.H. Ellisman, et al. 2011. Development of a Method for the Purification and Culture of Rodent Astrocytes. *Neuron*. 71:799-811.

Forsberg, K., P.A. Jonsson, P.M. Andersen, D. Bergemalm, K.S. Graffmo, M. Hultdin, J. Jacobsson, R. Rosquist, S.L. Marklund, and T. Brannstrom. 2010. Novel antibodies reveal inclusions containing non-native SOD1 in sporadic ALS patients. *PLoS One*. 5:e11552.

Forstermann, U., and W.C. Sessa. 2012. Nitric oxide synthases: regulation and function. *Eur Heart J*. 33:829-837, 837a-837d.

Frakes, A.E., L. Ferraiuolo, A.M. Haidet-Phillips, L. Schmelzer, L. Braun, C.J. Miranda, K.J. Ladner, A.K. Bevan, K.D. Foust, J.P. Godbout, et al. 2014. Microglia Induce Motor Neuron Death via the Classical NF-kappa B Pathway in Amyotrophic Lateral Sclerosis. *Neuron*. 81:1009-1023.

Fratta, P., P. Sivakumar, J. Humphrey, K. Lo, T. Ricketts, H. Oliveira, J.M. Brito-Armas, B. Kalmar, A. Ule, Y. Yu, et al. 2018. Mice with endogenous TDP-43 mutations exhibit gain of splicing function and characteristics of amyotrophic lateral sclerosis. *EMBO J*. 37.

Freibaum, B.D., Y. Lu, R. Lopez-Gonzalez, N.C. Kim, S. Almeida, K.H. Lee, N. Badders, M. Valentine, B.L. Miller, P.C. Wong, et al. 2015. GGGGCC repeat expansion in C9orf72 compromises nucleocytoplasmic transport. *Nature*. 525:129-133.

Freischmidt, A., T. Wieland, B. Richter, W. Ruf, V. Schaeffer, K. Muller, N. Marroquin, F. Nordin, A. Hubers, P. Weydt, et al. 2015. Haploinsufficiency of TBK1 causes familial ALS and fronto-temporal dementia. *Nature Neuroscience*. 18:631-+.

Frey, D., C. Schneider, L. Xu, J. Borg, W. Spooren, and P. Caroni. 2000. Early and selective loss of neuromuscular synapse subtypes with low sprouting competence in motoneuron diseases. *J Neurosci*. 20:2534-2542.

Fritz, E., P. Izaurieta, A. Weiss, F.R. Mir, P. Rojas, D. Gonzalez, F. Rojas, R.H. Brown, Jr., R. Madrid, and B. van Zundert. 2013. Mutant SOD1-expressing astrocytes release toxic factors that trigger motoneuron death by inducing hyperexcitability. *J Neurophysiol*. 109:2803-2814.

Garofalo, O., P.G.E. Kennedy, M. Swash, J.E. Martin, P. Luthert, B.H. Anderton, and P.N. Leigh. 1991. Ubiquitin and Heat-Shock Protein Expression in Amyotrophic-Lateral-Sclerosis. *Neuropath Appl Neuro*. 17:39-45.

Gasset-Rosa, F., S. Lu, H. Yu, C. Chen, Z. Melamed, L. Guo, J. Shorter, S. Da Cruz, and D.W. Cleveland. 2019. Cytoplasmic TDP-43 De-mixing Independent of Stress Granules Drives Inhibition of Nuclear Import, Loss of Nuclear TDP-43, and Cell Death. *Neuron*.

Genin, E.C., B. Madji Hounoum, S. Bannwarth, K. Fragaki, S. Lacas-Gervais, A. Mauri-Crouzet, F. Lespinasse, J. Neveu, B. Ropert, G. Auge, et al. 2019. Mitochondrial defect in muscle precedes neuromuscular junction degeneration and motor neuron death in CHCHD10(S59L/+) mouse. *Acta Neuropathol*.

Genin, E.C., M. Plutino, S. Bannwarth, E. Villa, E. Cisneros-Barroso, M. Roy, B. Ortega-Vila, K. Fragaki, F. Lespinasse, E. Pinero-Martos, et al. 2016. CHCHD10 mutations promote loss of mitochondrial cristae junctions with

impaired mitochondrial genome maintenance and inhibition of apoptosis. *Embo Mol Med*. 8:58-72.

Giannini, F., S. Battistini, M. Mancuso, G. Greco, C. Ricci, N. Volpi, A. Del Corona, S. Piazza, and G. Siciliano. 2010. D90A-SOD1 mutation in ALS: The first report of heterozygous Italian patients and unusual findings. *Amyotroph Lateral Scler*. 11:216-219.

Gibbs, K.L., B. Kalmar, E.R. Rhymes, A.D. Fellows, M. Ahmed, P. Whiting, C.H. Davies, L. Greensmith, and G. Schiavo. 2018. Inhibiting p38 MAPK alpha rescues axonal retrograde transport defects in a mouse model of ALS. *Cell Death Dis*. 9:596.

Gifondorwa, D.J., M.B. Robinson, C.D. Hayes, A.R. Taylor, D.M. Prevette, R.W. Oppenheim, J. Caress, and C.E. Milligan. 2007. Exogenous delivery of heat shock protein 70 increases lifespan in a mouse model of amyotrophic lateral sclerosis. *Journal of Neuroscience*. 27:13173-13180.

Gille, J.J.P., and H. Joenje. 1992. Cell-Culture Models for Oxidative Stress - Superoxide and Hydrogen-Peroxide Versus Normobaric Hyperoxia. *Mutat Res*. 275:405-414.

Gong, Y.H., A.S. Parsadanian, A. Andreeva, W.D. Snider, and J.L. Elliott. 2000. Restricted expression of G86R Cu/Zn superoxide dismutase in astrocytes results in astrocytosis but does not cause motoneuron degeneration. *Journal of Neuroscience*. 20:660-665.

Gopal, P.P., J.J. Nirschl, E. Klinman, and E.L. Holzbaur. 2017. Amyotrophic lateral sclerosis-linked mutations increase the viscosity of liquid-like TDP-43 RNP granules in neurons. *Proc Natl Acad Sci U S A*. 114:E2466-E2475.

Gorter, R.P., E. Nutma, M.C. Jahrei, J.C. de Jonge, R.A. Quinlan, P. van der Valk, J.M. van Noort, W. Baron, and S. Amor. 2018. Heat shock proteins are differentially expressed in brain and spinal cord: implications for multiple sclerosis. *Clin Exp Immunol*. 194:137-152.

Grabert, K., T. Michoel, M.H. Karavolos, S. Clohisey, J.K. Baillie, M.P. Stevens, T.C. Freeman, K.M. Summers, and B.W. McColl. 2016. Microglial brain region-dependent diversity and selective regional sensitivities to aging. *Nat Neurosci*. 19:504-516.

Greenway, M.J., P.M. Andersen, C. Russ, S. Ennis, S. Cashman, C. Donaghy, V. Patterson, R. Swingler, D. Kieran, J. Prehn, et al. 2006. ANG mutations segregate with familial and 'sporadic' amyotrophic lateral sclerosis. *Nat Genet*. 38:411-413.

Guo, L., H.J. Kim, H. Wang, J. Monaghan, F. Freyermuth, J.C. Sung, K. O'Donovan, C.M. Fare, Z. Diaz, N. Singh, et al. 2018. Nuclear-Import Receptors Reverse Aberrant Phase Transitions of RNA-Binding Proteins with Prion-like Domains. *Cell*. 173:677-692 e620.

Gurney, M.E., H.F. Pu, A.Y. Chiu, M.C. Dalcanto, C.Y. Polchow, D.D. Alexander, J. Caliendo, A. Hentati, Y.W. Kwon, H.X. Deng, et al. 1994. Motor-Neuron Degeneration in Mice That Express a Human Cu,Zn Superoxide-Dismutase Mutation. *Science*. 264:1772-1775.

Guyton, K.Z., Q. Xu, and N.J. Holbrook. 1996. Induction of the mammalian stress response gene GADD153 by oxidative stress: role of AP-1 element. *Biochem J*. 314 (Pt 2):547-554.

Guzhova, I., K. Kislyakova, O. Moskaliova, I. Fridlanskaya, M. Tytell, M. Cheetham, and B. Margulis. 2001. In vitro studies show that Hsp70 can be released by glia and that exogenous Hsp70 can enhance neuronal stress tolerance. *Brain Res*. 914:66-73.

Guzhova, I.V., Z.A. Darieva, A.R. Melo, and B.A. Margulis. 1997. Major stress protein Hsp70 interacts with NF-kB regulatory complex in human T-lymphoma cells. *Cell Stress Chaperon*. 2:132-139.

Haenseler, W., S.N. Sansom, J. Buchrieser, S.E. Newey, C.S. Moore, F.J. Nicholls, S. Chintawar, C. Schnell, J.P. Antel, N.D. Allen, et al. 2017. A Highly Efficient Human Pluripotent Stem Cell Microglia Model Displays a Neuronal-Co-culture-Specific Expression Profile and Inflammatory Response. *Stem Cell Reports*. 8:1727-1742.

Haidet-Phillips, A.M., M.E. Hester, C.J. Miranda, K. Meyer, L. Braun, A. Frakes, S. Song, S. Likhite, M.J. Murtha, K.D. Foust, et al. 2011. Astrocytes from familial and sporadic ALS patients are toxic to motor neurons. *Nat Biotechnol*. 29:824-828.

Hall, C.E., Z. Yao, M. Choi, G.E. Tyzack, A. Serio, R. Luisier, J. Harley, E. Preza, C. Arber, S.J. Crisp, et al. 2017. Progressive Motor Neuron Pathology and the Role of Astrocytes in a Human Stem Cell Model of VCP-Related ALS. *Cell Rep*. 19:1739-1749.

Hall, E.D., J.A. Oostveen, and M.E. Gurney. 1998. Relationship of microglial and astrocytic activation to disease onset and progression in a transgenic model of familial ALS. *Glia*. 23:249-256.

Hamby, M.E., J.A. Hewett, and S.J. Hewett. 2006. TGF-beta 1 potentiates astrocytic nitric oxide production by expanding the population of astrocytes that express NOS-2. *Glia*. 54:566-577.

Hansen, J.J., A. Durr, I. Cournu-Rebeix, C. Georgopoulos, D. Ang, M.N. Nielsen, C.S. Davoine, A. Brice, B. Fontaine, N. Gregersen, et al. 2002. Hereditary spastic paraplegia SPG13 is associated with a mutation in the gene encoding the mitochondrial chaperonin Hsp60. *American Journal of Human Genetics*. 70:1328-1332.

Hara, M., K. Kobayakawa, Y. Ohkawa, H. Kumamaru, K. Yokota, T. Saito, K. Kijima, S. Yoshizaki, K. Harimaya, Y. Nakashima, et al. 2017. Interaction of reactive astrocytes with type I collagen induces astrocytic scar formation through the integrin-N-cadherin pathway after spinal cord injury. *Nat Med*. 23:818-828.

Hardiman, O., A. Al-Chalabi, A. Chio, E.M. Corr, G. Logroscino, W. Robberecht, P.J. Shaw, Z. Simmons, and L.H. van den Berg. 2017. Amyotrophic lateral sclerosis. *Nat Rev Dis Primers*. 3:17071.

Hargitai, J., H. Lewis, I. Boros, T. Racz, A. Fiser, I. Kurucz, I. Benjamin, L. Vigh, Z. Penzes, P. Csermely, et al. 2003. Bimoclomol, a heat shock protein co-inducer, acts by the prolonged activation of heat shock factor-1. *Biochem Bioph Res Co*. 307:689-695.

Harraz, M.M., J.J. Marden, W. Zhou, Y. Zhang, A. Williams, V.S. Sharov, K. Nelson, M. Luo, H. Paulson, C. Schoneich, et al. 2008. SOD1 mutations disrupt redox-sensitive Rac regulation of NADPH oxidase in a familial ALS model. *J Clin Invest*. 118:659-670.

Hartl, F.U., A. Bracher, and M. Hayer-Hartl. 2011. Molecular chaperones in protein folding and proteostasis. *Nature*. 475:324-332.

Havasi, A., Z.J. Li, Z.Y. Wang, J.L. Martin, V. Botla, K. Ruchalski, J.H. Schwartz, and S.C. Borkan. 2008. Hsp27 inhibits Bax activation and apoptosis via a phosphatidylinositol 3-kinase-dependent mechanism. *Journal of Biological Chemistry*. 283:12305-12313.

Hayden, M.S., and S. Ghosh. 2008. Shared principles in NF-kappa B signaling. *Cell*. 132:344-362.

Haynes, C.M., and D. Ron. 2010. The mitochondrial UPR - protecting organelle protein homeostasis. *J Cell Sci*. 123:3849-3855.

Heiman-Patterson, T.D., J.S. Deitch, E.P. Blankenhorn, K.L. Erwin, M.J. Perreault, B.K. Alexander, N. Byers, I. Toman, and G.M. Alexander. 2005. Background and gender effects on survival in the TgN(SOD1-G93A)1Gur mouse model of ALS. *J Neurol Sci*. 236:1-7.

Heneka, M.T., A. Sharp, T. Klockgether, V. Gavrilyuk, and D.L. Feinstein. 2000. The heat shock response inhibits NF-kappaB activation, nitric oxide synthase type 2 expression, and macrophage/microglial activation in brain. *J Cereb Blood Flow Metab*. 20:800-811.

Henkel, J.S., J.I. Engelhardt, L. Siklos, E.P. Simpson, S.H. Kim, T. Pan, J.C. Goodman, T. Siddique, D.R. Beers, and S.H. Appel. 2004. Presence of dendritic cells, MCP-1, and activated microglia/macrophages in amyotrophic lateral sclerosis spinal cord tissue. *Ann Neurol*. 55:221-235.

Hensley, K., H. Abdel-Moaty, J. Hunter, M. Mhatre, S. Mou, K. Nguyen, T. Potapova, Q.N. Pye, M. Qi, H. Rice, et al. 2006. Primary glia expressing the G93A-SOD1 mutation present a neuroinflammatory phenotype and provide a cellular system for studies of glial inflammation. *J Neuroinflamm*. 3.

Hensley, K., J. Fedynyshyn, S. Ferrell, R.A. Floyd, B. Gordon, P. Grammas, L. Hamdheydari, M. Mhatre, S. Mou, Q.N. Pye, et al. 2003. Message and protein-level elevation of tumor necrosis factor alpha (TNF alpha) and TNF alpha-modulating cytokines in spinal cords of the G93A-SOD1 mouse model for amyotrophic lateral sclerosis. *Neurobiol Dis*. 14:74-80.

Hochstim, C., B. Deneen, A. Lukaszewicz, Q. Zhou, and D.J. Anderson. 2008. Identification of positionally distinct astrocyte subtypes whose identities are specified by a homeodomain code. *Cell*. 133:510-522.

Holm, T.H., D. Draeby, and T. Owens. 2012. Microglia are required for astroglial Toll-like receptor 4 response and for optimal TLR2 and TLR3 response. *Glia*. 60:630-638.

Horibe, T., and N.J. Hoogenraad. 2007. The chop gene contains an element for the positive regulation of the mitochondrial unfolded protein response. *PLoS One*. 2:e835.

Hough, M.A., J.G. Grossmann, S.V. Antonyuk, R.W. Strange, P.A. Doucette, J.A. Rodriguez, L.J. Whitson, P.J. Hart, L.J. Hayward, J.S. Valentine, et al. 2004. Dimer destabilization in superoxide dismutase may result in disease-causing properties: Structures of motor neuron disease mutants. *P Natl Acad Sci USA*. 101:5976-5981.

Ialenti, A., P. Di Meglio, F. D'Acquisto, B. Pisano, P. Maffia, G. Grassia, M. Di Rosa, and A. Ianaro. 2005. Inhibition of cyclooxygenase-2 gene expression by the heat shock response in J774 murine macrophages. *European Journal of Pharmacology*. 509:89-96.

Igoudjil, A., J. Magrane, L.R. Fischer, H.J. Kim, I. Hervias, M. Dumont, C. Cortez, J.D. Glass, A.A. Starkov, and G. Manfredi. 2011. In vivo pathogenic role of mutant SOD1 localized in the mitochondrial intermembrane space. *J Neurosci*. 31:15826-15837.

Ikiz, B., M.J. Alvarez, D.B. Re, V. Le Verche, K. Politi, F. Lotti, S. Phani, R. Pradhan, C. Yu, G.F. Croft, et al. 2015. The Regulatory Machinery of Neurodegeneration in In Vitro Models of Amyotrophic Lateral Sclerosis. *Cell Rep*. 12:335-345.

Israelson, A., N. Arbel, S. Da Cruz, H. Ilieva, K. Yamanaka, V. Shoshan-Barmatz, and D.W. Cleveland. 2010. Misfolded mutant SOD1 directly inhibits

VDAC1 conductance in a mouse model of inherited ALS. *Neuron*. 67:575-587.

Ito, Y., D. Ofengeim, A. Najafov, S. Das, S. Saberi, Y. Li, J. Hitomi, H. Zhu, H. Chen, L. Mayo, et al. 2016. RIPK1 mediates axonal degeneration by promoting inflammation and necroptosis in ALS. *Science*. 353:603-608.

Jaarsma, D., E.D. Haasdijk, J.A. Grashorn, R. Hawkins, W. van Duijn, H.W. Verspaget, J. London, and J.C. Holstege. 2000. Human Cu/Zn superoxide dismutase (SOD1) overexpression in mice causes mitochondrial vacuolization, axonal degeneration, and premature motoneuron death and accelerates motoneuron disease in mice expressing a familial amyotrophic lateral sclerosis mutant SOD1. *Neurobiol Dis*. 7:623-643.

Jaarsma, D., F. Rognoni, W. van Duijn, H.W. Verspaget, E.D. Haasdijk, and J.C. Holstege. 2001. CuZn superoxide dismutase (SOD1) accumulates in vacuolated mitochondria in transgenic mice expressing amyotrophic lateral sclerosis-linked SOD1 mutations. *Acta Neuropathologica*. 102:293-305.

Jaarsma, D., E. Teuling, E.D. Haasdijk, C.I. De Zeeuw, and C.C. Hoogenraad. 2008. Neuron-specific expression of mutant superoxide dismutase is sufficient to induce amyotrophic lateral sclerosis in transgenic mice. *Journal of Neuroscience*. 28:2075-2088.

Jafarian-Tehrani, M., G. Louin, N.C. Royo, V.C. Besson, G.A. Bohme, M. Plotkine, and C. Marchand-Verrecchia. 2005. 1400W, a potent selective inducible NOS inhibitor, improves histopathological outcome following traumatic brain injury in rats. *Nitric Oxide*. 12:61-69.

Johnson, J.O., J. Mandrioli, M. Benatar, Y. Abramzon, V.M. Van Deerlin, J.Q. Trojanowski, J.R. Gibbs, M. Brunetti, S. Gronka, J. Wuu, et al. 2010. Exome Sequencing Reveals VCP Mutations as a Cause of Familial ALS. *Neuron*. 68:857-864.

Johnson, J.O., E.P. Pioro, A. Boehringer, R. Chia, H. Feit, A.E. Renton, H.A. Pliner, Y. Abramzon, G. Marangi, B.J. Winborn, et al. 2014. Mutations in the Matrin 3 gene cause familial amyotrophic lateral sclerosis. *Nat Neurosci*. 17:664-666.

Johnston, J.A., M.J. Dalton, M.E. Gurney, and R.R. Kopito. 2000. Formation of high molecular weight complexes of mutant Cu, Zn-superoxide dismutase in a mouse model for familial amyotrophic lateral sclerosis. *Proc Natl Acad Sci U S A*. 97:12571-12576.

Joyce, P.I., P. McGoldrick, R.A. Saccon, W. Weber, P. Fratta, S.J. West, N. Zhu, S. Carter, V. Phatak, M. Stewart, et al. 2015. A novel SOD1-ALS mutation separates central and peripheral effects of mutant SOD1 toxicity. *Hum Mol Genet*. 24:1883-1897.

Juneja, T., M.A. Pericak-Vance, N.G. Laing, S. Dave, and T. Siddique. 1997. Prognosis in familial amyotrophic lateral sclerosis: progression and survival in patients with glu100gly and ala4val mutations in Cu,Zn superoxide dismutase. *Neurology*. 48:55-57.

Jung, C., C.M. Higgins, and Z. Xu. 2002. Mitochondrial electron transport chain complex dysfunction in a transgenic mouse model for amyotrophic lateral sclerosis. *J Neurochem*. 83:535-545.

Kabashi, E., J.N. Agar, Y. Hong, D.M. Taylor, S. Minotti, D.A. Figlewicz, and H.D. Durham. 2008. Proteasomes remain intact, but show early focal alteration in their composition in a mouse model of amyotrophic lateral sclerosis. *Journal of Neurochemistry*. 105:2353-2366.

Kabashi, E., J.N. Agar, M.J. Strong, and H.D. Durham. 2012. Impaired proteasome function in sporadic amyotrophic lateral sclerosis. *Amyotroph Lateral Sc*. 13:367-371.

Kabashi, E., J.N. Agar, D.M. Taylor, S. Minotti, and H.D. Durham. 2004. Focal dysfunction of the proteasome: a pathogenic factor in a mouse model of amyotrophic lateral sclerosis. *J Neurochem*. 89:1325-1335.

Kabuta, T., Y. Suzuki, and K. Wada. 2006. Degradation of amyotrophic lateral sclerosis-linked mutant Cu,Zn-superoxide dismutase proteins by macroautophagy and the proteasome. *J Biol Chem*. 281:30524-30533.

Kaiser, M., I. Maletzki, S. Hulsmann, B. Holtmann, W. Schulz-Schaeffer, F. Kirchhoff, M. Bahr, and C. Neusch. 2006. Progressive loss of a glial potassium channel (KCNJ10) in the spinal cord of the SOD1 (G93A) transgenic mouse model of amyotrophic lateral sclerosis. *Journal of Neurochemistry*. 99:900-912.

Kalmar, B., G. Burnstock, G. Vrbova, R. Urbanics, P. Csermely, and L. Greensmith. 2002. Upregulation of heat shock proteins rescues motoneurones from axotomy-induced cell death in neonatal rats. *Experimental Neurology*. 176:87-97.

Kalmar, B., and L. Greensmith. 2017. Cellular Chaperones As Therapeutic Targets in ALS to Restore Protein Homeostasis and Improve Cellular Function. *Front Mol Neurosci*. 10.

Kalmar, B., C.H. Lu, and L. Greensmith. 2014. The role of heat shock proteins in Amyotrophic Lateral Sclerosis: The therapeutic potential of Arimoclomol. *Pharmacol Ther*. 141:40-54.

Kalmar, B., S. Novoselov, A. Gray, M.E. Cheetham, B. Margulis, and L. Greensmith. 2008. Late stage treatment with arimoclomol delays disease progression and prevents protein aggregation in the SOD1 mouse model of ALS. *J Neurochem*. 107:339-350.

Kamakura, S., K. Oishi, T. Yoshimatsu, M. Nakafuku, N. Masuyama, and Y. Gotoh. 2004. Hes binding to STAT3 mediates crosstalk between Notch and JAK-STAT signalling. *Nat Cell Biol*. 6:547-554.

Kang, B.H., J. Plescia, T. Dohi, J. Rosa, S.J. Doxsey, and D.C. Altieri. 2007. Regulation of tumor cell mitochondrial homeostasis by an organelle-specific Hsp90 chaperone network. *Cell*. 131:257-270.

Kang, B.H., J. Plescia, H.Y. Song, M. Meli, G. Colombo, K. Beebe, B. Scroggins, L. Neckers, and D.C. Altieri. 2009. Combinatorial drug design targeting multiple cancer signaling networks controlled by mitochondrial Hsp90. *J Clin Invest*. 119:454-464.

Kang, S.H., Y. Li, M. Fukaya, I. Lorenzini, D.W. Cleveland, L.W. Ostrow, J.D. Rothstein, and D.E. Bergles. 2013. Degeneration and impaired regeneration of gray matter oligodendrocytes in amyotrophic lateral sclerosis. *Nat Neurosci*. 16:571-579.

Kanning, K.C., A. Kaplan, and C.E. Henderson. 2010. Motor neuron diversity in development and disease. *Annu Rev Neurosci*. 33:409-440.

Kato, S., H. Hayashi, K. Nakashima, E. Nanba, M. Kato, A. Hirano, I. Nakano, K. Asayama, and E. Ohama. 1997. Pathological characterization of astrocytic hyaline inclusions in familial amyotrophic lateral sclerosis. *American Journal of Pathology*. 151:611-620.

Kawahara, Y., K. Ito, H. Sun, H. Aizawa, I. Kanazawa, and S. Kwak. 2004. Glutamate receptors: RNA editing and death of motor neurons. *Nature*. 427:801.

Kelley, K.W., L. Ben Haim, L. Schirmer, G.E. Tyzack, M. Tolman, J.G. Miller, H.H. Tsai, S.M. Chang, A.V. Molofsky, Y.J. Yang, et al. 2018. Kir4.1-Dependent Astrocyte-Fast Motor Neuron Interactions Are Required for Peak Strength. *Neuron*. 98:306-+.

Kennedy, D., R. Jager, D.D. Mosser, and A. Samali. 2014. Regulation of Apoptosis by Heat Shock Proteins. *Iubmb Life*. 66:327-338.

Kerman, A., H.N. Liu, S. Croul, J. Bilbao, E. Rogaeva, L. Zinman, J. Robertson, and A. Chakrabartty. 2010. Amyotrophic lateral sclerosis is a non-amyloid disease in which extensive misfolding of SOD1 is unique to the familial form. *Acta Neuropathol*. 119:335-344.

Khakh, B.S., and M.V. Sofroniew. 2015. Diversity of astrocyte functions and phenotypes in neural circuits. *Nat Neurosci*. 18:942-952.

Kia, A., K. McAvoy, K. Krishnamurthy, D. Trotti, and P. Pasinelli. 2018. Astrocytes expressing ALS-linked mutant FUS induce motor neuron death through release of tumor necrosis factor-alpha. *Glia*. 66:1016-1033.

Kieran, D., M. Hafezparast, S. Bohnert, J.R.T. Dick, J. Martin, G. Schiavo, E.M.C. Fisher, and L. Greensmith. 2005. A mutation in dynein rescues axonal transport defects and extends the life span of ALS mice. *Journal of Cell Biology*. 169:561-567.

Kieran, D., B. Kalmar, J.R. Dick, J. Riddoch-Contreras, G. Burnstock, and L. Greensmith. 2004. Treatment with arimoclomol, a coinducer of heat shock proteins, delays disease progression in ALS mice. *Nat Med*. 10:402-405.

Kiernan, M.C., S. Vucic, B.C. Cheah, M.R. Turner, A. Eisen, O. Hardiman, J.R. Burrell, and M.C. Zoing. 2011. Amyotrophic lateral sclerosis. *Lancet*. 377:942-955.

Kim, H., J. Yang, M.J. Kim, S. Choi, J.R. Chung, J.M. Kim, Y.H. Yoo, J. Chung, and H. Koh. 2016. Tumor Necrosis Factor Receptor-associated Protein 1 (TRAP1) Mutation and TRAP1 Inhibitor Gamitrinib-triphenylphosphonium (G-TPP) Induce a Forkhead Box O (FOXO)-dependent Cell Protective Signal from Mitochondria. *J Biol Chem*. 291:1841-1853.

Kim, H.J., N.C. Kim, Y.D. Wang, E.A. Scarborough, J. Moore, Z. Diaz, K.S. MacLea, B. Freibaum, S. Li, A. Molliex, et al. 2013. Mutations in prion-like domains in hnRNPA2B1 and hnRNPA1 cause multisystem proteinopathy and ALS. *Nature*. 495:467-473.

Kim, K., S.G. Lee, T.P. Kegelman, Z.Z. Su, S.K. Das, R. Dash, S. Dasgupta, P.M. Barral, M. Hedvat, P. Diaz, et al. 2011. Role of excitatory amino acid transporter-2 (EAAT2) and glutamate in neurodegeneration: opportunities for developing novel therapeutics. *J Cell Physiol*. 226:2484-2493.

Kirkinezos, I.G., S.R. Bacman, D. Hernandez, J.O. Cossio, L.J. Arias, M.A. Perez-Pinzon, W.G. Bradley, and C.T. Moraes. 2005. Cytochrome c association with the inner mitochondrial membrane is impaired in the CNS of G93A-SOD1 mice. *Journal of Neuroscience*. 25:164-172.

Kiskinis, E., J. Sandoe, L.A. Williams, G.L. Boulting, R. Moccia, B.J. Wainger, S. Han, T. Peng, S. Thams, S. Mikkilineni, et al. 2014. Pathways disrupted in human ALS motor neurons identified through genetic correction of mutant SOD1. *Cell Stem Cell*. 14:781-795.

Kleinert, H., A. Pautz, K. Linker, and P.M. Schwarz. 2004. Regulation of the expression of inducible nitric oxide synthase. *Eur J Pharmacol*. 500:255-266.

Kleizen, B., and I. Braakman. 2004. Protein folding and quality control in the endoplasmic reticulum. *Curr Opin Cell Biol*. 16:343-349.

Kong, J., and Z. Xu. 1998. Massive mitochondrial degeneration in motor neurons triggers the onset of amyotrophic lateral sclerosis in mice expressing a mutant SOD1. *J Neurosci*. 18:3241-3250.

Kong, L.Y., M.K. McMillian, R. Maronpot, and J.S. Hong. 1996. Protein tyrosine kinase inhibitors suppress the production of nitric oxide in mixed glia, microglia-enriched or astrocyte-enriched cultures. *Brain Res*. 729:102-109.

Krencik, R., J.P. Weick, Y. Liu, Z.J. Zhang, and S.C. Zhang. 2011. Specification of transplantable astroglial subtypes from human pluripotent stem cells. *Nature Biotechnology*. 29:528-U592.

Kumar, V., G.M. Hasan, and M.I. Hassan. 2017. Unraveling the Role of RNA Mediated Toxicity of C9orf72 Repeats in C9-FTD/ALS. *Front Neurosci*. 11:711.

Kwiatkowski, T.J., Jr., D.A. Bosco, A.L. Leclerc, E. Tamrazian, C.R. Vanderburg, C. Russ, A. Davis, J. Gilchrist, E.J. Kasarskis, T. Munsat, et al. 2009. Mutations in the FUS/TLS gene on chromosome 16 cause familial amyotrophic lateral sclerosis. *Science*. 323:1205-1208.

Lagier-Tourenne, C., M. Polymenidou, K.R. Hutt, A.Q. Vu, M. Baughn, S.C. Huelga, K.M. Clutario, S.C. Ling, T.Y. Liang, C. Mazur, et al. 2012. Divergent roles of ALS-linked proteins FUS/TLS and TDP-43 intersect in processing long pre-mRNAs. *Nat Neurosci*. 15:1488-1497.

Lautenschlager, J., T. Prell, J. Ruhmer, L. Weidemann, O.W. Witte, and J. Grosskreutz. 2013. Overexpression of human mutated G93A SOD1 changes dynamics of the ER mitochondria calcium cycle specifically in mouse embryonic motor neurons. *Exp Neurol*. 247:91-100.

Leak, R.K. 2014. Heat shock proteins in neurodegenerative disorders and aging. *J Cell Commun Signal*. 8:293-310.

Lee, J., H. Ryu, and N.W. Kowall. 2009. Differential regulation of neuronal and inducible nitric oxide synthase (NOS) in the spinal cord of mutant SOD1 (G93A) ALS mice. *Biochem Biophys Res Commun*. 387:202-206.

Lee, Y., B.M. Morrison, Y. Li, S. Lengacher, M.H. Farah, P.N. Hoffman, Y. Liu, A. Tsingalia, L. Jin, P.W. Zhang, et al. 2012. Oligodendroglia metabolically support axons and contribute to neurodegeneration. *Nature*. 487:443-448.

Leichsenring, A., B. Linnartz, X.R. Zhu, H. Lubbert, and C.C. Stichel. 2006. Ascending neuropathology in the CNS of a mutant SOD1 mouse model of amyotrophic lateral sclerosis. *Brain Res*. 1096:180-195.

Leroux, P.D., and T.A. Reh. 1994. Regional Differences in Glial-Derived Factors That Promote Dendritic Outgrowth from Mouse Cortical-Neurons in-Vitro. *Journal of Neuroscience*. 14:4639-4655.

Levine, J.B., J. Kong, M. Nadler, and Z. Xu. 1999. Astrocytes interact intimately with degenerating motor neurons in mouse amyotrophic lateral sclerosis (ALS). *Glia*. 28:215-224.

Li, Q.A., C. Vande Velde, A. Israelson, J. Xie, A.O. Bailey, M.Q. Dong, S.J. Chun, T. Roy, L. Winer, J.R. Yates, et al. 2010. ALS-linked mutant superoxide dismutase 1 (SOD1) alters mitochondrial protein composition and decreases protein import. *P Natl Acad Sci USA*. 107:21146-21151.

Li, X.J., X.Q. Zhang, M.A. Johnson, Z.B. Wang, T. LaVaute, and S.C. Zhang. 2009. Coordination of sonic hedgehog and Wnt signaling determines ventral and dorsal telencephalic neuron types from human embryonic stem cells. *Development*. 136:4055-4063.

Liao, B., W.H. Zhao, D.R. Beers, J.S. Henkel, and S.H. Appel. 2012. Transformation from a neuroprotective to a neurotoxic microglial

phenotype in a mouse model of ALS. *Experimental Neurology*. 237:147-152.
Liao, J., L.A. Lowthert, N. Ghori, and M.B. Omary. 1995. The 70-Kda Heat-Shock Proteins Associate with Glandular Intermediate Filaments in an Atp-Dependent Manner. *Journal of Biological Chemistry*. 270:915-922.
Liddelow, S.A., and B.A. Barres. 2017. Reactive Astrocytes: Production, Function, and Therapeutic Potential. *Immunity*. 46:957-967.
Liddelow, S.A., K.A. Guttenplan, L.E. Clarke, F.C. Bennett, C.J. Bohlen, L. Schirmer, M.L. Bennett, A.E. Munch, W.S. Chung, T.C. Peterson, et al. 2017. Neurotoxic reactive astrocytes are induced by activated microglia. *Nature*. 541:481-487.
Lisanti, S., M. Tavecchio, Y.C. Chae, Q. Liu, A.K. Brice, M.L. Thakur, L.R. Languino, and D.C. Altieri. 2014. Deletion of the mitochondrial chaperone TRAP-1 uncovers global reprogramming of metabolic networks. *Cell Rep*. 8:671-677.
Liu, D.X., J. Wen, J. Liu, and L.P. Li. 1999. The roles of free radicals in amyotrophic lateral sclerosis: reactive oxygen species and elevated oxidation of protein, DNA, and membrane phospholipids. *Faseb Journal*. 13:2318-2328.
Liu, J., C. Lillo, P.A. Jonsson, C.V. Velde, C.M. Ward, T.M. Miller, J.R. Subramaniam, J.D. Rothstein, S. Marklund, P.M. Andersen, et al. 2004. Toxicity of familial ALS-linked SOD1 mutants from selective recruitment to spinal mitochondria. *Neuron*. 43:5-17.
Liu, J., L.A. Shinobu, C.M. Ward, D. Young, and D.W. Cleveland. 2005. Elevation of the Hsp70 chaperone does not effect toxicity in mouse models of familial amyotrophic lateral sclerosis. *Journal of Neurochemistry*. 93:875-882.
Lopez-Erauskin, J., T. Tadokoro, M.W. Baughn, B. Myers, M. McAlonis-Downes, C. Chillon-Marinas, J.N. Asiaban, J. Artates, A.T. Bui, A.P. Vetto, et al. 2018. ALS/FTD-Linked Mutation in FUS Suppresses Intra-axonal Protein Synthesis and Drives Disease Without Nuclear Loss-of-Function of FUS. *Neuron*.
Lopez-Gonzalez, R., Y.B. Lu, T.F. Gendron, A. Karydas, H. Tran, D.J. Yang, L. Petrucelli, B.L. Miller, S. Almeida, and F.B. Gao. 2016. Poly(GR) in C9ORF72-Related ALS/FTD Compromises Mitochondrial Function and Increases Oxidative Stress and DNA Damage in iPSC-Derived Motor Neurons. *Neuron*. 92:383-391.
Lou, E., S. Fujisawa, A. Morozov, A. Barlas, Y. Romin, Y. Dogan, S. Gholami, A.L. Moreira, K. Manova-Todorova, and M.A.S. Moore. 2012. Tunneling Nanotubes Provide a Unique Conduit for Intercellular Transfer of Cellular Contents in Human Malignant Pleural Mesothelioma. *Plos One*. 7.
Luisier, R., G.E. Tyzack, C.E. Hall, J.S. Mitchell, H. Devine, D.M. Taha, B. Malik, I. Meyer, L. Greensmith, J. Newcombe, et al. 2018. Intron retention and nuclear loss of SFPQ are molecular hallmarks of ALS. *Nature Communications*. 9.
Luty, A.A., J.B. Kwok, C. Dobson-Stone, C.T. Loy, K.G. Coupland, H. Karlstrom, T. Sobow, J. Tchorzewska, A. Maruszak, M. Barcikowska, et al. 2010. Sigma nonopioid intracellular receptor 1 mutations cause frontotemporal lobar degeneration-motor neuron disease. *Ann Neurol*. 68:639-649.
Mackenzie, I.R., E.H. Bigio, P.G. Ince, F. Geser, M. Neumann, N.J. Cairns, L.K. Kwong, M.S. Forman, J. Ravits, H. Stewart, et al. 2007. Pathological TDP-43 distinguishes sporadic amyotrophic lateral sclerosis from amyotrophic lateral sclerosis with SOD1 mutations. *Ann Neurol*. 61:427-434.

Mackenzie, I.R., A.M. Nicholson, M. Sarkar, J. Messing, M.D. Purice, C. Pottier, K. Annu, M. Baker, R.B. Perkerson, A. Kurti, et al. 2017. TIA1 Mutations in Amyotrophic Lateral Sclerosis and Frontotemporal Dementia Promote Phase Separation and Alter Stress Granule Dynamics. *Neuron*. 95:808-816 e809.

Madji Hounoum, B., S. Mavel, E. Coque, F. Patin, P. Vourc'h, S. Marouillat, L. Nadal-Desbarats, P. Emond, P. Corcia, C.R. Andres, et al. 2017. Wildtype motoneurons, ALS-Linked SOD1 mutation and glutamate profoundly modify astrocyte metabolism and lactate shuttling. *Glia*. 65:592-605.

Magnoni, R., J. Palmfeldt, J.H. Christensen, M. Sand, F. Maltecca, T.J. Corydon, M. West, G. Casari, and P. Bross. 2013. Late onset motoneuron disorder caused by mitochondrial Hsp60 chaperone deficiency in mice. *Neurobiol Dis*. 54:12-23.

Magrane, J., I. Hervias, M.S. Henning, M. Damiano, H. Kawamata, and G. Manfredi. 2009. Mutant SOD1 in neuronal mitochondria causes toxicity and mitochondrial dynamics abnormalities. *Human Molecular Genetics*. 18:4552-4564.

Magrane, J., and G. Manfredi. 2009. Mitochondrial function, morphology, and axonal transport in amyotrophic lateral sclerosis. *Antioxid Redox Signal*. 11:1615-1626.

Marchetto, M.C., A.R. Muotri, Y. Mu, A.M. Smith, G.G. Cezar, and F.H. Gage. 2008. Non-cell-autonomous effect of human SOD1 G37R astrocytes on motor neurons derived from human embryonic stem cells. *Cell Stem Cell*. 3:649-657.

Marcuccilli, C.J., S.K. Mathur, R.I. Morimoto, and R.J. Miller. 1996. Regulatory differences in the stress response of hippocampal neurons and glial cells after heat shock. *Journal of Neuroscience*. 16:478-485.

Marden, J.J., M.M. Harraz, A.J. Williams, K. Nelson, M. Luo, H. Paulson, and J.F. Engelhardt. 2007. Redox modifier genes in amyotrophic lateral sclerosis in mice. *J Clin Invest*. 117:2913-2919.

Marino Gammazza, A., R. Colangeli, G. Orban, M. Pierucci, G. Di Gennaro, M. Lo Bello, A. D'Aniello, F. Bucchieri, C. Pomara, M. Valentino, et al. 2015. Hsp60 response in experimental and human temporal lobe epilepsy. *Sci Rep*. 5:9434.

Markovinovic, A., R. Cimbro, T. Ljutic, J. Kriz, B. Rogelj, and I. Munitic. 2017. Optineurin in amyotrophic lateral sclerosis: Multifunctional adaptor protein at the crossroads of different neuroprotective mechanisms. *Progress in Neurobiology*. 154:1-20.

Martin, L.J., Z. Liu, K. Chen, A.C. Price, Y. Pan, J.A. Swaby, and W.C. Golden. 2007. Motor neuron degeneration in amyotrophic lateral sclerosis mutant superoxide dismutase-1 transgenic mice: mechanisms of mitochondriopathy and cell death. *J Comp Neurol*. 500:20-46.

Martin, R., R. Bajo-Graneras, R. Moratalla, G. Perea, and A. Araque. 2015. Circuit-specific signaling in astrocyte-neuron networks in basal ganglia pathways. *Glia*. 63:E214-E215.

Martinus, R.D., G.P. Garth, T.L. Webster, P. Cartwright, D.J. Naylor, P.B. Hoj, and N.J. Hoogenraad. 1996. Selective induction of mitochondrial chaperones in response to loss of the mitochondrial genome. *Eur J Biochem*. 240:98-103.

Maruyama, H., H. Morino, H. Ito, Y. Izumi, H. Kato, Y. Watanabe, Y. Kinoshita, M. Kamada, H. Nodera, H. Suzuki, et al. 2010. Mutations of optineurin in amyotrophic lateral sclerosis. *Nature*. 465:223-226.

Masgras, I., C. Sanchez-Martin, G. Colombo, and A. Rasola. 2017. The Chaperone TRAP1 As a Modulator of the Mitochondrial Adaptations in Cancer Cells. *Front Oncol*. 7:58.

Mateju, D., T.M. Franzmann, A. Patel, A. Kopach, E.E. Boczek, S. Maharana, H.O. Lee, S. Carra, A.A. Hyman, and S. Alberti. 2017. An aberrant phase transition of stress granules triggered by misfolded protein and prevented by chaperone function. *EMBO J*. 36:1669-1687.

Matsumoto, G., A. Stojanovic, C.I. Holmberg, S. Kim, and R.I. Morimoto. 2005. Structural properties and neuronal toxicity of amyotrophic lateral sclerosis-associated Cu/Zn superoxide dismutase 1 aggregates. *Journal of Cell Biology*. 171:75-85.

Mattiazzi, M., M. D'Aurelio, C.D. Gajewski, K. Martushova, M. Kiaei, M.F. Beal, and G. Manfredi. 2002. Mutated human SOD1 causes dysfunction of oxidative phosphorylation in mitochondria of transgenic mice. *Journal of Biological Chemistry*. 277:29626-29633.

McCarthy, K.D., and J. de Vellis. 1980. Preparation of separate astroglial and oligodendroglial cell cultures from rat cerebral tissue. *J Cell Biol*. 85:890-902.

McCombe, P.A., and R.D. Henderson. 2010. Effects of gender in amyotrophic lateral sclerosis. *Gend Med*. 7:557-570.

Meissner, F., K. Molawi, and A. Zychlinsky. 2010. Mutant superoxide dismutase 1-induced IL-1beta accelerates ALS pathogenesis. *Proc Natl Acad Sci U S A*. 107:13046-13050.

Melamed, Z., J. Lopez-Erauskin, M.W. Baughn, O. Zhang, K. Drenner, Yingsun, F. Freyermuth, M.A. McMahons, M.S. Beccari, J.W. Artates, et al. 2019. Premature polyadenylation-mediated loss of stathmin-2 is a hallmark of TDP-43-dependent neurodegeneration. *Nature Neuroscience*. 22:180-+.

Meyer, H., and C.C. Weihl. 2014. The VCP/p97 system at a glance: connecting cellular function to disease pathogenesis. *Journal of Cell Science*. 127:3877-3883.

Meyer, K., L. Ferraiuolo, C.J. Miranda, S. Likhite, S. McElroy, S. Renusch, D. Ditsworth, C. Lagier-Tourenne, R.A. Smith, J. Ravits, et al. 2014. Direct conversion of patient fibroblasts demonstrates non-cell autonomous toxicity of astrocytes to motor neurons in familial and sporadic ALS. *P Natl Acad Sci USA*. 111:829-832.

Migheli, A., R. Piva, C. Atzori, D. Troost, and D. Schiffer. 1997. c-Jun, JNK/SAPK kinases and transcription factor NF-kappa B are selectively activated in astrocytes, but not motor neurons, in amyotrophic lateral sclerosis. *J Neuropathol Exp Neurol*. 56:1314-1322.

Milanese, M., S. Zappettini, F. Onofri, L. Musazzi, D. Tardito, T. Bonifacino, M. Messa, G. Racagni, C. Usai, F. Benfenati, et al. 2011. Abnormal exocytotic release of glutamate in a mouse model of amyotrophic lateral sclerosis. *Journal of Neurochemistry*. 116:1028-1042.

Miller, S.J., J.C. Glatzer, Y.C. Hsieh, and J.D. Rothstein. 2018. Cortical astroglia undergo transcriptomic dysregulation in the G93A SOD1 ALS mouse model. *J Neurogenet*. 32:322-335.

Mitchell, J., P. Paul, H.J. Chen, A. Morris, M. Payling, M. Falchi, J. Habgood, S. Panoutsou, S. Winkler, V. Tisato, et al. 2010. Familial amyotrophic lateral sclerosis is associated with a mutation in D-amino acid oxidase. *P Natl Acad Sci USA*. 107:7556-7561.

Mitsumoto, A., A. Takeuchi, K. Okawa, and Y. Nakagawa. 2002. A subset of newly synthesized polypeptides in mitochondria from human endothelial cells exposed to hydroperoxide stress. *Free Radic Biol Med*. 32:22-37.

Mizielinska, S., S. Gronke, T. Niccoli, C.E. Ridler, E.L. Clayton, A. Devoy, T. Moens, F.E. Norona, I.O.C. Woollacott, J. Pietrzyk, et al. 2014. C9orf72 repeat expansions cause neurodegeneration in Drosophila through arginine-rich proteins. *Science*. 345:1192-1194.

Moehle, E.A., K. Shen, and A. Dillin. 2019. Mitochondrial proteostasis in the context of cellular and organismal health and aging. *J Biol Chem*. 294:5396-5407.

Mohammadi, B., K. Krampfl, H. Moschref, R. Dengler, and J. Bufler. 2001. Interaction of the neuroprotective drug riluzole with GABA(A) and glycine receptor channels. *Eur J Pharmacol*. 415:135-140.

Molliex, A., J. Temirov, J. Lee, M. Coughlin, A.P. Kanagaraj, H.J. Kim, T. Mittag, and J.P. Taylor. 2015. Phase separation by low complexity domains promotes stress granule assembly and drives pathological fibrillization. *Cell*. 163:123-133.

Molofsky, A.V., K.W. Kelley, H.H. Tsai, S.A. Redmond, S.M. Chang, L. Madireddy, J.R. Chan, S.E. Baranzini, E.M. Ullian, and D.H. Rowitch. 2014. Astrocyte-encoded positional cues maintain sensorimotor circuit integrity. *Nature*. 509:189-194.

Montesano Gesualdi, N., G. Chirico, G. Pirozzi, E. Costantino, M. Landriscina, and F. Esposito. 2007. Tumor necrosis factor-associated protein 1 (TRAP-1) protects cells from oxidative stress and apoptosis. *Stress*. 10:342-350.

Mordes, D.A., M. Prudencio, L.D. Goodman, J.R. Klim, R. Moccia, F. Limone, O. Pietilainen, K. Chowdhary, D.W. Dickson, R. Rademakers, et al. 2018. Dipeptide repeat proteins activate a heat shock response found in C9ORF72-ALS/FTLD patients. *Acta Neuropathol Com*. 6.

Morel, L., M.S.R. Chiang, H. Higashimori, T. Shoneye, L.K. Iyer, J. Yelick, A. Tai, and Y.J. Yang. 2017. Molecular and Functional Properties of Regional Astrocytes in the Adult Brain. *Journal of Neuroscience*. 37:8706-8717.

Morimoto, R.I., P.E. Kroeger, and J.J. Cotto. 1996. The transcriptional regulation of heat shock genes: a plethora of heat shock factors and regulatory conditions. *EXS*. 77:139-163.

Morrison, S.J., S.E. Perez, Z. Qiao, J.M. Verdi, C. Hicks, G. Weinmaster, and D.J. Anderson. 2000. Transient notch activation initiates an irreversible switch from neurogenesis to gliogenesis by neural crest stem cells. *Cell*. 101:499-510.

Mosser, D.D., P.T. Kotzbauer, K.D. Sarge, and R.I. Morimoto. 1990. In vitro activation of heat shock transcription factor DNA-binding by calcium and biochemical conditions that affect protein conformation. *Proc Natl Acad Sci U S A*. 87:3748-3752.

Mounier, N., and A.P. Arrigo. 2002. Actin cytoskeleton and small heat shock proteins: how do they interact? *Cell Stress Chaperon*. 7:167-176.

Munch, C., and J.W. Harper. 2016. Mitochondrial unfolded protein response controls matrix pre-RNA processing and translation. *Nature*. 534:710-713.

Munch, C., J. O'Brien, and A. Bertolotti. 2011. Prion-like propagation of mutant superoxide dismutase-1 misfolding in neuronal cells. *P Natl Acad Sci USA*. 108:3548-3553.

Murakami, T., S. Qamar, J.Q. Lin, G.S.K. Schierle, E. Rees, A. Miyashita, A.R. Costa, R.B. Dodd, F.T.S. Chan, C.H. Michel, et al. 2015. ALS/FTD Mutation-Induced Phase Transition of FUS Liquid Droplets and Reversible

Hydrogels into Irreversible Hydrogels Impairs RNP Granule Function. *Neuron*. 88:678-690.

Nagai, M., D.B. Re, T. Nagata, A. Chalazonitis, T.M. Jessell, H. Wichterle, and S. Przedborski. 2007. Astrocytes expressing ALS-linked mutated SOD1 release factors selectively toxic to motor neurons. *Nat Neurosci*. 10:615-622.

Nakashima, K., M. Yanagisawa, H. Arakawa, N. Kimura, T. Hisatsune, M. Kawabata, K. Miyazono, and T. Taga. 1999. Synergistic signaling in fetal brain by STAT3-Smad1 complex bridged by p300. *Science*. 284:479-482.

Nardo, G., M.C. Trolese, M. Tortarolo, A. Vallarola, M. Freschi, L. Pasetto, V. Bonetto, and C. Bendotti. 2016. New Insights on the Mechanisms of Disease Course Variability in ALS from Mutant SOD1 Mouse Models. *Brain Pathol*. 26:237-247.

Neumann, M., D.M. Sampathu, L.K. Kwong, A.C. Truax, M.C. Micsenyi, T.T. Chou, J. Bruce, T. Schuck, M. Grossman, C.M. Clark, et al. 2006. Ubiquitinated TDP-43 in frontotemporal lobar degeneration and amyotrophic lateral sclerosis. *Science*. 314:130-133.

Nguyen, D.K.H., R. Thombre, and J. Wang. 2019. Autophagy as a common pathway in amyotrophic lateral sclerosis. *Neurosci Lett*. 697:34-48.

Nguyen, H.P., C. Van Broeckhoven, and J. van der Zee. 2018. ALS Genes in the Genomic Era and their Implications for FTD. *Trends Genet*. 34:404-423.

Nguyen, K.T., L.E. Garcia-Chacon, J.N. Barretta, E.F. Barrett, and G. David. 2009. The Psi(m) depolarization that accompanies mitochondrial Ca2+ uptake is greater in mutant SOD1 than in wild-type mouse motor terminals. *P Natl Acad Sci USA*. 106:2007-2011.

Niccoli, T., L. Partridge, and A.M. Isaacs. 2017. Ageing as a risk factor for ALS/FTD. *Human Molecular Genetics*. 26:R105-R113.

Nicolas, A., K.P. Kenna, A.E. Renton, N. Ticozzi, F. Faghri, R. Chia, J.A. Dominov, B.J. Kenna, M.A. Nalls, P. Keagle, et al. 2018. Genome-wide Analyses Identify KIF5A as a Novel ALS Gene. *Neuron*. 97:1268-+.

Niedermeyer, S., M. Murn, and P.J. Choi. 2019. Respiratory Failure in Amyotrophic Lateral Sclerosis. *Chest*. 155:401-408.

Nijssen, J., L.H. Comley, and E. Hedlund. 2017. Motor neuron vulnerability and resistance in amyotrophic lateral sclerosis. *Acta Neuropathol*. 133:863-885.

Nikodemova, M., A.L. Small, S.M. Smith, G.S. Mitchell, and J.J. Watters. 2014. Spinal but not cortical microglia acquire an atypical phenotype with high VEGF, galectin-3 and osteopontin, and blunted inflammatory responses in ALS rats. *Neurobiol Dis*. 69:43-53.

Nishimura, A.L., M. Mitne-Neto, H.C.A. Silva, A. Richieri-Costa, S. Middleton, D. Cascio, F. Kok, J.R.M. Oliveira, T. Gillingwater, J. Webb, et al. 2004. A mutation in the vesicle-trafficking protein VAPB causes late-onset spinal muscular atrophy and amyotrophic lateral sclerosis. *American Journal of Human Genetics*. 75:822-831.

Nishimura, R.N., B.E. Dwyer, K. Clegg, R. Cole, and J. de Vellis. 1991. Comparison of the heat shock response in cultured cortical neurons and astrocytes. *Brain Res Mol Brain Res*. 9:39-45.

Noack, H., H. Possel, S. Chatterjee, G. Keilhoff, and G. Wolf. 2000. Nitrosative stress in primary glial cultures after induction of the inducible isoform of nitric oxide synthase (i-NOS). *Toxicology*. 148:133-142.

Noble, M., J.E. Davies, M. Mayer-Proschel, C. Proschel, and S.J. Davies. 2011. Precursor cell biology and the development of astrocyte transplantation therapies: lessons from spinal cord injury. *Neurotherapeutics*. 8:677-693.

Nwaobi, S.E., V.A. Cuddapah, K.C. Patterson, A.C. Randolph, and M.L. Olsen. 2016. The role of glial-specific Kir4.1 in normal and pathological states of the CNS. *Acta Neuropathologica*. 132:1-21.

O'Rourke, J.G., L. Bogdanik, A. Yanez, D. Lall, A.J. Wolf, A.K.M.G. Muhammad, R. Ho, S. Carmona, J.P. Vit, J. Zarrow, et al. 2016. C9orf72 is required for proper macrophage and microglial function in mice. *Science*. 351:1324-1329.

Oakes, J.A., M.C. Davies, and M.O. Collins. 2017. TBK1: a new player in ALS linking autophagy and neuroinflammation. *Molecular Brain*. 10.

Oberheim, N.A., S.A. Goldman, and M. Nedergaard. 2012. Heterogeneity of astrocytic form and function. *Methods Mol Biol*. 814:23-45.

Okado-Matsumoto, A., and I. Fridovich. 2002. Amyotrophic lateral sclerosis: a proposed mechanism. *Proc Natl Acad Sci U S A*. 99:9010-9014.

Okamoto, T., R. Ishida, H. Yamamoto, M. Tanabe-Ishida, A. Haga, H. Takahashi, K. Takahashi, D. Goto, E. Grave, and H. Itoh. 2015. Functional structure and physiological functions of mammalian wild-type HSP60. *Arch Biochem Biophys*. 586:10-19.

Ostermann, J., A.L. Horwich, W. Neupert, and F.U. Hartl. 1989. Protein folding in mitochondria requires complex formation with hsp60 and ATP hydrolysis. *Nature*. 341:125-130.

Ouali Alami, N., C. Schurr, F. Olde Heuvel, L. Tang, Q. Li, A. Tasdogan, A. Kimbara, M. Nettekoven, G. Ottaviani, C. Raposo, et al. 2018. NF-kappaB activation in astrocytes drives a stage-specific beneficial neuroimmunological response in ALS. *EMBO J*.

Pagliarini, D.J., S.E. Calvo, B. Chang, S.A. Sheth, S.B. Vafai, S.E. Ong, G.A. Walford, C. Sugiana, A. Boneh, W.K. Chen, et al. 2008. A mitochondrial protein compendium elucidates complex I disease biology. *Cell*. 134:112-123.

Papadeas, S.T., S.E. Kraig, C. O'Banion, A.C. Lepore, and N.J. Maragakis. 2011. Astrocytes carrying the superoxide dismutase 1 (SOD1G93A) mutation induce wild-type motor neuron degeneration in vivo. *Proc Natl Acad Sci U S A*. 108:17803-17808.

Park, H.K., H. Jeong, E. Ko, G. Lee, J.E. Lee, S.K. Lee, A.J. Lee, J.Y. Im, S. Hu, S.H. Kim, et al. 2017. Paralog Specificity Determines Subcellular Distribution, Action Mechanism, and Anticancer Activity of TRAP1 Inhibitors. *J Med Chem*. 60:7569-7578.

Park, K.J., R.B. Gaynor, and Y.T. Kwak. 2003. Heat shock protein 27 association with the I kappa B kinase complex regulates tumor necrosis factor alpha-induced NF-kappa B activation. *Journal of Biological Chemistry*. 278:35272-35278.

Parkinson, N., P.G. Ince, M.O. Smith, R. Highley, G. Skibinski, P.M. Andersen, K.E. Morrison, H.S. Pall, O. Hardiman, J. Collinge, et al. 2006. ALS phenotypes with mutations in CHMP2B (charged multivesicular body protein 2B). *Neurology*. 67:1074-1077.

Parone, P.A., S. Da Cruz, J.S. Han, M. McAlonis-Downes, A.P. Vetto, S.K. Lee, E. Tseng, and D.W. Cleveland. 2013. Enhancing mitochondrial calcium buffering capacity reduces aggregation of misfolded SOD1 and motor neuron cell death without extending survival in mouse models of inherited amyotrophic lateral sclerosis. *J Neurosci*. 33:4657-4671.

Patani, R. 2016. Generating Diverse Spinal Motor Neuron Subtypes from Human Pluripotent Stem Cells. *Stem Cells International*.

Patani, R., A.J. Hollins, T.M. Wishart, C.A. Puddifoot, S. Alvarez, A.R. de Lera, D.J.A. Wyllie, D.A.S. Compston, R.A. Pedersen, T.H. Gillingwater, et al. 2011. Retinoid-independent motor neurogenesis from human embryonic stem cells reveals a medial columnar ground state. *Nature Communications*. 2.

Pedrini, S., D. Sau, S. Guareschi, M. Bogush, R.H. Brown, Jr., N. Naniche, A. Kia, D. Trotti, and P. Pasinelli. 2010. ALS-linked mutant SOD1 damages mitochondria by promoting conformational changes in Bcl-2. *Hum Mol Genet*. 19:2974-2986.

Pehar, M., P. Cassina, M.R. Vargas, R. Castellanos, L. Viera, J.S. Beckman, A.G. Estevez, and L. Barbeito. 2004. Astrocytic production of nerve growth factor in motor neuron apoptosis: implications for amyotrophic lateral sclerosis. *J Neurochem*. 89:464-473.

Perng, M.D., L. Cairns, P. van den IJssel, A. Prescott, A.M. Hutcheson, and R.A. Quinlan. 1999. Intermediate filament interactions can be altered by HSP27 and alpha B-crystallin. *Journal of Cell Science*. 112:2099-2112.

Perriot, S., A. Mathias, G. Perriard, M. Canales, N. Jonkmans, N. Merienne, C. Meunier, L. El Kassar, A.L. Perrier, D.A. Laplaud, et al. 2018. Human Induced Pluripotent Stem Cell-Derived Astrocytes Are Differentially Activated by Multiple Sclerosis-Associated Cytokines. *Stem Cell Reports*. 11:1199-1210.

Perry, S.W., J.P. Norman, J. Barbieri, E.B. Brown, and H.A. Gelbard. 2011. Mitochondrial membrane potential probes and the proton gradient: a practical usage guide. *Biotechniques*. 50:98-115.

Phatnani, H.P., P. Guarnieri, B.A. Friedman, M.A. Carrasco, M. Muratet, S. O'Keeffe, C. Nwakeze, F. Pauli-Behn, K.M. Newberry, S.K. Meadows, et al. 2013. Intricate interplay between astrocytes and motor neurons in ALS. *P Natl Acad Sci USA*. 110:E756-E765.

Philips, T., A. Bento-Abreu, A. Nonneman, W. Haeck, K. Staats, V. Geelen, N. Hersmus, B. Kusters, L. Van Den Bosch, P. Van Damme, et al. 2013. Oligodendrocyte dysfunction in the pathogenesis of amyotrophic lateral sclerosis. *Brain*. 136:471-482.

Philips, T., and J.D. Rothstein. 2014. Glial cells in amyotrophic lateral sclerosis. *Experimental Neurology*. 262:111-120.

Philips, T., and J.D. Rothstein. 2015. Rodent Models of Amyotrophic Lateral Sclerosis. *Curr Protoc Pharmacol*. 69:5 67 61-21.

Phukan, J., M. Elamin, P. Bede, N. Jordan, L. Gallagher, S. Byrne, C. Lynch, N. Pender, and O. Hardiman. 2012. The syndrome of cognitive impairment in amyotrophic lateral sclerosis: a population-based study. *J Neurol Neurosurg Psychiatry*. 83:102-108.

Pickrell, A.M., and R.J. Youle. 2015. The roles of PINK1, parkin, and mitochondrial fidelity in Parkinson's disease. *Neuron*. 85:257-273.

Plun-Favreau, H., V.S. Burchell, K.M. Holmstrom, Z. Yao, E. Deas, K. Cain, V. Fedele, N. Moisoi, M. Campanella, L.M. Martins, et al. 2012. HtrA2 deficiency causes mitochondrial uncoupling through the F1F0-ATP synthase and consequent ATP depletion. *Cell Death & Disease*. 3.

Plun-Favreau, H., S. Gandhi, A. Wood-Kaczmar, E. Deas, Z. Yao, and N.W. Wood. 2008. What Have PINK1 and HtrA2 Genes Told Us about the Role of Mitochondria in Parkinson's Disease? *Mitochondria and Oxidative Stress in Neurodegenerative Disorders*. 1147:30-36.

Plun-Favreau, H., K. Klupsch, N. Moisoi, S. Gandhi, S. Kjaer, D. Frith, K. Harvey, E. Deas, R.J. Harvey, N. McDonald, et al. 2007. The mitochondrial protease HtrA2 is regulated by Parkinson's disease-associated kinase PINK1. *Nat Cell Biol*. 9:1243-U1263.

Polymenidou, M., C. Lagier-Tourenne, K.R. Hutt, S.C. Huelga, J. Moran, T.Y. Liang, S.C. Ling, E. Sun, E. Wancewicz, C. Mazur, et al. 2011. Long pre-mRNA depletion and RNA missplicing contribute to neuronal vulnerability from loss of TDP-43. *Nat Neurosci*. 14:459-468.

Pramatarova, A., J. Laganiere, J. Roussel, K. Brisebois, and G.A. Rouleau. 2001. Neuron-specific expression of mutant superoxide dismutase 1 in transgenic mice does not lead to motor impairment. *J Neurosci*. 21:3369-3374.

Preville, X., F. Salvemini, S. Giraud, S. Chaufour, C. Paul, G. Stepien, M.V. Ursini, and A.P. Arrigo. 1999. Mammalian small stress proteins protect against oxidative stress through their ability to increase glucose-6-phosphate dehydrogenase activity and by maintaining optimal cellular detoxifying machinery. *Experimental Cell Research*. 247:61-78.

Pridgeon, J.W., J.A. Olzmann, L.S. Chin, and L. Li. 2007. PINK1 protects against oxidative stress by phosphorylating mitochondrial chaperone TRAP1. *PLoS Biol*. 5:e172.

Puls, I., C. Jonnakuty, B.H. LaMonte, E.L. Holzbaur, M. Tokito, E. Mann, M.K. Floeter, K. Bidus, D. Drayna, S.J. Oh, et al. 2003. Mutant dynactin in motor neuron disease. *Nat Genet*. 33:455-456.

Rakhit, R., J.P. Crow, J.R. Lepock, L.H. Kondejewski, N.R. Cashman, and A. Chakrabartty. 2004. Monomeric Cu,Zn-superoxide dismutase is a common misfolding intermediate in the oxidation models of sporadic and familial amyotrophic lateral sclerosis. *Journal of Biological Chemistry*. 279:15499-15504.

Rakhit, R., J. Robertson, C. Vande Velde, P. Horne, D.M. Ruth, J. Griffin, D.W. Cleveland, N.R. Cashman, and A. Chakrabartty. 2007. An immunological epitope selective for pathological monomer-misfolded SOD1 in ALS. *Nature Medicine*. 13:754-759.

Ran, R., A. Lu, L. Zhang, Y. Tang, H. Zhu, H. Xu, Y. Feng, C. Han, G. Zhou, A.C. Rigby, et al. 2004. Hsp70 promotes TNF-mediated apoptosis by binding IKK gamma and impairing NF-kappa B survival signaling. *Genes Dev*. 18:1466-1481.

Raoul, C., A.G. Estevez, H. Nishimune, D.W. Cleveland, O. deLapeyriere, C.E. Henderson, G. Haase, and B. Pettmann. 2002. Motoneuron death triggered by a specific pathway downstream of Fas: Potentiation by ALS-linked SOD1 mutations. *Neuron*. 35:1067-1083.

Ratovitski, T., L.B. Corson, J. Strain, P. Wong, D.W. Cleveland, V.C. Culotta, and D.R. Borchelt. 1999. Variation in the biochemical/biophysical properties of mutant superoxide dismutase 1 enzymes and the rate of disease progression in familial amyotrophic lateral sclerosis kindreds. *Human Molecular Genetics*. 8:1451-1460.

Re, D.B., V. Le Verche, C. Yu, M.W. Amoroso, K.A. Politi, S. Phani, B. Ikiz, L. Hoffmann, M. Koolen, T. Nagata, et al. 2014. Necroptosis drives motor neuron death in models of both sporadic and familial ALS. *Neuron*. 81:1001-1008.

Reaume, A.G., J.L. Elliott, E.K. Hoffman, N.W. Kowall, R.J. Ferrante, D.F. Siwek, H.M. Wilcox, D.G. Flood, M.F. Beal, R.H. Brown, Jr., et al. 1996. Motor

neurons in Cu/Zn superoxide dismutase-deficient mice develop normally but exhibit enhanced cell death after axonal injury. *Nat Genet*. 13:43-47.
Reddi, A.R., and V.C. Culotta. 2013. SOD1 Integrates Signals from Oxygen and Glucose to Repress Respiration. *Cell*. 152:224-235.
Regan, M.R., Y.H. Huang, Y.S. Kim, M.I. Dykes-Hoberg, L. Jin, A.M. Watkins, D.E. Bergles, and J.D. Rothstein. 2007. Variations in promoter activity reveal a differential expression and physiology of glutamate transporters by glia in the developing and mature CNS. *J Neurosci*. 27:6607-6619.
Renton, A.E., A. Chio, and B.J. Traynor. 2014. State of play in amyotrophic lateral sclerosis genetics. *Nat Neurosci*. 17:17-23.
Renton, A.E., E. Majounie, A. Waite, J. Simon-Sanchez, S. Rollinson, J.R. Gibbs, J.C. Schymick, H. Laaksovirta, J.C. van Swieten, L. Myllykangas, et al. 2011. A Hexanucleotide Repeat Expansion in C9ORF72 Is the Cause of Chromosome 9p21-Linked ALS-FTD. *Neuron*. 72:257-268.
Richter, B., D.A. Sliter, L. Herhaus, A. Stolz, C. Wang, P. Beli, G. Zaffagnini, P. Wild, S. Martens, S.A. Wagner, et al. 2016. Phosphorylation of OPTN by TBK1 enhances its binding to Ub chains and promotes selective autophagy of damaged mitochondria. *Proc Natl Acad Sci U S A*. 113:4039-4044.
Ritossa, F. 1962. New Puffing Pattern Induced by Temperature Shock and Dnp in Drosophila. *Experientia*. 18:571-&.
Robinson, M.B., J.L. Tidwell, T. Gould, A.R. Taylor, J.M. Newbern, J. Graves, M. Tytell, and C.E. Milligan. 2005. Extracellular heat shock protein 70: a critical component for motoneuron survival. *J Neurosci*. 25:9735-9745.
Rojas, F., N. Cortes, S. Abarzua, A. Dyrda, and B. van Zundert. 2014. Astrocytes expressing mutant SOD1 and TDP43 trigger motoneuron death that is mediated via sodium channels and nitroxidative stress. *Front Cell Neurosci*. 8:24.
Rosen, D.R. 1993. Mutations in Cu/Zn superoxide dismutase gene are associated with familial amyotrophic lateral sclerosis. *Nature*. 364:362.
Rossi, D., L. Brambilla, C.F. Valori, C. Roncoroni, A. Crugnola, T. Yokota, D.E. Bredesen, and A. Volterra. 2008. Focal degeneration of astrocytes in amyotrophic lateral sclerosis. *Cell Death Differ*. 15:1691-1700.
Rothstein, J.D., G. Tsai, R.W. Kuncl, L. Clawson, D.R. Cornblath, D.B. Drachman, A. Pestronk, B.L. Stauch, and J.T. Coyle. 1990. Abnormal excitatory amino acid metabolism in amyotrophic lateral sclerosis. *Ann Neurol*. 28:18-25.
Rothstein, J.D., M. Van Kammen, A.I. Levey, L.J. Martin, and R.W. Kuncl. 1995a. Selective loss of glial glutamate transporter GLT-1 in amyotrophic lateral sclerosis. *Ann Neurol*. 38:73-84.
Rothstein, J.D., M. Vankammen, A.I. Levey, L.J. Martin, and R.W. Kuncl. 1995b. Selective Loss of Glial Glutamate Transporter Glt-1 in Amyotrophic-Lateral-Sclerosis. *Annals of Neurology*. 38:73-84.
Rudnick, N.D., C.J. Griffey, P. Guarnieri, V. Gerbino, X. Wang, J.A. Piersaint, J.C. Tapia, M.M. Rich, and T. Maniatis. 2017. Distinct roles for motor neuron autophagy early and late in the SOD1(G93A) mouse model of ALS. *Proc Natl Acad Sci U S A*. 114:E8294-E8303.
Runkel, E.D., S. Liu, R. Baumeister, and E. Schulze. 2013. Surveillance-activated defenses block the ROS-induced mitochondrial unfolded protein response. *PLoS Genet*. 9:e1003346.
Saberi, S., J.E. Stauffer, D.J. Schulte, and J. Ravits. 2015. Neuropathology of Amyotrophic Lateral Sclerosis and Its Variants. *Neurol Clin*. 33:855-876.

Saccon, R.A., R.K. Bunton-Stasyshyn, E.M. Fisher, and P. Fratta. 2013. Is SOD1 loss of function involved in amyotrophic lateral sclerosis? *Brain*. 136:2342-2358.

Sako, W., H. Ito, M. Yoshida, H. Koizumi, M. Kamada, K. Fujita, Y. Hashizume, Y. Izumi, and R. Kaji. 2012. Nuclear factor kappa B expression in patients with sporadic amyotrophic lateral sclerosis and hereditary amyotrophic lateral sclerosis with optineurin mutations. *Clin Neuropathol*. 31:418-423.

Sala, A.J., L.C. Bott, and R.I. Morimoto. 2017. Shaping proteostasis at the cellular, tissue, and organismal level. *Journal of Cell Biology*. 216:1231-1241.

San Gil, R., L. Ooi, J.J. Yerbury, and H. Ecroyd. 2017. The heat shock response in neurons and astroglia and its role in neurodegenerative diseases. *Mol Neurodegener*. 12:65.

Sasaki, S. 2011. Autophagy in spinal cord motor neurons in sporadic amyotrophic lateral sclerosis. *J Neuropathol Exp Neurol*. 70:349-359.

Sasaki, S., and M. Iwata. 2007. Mitochondrial alterations in the spinal cord of patients with sporadic amyotrophic lateral sclerosis. *J Neuropathol Exp Neurol*. 66:10-16.

Satoh, J.I., and S.U. Kim. 1995. Differential Expression of Heat-Shock Protein Hsp27 in Human Neurons and Glial-Cells in Culture. *Journal of Neuroscience Research*. 41:805-818.

Saura, J. 2007. Microglial cells in astroglial cultures: a cautionary note. *J Neuroinflammation*. 4:26.

Saura, J., E. Angulo, A. Ejarque, V. Casado, J.M. Tusell, R. Moratalla, J.F. Chen, M.A. Schwarzschild, C. Lluis, R. Franco, et al. 2005. Adenosine A(2A) receptor stimulation potentiates nitric oxide release by activated microglia. *Journal of Neurochemistry*. 95:919-929.

Saura, J., J.M. Tusell, and J. Serratosa. 2003. High-yield isolation of murine microglia by mild trypsinization. *Glia*. 44:183-189.

Schapira, A.H., J.M. Cooper, D. Dexter, P. Jenner, J.B. Clark, and C.D. Marsden. 1989. Mitochondrial complex I deficiency in Parkinson's disease. *Lancet*. 1:1269.

Schnell, L., S. Fearn, H. Klassen, M.E. Schwab, and V.H. Perry. 1999. Acute inflammatory responses to mechanical lesions in the CNS: differences between brain and spinal cord. *Eur J Neurosci*. 11:3648-3658.

Sciacovelli, M., G. Guzzo, V. Morello, C. Frezza, L. Zheng, N. Nannini, F. Calabrese, G. Laudiero, F. Esposito, M. Landriscina, et al. 2013. The mitochondrial chaperone TRAP1 promotes neoplastic growth by inhibiting succinate dehydrogenase. *Cell Metab*. 17:988-999.

Serio, A., B. Bilican, S.J. Barmada, D.M. Ando, C. Zhao, R. Siller, K. Burr, G. Haghi, D. Story, A.L. Nishimura, et al. 2013. Astrocyte pathology and the absence of non-cell autonomy in an induced pluripotent stem cell model of TDP-43 proteinopathy. *Proc Natl Acad Sci U S A*. 110:4697-4702.

Serio, A., and R. Patani. 2018. Concise Review: The Cellular Conspiracy of Amyotrophic Lateral Sclerosis. *Stem Cells*. 36:293-303.

Shahheydari, H., A. Ragagnin, A.K. Walker, R.P. Toth, M. Vidal, C.J. Jagaraj, E.R. Perri, A. Konopka, J.M. Sultana, and J.D. Atkin. 2017. Protein Quality Control and the Amyotrophic Lateral Sclerosis/Frontotemporal Dementia Continuum. *Front Mol Neurosci*. 10.

Sharp, P.S., M.T. Akbar, S. Bouri, A. Senda, K. Joshi, H.J. Chen, D.S. Latchman, D.J. Wells, and J. de Belleroche. 2008. Protective effects of heat shock

protein 27 in a model of ALS occur in the early stages of disease progression. *Neurobiol Dis*. 30:42-55.
Sharp, P.S., J.R. Dick, and L. Greensmith. 2005. The effect of peripheral nerve injury on disease progression in the SOD1(G93A) mouse model of amyotrophic lateral sclerosis. *Neuroscience*. 130:897-910.
Shaw, B.F., H.L. Lelie, A. Durazo, A.M. Nersissian, G. Xu, P.K. Chan, E.B. Gralla, A. Tiwari, L.J. Hayward, D.R. Borchelt, et al. 2008. Detergent-insoluble aggregates associated with amyotrophic lateral sclerosis in transgenic mice contain primarily full-length, unmodified superoxide dismutase-1. *Journal of Biological Chemistry*. 283:8340-8350.
Sheppard, P.W., X.Y. Sun, M. Khammash, and R.G. Giffard. 2014. Overexpression of Heat Shock Protein 72 Attenuates NF-kappa B Activation Using a Combination of Regulatory Mechanisms in Microglia. *Plos Computational Biology*. 10.
Shi, Y., P. Kirwan, and F.J. Livesey. 2012. Directed differentiation of human pluripotent stem cells to cerebral cortex neurons and neural networks. *Nat Protoc*. 7:1836-1846.
Shibata, N., R. Nagai, K. Uchida, S. Horiuchi, S. Yamada, A. Hirano, M. Kawaguchi, T. Yamamoto, S. Sasaki, and M. Kobayashi. 2001. Morphological evidence for lipid peroxidation and protein glycoxidation in spinal cords from sporadic amyotrophic lateral sclerosis patients. *Brain Research*. 917:97-104.
Shin, D.I., and Y.J. Oh. 2014. Tumor Necrosis Factor-Associated Protein 1 (TRAP1) is Released from the Mitochondria Following 6-hydroxydopamine Treatment. *Exp Neurobiol*. 23:65-76.
Shin, J.E., S. Geisler, and A. DiAntonio. 2014. Dynamic regulation of SCG10 in regenerating axons after injury. *Exp Neurol*. 252:1-11.
Shinder, G.A., M.C. Lacourse, S. Minotti, and H.D. Durham. 2001. Mutant Cu/Zn-superoxide dismutase proteins have altered solubility and interact with heat shock/stress proteins in models of amyotrophic lateral sclerosis. *Journal of Biological Chemistry*. 276:12791-12796.
Siegelin, M.D., T. Dohi, C.M. Raskett, G.M. Orlowski, C.M. Powers, C.A. Gilbert, A.H. Ross, J. Plescia, and D.C. Altieri. 2011. Exploiting the mitochondrial unfolded protein response for cancer therapy in mice and human cells. *J Clin Invest*. 121:1349-1360.
Sirko, S., G. Behrendt, P. Johansson, N. Plesnila, K. Grobe, L. Dimou, and M. Gotz. 2013. Reactive Glia Acquire Stem Cell Properties in Response to Sonic Hedgehog in the Injured Brain. *Glia*. 61:S197-S197.
Sloan, S.A., and B.A. Barres. 2013. Glia as primary drivers of neuropathology in TDP-43 proteinopathies. *Proc Natl Acad Sci U S A*. 110:4439-4440.
Smith, B.N., N. Ticozzi, C. Fallini, A.S. Gkazi, S. Topp, K.P. Kenna, E.L. Scotter, J. Kost, P. Keagle, J.W. Miller, et al. 2014. Exome-wide rare variant analysis identifies TUBA4A mutations associated with familial ALS. *Neuron*. 84:324-331.
Smith, B.N., S.D. Topp, C. Fallini, H. Shibata, H.J. Chen, C. Troakes, A. King, N. Ticozzi, K.P. Kenna, A. Soragia-Gkazi, et al. 2017a. Mutations in the vesicular trafficking protein annexin A11 are associated with amyotrophic lateral sclerosis. *Sci Transl Med*. 9.
Smith, E.F., P.J. Shaw, and K.J. De Vos. 2017b. The role of mitochondria in amyotrophic lateral sclerosis. *Neurosci Lett*.
Sofroniew, M.V. 2009. Molecular dissection of reactive astrogliosis and glial scar formation. *Trends Neurosci*. 32:638-647.

Sofroniew, M.V., and H.V. Vinters. 2010. Astrocytes: biology and pathology. *Acta Neuropathol*. 119:7-35.

Sola, C., C. Casal, J.M. Tusell, and J. Serratosa. 2002. Astrocytes enhance lipopolysaccharide-induced nitric oxide production by microglial cells. *European Journal of Neuroscience*. 16:1275-1283.

Song, H., C.F. Stevens, and F.H. Gage. 2002. Astroglia induce neurogenesis from adult neural stem cells. *Nature*. 417:39-44.

Song, H.Y., J.D. Dunbar, Y.X. Zhang, D.Q. Guo, and D.B. Donner. 1995. Identification of a Protein with Homology to Hsp90 That Binds the Type-1 Tumor-Necrosis-Factor Receptor. *Journal of Biological Chemistry*. 270:3574-3581.

Song, S., C.J. Miranda, L. Braun, K. Meyer, A.E. Frakes, L. Ferraiuolo, S. Likhite, A.K. Bevan, K.D. Foust, M.J. McConnell, et al. 2016. Major histocompatibility complex class I molecules protect motor neurons from astrocyte-induced toxicity in amyotrophic lateral sclerosis. *Nature Medicine*. 22:397-+.

Song, W., Y. Song, B. Kincaid, B. Bossy, and E. Bossy-Wetzel. 2013. Mutant SOD1G93A triggers mitochondrial fragmentation in spinal cord motor neurons: neuroprotection by SIRT3 and PGC-1alpha. *Neurobiol Dis*. 51:72-81.

Soreq, L., U.K.B.E. Consortium, C. North American Brain Expression, J. Rose, E. Soreq, J. Hardy, D. Trabzuni, M.R. Cookson, C. Smith, M. Ryten, et al. 2017. Major Shifts in Glial Regional Identity Are a Transcriptional Hallmark of Human Brain Aging. *Cell Rep*. 18:557-570.

Sreedharan, J., I.P. Blair, V.B. Tripathi, X. Hu, C. Vance, B. Rogelj, S. Ackerley, J.C. Durnall, K.L. Williams, E. Buratti, et al. 2008. TDP-43 mutations in familial and sporadic amyotrophic lateral sclerosis. *Science*. 319:1668-1672.

Stathopulos, P.B., J.A.O. Rumfeldt, G.A. Scholz, R.A. Irani, H.E. Frey, R.A. Hallewell, J.R. Lepock, and E.M. Meiering. 2003. Cu/Zn superoxide dismutase mutants associated with amyotrophic lateral sclerosis show enhanced formation of aggregates in vitro. *P Natl Acad Sci USA*. 100:7021-7026.

Statland, J.M., R.J. Barohn, A.L. McVey, J.S. Katz, and M.M. Dimachkie. 2015. Patterns of Weakness, Classification of Motor Neuron Disease, and Clinical Diagnosis of Sporadic Amyotrophic Lateral Sclerosis. *Neurol Clin*. 33:735-748.

Staunton, C.A., R. Barrett-Jolley, L. Djouhri, and T. Thippeswamy. 2018. Inducible nitric oxide synthase inhibition by 1400W limits pain hypersensitivity in a neuropathic pain rat model. *Exp Physiol*. 103:535-544.

Stowell, R.D., E.L. Wong, H.N. Batchelor, M.S. Mendes, C.E. Lamantia, B.S. Whitelaw, and A.K. Majewska. 2018. Cerebellar microglia are dynamically unique and survey Purkinje neurons in vivo. *Dev Neurobiol*. 78:627-644.

Sturtz, L.A., K. Diekert, L.T. Jensen, R. Lill, and V.C. Culotta. 2001. A fraction of yeast Cu,Zn-superoxide dismutase and its metallochaperone, CCS, localize to the intermembrane space of mitochondria. A physiological role for SOD1 in guarding against mitochondrial oxidative damage. *J Biol Chem*. 276:38084-38089.

Sulejczak, D., S.J. Chrapusta, D. Dziewulska, and J. Rafalowska. 2015. NF-kappaB deficit in spinal motoneurons in patients with sporadic amyotrophic lateral sclerosis--a pilot study. *Folia Neuropathol*. 53:367-376.

Sun, S., Y. Sun, S.C. Ling, L. Ferraiuolo, M. McAlonis-Downes, Y. Zou, K. Drenner, Y. Wang, D. Ditsworth, S. Tokunaga, et al. 2015. Translational profiling identifies a cascade of damage initiated in motor neurons and spreading to glia in mutant SOD1-mediated ALS. *Proc Natl Acad Sci U S A*. 112:E6993-7002.

Swarup, V., D. Phaneuf, N. Dupre, S. Petri, M. Strong, J. Kriz, and J.P. Julien. 2011. Deregulation of TDP-43 in amyotrophic lateral sclerosis triggers nuclear factor kappaB-mediated pathogenic pathways. *J Exp Med*. 208:2429-2447.

Tang, H., J. Li, X. Liu, G. Wang, M. Luo, and H. Deng. 2016. Down-regulation of HSP60 Suppresses the Proliferation of Glioblastoma Cells via the ROS/AMPK/mTOR Pathway. *Sci Rep*. 6:28388.

Tarassishin, L., H.S. Suh, and S.C. Lee. 2014. LPS and IL-1 differentially activate mouse and human astrocytes: role of CD14. *Glia*. 62:999-1013.

Tashiro, Y., M. Urushitani, H. Inoue, M. Koike, Y. Uchiyama, M. Komatsu, K. Tanaka, M. Yamazaki, M. Abe, H. Misawa, et al. 2012. Motor Neuron-specific Disruption of Proteasomes, but Not Autophagy, Replicates Amyotrophic Lateral Sclerosis. *Journal of Biological Chemistry*. 287:42984-42994.

Tatsuta, T. 2009. Protein quality control in mitochondria. *J Biochem*. 146:455-461.

Taylor, J.P., R.H. Brown, Jr., and D.W. Cleveland. 2016. Decoding ALS: from genes to mechanism. *Nature*. 539:197-206.

Ticozzi, N., C. Vance, A.L. LeClerc, P. Keagle, J.D. Glass, D. McKenna-Yasek, P.C. Sapp, V. Silani, D.A. Bosco, C.E. Shaw, et al. 2011. Mutational Analysis Reveals the FUS Homolog TAF15 as a Candidate Gene for Familial Amyotrophic Lateral Sclerosis. *Am J Med Genet B*. 156b:285-290.

Tong, J.B., C. Huang, F.F. Bi, Q.X. Wu, B. Huang, X.H. Liu, F. Li, H.X. Zhou, and X.G. Xia. 2013. Expression of ALS-linked TDP-43 mutant in astrocytes causes non-cell-autonomous motor neuron death in rats. *Embo Journal*. 32:1917-1926.

Trautinger, F., I. KindasMugge, R.M. Knobler, and H. Honigsmann. 1996. Stress proteins in the cellular response to ultraviolet radiation. *J Photoch Photobio B*. 35:141-148.

Tsai, H.H., H. Li, L.C. Fuentealba, A.V. Molofsky, R. Taveira-Marques, H. Zhuang, A. Tenney, A.T. Murnen, S.P. Fancy, F. Merkle, et al. 2012. Regional astrocyte allocation regulates CNS synaptogenesis and repair. *Science*. 337:358-362.

Tsang, C.K., Y. Liu, J. Thomas, Y.J. Zhang, and X.F.S. Zheng. 2014. Superoxide dismutase 1 acts as a nuclear transcription factor to regulate oxidative stress resistance. *Nature Communications*. 5.

Tsvetkov, A.S., M. Arrasate, S. Barmada, D.M. Ando, P. Sharma, B.A. Shaby, and S. Finkbeiner. 2013. Proteostasis of polyglutamine varies among neurons and predicts neurodegeneration. *Nat Chem Biol*. 9:586-U591.

Tummala, H., C. Jung, A. Tiwari, C.M. Higgins, L.J. Hayward, and Z. Xu. 2005. Inhibition of chaperone activity is a shared property of several Cu,Zn-superoxide dismutase mutants that cause amyotrophic lateral sclerosis. *J Biol Chem*. 280:17725-17731.

Turner, M.R., A. Al-Chalabi, A. Chio, O. Hardiman, M.C. Kiernan, J.D. Rohrer, J. Rowe, W. Seeley, and K. Talbot. 2017. Genetic screening in sporadic ALS and FTD. *J Neurol Neurosurg Psychiatry*. 88:1042-1044.

Tyzack, G., A. Lakatos, and R. Patani. 2016. Human Stem Cell-Derived Astrocytes: Specification and Relevance for Neurological Disorders. *Curr Stem Cell Rep*. 2:236-247.

Tyzack, G.E., C.E. Hall, C.R. Sibley, T. Cymes, S. Forostyak, G. Carlino, I.F. Meyer, G. Schiavo, S.C. Zhang, G.M. Gibbons, et al. 2017. A neuroprotective astrocyte state is induced by neuronal signal EphB1 but fails in ALS models. *Nature Communications*. 8.

Tyzack, G.E., R. Luisier, D.M. Taha, J. Neeves, M. Modic, J.S. Mitchell, I. Meyer, L. Greensmith, J. Newcombe, J. Ule, et al. 2019. Widespread FUS mislocalization is a molecular hallmark of amyotrophic lateral sclerosis. *Brain*.

Urushitani, M., A. Sik, T. Sakurai, N. Nukina, R. Takahashi, and J.P. Julien. 2006. Chromogranin-mediated secretion of mutant superoxide dismutase proteins linked to amyotrophic lateral sclerosis. *Nature Neuroscience*. 9:108-118.

van Blitterswijk, M., M.A. van Es, E.A. Hennekam, D. Dooijes, W. van Rheenen, J. Medic, P.R. Bourque, H.J. Schelhaas, A.J. van der Kooi, M. de Visser, et al. 2012. Evidence for an oligogenic basis of amyotrophic lateral sclerosis. *Hum Mol Genet*. 21:3776-3784.

Van Damme, P., D. Braeken, G. Callewaert, W. Robberecht, and L. Van den Bosch. 2005a. GluR2 deficiency accelerates motor neuron degeneration in a mouse model of amyotrophic lateral sclerosis. *J Neuropath Exp Neur*. 64:605-612.

van Damme, P., M. Dewil, W. Robberecht, and L. van den Bosch. 2005b. Excitotoxicity and Amyotrophic Lateral Sclerosis. *Neurodegenerative Diseases*. 2:147-159.

Van Damme, P., L. Van Den Bosch, E. Van Houtte, G. Callewaert, and W. Robberecht. 2002. GluR2-dependent properties of AMPA receptors determine the selective vulnerability of motor neurons to excitotoxicity. *Journal of the Neurological Sciences*. 199:S34-S34.

Vance, C., B. Rogelj, T. Hortobagyi, K.J. De Vos, A.L. Nishimura, J. Sreedharan, X. Hu, B. Smith, D. Ruddy, P. Wright, et al. 2009. Mutations in FUS, an RNA processing protein, cause familial amyotrophic lateral sclerosis type 6. *Science*. 323:1208-1211.

Vande Velde, C., K.K. McDonald, Y. Boukhedimi, M. McAlonis-Downes, C.S. Lobsiger, S. Bel Hadj, A. Zandona, J.P. Julien, S.B. Shah, and D.W. Cleveland. 2011. Misfolded SOD1 associated with motor neuron mitochondria alters mitochondrial shape and distribution prior to clinical onset. *PLoS One*. 6:e22031.

Vandoorne, T., K. De Bock, and L. Van Den Bosch. 2018. Energy metabolism in ALS: an underappreciated opportunity? *Acta Neuropathologica*. 135:489-509.

Varcianna, A., M.A. Myszczynska, L.M. Castelli, B. O'Neill, Y. Kim, J. Talbot, S. Nyberg, I. Nyamali, P.R. Heath, M.J. Stopford, et al. 2019. Micro-RNAs secreted through astrocyte-derived extracellular vesicles cause neuronal network degeneration in C9orf72 ALS. *Ebiomedicine*. 40:626-635.

Vigh, L., P.N. Literati, I. Horvath, Z. Torok, G. Balogh, A. Glatz, E. Kovacs, I. Boros, P. Ferdinandy, B. Farkas, et al. 1997. Bimoclomol: a nontoxic, hydroxylamine derivative with stress protein-inducing activity and cytoprotective effects. *Nat Med*. 3:1150-1154.

Vijayvergiya, C., M.F. Beal, J. Buck, and G. Manfredi. 2005. Mutant superoxide dismutase 1 forms aggregates in the brain mitochondrial matrix of amyotrophic lateral sclerosis mice. *J Neurosci*. 25:2463-2470.

Vleminckx, V., P. Van Damme, K. Goffin, H. Delye, L. Van den Bosch, and W. Robberecht. 2002. Upregulation of HSP27 in a transgenic model of ALS. *J Neuropath Exp Neur*. 61:968-974.

Voos, W. 2013. Chaperone-protease networks in mitochondrial protein homeostasis. *Biochim Biophys Acta*. 1833:388-399.

Wang, L., D.H. Gutmann, and R.P. Roos. 2011. Astrocyte loss of mutant SOD1 delays ALS disease onset and progression in G85R transgenic mice. *Hum Mol Genet*. 20:286-293.

Wang, W.Z., L.W. Wang, J.J. Lu, S.L. Siedlak, H. Fujioka, J.J. Liang, S.R. Jiang, X.P. Ma, Z. Jiang, E.L. da Rocha, et al. 2016. The inhibition of TDP-43 mitochondrial localization blocks its neuronal toxicity. *Nature Medicine*. 22:869-+.

Watanabe, M., M. Dykes-Hoberg, V.C. Culotta, D.L. Price, P.C. Wong, and J.D. Rothstein. 2001. Histological evidence of protein aggregation in mutant SOD1 transgenic mice and in amyotrophic lateral sclerosis neural tissues. *Neurobiol Dis*. 8:933-941.

Webster, C.P., E.F. Smith, C.S. Bauer, A. Moller, G.M. Hautbergue, L. Ferraiuolo, M.A. Myszczynska, A. Higginbottom, M.J. Walsh, A.J. Whitworth, et al. 2016. The C9orf72 protein interacts with Rab1a and the ULK1 complex to regulate initiation of autophagy. *Embo Journal*. 35:1656-1676.

Webster, C.P., E.F. Smith, P.J. Shaw, and K.J. De Vos. 2017. Protein Homeostasis in Amyotrophic Lateral Sclerosis: Therapeutic Opportunities? *Front Mol Neurosci*. 10:123.

Wei, J.P.J., C. Srinivasan, H. Han, J.S. Valentine, and E.B. Gralla. 2001. Evidence for a novel role of copper-zinc superoxide dismutase in zinc metabolism. *Journal of Biological Chemistry*. 276:44798-44803.

Welch, W.J., H.S. Kang, R.P. Beckmann, and L.A. Mizzen. 1991. Response of mammalian cells to metabolic stress; changes in cell physiology and structure/function of stress proteins. *Curr Top Microbiol Immunol*. 167:31-55.

Westerheide, S.D., J. Anckar, S.M. Stevens, L. Sistonen, and R.I. Morimoto. 2009. Stress-Inducible Regulation of Heat Shock Factor 1 by the Deacetylase SIRT1. *Science*. 323:1063-1066.

Weydt, P., E.C. Yuen, B.R. Ransom, and T. Moller. 2004. Increased cytotoxic potential of microglia from ALS-transgenic mice. *Glia*. 48:179-182.

Wilhelmsson, U., E.A. Bushongt, D.L. Price, B.L. Smarr, V. Phung, M. Terada, M.H. Ellisman, and M. Pekny. 2006. Redefining the concept of reactive astrocytes as cells that remain within their unique domains upon reaction to injury. *P Natl Acad Sci USA*. 103:17513-17518.

Woerner, A.C., F. Frottin, D. Hornburg, L.R. Feng, F. Meissner, M. Patra, J. Tatzelt, M. Mann, K.F. Winklhofer, F.U. Hartl, et al. 2016. Cytoplasmic protein aggregates interfere with nucleocytoplasmic transport of protein and RNA. *Science*. 351:173-176.

Wong, H.R., M. Ryan, and J.R. Wispe. 1997. The heat shock response inhibits inducible nitric oxide synthase gene expression by blocking I kappa-B degradation and NF-kappa B nuclear translocation. *Biochem Biophys Res Commun*. 231:257-263.

Wong, P.C., C.A. Pardo, D.R. Borchelt, M.K. Lee, N.G. Copeland, N.A. Jenkins, S.S. Sisodia, D.W. Cleveland, and D.L. Price. 1995. An adverse property

of a familial ALS-linked SOD1 mutation causes motor neuron disease characterized by vacuolar degeneration of mitochondria. *Neuron*. 14:1105-1116.

Wu, C.H., C. Fallini, N. Ticozzi, P.J. Keagle, P.C. Sapp, K. Piotrowska, P. Lowe, M. Koppers, D. McKenna-Yasek, D.M. Baron, et al. 2012. Mutations in the profilin 1 gene cause familial amyotrophic lateral sclerosis. *Nature*. 488:499-+.

Wu, D.C., D.B. Re, M. Nagai, H. Ischiropoulos, and S. Przedborski. 2006. The inflammatory NADPH oxidase enzyme modulates motor neuron degeneration in amyotrophic lateral sclerosis mice. *Proc Natl Acad Sci U S A*. 103:12132-12137.

Wu, Y., J. Liu, Z. Zhang, H. Huang, J. Shen, S. Zhang, Y. Jiang, L. Luo, and Z. Yin. 2009. HSP27 regulates IL-1 stimulated IKK activation through interacting with TRAF6 and affecting its ubiquitination. *Cell Signal*. 21:143-150.

Xiao, Q., W. Zhao, D.R. Beers, A.A. Yen, W. Xie, J.S. Henkel, and S.H. Appel. 2007. Mutant SOD1(G93A) microglia are more neurotoxic relative to wild-type microglia. *J Neurochem*. 102:2008-2019.

Xiao, S., L. MacNair, P. McGoldrick, P.M. McKeever, J.R. McLean, M. Zhang, J. Keith, L. Zinman, E. Rogaeva, and J. Robertson. 2015. Isoform-specific antibodies reveal distinct subcellular localizations of C9orf72 in amyotrophic lateral sclerosis. *Ann Neurol*. 78:568-583.

Xiao, X.Z., X.X. Zuo, A.A. Davis, D.R. McMillan, B.B. Curry, J.A. Richardson, and I.J. Benjamin. 1999. HSF1 is required for extra-embryonic development, postnatal growth and protection during inflammatory responses in mice. *Embo Journal*. 18:5943-5952.

Xie, Q.W., Y. Kashiwabara, and C. Nathan. 1994. Role of Transcription Factor Nf-Kappa-B/Rel in Induction of Nitric-Oxide Synthase. *Journal of Biological Chemistry*. 269:4705-4708.

Xie, Y., B. Zhou, M.Y. Lin, S. Wang, K.D. Foust, and Z.H. Sheng. 2015. Endolysosomal Deficits Augment Mitochondria Pathology in Spinal Motor Neurons of Asymptomatic fALS Mice. *Neuron*. 87:355-370.

Yamanaka, K., S.J. Chun, S. Boillee, N. Fujimori-Tonou, H. Yamashita, D.H. Gutmann, R. Takahashi, H. Misawa, and D.W. Cleveland. 2008. Astrocytes as determinants of disease progression in inherited amyotrophic lateral sclerosis. *Nat Neurosci*. 11:251-253.

Yamashita, H., J. Kawamata, K. Okawa, R. Kanki, T. Nakamizo, T. Hatayama, K. Yamanaka, R. Takahashi, and S. Shimohama. 2007. Heat-shock protein 105 interacts with and suppresses aggregation of mutant Cu/Zn superoxide dismutase: clues to a possible strategy for treating ALS. *J Neurochem*. 102:1497-1505.

Yanagisawa, M., K. Nakashima, T. Takizawa, W. Ochiai, H. Arakawa, and T. Taga. 2001. Signaling crosstalk underlying synergistic induction of astrocyte differentiation by BMPs and IL-6 family of cytokines. *Febs Letters*. 489:139-143.

Yenari, M.A., J. Liu, Z. Zheng, Z.S. Vexler, J.E. Lee, and R.G. Giffard. 2005. Antiapoptotic and anti-inflammatory mechanisms of heat-shock protein protection. *Ann N Y Acad Sci*. 1053:74-83.

Yerbury, J.J., D. Gower, L. Vanags, K. Roberts, J.A. Lee, and H. Ecroyd. 2013. The small heat shock proteins alpha B-crystallin and Hsp27 suppress SOD1 aggregation in vitro. *Cell Stress Chaperon*. 18:251-257.

Yin, H.Z., and J.H. Weiss. 2012. Marked synergism between mutant SOD1 and glutamate transport inhibition in the induction of motor neuronal degeneration in spinal cord slice cultures. *Brain Research*. 1448:153-162.

Yoshida, S., S. Tsutsumi, G. Muhlebach, C. Sourbier, M.J. Lee, S. Lee, E. Vartholomaiou, M. Tatokoro, K. Beebe, N. Miyajima, et al. 2013. Molecular chaperone TRAP1 regulates a metabolic switch between mitochondrial respiration and aerobic glycolysis. *Proc Natl Acad Sci U S A*. 110:E1604-1612.

Zamanian, J.L., L. Xu, L.C. Foo, N. Nouri, L. Zhou, R.G. Giffard, and B.A. Barres. 2012. Genomic analysis of reactive astrogliosis. *J Neurosci*. 32:6391-6410.

Zhang, J., H. Ito, R. Wate, S. Ohnishi, S. Nakano, and H. Kusaka. 2006. Altered distributions of nucleocytoplasmic transport-related proteins in the spinal cord of a mouse model of amyotrophic lateral sclerosis. *Acta Neuropathol*. 112:673-680.

Zhang, K., C.J. Donnelly, A.R. Haeusler, J.C. Grima, J.B. Machamer, P. Steinwald, E.L. Daley, S.J. Miller, K.M. Cunningham, S. Vidensky, et al. 2015. The C9orf72 repeat expansion disrupts nucleocytoplasmic transport. *Nature*. 525:56-61.

Zhang, L., P. Karsten, S. Hamm, J.H. Pogson, A.K. Muller-Rischart, N. Exner, C. Haass, A.J. Whitworth, K.F. Winklhofer, J.B. Schulz, et al. 2013. TRAP1 rescues PINK1 loss-of-function phenotypes. *Hum Mol Genet*. 22:2829-2841.

Zhang, P.L., M.Y. Lun, C.M. Schworer, T.M. Blasick, K.K. Masker, J.B. Jones, and D.J. Carey. 2008. Heat shock protein expression is highly sensitive to ischemia-reperfusion injury in rat kidneys. *Ann Clin Lab Sci*. 38:57-64.

Zhang, Q., M.J. Lenardo, and D. Baltimore. 2017. 30 Years of NF-kappa B: A Blossoming of Relevance to Human Pathobiology. *Cell*. 168:37-57.

Zhang, Y., S.A. Sloan, L.E. Clarke, C. Caneda, C.A. Plaza, P.D. Blumenthal, H. Vogel, G.K. Steinberg, M.S.B. Edwards, G. Li, et al. 2016. Purification and Characterization of Progenitor and Mature Human Astrocytes Reveals Transcriptional and Functional Differences with Mouse. *Neuron*. 89:37-53.

Zhao, Q., J. Wang, I.V. Levichkin, S. Stasinopoulos, M.T. Ryan, and N.J. Hoogenraad. 2002. A mitochondrial specific stress response in mammalian cells. *EMBO J*. 21:4411-4419.

Zhao, W., D.R. Beers, J.S. Henkel, W. Zhang, M. Urushitani, J.P. Julien, and S.H. Appel. 2010. Extracellular mutant SOD1 induces microglial-mediated motoneuron injury. *Glia*. 58:231-243.

Zhao, W., W. Xie, W. Le, D.R. Beers, Y. He, J.S. Henkel, E.P. Simpson, A.A. Yen, Q. Xiao, and S.H. Appel. 2004. Activated microglia initiate motor neuron injury by a nitric oxide and glutamate-mediated mechanism. *J Neuropathol Exp Neurol*. 63:964-977.

Zhao, W.H., D.R. Beers, S. Bell, J.H. Wang, S.X. Wen, R.H. Baloh, and S.H. Appel. 2015. TDP-43 activates microglia through NF-kappa B and NLRP3 inflammasome. *Experimental Neurology*. 273:24-35.

Zheng, Z., J.Y. Kim, H.L. Ma, J.E. Lee, and M.A. Yenari. 2008. Anti-inflammatory effects of the 70 kDa heat shock protein in experimental stroke. *J Cerebr Blood F Met*. 28:53-63.

Zhou, L., and D.Y. Zhu. 2009. Neuronal nitric oxide synthase: structure, subcellular localization, regulation, and clinical implications. *Nitric Oxide*. 20:223-230.